HYDRAULIC PERFORMANCE EVALUATION OF MULTI-LAYERED COVER SYSTEM FOR NEAR SURFACE DISPOSAL FACILITY

Thesis

submitted in partial fulfilment of the requirements

for the degree of

Doctor of Philosophy

by

Janarul Shaikh

(Roll No. 146104004)

Department of Civil Engineering
Indian Institute of Technology Guwahati
Guwahati 781039, Assam, India

December 2019

भारतीय प्रौद्योगिकी संस्थान गुवाहाटी
Indian Institute of Technology Guwahati

CERTIFICATE

This is to certify that the thesis titled "**Hydraulic Performance Evaluation of Multi-layered Cover System for Near Surface Disposal Facility**" submitted by Janarul Shaikh to the Indian Institute of Technology Guwahati, for the award of the degree of Doctor of Philosophy in Civil Engineering is a record of bonafide research work carried out by him under my supervision and guidance. The thesis work, in my opinion, has reached the requisite standard fulfilling the requirement for the degree of Doctor of Philosophy.

Date: 23-12-2019
Place: IIT Guwahati

Prof. Sreedeep Sekharan
Department of Civil Engineering
Indian Institute of Technology Guwahati
Guwahati 781039, Assam, India

भारतीय प्रौद्योगिकी संस्थान गुवाहाटी
Indian Institute of Technology Guwahati

STATEMENT

I do hereby declare that the matter embodied in this thesis is the results of investigations carried out by me in the Department of Civil Engineering, Indian Institute of Technology Guwahati, Assam, India.

In keeping with the general practice of reporting scientific observations, due acknowledgements have been made wherever the work described is based on the findings of the other investigators.

Place: IIT Guwahati

Date: 23-12-2019

Janarul Shaikh

(Roll No. 146104004)

भारतीय प्रौद्योगिकी संस्थान गुवाहाटी
Indian Institute of Technology Guwahati

ACKNOWLEDGEMENT

I would like to express my sincere gratitude and heartfelt thanks to my thesis supervisor Prof. Sreedeep Sekharan for his excellent technical guidance and constant encouragement. I am very thankful to him for the freedom that he had given me for working comfortably throughout this research study and all his valuable time that he had spent for supervising me. I would always be indebted to him for the kind nature that he had showed to me during my difficult time. I would be highly grateful to him for his precious advice, which will keep me motivated for achieving success in my career.

I would like to thank the doctoral committee members Dr. Arindam Dey, Dr. Anil Kumar Mishra and Dr. Tadikonda Venkata Bharat for their constructive comments and suggestions that helped me immensely to carry out my study.

I would like to thankfully acknowledge board of research in nuclear sciences (BRNS), Department of Atomic Energy (DAE), India for the financial support provided for the work reported in this thesis vide project no. 2013/36/06-BRNS. I am also thankful to Dr. Ravi Ranjan Rakesh, the scientific officer, Bhabha Atomic Research Centre (BARC) for his valuable inputs.

I highly appreciate Ministry of Human Resource Development (MHRD) of my country India for providing me the fellowship to support my educational needs. I would like to thank the Director of the Institute, the Deans, the Registrars and all the office staffs of various sections for strengthening research and academic environment in the Institute. I also extend my thanks to the Head, the teaching faculty, the laboratory and office staffs of Civil Engineering Department for their kind co-operations during my needful time. I am thankful to the doctors and medical staffs of IITG Hospital for taking care of my health issues. I am thankful to all my friends who helped me in many ways during my study. Few of them are Sudheer, Krishanu, Bhanu, Doordarshi, Biplab, Abhishek, Shankar, Suchit, Yagom, Jumrik and Bordoloi et al.

I am indebted to my tutor late Mr. Abdur Rafique Sir and to Al-Ameen Mission for inculcating strong perseverance, enormous patience and positive attitude in me.

I would like to respect my mother Ambia Bibi and my father Yearfor Shaikh for their endless love and affection, which always keeps me strong and energetic. I am thankful to my brother Mr. Monirul Sk., Sister Mrs. Nasin Banu and all others of my family. I am very thankful to my wife Mrs. Sahida (Runi) for supporting me patiently during the period of troubles.

I would also like to remember the Almighty God who blessed me with my daughter Jasmine and my son Alameen as the constant inspiration for this achievement of my life.

Date: 23-12-2019 **Janarul Shaikh**

भारतीय प्रौद्योगिकी संस्थान गुवाहाटी
Indian Institute of Technology Guwahati

ABSTRACT

Engineered multi-layered cover system (MLCS) are constructed over near surface waste disposal facilities (NSDF) after the operational closure for minimizing rain water ingress into the underlying wastes. There are different types of MLCS, which are applicable for a given climatic condition. The relevant literature advocates clay based hydraulic barrier as the MLCS for high humid high intensity rainfall regions like Indian subcontinent. There are not many studies that evaluate the hydraulic performance of MLCS relevant to the tropical climate of India. The main objective of this study is to investigate the hydraulic performance efficiency of the MLCS for the tropical Indian climate. This was accomplished by conducting controlled laboratory percolation study under constant ponding depth for different configurations of MLCS for a duration of 900 days. The role of inclusion of geosynthetic clay liner (GCL) and fly ash in the MLCS was studied based on the laboratory results. A field MLCS was constructed for studying the percolation characteristics under realistic soil-atmosphere boundary condition for a period of 800 days. The laboratory and field MLCS were simulated numerically using HYDRUS 2D finite element code for identifying the appropriate hydraulic characteristic input and boundary conditions. Based on this, the climate change impact on MLCS was investigated with and without considering material performance deterioration for a duration of 87 years.

The numerical simulation of laboratory MLCS column matched well with wetting water retention characteristics as compared to drying and predicted results. The numerical analysis of field MLCS indicated the appropriateness of drying water retention characteristic input for simulating the alternate wetting and drying conditions. The MLCS with GCL resulted in 36 % cost benefit and performed efficiently despite using relatively permeable fly ash in the surface layer. In the absence of GCL, MLCS underperformed when fly ash was added to the surface layer. The field study of MLCS revealed that the input atmospheric boundary condition based on Penman-Monteith evapotranspiration model gave comparable numerical and measured results. The effect of 800 days of weather variation was found to be significant for surface layer (SL), and marginal for both drainage and barrier layers (DL and BL). Vegetation growth and desiccation cracks on the SL hardly affected the moisture dynamics in the BL for this duration. The numerical simulation of long-term climate change impact of 87 years exhibited high sensitivity of SL to the atmospheric variants by undergoing cyclic wetting and drying. The simulation results indicated that the provision of MLCS without GCL restrict water interaction with the waste by 13 and 18 years with and without considering material deterioration, respectively. The provision of GCL in the MLCS delayed the water interaction with the waste by 25 and 42 years with and without considering material deterioration, respectively.

Keywords: Hazardous waste; landfill cover system; hydraulic performance; percolation; water content; matric suction; numerical modelling; climate change impact

भारतीय प्रौद्योगिकी संस्थान गुवाहाटी
Indian Institute of Technology Guwahati

TABLE OF CONTENTS

भारतीय प्रौद्योगिकी संस्थान गुवाहाटी
Indian Institute of Technology Guwahati

LIST OF FIGURES

LIST OF TABLES

NOTATIONS

θ	Volumetric water content ($m^3.m^{-3}$)
θ_c	Computed volumetric water content
θ_m	Measured volumetric water content
θ_{mr}	Revised volumetric water content
θ_f	Final volumetric water content at the end of a particular time duration
θ_i	Initial volumetric water content at the beginning of a particular time duration
θ_s	Saturated volumetric water content ($m^3.m^{-3}$)
θ_r	Residual volumetric water content ($m^3.m^{-3}$)
θ_i	Initial volumetric water content ($m^3.m^{-3}$)
θ_x	Measured or simulated volumetric water content at a column depth of *x* cm (*x* = 10, 20, 30, 40, 60, and 100 cm) ($m^3.m^{-3}$)
ψ	Soil water potential/Soil suction (kPa)
ψ_t	Total soil water potential (kPa)
ψ_m	Matric soil water potential (kPa)
ψ_o	Osmotic soil water potential (kPa)
ψ_g	Gravitational soil water potential (kPa)
ψ_p	Soil water potential due pressure head (kPa)
ψ_{aev}	Air entry value
ε_a	Dielectric constant (–)
T	Temperature (°C)
q	Rate of water flux
w	Gravimetric water content
V	Voltage (volt)
a_0, a_1	Calibration parameters

A, B, C, D	Calibration parameters
a, b	Calibration parameter
ΔS	Change in soil water storage
V_G	Geometric volume of soil
H	Pressure head (cm)
t	Time (days)
t_d	Time of deviation from initial condition (days)
t_s	Time of saturation (days)
TP_x	Time interval taken form deviation to saturation of volumetric water content a column depth of *x* cm (*x* = 10, 20, 30, 40, 60, and 100 cm) (days)
k	Unsaturated hydraulic conductivity (m/s)
k_s	Saturated hydraulic conductivity (m/s)
k_r	Relative hydraulic conductivity (m/s)
α	van Genuchten parameters (cm^{-1})
n	van Genuchten parameters (–)
G	Specific gravity (–)
ρ_d	Dry density (g/cm^3)
ρ_w	Density of water (g/cm^3)
C	Percentage of cost-benefit (%)
C_B	Cost of bentonite (USD)
C_{B+G}	Cost of bentonite and GCL (USD)
d	Diameter of test column (m)
h	Saturated height of barrier layer (m)
P	Percentage of bentonite used for barrier layer (%)
R_B	Bentonite price (USD/kg)
R_G	GCL price (USD/m^2)

ABBREVIATIONS

NSDF	Near surface disposal facility
MLCS	Multi-layered landfill cover system
CS	Cover system
USEPA	United states environmental protection agency
RCRA	Resource conservation and recovery act
USDOE	United states department of energy
ASTM	American society of testing and materials
IS	Indian standard
FE	Finite element
ITRC	Interstate technology and recovery council
CERCLA	Comprehensive environmental response, compensation & liability act
ACAP	Alternative cover assessment programme
HELP	Hydrological evaluation of landfill performance
ET	Evapotranspiration
CB	Capillary barrier
CCL	Compacted clay liner
GCL	Geosynthetic clay liner
GMB	Geomembrane
GTX	Geotextile
GN	Geonet
GC	Geocomposite
LLDPE	Linear low-density polyethylene
HDPE	High density polyethylene
MSW	Municipal solid waste
HW	Hospital waste

WCR	Water content reflectometer
TDR	Time domain reflectometry
SL	Surface layer
DL	Drainage layer
BL	Barrier layer
RS	Red soil
BS	Black soil
MS	Medium sand
FA	Fly ash
BN	Bentonite
RF	Red soil-fly ash mix (1:1)
BF	Black soil-fly ash mix (1:1)
RB	Red soil-bentonite mix (7:3)
BB	Black soil-bentonite mix (7:3)
FB	Fly ash-bentonite mix (7:3)
MDD	Maximum dry density
OMC	Optimum moisture content
CEC	Cation exchange capacity
PP	Profile probe
PPS	Profile probe sensor
PVC	Polyvinyl chloride
TP	Transition period
SWCC	Soil water characteristic curve
vG	van Genuchten
PM	Penman-Monteith
JH	Jensen-Haise
HS	Hargreaves-Samani

BC	Blaney-Criddle
PT	Preistley Taylor
LAI	Leaf area index
CIT	Crack intensity factor
Csec	Central section
Msec	Middle section
Tsec	Toe section
EM	Electromagnetic
FE	Finite element
WHP	Wetting hydraulic parameters
DHP	Drying hydraulic parameters
PHP	Predicted hydraulic parameters
OM	Organic matter (%)
C1	Multi-layered cover system having red soil as surface layer, medium sand as drainage layer, and 7: 3 red soil-bentonite mix as barrier layer
C2	Multi-layered over system having 1:1 red soil-fly ash mix as surface layer, medium sand as drainage layer, and 7: 3 red soil-bentonite mix as barrier layer along with 1 cm thick geosythetic clay liner on its top as additional hydraulic barrier
C3	Multi-layered cover system having black soil as surface layer, medium sand as drainage layer, and 7: 3 black soil-bentonite mix as barrier layer
C4	Multi-layered cover system having 1:1 black soil-fly ash mix as surface layer, medium sand as drainage layer, and 7: 3 fly ash-bentonite mix as barrier layer
SDSM	Statistical down scaling model

Chapter 1
Introduction

1.1 General

The engineering approach of containing excessively large quantity of waste generated from domestic, industrial and energy sectors are through well-designed near surface disposal facilities (NSDFs). The disposed wastes should impose minimum risk to the future generation and ecosystem (Allen and Taylor 2006; Daniel et al. 2002). Therefore, NSDFs after reaching their full capacity need to be isolated from surrounding environment for sufficiently long period (> 100 years) to ensure minimal effect of waste on useful resources (Francisca and Glatstein 2010; Zhang et al. 2017). This can be achieved by constructing a well-designed cover system over the NSDF to minimize water infiltration into the underlying wastes. Such an approach is also mandatory to securing non-engineered surface waste dumps, which pose a high risk to surrounding environment. The provision of cover system can effectively reduce leachate generation and hence reduce the possibility of ground water and geoenvironment contamination in the case of both engineered and non-engineered waste disposal (Rowe 2011; Xue et al. 2013).

There are different types of cover system developed over the past few decades (Barnswell and Dwyer 2011; Khapre et al. 2017; Rahardjo et al. 2012), which are either single layered simple covers or a more complex multi-layered. Among them, the cover system based on evapotranspiration (ET) and capillary barrier (CB) action, are popularly used. ET and CB cover system are mostly suitable for arid and semi-arid regions where the average annual rainfall ranges from 100 mm to 600 mm (Sadek et al. 2007; Schneider et al. 2012). However, these cover systems were found to be inadequate for humid regions with average annual rainfall more than 1000 mm (Ng et al. 2015; Zhang and Sun 2014). Previous literature (Abdolahzadeh et al. 2011; Bonaparte et al. 2002) advocates hydraulic barrier multi-layered cover system (MLCS) for humid sites. It is reviewed that the MLCS are susceptible to various factors affecting its long-term hydraulic performance. Some of the primary factors are climatic conditions, plant species, topographic features and ecological system of the site (Qian et al. 2010). Various design parameters of different cover have been studied to explore the appropriate cover materials and configurations (Daniel et al. 2002; Reddy et al. 2010). Several research demonstrated the significance of the study on unsaturated flow conditions, water balance and hydrological processes within

the MLCS (Bohnhoff et al. 2009; Ogorzalek et al. 2008). Several water infiltration tests of MLCS column were previously performed to investigate hydraulic barrier efficiency of MLCS under controlled conditions (McCartney and Zornberg 2010; Rahardjo et al. 2012). Field studies on various configurations of the MLCS under different weather conditions were also conducted in last few decades (Albright et al. 2012; Apiwantragoon et al. 2015; Ng et al. 2019a). Moreover, experimental results of MLCS were compared with its numerical simulations to investigate its long-term performance efficiency (Aljaradin and Persson 2015; Li et al. 2013; Schnabel et al. 2005). The previous studies (Daniel et al. 2002; Luellen and Brydges 2005; Sinnathamby et al. 2014) also reveal that the cover system must be capable of surviving extreme conditions as well as accommodating changes in the properties of component materials due to degradation caused by various climate adversities.

No studies exist for catastrophic scenarios of flood wherein the cover system was inundated by water for an extended period. This is essential in view of recent cases of extreme meteorological events occurring due to climate change (Kundzewicz et al. 2013). Such situations are evidently seen in northeast India where there is the overflow of the Brahmaputra river, resulting in constant ponding condition in some areas for a few months (Dhar and Nandargi 2000). Very recently, other western states of India, Kerala, and Maharashtra, have also experienced constant water ponding due to heavy rainfall for hours (Francis and Gadgil 2006). Based on the literature reviewed, it is noted that there are not many studies that deals with the hydraulic performance assessment of MLCS for high humid high rainfall weather conditions (Ng et al. 2016 and 2019a). This is specifically true for the tropical weather conditions of Indian subcontinent wherein the average annual rainfall is found to be around 2500 mm. There are no studies in the literature to advance the understanding long-term climate change impact on the hydraulic performance of MLCS. Hence, it is not feasible to prepare site specific design techniques for constructing an economic MLCS which can endure hostile weather impacts experienced in Indian subcontinent. In addition to this, investigations are required for exploring the suitability of utilizing the alternate materials like geosynthetic clay liner, fly ash and asphalt concrete in cover system for specific applications.

The objective and scopes of the present research work is outlined for investigating the hydraulic performance of MLCS under high humid, high rainfall conditions, for this purpose, a controlled laboratory investigation was performed for assessing the percolation characteristics of different configurations of MLCS under constant water ponding boundary condition for an extended period of 900 days. This was followed by constructing and

monitoring a pilot field scale MLCS subjected to high rainfall condition of north-east India for a period of 800 days. Numerical simulations were performed for both laboratory and field MLCS to gain confidence on the appropriateness of input water retention characteristics and boundary conditions. Based on this understanding, the climate change impact on MLCS was performed for a duration of 87 years with and without considering material performance deterioration. The main purpose of this study is to aid in the development of best possible configuration of MLCS using locally available soil, coal combustion residue (in combination with soils) at less cost. It is believed that the proposed research can become a reference guideline for constructing MLCS in a high humid, high rainfall location like Indian subcontinent.

1.2 Motivation for the study

In most developing countries, there is an urgent necessity to develop site-specific design guidelines for constructing multi-layered cover system (MLCS) over the near surface disposal facility after its full capacity. This requires clear understanding about numerous governing factors, which plays very significant role in MLCS design and its performance. The long-term hydraulic performance assessment of MLCS becomes a necessity for tropical weather where there is continuous short-term cycles of drying and wetting. The fatigue stress induced in soils and its effect on overall hydraulic performance of MLCS need to be understood in detail. Since the expected design life of MLCS is more than 100 years, it is invariably necessary to understand the climate change impact on the performance of MLCS. Such needs have motivated this research work to cater to the requirement of MLCS to be constructed over NSDFs in high humid, high rainfall regions.

1.3 Outline of the thesis

The thesis is organized in eight chapters as follows.

- **Chapter 1** gives a general overview of the thesis, motivation behind this research work and its importance.
- **Chapter 2** reviews the literature comprehensively on the background research and identifies the gap areas. The objective and scope of the study are also listed in this chapter.
- **Chapter 3** deals with basic characterization of soil materials, the details of the methodologies, and the theoretical concepts adopted in this study to meet the research objectives.

➢ **Chapter 4** describes the performance evaluation of the water content sensors (profile probe and 5TM), and summarizes the soil specific calibration parameters which were used for further measurements.

➢ **Chapter 5** demonstrates the controlled laboratory evaluation of four different configurations of MLCS columns under constant water ponding. In the chapter, these test results were also compared with simulated results from the numerical analyses by considering three different sets of soil hydraulic parameters.

➢ **Chapter 6** discusses the results of the field test of a trial MLCS constructed in the field and exposed to natural weather condition for 800 days spanning from May 2016 to July 2018. Based on five different sets of time variable boundary conditions and three different sets of hydraulic properties, numerical simulations were carried out in the chapter for comparing with the field observations.

➢ **Chapter 7** explains the climate change impact assessment of water percolation characteristics of MLCS. The futuristic climate parameters of 87 years forecasted by statistical down scaling model (SDSM) technique, were utilized in the chapter for assigning time variable boundary condition in numerical analyses.

➢ **Chapter 8** finally, lists conclusions of the study. The limitations and future work of the study is also presented in the chapter.

Chapter 2
Literature Review

2.1 General

Multi-layered cover system (MLCS) are provided over waste containment facility after it reaches its full capacity. This chapter provides a comprehensive review of different types of cover systems with varying configuration reported in the literature. A review of laboratory column studies is presented to understand its role in evaluating long-term hydraulic performance of different MLCS. In continuation, several case studies on the pilot cover systems under different climatic conditions have been reviewed. Numerical modeling plays a significant role in studying the long-term performance of MLCS. A detailed review of various numerical tools (software codes) used for evaluating performance of MLCS is presented. Finally, a critical appraisal was presented to summarize the research gaps in the existing literature followed by the objective and scopes of the present research.

2.2 Classification of landfill cover system

The primary design aspect of the cover system is to minimize water infiltration into underlying waste (USEPA 1989a). The cover system is composed of different individual layers, which function to fulfill the specific purpose (Hauser et al. 2001). The environmental protection agency, United States of America (USEPA) (Landreth et al. 1991; USEPA 1989b) recommended design criteria for a general cover system for near surface hazardous landfill. Resource conservation and recovery act (RCRA) is a regulatory document that acts as guideline for design of various covers (Barnswell and Dwyer 2011; Khire et al. 2000; McGuire et al. 2009). The RCRA initially defined conventional cover systems for solid waste and hazardous waste landfills. Further, few emerging alternate cover configurations namely evapotranspiration, anisotropic and capillary barrier covers have been explored by department of energy, United States of America (USDOE 2000). Various cover systems are briefly discussed in this section.

Multi-layered covers (RCRA subtitle C) are commonly implemented for hazardous landfills (Landreth et al. 1991) with its configurations shown in Fig. 2.1A. Design of each individual layer is done based on site and project specific conditions**.** Compacted clay layer (CCL) are generally used as hydraulic barriers in these cover systems (USEPA 1989b). However, it is vulnerable to environmental influences such as desiccation cracking, freeze

thaw cycles, rainfall infiltration, etc. Hence, a buffer layer is provided on the surface to protect the clay layer, as shown in Fig. 2.1B (Landreth and Carson 1991). Basic covers (RCRA subtitle D) are generally used in non-hazardous landfills (Morris and Stormont 1997). The performance of these cover systems essentially depend on the permeability of the compacted clay layer (Hauser et al. 2001).

In recent years, the use of capillary barrier covers in arid to semi-arid climatic regions is gaining popularity due to its improved performance (Harnas et al. 2014; Tami et al. 2003). These covers consist of a coarser layer underlying a finer layer as shown in Fig. 2.2A. Due to difference in pore size distribution and capillary suction forces, such configuration creates a capillary tension in upper layer, which results in temporary water storage in upper fine layer (Stormont and Anderson 1999). This stored water can ultimately be removed by evaporation, transpiration, and lateral drainage to minimize percolation (Stormont and Morris 1999). Such barriers are effective when combined effect of transpiration, evaporation, and lateral drainage are higher than the precipitation (Qian et al. 2010). Evapotranspiration (ET) cover consists of a vegetated soil layer that limits deep drainage by storing water until it is removed by ET (Jacobson et al. 2005; Mccartney and Zornberg 2002; Scanlon et al. 2005b; Zornberg et al. 2003), as shown in Fig. 2.2B. Surface soil in such covers is selected to have high water storage capacity to limit deep percolation during seasons of high precipitation (Forman and Anderson 2005; Hauser et al. 2005; Madalinski et al. 2003). ET cover performance also depends on type of vegetation as plant roots remove water through transpiration (Nyhan 2005; Rock et al. 2012; Schneider et al. 2012; Zhang and Sun 2014; Zhang et al. 2017).

Anisotropic covers are modified form of capillary barrier covers, which are designed to promote lateral drainage of water while avoiding deep percolation (Parent and Cabral 2006). In such systems, there is a wide variation of soil properties and compaction state in each layer. This results in development of different capillary forces in each layer enhancing lateral drainage (Abdolahzadeh et al. 2011). A typical anisotropic cover is depicted in Fig. 2.3A. Geosynthetic clay liner **(**GCL) covers are similar to conventional multi-layer covers, as shown in Fig. 2.3B. Only difference is the use of GCL in place of CCL or along with CCL (Park and Fleming 2006; Zornberg et al. 2010). GCL is a factory-made product that comes in rolls of bentonite sandwiched geotextiles or bentonite adhesively bonded with geo-membrane (GMB). Use of GCL as the sole barrier or as a composite with geomembrane (GMB) is rapidly gaining acceptance (Benson et al. 2010; Bouazza et al. 2002; Christopher 1991; Sun et al. 2010).

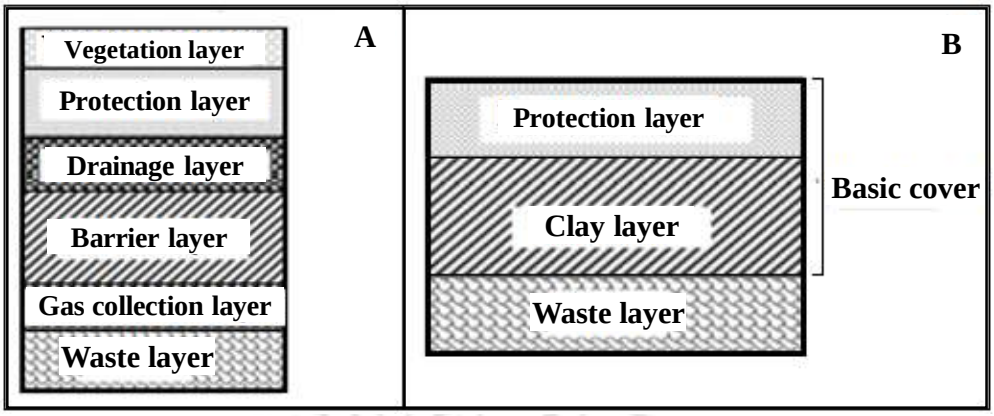

Fig. 2.1 (A) RCRA subtitle C cover and (B) RCRA subtitle D cover (USEPA 1989b)

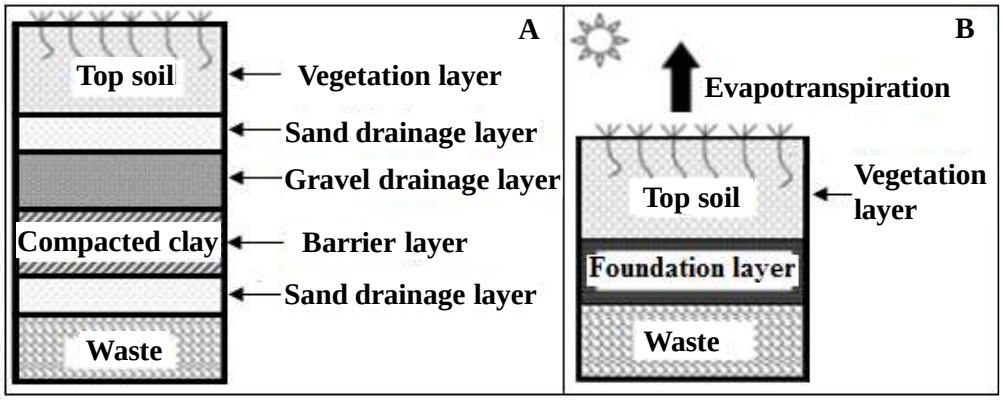

Fig. 2.2 (A) Capillary barrier cover and (B) Evapotranspiration cover (USDOE 2000)

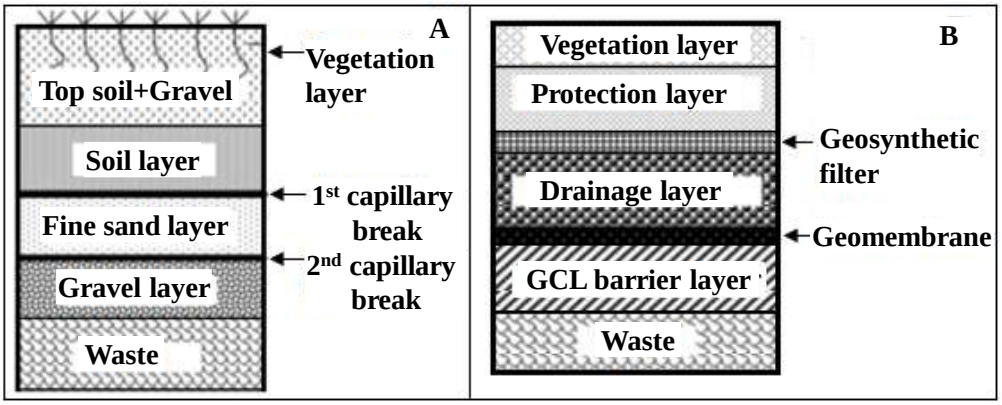

Fig. 2.3 (A) Anisotropic barrier cover and (B) GCL cover (USEPA 1989a)

The conductive barrier cover shown in Fig. 2.4 A, employs the capillary barrier phenomenon to divert water away from the waste (Khire et al. 1999; Morris and Stormont 1998; Stormont 1996). The conductive layer consists of a highly permeable material, such as coarse gravel, underlying a fine-grained material. Because of the differences in saturated

hydraulic conductivity between the two layers (ideally about a factor of 1000), a capillary break is formed at the interface of the two layers (Kampf and Montenegro 1997). Water is diverted laterally in the finer textured soil above the layer interface when it is at a negative capillary tension (Zhan et al. 2014). Under these conditions, the barrier prevents liquid from crossing the capillary break. The barrier will continue to operate as long as the overlying low-permeability zone does not saturate (Ogorzalek et al. 2008). Upon saturation, efficiency of this barrier is reduced (Li et al. 2013).

Vegetated soil cover presented in Fig. 2.4 B, plays a vital role in the management of water through protection of the surface layer against erosion through removal of soil moisture by plant transpiration (MacDonald et al. 2008; Salt et al. 2006). If the design is based on an optimum combination of soil type, soil depth, surface slope and vegetation species, then storage and removal of soil moisture is maximized by plant transpiration and evaporation (Song et al. 2017). All NSDFs that use a soil cover, as a part of final closure system, can be benefitted from use of a well-designed vegetation cover (Khapre et al. 2017; Lamb et al. 2014). In humid environments, evapotranspiration may remove up to 80% of water infiltrated into cover soil (Smirnova et al. 2011). In arid and semi-arid environments, vegetation cover may remove 100% of infiltrated moisture from cap soils (Abichou et al. 2012). Thus, vegetation cover is highly effective means of managing soil moisture in a repository closure cap, particularly if care is taken in selecting plant species and vegetation procedure (Ng et al. 2019a; b; Yuen et al. 2010). Table 2.1 summarizes the different types of cover system and also presents the cover specific climate suitability, working mechanism and special material utilization.

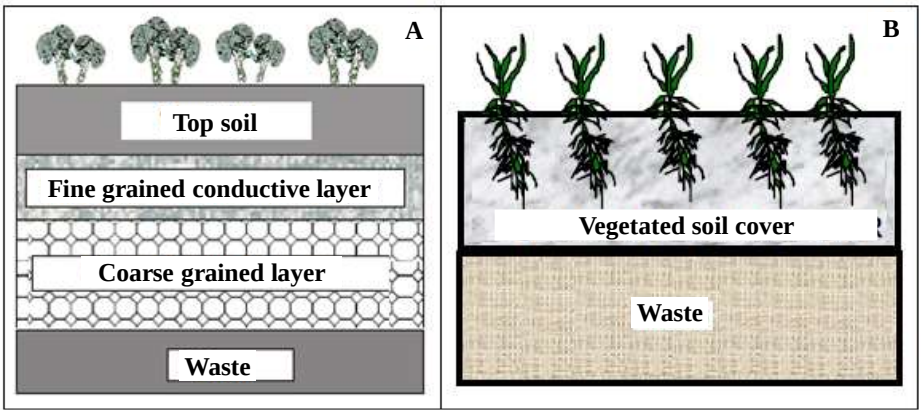

Fig. 2.4 (A) Conductive barrier cover and (B) vegetated soil cover (IAEA 2001)

Table 2.1 Different types of cover system for landfill application

Type of cover system	No. of layer	Suitable climate				Capillary break	Vegetation growth	Lateral drainage	Use of GCL/GMB	Reference
		Arid	Semi arid	Humid	High humid					
RCRA subtitle C (Multi-layered)	4	X	X	✓	✓	Optional	Required	Required	Optional	USEPA 1989b; Landreth et al. 1991; Landreth and Carson 1991
RCRA subtitle D (Basic)	1	✓	✓	X	X	Optional	Optional	Optional	Not used	Morris and Stormont 1997; Hauser et al. 2001
Capillary barrier	2	X	✓	✓	X	Required	Optional	Optional	Not used	Harnas et al. 2014; Tami et al. 2003; Stormont and Anderson 1999; Stormont and Morris 1999
Evapotranspiration	1	X	✓	✓	X	Optional	Required	Not used	Not used	Jacobson et al. 2005; Mccartney and Zornberg 2002; Scanlon et al. 2005b; Zornberg et al. 2003
Anisotropic barrier	3	X	✓	✓	✓	Required	Optional	Optional	Not used	Forman and Anderson 2005; Hauser et al. 2005; Madalinski et al. 2003
GCL barrier	3	X	X	✓	✓	Optional	Optional	Optional	Required	Benson et al. 2010; Bouazza et al. 2002; Christopher 1991; Sun et al. 2010; Park and Fleming 2006; Zornberg et al. 2010
Conductive barrier	2	X	✓	✓	X	Required	Optional	Optional	Not used	Khire et al. 1999; Morris and Stormont 1998; Stormont 1996; Qian et al. 2010
Vegetated barrier	1	X	✓	✓	X	Optional	Required	Not used	Not used	MacDonald et al. 2008; Salt et al. 2006; Khapre et al. 2017; Lamb et al. 2014; Yuen et al. 2010

Notes: RCRA = Resource conservation and recovery act, GCL = geosynthetic clay liner, GMB = Geomembranes

2.3 Configuration and materials for various component layer

Landfill cover system is more often expected to last for hundreds of years or longer (ITRC 2003; Morris 1990; Richardson and Waugh 1996). It is primarily designed as an integral component of a larger dynamic ecosystem (USEPA 1989a; b). Inevitable changes in physical and biological conditions must be understood to ensure long-term performance efficiency of the cover system (Landreth et al. 1991). There are several factors for setting an effective configuration of each component layer in cover system. Hence, it is made of multiple component layers namely (i) surface layer, (ii) protection layer, (iii) drainage layer, (iv) barrier layer, (v) gas collection layer, and (vi) foundation layer (Koerner and Daniel 1997). An effort has been made in the following sub-sections to review various configurations and materials of each cover layer. Table 2.2 summarizes layer specific configurations and materials of the MLCS.

2.3.1 Surface layer

The minimum thickness of surface layer is established based on consideration of the rooting depth of any surface vegetation, anticipated erosion rate, and construction tolerances (Øygarden et al. 1997). For shallow-rooted plants such as certain grasses, a 150 mm thick layer of soil usually provides adequate rooting depth (Zhan et al. 2007). Thus, the minimum thickness of a vegetated surface layer is generally 150 mm (USEPA 1989b). If plants with deeper roots are planted, the thickness of the topsoil should be increased to accommodate the root growth. In some cases (ITRC 2003), the combined layer of the surface layer and protection layer are referred as cover soil. This has a typical minimum thickness of 450 to 600 mm for cover systems with hydraulic barriers considering the plant rooting depth. For cover systems with evapotranspiration or capillary barriers, Landreth et al. (1991) recommends a minimum cover soil thickness of 900 mm or greater. In United States of America, most landfill cover system top decks are designed to have an inclination in the range of 2 to 5%, after accounting for settlement, to promote surface runoff (Landreth et al. 1991; Maqsoud et al. 2011; Nyhan et al. 1997). Based on these literature slopes flatter than 2% may cause water to inpound on the surface, if localized settlements occur, and are usually avoided. Excessive erosion or slope instability increases as the cover system inclination increases (Morris and Stormont 1998). The most common material used to construct the surface layer is locally available topsoil. It is important that topsoil contain adequate organic matter and plant nutrients. An increasingly common practice is to amend topsoil with organic matter. The organic matter in these materials helps to promote growth

of vegetation. Erosion-resistant materials such as soil-gravel mixtures, gravel, riprap, geo-synthetic erosion control materials, may be utilized to help in reducing erosion. In addition to these, the use of asphalt concrete, articulated block systems, construction and demolition wastes, and lightweight manufactured aggregates can be used.

2.3.2 Protection layer

As previously mentioned the thicknesses of cover soils (surface layer plus protection layer) are often in the range of 450 to 600 mm, although thicknesses greater than 1 m are sometimes necessary to meet other design requirements. The protection layer may need to be still thicker if both vegetative support and protection from bio-intrusion are required (USEPA 1989b). The typical thickness of a bio-intrusion-resistant cobble layer is about 500 to 1000 mm (Bonaparte et al. 2002). The provision of side slope for protection layer is avoided as it effects moisture storage layer to support the healthy growth of plant roots (Sayer et al. 2005; Smirnova et al. 2011). However, for lateral drainage purpose it is sloped just as much as the overlying surface layer where no plant growth is intended. The protection layer is usually constructed from locally available soil. According to Bonaparte et al. (2002), medium-textured soils, such as loams, have the best overall characteristics for seed germination and the development of plant root systems. Fine-textured soils, such as silts and clays, have excellent water-holding capability, which provides roots with water for plant growth but limits the transport of oxygen to plant roots. In addition, fine-textured soils are vulnerable to cracking when desiccated. If the primary role of the protection layer is to prevent bio-intrusion, cobbles, asphaltic concrete, recycled concrete pavement, or similar materials needs to be provided (Koerner and Daniel 1997).

2.3.3 Drainage layer

The recommended minimum thickness of a granular drainage layer is usually 30 cm (Bonaparte et al. 2002; USEPA 1989b). This allows sufficient thickness for ease of construction and to avoid damage to underlying geosynthetics, such as a geomembrane (you have not changed the symbol GMB). It is possible to construct thinner granular drainage layer of thickness of about 15 cm or less, but granular drainage layers thinner than 30 cm are not very common (Palmeira and Silva 2007). To prevent clogging of internal drainage layers, it is often necessary to install a filter layer directly over granular materials (Rowe 2005). It is very essential for a drainage layer to provide an effective side slope to ease and promote the lateral movement of the infiltrated water toward the outside of cover

system (Daniel et al. 1993b). As the case, a side slope of more than 2% is supposed to be appropriate (USEPA 1989b). Based on previous literature (Koerner and Daniel 1997), both granular materials (typically sand or gravel), Geotextile (GTX), Geonet (GN), and Geocomposite (GC) are generally used as drainage layer material in cover systems. The granular material used should have adequate hydraulic conductivity for laterally draining out the permeated water to minimize the buildup of hydraulic head above the hydraulic barrier. Moreover, in case of filter layer adequate hydraulic transmissivity is required to convey the design flow rate.

2.3.4 Hydraulic barrier layer

Materials used for hydraulic barriers include GMBs, GCLs, and CCLs. Choices in the composite category typically are GMB/GCL, GMB/CCL, or GM/GCL/CCL. A cover system with a composite barrier allows less percolation than a cover system with only GMB, GCL, or CCL barrier alone. Each type of barrier has advantages and disadvantages. No single type is optimal for all cover systems. The thickness of a GMB used in a cover system is selected based upon several factors, the most important of which is durability (Brachman and Gudina 2008). The GMBs should be adequately thick to resist construction damage and puncture. The minimum recommended thickness for this purpose is 0.75 mm (Brachman and Sabir 2010). The GCLs are manufactured with a nominal clay thickness of 5 mm. Like GMBs, GCLs are thin and may potentially be punctured during installation. Unlike GMBs, however, GCLs possess significant self-sealing capability due to the swelling of dry bentonite upon hydration or the plastic flow of hydrated bentonite (Rowe 2012, 2014). Several studies (Daniel et al. 1993a; James et al. 1997) investigated the advantages and disadvantages of GCLs as the landfill cover material. The CCLs offer the advantage over GMBs and GCLs. The CCLs are constructed in layers called lifts that typically have a thickness before compaction (loose lift) of 20 to 25 cm and a thickness after compaction (compacted lift) of not more than 15 cm (Gross 2003; ITRC 2003). Typically, three to six lifts are used to produce a CCL hydraulic barrier with a final thickness of 45 to 90 cm. A minimum of three compacted lifts is recommended. If the CCL hydraulic barrier is not overlain by a GMB, four of more compacted lifts is preferred (USEPA 1989a; b). Historically, CCLs have been the most frequently used cover system barrier material. Previous literature (Bonaparte et al. 2002; Caldwell and Reith 1993; Daniel and Wu 1993) explored the potentials of CCLs to be used as landfill cover materials.

Table 2.2 Configurations of various layers of landfill cover systems

Cover layer	Thickness (cm)	Slope (%)	Required soil properties	Component materials	Main functions	Deterioration associated	Literature reviewed
Surface layer	15 – 90	2 – 10	$10^{-8} \leq k_s \leq 10^{-3}$	native soil, soil-gravel mix, gravel, riprap, asphalt concrete, debris, etc.	(1) supports vegetation growth, (2) maximizes evapotranspiration, (3) facilitates surface runoff	erosion, corrosion, desiccation, freeze-thaw cycles, wet-dry cycles, bio intrusion, etc.	USEPA 1989; Landreth et al. 1991; Bonaparte et al 2002; Zhan et al. 2007; Maqsoud et al. 2011
Protection layer	45 – 100	2 – 5	$10^{-8} \leq k_s \leq 10^{-5}$	local soil, fine-medium textured soil, cobbles, asphalt concrete, recycled concrete	(1) prevents desiccation, root penetration, Bio-intrusion, (2) stores meteoric water, (3) protects underlying layers etc.	corrosion, desiccation, freeze-thaw cycles, wet-dry cycles, bio intrusion, etc.	USEPA 1989; ITRC 2003; Koerner and Daniel 1997; USDOE 2000 Bonaparte et al. 2002; Sayer et al. 2005; Smirnova et al. 2011
Drainage layer	15 – 30	2 – 5	$k_s \geq 10^{-5}$	sand, gravel, Geo-net,	reduces pore water pressure on the underlying barrier layer by draining out liquid laterally	root penetration, invasion of fines, clogging	Daniel et al. 1993a and b; Rowe 2005; Palmeira and Silva 2007
Hydraulic barrier layer	30 – 90 cm for CCL, 5 – 10 mm for GCL, 0.5 – 2 mm for GMB,	2 – 5	$k_s \leq 10^{-9}$	CCL: Local soil/ sand + bentonite/lime/cement (20-30%). GCL: Adhesively bonded, Switch bonded, Needle punched type GMB: LLDPE, HDPE, etc.	(1) prevent percolation of water into the underlying waste, (2) Deter the migration of landfill gas into the environment	freeze/thaw, desiccation, wet dry cycle,	Caldwell and Reith 1993; Gross 2003 James et al. 1997; Brachman and Sabir 2010
Gas collection layer	30 – 45	_	$k_s \geq 10^{-4}$	coarse sand, highly permeable soil	reduces the potential pressure within the landfill by collecting gases.	clogging	Koerner et al. 1998; Daniel and Wu 1993
Foundation layer	≥ 30	_	$10^{-8} \leq k_s \leq 10^{-5}$	locally available soil	provides a firm subgrade for placement of overlying layers	differential settlement	Jesionek and Dunn 1995; Bonaparte et al. 2002

Notes: k_s = saturated hydraulic conductivity (m/s), CCL = compacted clay liner, GCL = geosynthetic clay liner, GMB = Geomembranes, LLDPE = linear low-density polyethylene, HDPE = high density polyethylene

2.3.5 Gas collection layer

A minimum thickness for a granular gas collection layer is usually recommended as 30 cm. A geotextile filter layer may be required between the gas collection layer and CCL to prevent excessive clogging. Like drainage layers, gas collection layers may be constructed of granular materials or geosynthetics. The material used should have adequate gas transmissivity to minimize the built up of gas pressures beneath the barrier and to convey the design gas flow rate. Granular gas collection materials are normally composed of relatively clean sand or gravel. When a granular material is used, a separation (typically a GTX) may be needed between the granular material and the overlying barrier (Koerner 1998).

2.3.6 Foundation layer

The thickness of the foundation layer is selected based on site-specific criteria and proposed end use of the cover system. The minimum thickness of a foundation layer is usually recommended to be 30 cm. When the foundation layer is designed to attenuate the waste differential settlements, it may be several meters thick (Koerner and Daniel 1997; Landreth and Carson 1991). Materials most often used for the foundation layer include locally available soils. Soil used for foundation layer varied from silt to clay loam, with reported hydraulic conductivity ranging from 10^{-9} to 10^{-5} m/s (Landreth et al. 1991). In a few situations, waste material can be used to construct the foundation layer. If constructed of granular material, the foundation layer may also serve as a gas collection layer.

2.4 Post-closure issues of cover system

Cover systems designed for long-term performance need to consider ecological and biological processes that could affect cover system characteristics after installation, including changes in the physical and hydraulic properties of the cover materials over time. Internal and external hydrologic control features, and additional design features need to be incorporated into MLCS to limit infiltration; withstand surface erosion; deter plant root penetration, animal intrusion (bio-intrusion); minimize clogging of drainage layer due to invasion of fine-grained materials; and minimize damage due to frost (freeze/thaw) and desiccation. Table 2.3 summarizes important post closure issues associated with cover system. The following subsection reviews a few of these issues which are very crucial for cover design consideration.

2.4.1 Steep waste slope and cover erosion

Occasionally, in the closure of landfills, it is necessary to address the issue of steep existing waste slopes. One option is to cut the slope back to a shallower grade by excavation and then relocate the excavated waste either on-site or off-site at another landfill. The advantage of this approach is that it increases the stability of the waste mass and results in a final slope inclination within the conventional range for cover systems. Disadvantages associated with waste excavation and relocation include construction-related instability, health and safety concerns associated with exposing the waste, leachate generation, nuisance (e.g., odor) and cost. Several alternative approaches exist for constructing cover systems over steep waste slopes without need for waste excavation, or at least with very limited waste excavation. One of these alternatives include the use of cover system with steep slope. Long-term surface erosion problems should be anticipated when the steep cover slopes are used.

Erosion is one of the most important concern with respect to the surface layer. Excessive erosion can lead to exposure of underlying layers and can cause the cover system to be ineffective. Erosion can be controlled by managing surface-water runoff, minimizing seepage forces within the cover system soils, and selecting a surface layer material that can withstand the anticipated erosive stresses. Swope (1975) studied 24 landfill cover systems in USA and found that 33% had slight erosion, 40% had moderate erosion, and more than 20% had severe erosion. Gross et al. (2002) described several cases of significant cover system erosion, including one for a cover system with 60 m long 3H: 1V side slopes. To prevent ponding of rainwater, the soil surface should be uniformly graded and sloped about 3%. Slopes greater than 5%, likely promote erosion, unless preventive measures are provided (Koerner and Daniel 1997). According to Sherard et al. (1976), the erosion potential of soil is primarily a function of the size of the soil particles, inter-particle cohesive forces, and the velocity of the transporting fluid (air or water). Hence, soil-gravel mixtures or gravel veneers are often considered as a surface layer for cover systems constructed at arid and semi-arid sites (Gray and Sotir 1996). The time of completion of cover system construction can influence the erosion potential (Bonaparte et al. 2002).

2.4.2 Dry-wet cycles and desiccation crack

The potential for dry-wet cycles to affect the integrity of CCLs and GCLs should be considered whenever these materials are used as hydraulic barriers. Cyclic wetting and drying can have a significant impact on the hydraulic conductivity of CCLs. As drying

progresses, shrinkage occurs and reaches a limit at which cracking can occur due to desiccation. It gradually progresses deeper into the CCL until a pathway of water migration becomes available. Previous study (Khire et al. 1997, 1999) has shown that severe desiccation can occur to depths of up to 1 m, and it is recommended that at least 1.2 m of cover soil to be used for protecting the CCL from cracking. The literature has suggested that the key process of desiccation crack formation needs to be understood in assessment of landfill cap performance under anticipated climate change scenario (Sinnathamby et al. 2014). Depending on chemistry of permeating water, GCLs may or may not be vulnerable to permanent damage from desiccation. When permeated with contaminated solution, GCLs are less vulnerable than CCLs to permanent damage from desiccation, because of swelling and self-healing capability of bentonite (Boardman and Daniel 1996; Lin and Benson 2000). It was suggested that the best approach for protection of a CCL or GCL from desiccation is to place a GMB over the barrier, and then cover the GMB with soil.

2.4.3 Freeze thaw cycles and frost penetration

The protection layer is generally designed with the intent of preventing underlying layers from freezing. This is especially a concern in cold climates. The potential for freeze-thaw of hydraulic barrier should be evaluated. As temperatures drop and soil layers within the cover system freeze, water drawn towards the freezing front can cause desiccation, freeze-thaw cracking, and frost heaving (Othman and Benson 1993). Desiccation and frost cracking may cause CCLs located within the frost zone to have increased permeability to water and gas. The CCL hydraulic conductivity increases by one to two orders of magnitude (Othman et al. 1994). The CCLs appear to be vulnerable to damage from freeze-thaw action according to the previous study (Wong and Haug 1991). To avoid damage to CCLs, the protection and overlying surface layers should be thick enough to place CCL below the maximum depth of frost penetration (Benson and Othman 1993). If the barrier is within the zone of frost penetration, then the impact of frost upon the barrier materials should be considered. Frost is generally believed to have no effect on GMBs (Comer et al. 1995). Laboratory data (Hewitt and Daniel 1997) as well as field data (Kraus et al. 1997; Sterpi 2015) suggest that GCLs can withstand multiple cycles of freeze-thaw with little or no adverse effect on its hydraulic conductivity.

Table 2.3 Various post closure issues associated with landfill cover system

Various issues	Cause	Effect	Prevention	Literature reviewed
Erosion	slopes greater than 5%, excessive surface runoff	progressively leads to exposure of underlying layers	using a suitable erosion resisting material for surface layer	Swope 1975; Sherard et al. 1976; Gross et al. 2002
Desiccation cracks	cyclic wetting drying	gradually increases water/gas permeability of CCL/GCL	placing a GMB followed by thick soil mass over the CCL/GCL	Khire et al. 1997, 1999; Lin and Benson 2000
Frost penetration	cyclic freezing thawing	water/gas permeability of CCL/GCL gradually increases	placing a GMB followed by thick soil mass over the CCL/GCL	Sterpi 2015; Othman et al. 1994; Wong and Haug 1991
Bio-intrusion	burrowing by animals like rabbits, rats, mice, fox, etc.	destroys the integrity of underlying components	employing GMB made from HDPE and welded wire mesh	Steiniger 1968; Bonaparte et al. 2002
Root penetration	healthy growth of vegetation with deep roots	increases the hydraulic conductivity of various layers	allowing growth of plants with shallow roots	Suter et al. 1993; Lamb et al. 2014; Ng et al. 2019a and b
Rainwater percolation	heavy and prolonged rainfall	forms harmful leachate by interacting with underlying waste	enhancing lateral drainage and using less permeable material in hydraulic barrier layer	Gross et al. 1997; Othman et al. 2002; Landreth et al. 1991
Clogging	invasion of fine particles from the overlying layers	leads to slope instability by increasing pore water pressure on the underlying barrier layer	installing GTX filter above the drainage layer	Jaisi et al. 2005; Reddy et al. 2008, 2010; Rowe and Yu 2012
Differential settlement	reduction in shear strength due to change in soil fabric	ruins cover integrity by disturbing slope stability	using needle punched GCLs along with less permeable soil of higher strength	LaGatta et al. 1997; Daniel et al. 1993a; Othman et al. 1994
Waste compression	biodegradation of organic component	causes differential settlement	removing organic component	Sharma and Lewis 1994; Daniel et al. 2002
Gas emission	decomposition of organic matter	increases uplift pressure inside the cover system	dumping waste with less organic matter	Bonaparte et al. 2002; Koerner et al. 2002
Degradation	Adverse impact of climate	Deteriorates properties of cover materials	Selecting proper cover materials	Mitchell and Jaber 1990; Hsuan and Koerner 1998

2.4.4 Accidental human and animal intrusion

Accidental human intrusion has generally not been a design consideration for cover systems on most landfills or waste remediation sites. Essentially the type of waste for which accidental human intrusion has been a design consideration is radioactive waste. Human intrusion into Municipal solid waste (MSW) or Hospital Waste (HW) could also be dangerous to the intruder. No amount of thickness can prevent intentional intrusion, such as drilling a boring or digging a deep utility excavation (Bonaparte et al. 2002). For radioactive waste, the protection layer may need to provide cover system with a high level of protection from intrusion by burrowing animals like rabbits, rats, mice, fox, and etc. A GMB may also be viewed as a barrier to burrowing animals. Studies by Steiniger (1968) indicate that animals will not make their way through GMBs such as those made from HDPE and welded wire mesh.

2.4.5 Vegetation growth and root penetration

Vegetated cover soils should be thick enough to accommodate a healthy growth of plant roots and store sufficient water to support plant growth. Plants should generally have relatively shallow roots so that the roots do not penetrate too deep into the cover system because deep penetration threatens the integrity of underlying components. However, the penetration of plant roots below the protection layer is undesirable. The potential mechanisms by which plant roots can damage a cover system are summarized in previous study (Suter et al. 1993): (i) Roots may enter the drainage layer or gas collection layer and cause clogging, (ii) Roots may penetrate the hydraulic barrier, causing an increase in hydraulic conductivity, (iii) Decomposing roots leave channels for movement of water and vapors, (iv) Roots may desiccate CCLs, causing shrinking and cracking, (v) Uprooted trees may lead to soil erosion and leave depressions in the cover system, (vi) Roots may enter the wastes, take up constituent chemicals, and transport them to surface.

2.4.6 Water storage and percolation

For cover systems with a vegetated surface layer, it is critical that the cover soils be capable of retaining sufficient moisture to support plant growth. The greater the percentage of fines in a soil the greater the water retention after gravity drainage. Though plastic clays have a high field capacity, they are typically not used for the protection layer because they can desiccate and crack, providing preferential pathways for infiltrating water to bypass the clay matrix and thereby bypass storage. A soil's available water storage capacity depends

on its texture and density (Daniel et al. 1993a). Selection of hydraulic barrier depends on the allowable rate of water percolation through cover system. It is recommended that the percolation objective for the cover system be defined, at least qualitatively, prior to design. For example, if the cover system is for a MSW landfill, the design maximum percolation might be in the range of 0.1 to 1.0 mm/year (Koerner and Daniel 1997). GMB/GCL or GMB/CCL composite barriers have a representative efficiency of 99.9%, where efficiency is defined as the percentage of lateral drainage that flows from drainage layer rather than percolates through barrier layer (Gross et al. 1997; Othman et al. 2002).

2.4.7 Clogging of drainage layer

Drainage layer is included above hydraulic barrier layer to promote lateral drainage and prevent the buildup of hydraulic head in the cover system. The main issues with drainage layer design are related to flow capacity, transitions and outlets, and filtration. The drainage layer should be designed to have adequate flow capacity and to provide free-flow of water through proper transitions and outlets. In the absence of this, cover soils can become saturated, leading to increased erosion, high seepage forces, leading to an increased potential for slope instability. Previous research (Jaisi et al. 2005; Reddy et al. 2008, 2010; Yu and Rowe 2012) advocates the need for a goetextile filter above the drainage layer to minimize clogging of drainage layer due to fine-grained materials.

2.4.8 Prompt placement and intimate contact of geomembrane

Koerner (1998) suggested that the GMB should be placed over the CCL as soon as possible after the final lift of CCL is constructed to protect it from desiccation, freezing, and other stressors. Bowders et al. (1997) showed that the exposed GMB component can heat and cause desiccation of underlying clay soils over a period of a few weeks. Desiccation occurred more rapidly with black surfaced GMBs than with white-surfaced GMBs since the latter reflect radiant heat (Koerner and Koerner 1995). Regarding intimate contact of a GMB with an underlying CCL, surface of the CCL should be smooth rolled with a steel-drummed roller before the GMB is placed. Wrinkles form in the GMB after initial placement and subsequent heating during the day. Wrinkles are more pronounced in the stiffer and thicker GMBs (e.g. HDPE) (Koerner 1998). To reduce wrinkle formation, white-surfaced GMBs may be considered. On long side slopes, it may be preferable to use textured GMB rather than smooth GMB to decrease the size of GMB wrinkles. Giroud (1994) has shown analytically that GMB wrinkles are shorter and spaced closer together

when the shear strength between the GMB and the underlying material is increased. Therefore, based on the analysis, use of textured GMB decreases the potential for large wrinkle formation.

2.4.9 Shear strength and differential settlement

The impact of differential settlement on the hydraulic conductivity of GCLs overlain by a 0.6-m thick layer of pea gravel was evaluated by (LaGatta et al. 1997). The results of their evaluation indicate that intact and overlapped samples of needle punched GCLs can withstand angular distortions of 0.35 to 0.6, equivalent to tensile strains of 5 to 16%, while maintaining a saturated hydraulic conductivity of 1×10^{-9} m/s or less. Several factors may affect long-term shear strength properties of the cover system materials and interfaces. Researchers (Daniel et al. 1993a; Othman et al. 1994) have shown that many CCLs undergo significant change in soil fabric and reduction in shear strength because of freeze-thaw cycles. In addition, both heating and cooling result in soil moisture migration, which can cause changes in shear strength of layer material and interface.

2.4.10 Foul gas emission and radiation

The management to collect or control the landfill gas produced beneath the cover systems, is very important while designing a cover system. In case of a MSW landfill, it is required to prevent the emission of foul gas which is of concern to human health and environment. Subsurface gas migration may also lead to adverse groundwater quality impacts due to diffusion of volatile constituents from the gas phase to groundwater. Moreover, uncontrolled gas may produce uplift pressure which causes GMB bubbles displacing the cover soil. GMBs are generally the best barriers to gas. GCLs and CCLs also make very good gas barriers when they are at high degrees of saturation The need for a GTX filter between the gas collection layer and overlying hydraulic barrier should be evaluated (Bonaparte et al. 2002). Some radioactive wastes emit radon-222 ($^{222}R_n$) in the form of a heavier-than-air gas. Inhalation of radon gas at sufficient concentrations is a human health hazard. To attenuate the release of radon to the environment, the cover system may need to incorporate a radon gas barrier. Koerner et al. (2002) described that GMBs can also be used as barriers to radon gas release.

2.4.11 Compressibility of waste

The potential for waste settlement is highly dependent on the type of waste. Relative to most other wastes, MSW is highly compressible, due to its initial compressibility and the additional compressibility induced by the biodegradation of its organic component (Sharma and Lewis 1994). Materials such as mine waste, ash and slag, construction and demolition waste, and soil waste have relatively lower settlement potential (Holtz et al. 1981). The closure of landfill containing compressible waste is a challenging design issue due to its low bearing capacity. If the undrained shear strength of the near surface waste is less than 15 to 20 kPa, the waste may not be able to support a conventional cover system and the bearing capacity of the waste will be an important consideration in the design process (Daniel et al. 2002). Geosynthetic or GTX or geogrid reinforcement materials can be used to support cover systems over the waste.

2.4.12 Material degradation

Anticipated lifetime of barrier material should be considered in relation to required design lifetime of the cover system. For CCLs, the anticipated service life is difficult to assess due to the complex soil-water interaction. Clearly, the soil particles of a CCL will last for geologic time. If a CCL is protected from freeze-thaw and other environmental effects, and not subjected to excessive differential settlements, its anticipated service life is indefinitely long (Mitchell and Jaber 1990). The lifetime of a CCL is clearly material and site specific. Little information currently exists on the service life of GCLs. In absence of external degradation mechanisms, the service life of bentonite is indefinitely long. However, long-term bentonite degradation is a concern if there is potential for cation exchange. In addition, both durability and chemical compatibility are issues with respect to the reinforcing fibers or yarns of GCLs placed on side slopes (Koerner 1998). The service life of any GMB component of the cover system is dependent on how well the material is protected. The primary mechanism of degradation of a GMB hydraulic barrier in a cover system is oxidation of the polymers causing brittleness over a long time. The literature (Hsuan and Koerner 1998) indicate that the service life of commercially available high-density polyethylene (HDPE) GMBs is several hundred years.

2.5 Requirements of conceptual design criteria

Gross et al. (2002) present the results of a survey conducted for USEPA on problems and lessons learned at representative landfill facilities located throughout the

USA. The survey identified 69 modern landfill facilities that had experienced 80 liner or cover system problems. Almost 30% of the problems identified in the study involved landfill cover systems. The primary factor contributing to the cover system problem in most cases was inadequate design. The critical first steps in designing a landfill cover system involve: (i) developing the criteria that will be used to guide the design, (ii) preparing a conceptual design using these criteria, (iii) identifying data gaps based on the conceptual design and (iv) performing predesign studies to generate the data needed to prepare the detailed design, construction plans and specifications.

2.5.1 Elements of design

Based on previous literature (Bonaparte et al. 2002) there are few important questions that typically need to be addressed when considering the design of multi-layered cover system include: (1) What materials are available to construct each individual layer? (2) What thickness of each component layer material is needed? (3) What maximum slope inclination can be used with the surface layer material while providing acceptable erosion rates? (4) For vegetated cover systems, what plant species should be established? (5) How should surface-water runoff be managed? (6) What minimum slope inclination is required to promote runoff after accounting for settlement? (7) What temporary and permanent erosion control measures should be used? (8) What are the maximum design flow rate and allowable flow rate in the drainage layer? (9) How should drainage layer transitions and outlets be designed? (10) What is the expected performance of the hydraulic barrier in terms of quantity of water percolation through the layer? (11) What is the expected performance of the hydraulic barrier in terms of prevention of gas release to the atmosphere? (12) How much differential settlement is expected, what level of tensile strain will this create in the hydraulic barrier, and how is the barrier expected to perform under this stressor? (13) What is the likelihood that the hydraulic barrier will be subjected to wet-dry cycles and how is the barrier expected to perform under this stressor? (14) What is the likelihood that the hydraulic barrier will be subjected to freeze-thaw cycles and how is the barrier expected to perform under this stressor? (15) What hydraulic barrier properties are required to provide the required shear strength? (16) What is the likelihood that the hydraulic barrier will be subjected to bio-intrusion and how is the barrier expected to perform under this stressor? (17) What is the anticipated lifetime of the barrier material(s)? (18) How should gas collection layer transitions and outlets be designed? (19) How should the individual component layer be constructed? (20) What type and frequency of maintenance should be

employed for a particular layer if required? And (21) What type and frequency of monitoring should be employed for a particular layer if required?

2.5.2 Regulatory requirement

It needs to understand the regulatory closure requirements for different types of landfill to govern the environmental remediation for safe and healthy existence of the human beings on this earth. Some of the important regulations applicable to cover systems in United States of America, which has been followed all over the world for past few decades, are briefly reviewed in this section. The RCRA (Resource Conservation and Recovery Act) was primarily established to prevent future contamination that could result from solid waste landfills and to take a more prescriptive approach in its rule. According to RCRA Subtitle D and Subtitle C, cover system must be designed and constructed to (i) have a permeability less than or equal to the permeability of any bottom liner system or natural sub-soils present, or a permeability not greater than 1×10^{-7}cm/sec, whichever is less, (ii) minimize infiltration through the closed MSW by the use of an infiltration layer that contains a minimum 18-inches of earthen material, (iii) minimize erosion of the final cover by the use of an erosion layer of at least 6-inches thickness of earthen material that is capable of sustaining native plant growth, (iv) promote drainage and minimize erosion or abrasion of the cover and (v) accommodate settling and subsidence so that the cover's integrity is maintained.

The CERCLA (Comprehensive Environmental Response, Compensation and Liability Act) is of primary importance when considering environmental remediation and waste isolation. USEPA has managed the Superfund Program for the past 24 years since CERCLA was enacted in 1980. The USEPA defines institutional or legal controls that minimize the potential for human exposure to contamination by limiting land or resource use (Gross 2003). CERCLA establishes several key requirements with regard to the implementation of institutional controls for managing residual contaminants. CERCLA stresses the importance of permanent remedies and treatment technologies in cleaning up hazardous waste sites for removal of contaminants.

2.5.3 Climatic criteria

Climate significantly affects design and performance of cover system. Further, climatic factors greatly affect the types of vegetation that grows on a cover system. Previous researchers (Benson and Khire 1995; Bohnhoff et al. 2009; Zhan et al. 2014) studied the climatic criteria to be considered in the design of a cover system, which include the amount

and seasonal distribution of precipitation (Sinnathamby et al. 2014), duration of specific storm events, intensity of specific storm events, seasonal temperature variations and extremes, depth of frost penetration, quantity of snow melt, wind speed and direction, solar radiation and humidity.

2.5.4 Aesthetic and land use criteria

Aesthetic and land use criteria are gaining importance in the design of cover systems. The aesthetic enhancements that have been incorporated into cover systems include: (i) construction of an undulating side slope to provide a more natural looking landform (compared to long, planar side slope), (ii) planting of trees in terraces and (iii) construction of decorative block retaining walls. Increasingly, beneficial post-closure land uses are being considered in the design of cover systems for landfill closures and CERCLA remediation (ITRC 2003). The most common types of end uses are parks, hiking trails, sports fields, and golf courses (Bonaparte et al. 2002). The selected end use can have a significant impact on cover system design (Daniel et al. 2002). For example, if a site is to be used for a golf course or other facility with a vegetated surface layer that requires irrigation, the cover system may require an internal drainage layer and a barrier with a GMB to control percolation (Hauser et al. 2005).

2.5.5 Physical and engineering criteria

Previous researchers studied the physical criteria that should be considered in designing a cover system, which include the lateral limits of waste (Bennett 2007), property setback requirements (if any), height of facility above surrounding ground, side slope length and inclination (Wells and Crooks 1987), top deck length and inclination, depth of waste within the facility, type and thickness of interim cover (Nyhan et al. 1997), and potential for the waste to generate gas (Vangpaisal et al. 2008). Table 2.4 summarize the engineering criteria that are frequently considered in the design of RCRA or CERCLA cover systems.

Table 2.4 Common engineering criteria for different types of cover systems

Surface-Water Runoff Control ✓ Estimated peak flow rate ✓ Surface-water control structure design (benches, channels, and retention ponds)	**Erosion Control and Vegetation** ✓ Rill and inter-rill erosion ✓ Gully formation (tractive force analysis, critical distance for gully formation, permissible velocity analysis) ✓ Wind erosion ✓ Vegetation requirements (type, planting, fertilizer, amendments) ✓ Temporary and permanent erosion control material requirements
Slope Stability ✓ Foundation stability ✓ Waste mass stability ✓ Cover system veneer stability ✓ Pseudo-static stability analysis ✓ Other stability conditions	
Settlement (Total and Differential) ✓ Foundation total settlement ✓ Waste mass total settlement ✓ Foundation differential settlement ✓ Waste mass differential settlement	**Hydraulic Performance** ✓ Cover system water balance ✓ Percolation through cover system ✓ Water flow in drainage system ✓ Maximum head in drainage layer
Seismic Deformation Analysis ✓ Foundation liquefaction ✓ Waste mass deformation ✓ Cover system deformation	**Gas Emission Control** ✓ Gas emission rate analysis ✓ Gas flow and pressure in collection layer ✓ Gas collection system (active or passive) ✓ Gas treatment requirements
Soil Component Performance ✓ Erosion resistance of surface layer ✓ Bio-intrusion resistance ✓ Water storage capacity ✓ Frost penetration depth ✓ Drainage layer flow rate ✓ Drainage layer clogging potential ✓ Drainage layer outlet design ✓ Granular filter layer requirements ✓ Hydraulic soil barrier design (suitable soil availability, thickness, permeability)	**Geosynthetic Component Performance** ✓ GTX filter layer requirements ✓ GTX clogging potential ✓ GN/GC flow rate ✓ GN/GC clogging potential ✓ GN/GC compression resistance ✓ GN/GC outlet design ✓ GTX cushion layer requirements ✓ GMB design ✓ GCL design

2.5.6 Ecological criteria

A cover system should be designed as an integral component of a larger dynamic ecosystem for a high design life of around hundreds years, or longer (Koerner and Daniel 1997). Inevitable changes in physical and biological conditions should be taken into account to help ensure the long-term effectiveness of the cover system (Bonaparte et al. 2002). Only through a holistic ecological approach, the long-term maintenance requirements for cover systems can be minimized (Caldwell and Reith 1993).

2.6 Case studies on test plots of field cover systems

Omega Hills, Wisconsin

One of the first detailed field studies on the performance of CCLs in landfill cover systems was described by Montgomery and Parsons (1989, 1990). Three large test plots with different cover system shown in Fig. 2.5 were constructed on top of the closed Omega Hills landfill, Wisconsin and monitored for four years. The purpose of the field study was to compare the performance of the different cover system. Major observation from the study was that in a short period of time CCLs overlain by only 0.15 to 0.45 m of topsoil was subjected to desiccation, cracking, and increase in hydraulic conductivity.

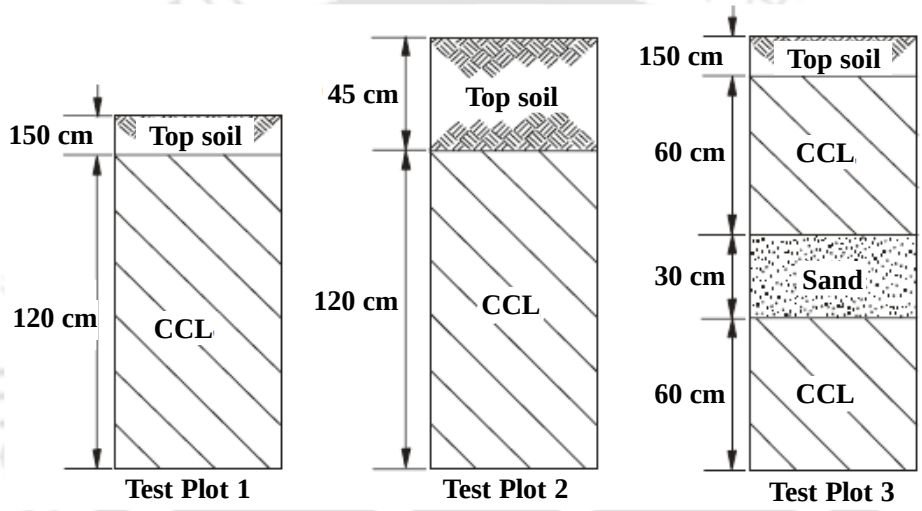

Fig. 2.5 Cross sections of cover system test plots at a landfill in Omega Hills, Wisconsin (modified from Montgomery and Parsons 1989).

Kettleman City, California

Corser and Cranston (1991) and Corser et al. (1992) constructed three test plots shown in Fig. 2.6 at a landfill in Kettleman City, California. Although the test plots were observed for only six months, significant deterioration of the CCLs was observed in test plots 1 and 3. Only test plot 2, in which the CCL was covered with a GMB and 0.6 m of topsoil, performed well. The observations from the test plots are consistent with those of Omega Hills and suggest that perhaps the only practical way to protect a CCL from desiccation is to cover it with a GMB overlain by a sufficiently thick layer of surface soil.

Hamburg, Germany

Melchior et al. (1994) and Melchior (1997 a, b) described a test program to date involving CCLs for cover systems. Test plots with four different cover system cross sections, shown in Fig. 2.7, were constructed on relatively flat (i.e., 4% slope) top deck of a MSW landfill in Hamburg, Germany. Climate, lateral drainage, runoff, percolation, soil moisture content, and soil water potential data were collected. The main finding of the study was: (i) The clayey sands tend to be less vulnerable to shrinkage cracking than clays (especially highly plastic clays) that contain relatively few coarse-grained particles. (ii) For long-term performance of CCL, it should be protected with both a GMB and a sufficiently thick layer of cover soil above the GMB. Furthermore, if a GCL is used in lieu of a CCL, the GCL must be chemically compatible with adjacent soils.

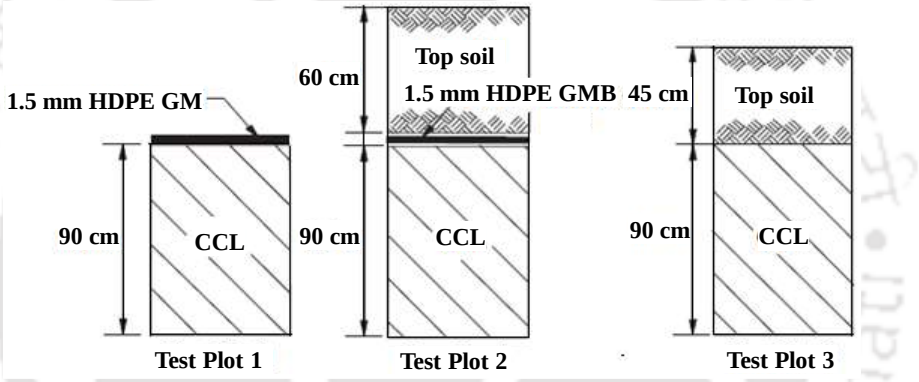

Fig. 2.6 Cross sections of cover system test plots at a Landfill in Kettleman City, California (modified from Corser and Cranston, 1991)

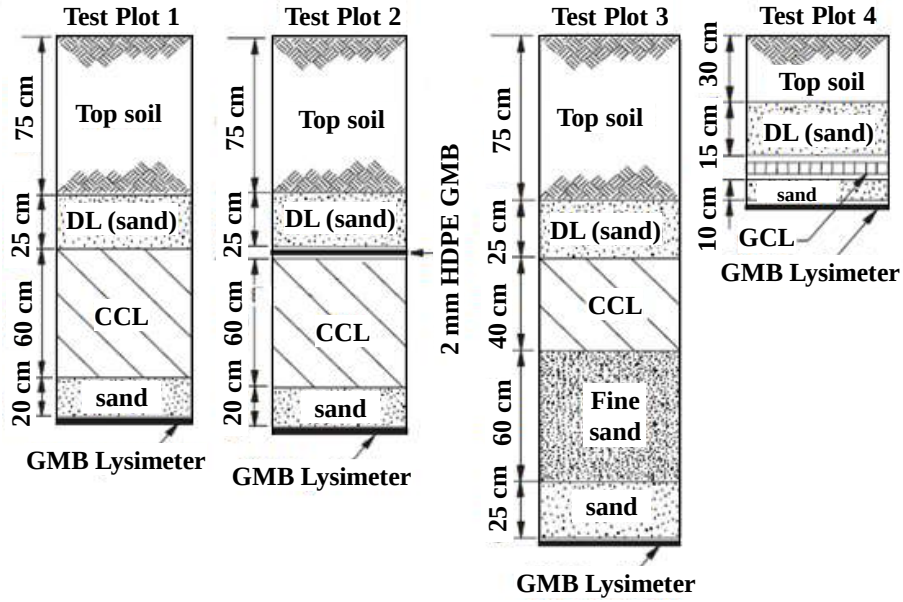

Fig. 2.7 Cross sections of cover system test plots at a landfill in Hamburg, Germany (modified from Melchior et al, 1994; Melchior, 1997a)

Albuquerque, New Mexico

Dwyer (1997, 1998, 2001) have described the construction and monitoring of six test plots with different cover system configurations (Fig. 2.8) at the Kirtland Air Force Base in Albuquerque, New Mexico. To provide good vegetation cover during the growing season, the plots were seeded with a mixture of warm season and cold season native grasses. The test plots were constructed in 1995 and 1996. Each test plot was 13 m wide by 100 m long, crowned in the middle, and sloped at 5%. Continuous water balance and meteorological data were collected for the test plots. The plots were heavily instrumented to quantify measurable water balance variables (precipitation, surface runoff, lateral drainage, percolation, and soil moisture changes). Instrumentation included collection lysimeters to monitor percolation and time domain reflectometry (TDR) moisture sensors to monitor the soil water content within the cover system.

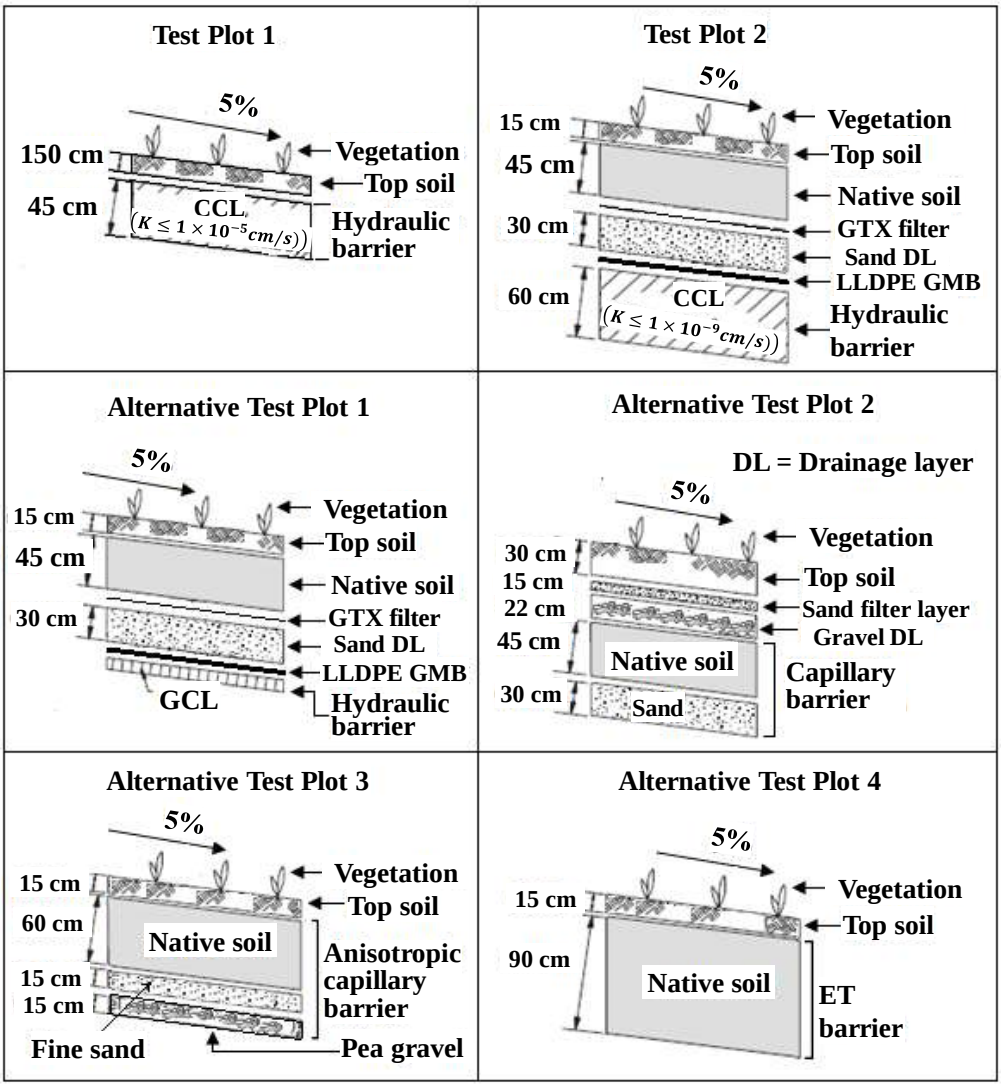

Fig. 2.8 Cross sections of cover system test plots at Kirtland Air Force Base in Albuquerque, New Mexico (modified from Dwyer, 1997)

Based on the above experiments, it was reported that the GCL cover did not perform as well as expected. The bentonite within the geosynthetic clay liner was desiccated, and could not fully repair itself during rewetting. The capillary barrier covers also showed a higher than expected percolation rate for the first year, but the rate slowed down as the surface vegetation thickened with native grasses and shrubs. The anisotropic barrier and ET cover was found to perform well essentially associated with the transpiration rate. This test plot revealed that in dry environments, a well-designed simple soil cover was not only the cheapest alternative but also the most effective at controlling infiltration.

Los Alamos, New Mexico

Nyhan et al. (1997) described the performance of sixteen test plots constructed at Los Alamos National Laboratory, New Mexico. The plots had four different cover system configurations, which were constructed with a slope of 5, 10, 15, and 20%. None of the plots was vegetated. Precipitation, runoff, lateral drainage, percolation, and soil water content were measured for each test plot. The four cover system cross sections that were constructed are (i) Test cover 1: conventional Los Alamos design with 0.15 m of loam topsoil, 0.76 m of silty sand, and 0.3 m of gravel; (ii) Test cover 2: EPA design with 0.15 m of loam topsoil, a GTX filter/separator, 0.3 m of drainage sand, and a 0.6 m thick bentonite clay-sand CCL; (iii) Test cover 3: loam capillary barrier design with 0.6 m of loam topsoil overlying 0.76 m of fine sand; (iv) Test cover 4: clay loam capillary barrier design with 0.6 m of clay loam topsoil overlying 0.76 m of fine sand. Results indicated that the test cover 2 performed better than the other cover system configurations with no evidence of percolation even though its CCL was protected by 0.45 m of soil. The highest amount of percolation was recorded for test cover 1.

Lysimeters at DOE Hanford Site

Fayer et al. (1992) compared field water balance for eight unvegetated lysimeters at USDOE's Hanford site with water balances simulated using UNSAT-H code. Soil profile in the lysimeters and simplified profile used for simulations are shown in Fig. 2.9. The uppermost soil in the lysimeters is a silt loam material. Soil profile in lysimeters is intended to simulate a capillary barrier.

The simulation was found to underestimate the amount of soil water storage during the spring and overestimate the amount of soil water storage during the winter. This was to

underestimation of evaporation in winter and overestimation of evaporation in summer. By decreasing evaporation, increasing saturated hydraulic conductivity of silt loam, and adding a snow cover, simulated soil water storage shows better agreement with measured soil water storage.

Hill Air Force Base

Paige et al. (1996) described calibrating Version 2 of the HELP model to field measurements from two cover system test plots constructed at Hill Air Force Base (Hill AFB), in Layton, Utah and monitored for a four-year period. The calibrated models were then used to simulate the long-term performance of the cover systems. Cross sections of the cover systems are shown in Fig. 2.10. After construction, the plots were vegetated with native grasses. Water balance data measured over the four-year monitoring period include precipitation, lateral flow in the sand drainage layer, percolation, soil moisture content, and runoff. Even with the site-specific calibration, significant differences between field and simulated water balance was noted. In particular, for the ET cover system, correlation between measured and predicted percolation was not good.

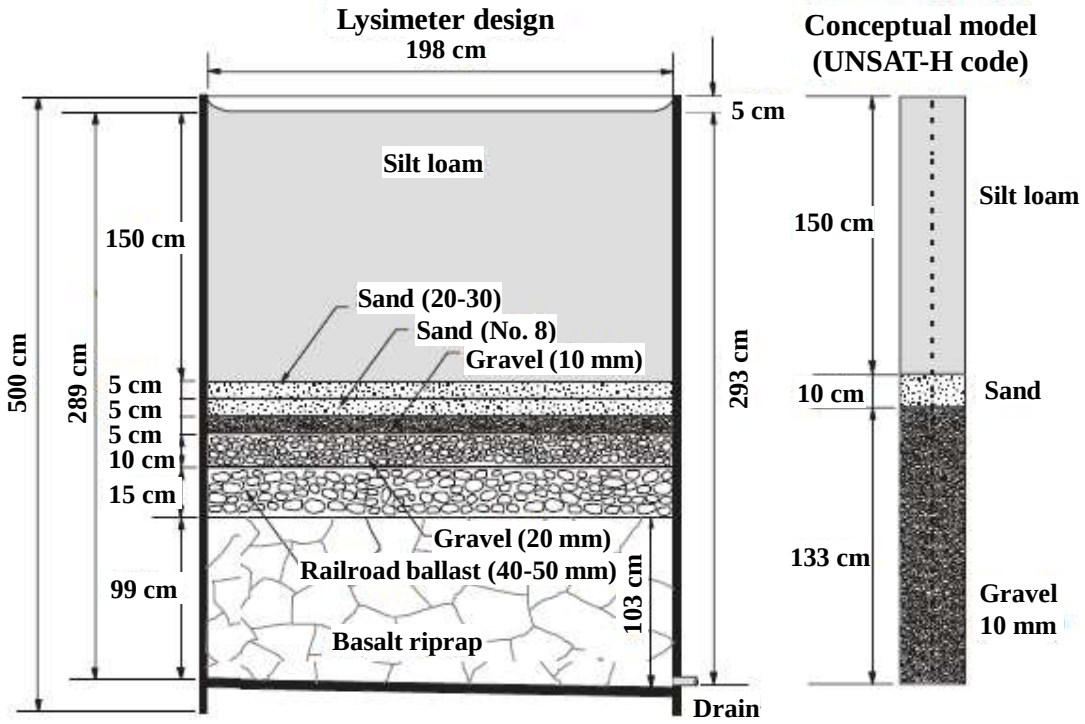

Fig. 2.9 Lysimeter design and conceptual model used to compare measured and simulated water balance for DOE Hanford site (from Fayer et al. 1992)

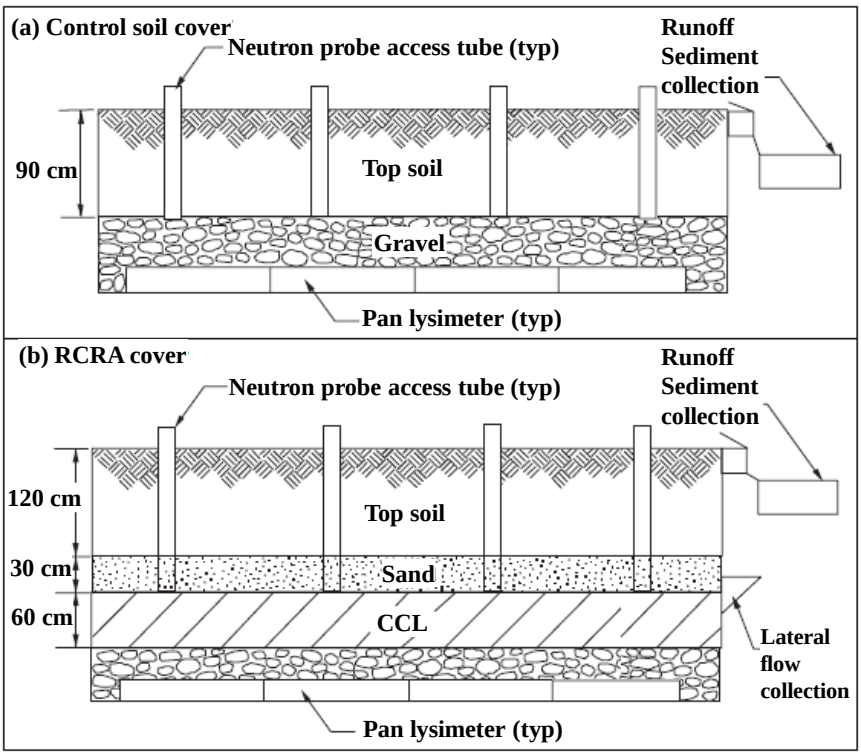

Fig. 2.10 Hill Air Force Base test plots: (a) ET-type cover system; and (b) hydraulic barrier-type cover system (from Paige et al. 1996)

2.7 Column study on cover system

A chronological review of the previous studies on cover system (CS) column test is summarized in Table 1 to highlight the importance of various methodologies. Based on the literature listed in Table 1, it was noted that different types of CS have evolved over the last few decades mainly based on two mechanisms known as evapotranspiration (ET) and capillary barrier (CB) action. The table also focuses on the inclusion of geosynthetic clay liner (GCL) and different recycled materials in MLCS for landfill application.

Stormont and Anderson (1999) have conducted infiltration tests using soil columns with different material combinations to study the capillary barrier effect. The soil column was 203 mm in diameter and 1000 mm high constructed using clear plexiglass cylinders. The different soil layers placed in the column were compacted using Proctor hammer in the calculated lift volume to achieve the desired density. Tensiometers and water content reflectometers (WCR) were employed for the measurement of suction and water content in the soil column. The study was carried out with three fine soils over coarse soil combinations. It was concluded that the lower coarser layer is critical for the performance of the capillary barrier. The coarser and uniform the lower layer, the better the performance of the capillary barrier. It was further stated that the capillary barrier so formed could be restored with repeated drying and wetting cycles.

Table 2.5 Reviewed literature on cover systems used for landfill application

References	Type of cover					Technique						Considerations for the study					
	Capillary barrier	Evapotranspiration	Monolithic	Three/multi-layer	Instrumented profile	Laboratory study	Numerical simulation	Lysimeter	Column study	Field study	Soil water content	Soil suction	Water percolation	Flood conditions	Vegetation	GCL inclusion	Recycled material
Woyshner and Yanful (1995)	X	✓	✓	X	✓	X	✓	X	X	✓	✓	X	X	X	X	X	X
Stormont (1996)	✓	X	X	X	X	X	X	X	X	X	X	✓	X	X	X	✓	X
Khire et al. (1997)	✓	✓	X	X	✓	X	✓	X	X	✓	✓	✓	X	X	✓	X	X
Nyhan et al. (1997)	✓	X	X	X	X	X	X	X	X	✓	✓	X	✓	X	✓	✓	X
Stormont and Anderson (1999)	✓	X	X	X	X	✓	X	X	✓	X	✓	✓	X	✓	X	X	X
Choo and Yanful (2000)	✓	X	X	X	✓	X	✓	X	✓	X	✓	✓	✓	X	X	X	X
Khire et al. (2000)	✓	X	X	X	✓	X	✓	✓	X	X	✓	✓	X	X	✓	X	X
Benson et al. (2001)	✓	X	X	X	✓	X	✓	✓	X	✓	✓	✓	✓	✓	✓	X	X
Hauser et al. (2001)	✓	✓	X	X	X	X	X	✓	X	✓	X	X	✓	X	✓	X	X
Dwyer (2003)	✓	✓	X	✓	✓	X	✓	X	X	✓	✓	✓	✓	X	✓	✓	X
Tami et al. (2003)	✓	X	X	X	X	✓	X	X	X	X	✓	✓	✓	X	X	X	X
Yanful et al. (2003)	X	✓	✓	X	✓	✓	✓	X	✓	X	✓	X	✓	X	X	X	X
Zornberg et al. (2003)	✓	✓	X	X	✓	X	✓	X	X	✓	✓	X	✓	X	✓	X	X
Albright et al. (2004)	✓	✓	X	✓	X	X	X	✓	X	✓	X	X	✓	X	X	✓	X
Yang et al. (2004a)	✓	X	X	X	X	✓	✓	X	✓	X	✓	✓	X	X	X	X	X
Yang et al. (2004b)	✓	X	X	X	✓	✓	X	X	✓	X	✓	✓	X	X	X	X	X
Iryo and Rowe (2005)	✓	X	X	X	✓	X	✓	X	X	X	✓	✓	✓	X	X	X	X
Luellen and Brydges (2005)	✓	X	X	X	✓	X	✓	X	X	X	X	X	X	X	X	✓	X
Scanlon et al. (2005b)	✓	✓	X	X	✓	X	✓	✓	X	✓	✓	✓	X	X	✓	✓	X
Albright et al. (2006a)	X	X	✓	X	X	✓	X	✓	X	✓	✓	X	X	X	✓	X	X
Albright et al. (2006b)	X	X	✓	X	X	X	X	✓	X	✓	✓	X	X	X	✓	✓	X
Krisdani et al. (2006)	✓	X	X	X	✓	✓	X	X	✓	X	✓	✓	X	X	X	X	X
Parent and Cabral (2006)	✓	X	X	X	✓	X	✓	X	X	X	✓	✓	X	X	X	X	X
Yanful et al. (2006)	✓	X	X	X	✓	X	✓	X	X	X	✓	✓	X	X	X	X	X
Yang et al. (2006)	✓	X	X	X	X	✓	✓	X	✓	X	✓	✓	X	X	X	X	X
Benson et al. (2007a)	X	✓	✓	X	X	✓	X	✓	X	✓	✓	✓	X	X	✓	✓	X
Benson et al. (2007b)	✓	✓	X	X	✓	✓	✓	✓	✓	✓	X	X	✓	✓	✓	X	X
Indrawan et al. (2007)	✓	X	X	X	✓	✓	✓	X	✓	X	✓	✓	X	X	X	X	X
Sadek et al. (2007)	X	X	✓	X	✓	X	✓	X	X	X	✓	✓	✓	X	✓	X	X
Ogorzalek et al. (2008)	✓	X	X	X	✓	X	✓	✓	X	X	✓	✓	✓	✓	X	✓	X
McGuire et al. (2009)	X	✓	✓	X	✓	✓	✓	✓	X	X	✓	✓	X	X	X	X	X
Zhang et al. (2009)	✓	✓	X	X	✓	✓	✓	✓	X	X	✓	✓	X	X	✓	X	X
Lewis and Sjostrom (2010)	X	X	✓	X	✓	✓	X	X	✓	X	X	✓	X	X	X	X	X
Melchior et al. (2010)	✓	X	X	✓	X	X	✓	✓	X	✓	✓	X	X	X	✓	X	X
Sun et al. (2010)	X	✓	✓	X	✓	✓	✓	✓	✓	X	✓	✓	X	X	X	✓	X
Qian et al. (2010)	✓	X	X	X	X	✓	X	X	X	X	X	✓	✓	X	X	X	X
Abdolahzadeh et al.(2011)	✓	X	X	X	✓	X	✓	X	X	✓	✓	✓	✓	X	X	X	X
Mijares et al. (2012)	X	X	✓	X	X	X	X	✓	X	✓	✓	X	✓	X	✓	X	X

Albright et al. (2012)	X	✓	✓	X	X	✓	X	✓	X	✓	X	X	✓	X	✓	X	X
Rahardjo et al. (2012)	✓	X	X	X	X	X	X	X	X	✓	✓	✓	X	X	✓	✓	X
Li et al. (2013)	✓	X	X	X	✓	X	✓	X	X	X	✓	✓	X	X	X	X	X
Harnas et al. (2014)	✓	X	X	X	X	✓	X	X	✓	X	✓	✓	X	X	X	X	✓
Zhang and Sun (2014)	✓	X	X	X	✓	X	✓	X	X	X	✓	✓	✓	X	✓	X	X
Ng et al. (2015)	X	X	X	✓	✓	✓	✓	X	X	X	✓	✓	X	X	X	✓	X
Coo et al. (2016)	X	X	X	✓	✓	✓	✓	X	✓	X	✓	✓	X	✓	✓	X	X
Ng et al. (2016)	X	X	X	✓	X	✓	X	X	✓	X	✓	✓	X	✓	X	X	X
Zhang et al. (2016)	✓	✓	X	X	✓	✓	✓	X	✓	X	✓	✓	✓	X	X	X	X
Rahardjo et al. (2016)	✓	X	X	X	✓	✓	✓	X	X	X	✓	✓	✓	X	X	X	✓
Khapre et al. (2017)	X	✓	✓	X	X	✓	X	X	X	X	✓	✓	X	X	X	X	X
Zhang et al. (2017)	X	X	✓	X	✓	X	✓	X	X	✓	✓	✓	X	X	X	X	X
Ng et al. (2019a)	X	X	X	✓	X	X	X	X	X	✓	✓	✓	X	X	✓	X	✓
Ng et al. (2019b)	X	X	X	✓	X	✓	X	X	✓	✓	✓	✓	X	✓	✓	X	✓
Tan et al. (2018)	✓	X	X	✓	X	✓	X	X	✓	X	✓	✓	✓	X	X	X	X

Choo and Yanful (2000) have studied transient water flow in homogenous soil and steady state flow in multilayer soil using analytical methods and finite element model. The results obtained from the simulation were compared with those obtained from laboratory column study. The laboratory column studies consisted of two separate columns in which a two layer and a three layered soil cover were packed into a Plexiglas column of internal diameter 0.108 m and length 1.022 m. A porous ceramic disk (high air entry) was fitted at the base of the column to allow movement of water and prevent flow of free air. The column was instrumented with tensiometers and time domain reflectometry (TDR) probes along the length to measure pressure and water content. The modelling and experimental results showed different trends for time greater than 3 days, which has been attributed to the presence of discontinuous water pockets in the columns. The authors also state that vapor transport by diffusion plays a significant role where evaporation occurs in soil, and hence should be included in the flow model for the simulation. The results obtained by authors emphasized the need for accurate knowledge of unsaturated hydraulic conductivity-pressure functions in flow modelling.

Yanful et al. (2003) have studied the flow of water through multi-layered soil cover by conducting laboratory column studies. Numerical simulations were also carried out with the help of a coupled liquid flow, vapor diffusion, and heat transfer finite element model. The layered soil cover studied was proposed for mine-waste soil cover, which intended to control oxygen diffusion and infiltration. Studies on column setups consisting of single clay till layer and three-layer soil cover (consisting of coarse soil, clayey till soil and fine soil) with thickness ratio of 3:8:5 (from top soil layer to bottom) were performed. The

evaporation columns measured 115mm in diameter and 255 mm in height and were instrumented using Time domain reflectometry (TDR) probe and thermocouple for measuring water content and temperature respectively. Saturation of the soil columns were performed using a 6.35 mm (internal diameter, ID) plastic tube connected to the bottom center hole of the column and to a mercury constant water supply system. Depending on soil type, the saturation pressure was varied from 5 to 40 kPa. The water supply and drainage system consisted of the same tube connected to a 1-l Mariotte bottle for maintaining a constant water level. Results obtained from the experiments agreed reasonably well with the predicted values from the modelling. Sand layers placed on top and bottom of the till layer worked as evaporation and drainage barriers, respectively. This ensured that the till layer remained saturated and performed effectively as an oxygen barrier. Modelling results further indicated coarse sand as the most suitable top evaporation protective layer.

Yang et al. (2004a) have described the construction and performance of a large-scale soil column for studying laboratory infiltration characteristics. Transparent acrylic cylinder (5mm thick and 190 mm ID) strengthened by vertical stiffeners and provided with a top acrylic cap and a bottom stainless steel base plate was used in the setup. Threaded holes were fabricated in the cylinder for the installation of TDR probes and tensiometers-transducer system. The mounting was done using specially designed stainless steel connector (double socket type). The mounting was done by either pre-drilling a hole in soil column or by inserting the ceramic cup at desired position during compaction. The positions of the holes were finalized on basis of seepage analysis using SEEP/W. All the joints were properly sealed using rubber O-rings and fastened using bolts and nuts. The water flow system employed consisted of constant head water tank, sensitive ball valve for flow regulation, rainfall distributor (perforated acrylic plate), overflow outlet for regulation of water head on the soil surface and percolation discharge using a pipe connected to a steel plate, which was recessed to accommodate a porous stone. The percolated water was collected and weighed, continuously using an electronic balance. The tensiometers, TDR and the electronic balance were connected to a data acquisition system for continuous data logging and storage. The experimental setup was found to be effective in infiltration studies.

Yang et al. (2004b) have investigated the capillary barrier effect by conducting infiltration tests on two layered soil columns with various combinations of materials (fine sand, medium sand, gravelly sand). The effectiveness of the barrier was judged by the

criteria of pore-water pressure change across the interface and the final water storage. The use of gravels as the coarser layer was found to be more effective as a capillary barrier as it had better water storage and the water entry value was lower. The water entry value was found to be approximately equal to the residual matric suction value of the soil. The maximum matric suction developed in the soil column was found to be either one or two times the residual matric suction. It was also reported that the ultimate pore-water pressure profile in the soil column does not reach hydrostatic equilibrium as predicted theoretically. Based on this observation the authors have proposed an idealized ultimate pore-water pressure profile, which can be useful for estimating negative pore-water pressure in the soil when water table is deep. It has been further pointed out that the SWCC of a soil using the drying capillary rise open tube can provide consistent and accurate results only up to matric suction range of two times the residual water matric suction of the soil.

Yang et al. (2006) have conducted laboratory investigations on the vertical infiltration of two soil columns of finer over coarser soils subjected to simulated rainfalls. The finer material used in the column were two different locally available clay and the coarser layer consisted of fine or medium sand. SWCCs associated with the drying and wetting of the soil column were plotted and it was observed that the curves so obtained were secondary or scanning curves. It was also concluded that these relationships between matric suction and volumetric water content are not unique and are dependent on the drying and wetting histories of the soil. Transient processes with delayed response and instantaneous response of pore water pressure and water content due to rainfall intensity were observed in separate cases of column study. The delayed response indicated the redistribution process of soil water during infiltration. The test results further indicated that the coarser layer restricted the increase of pore water pressure in the upper clay layer during infiltration. The authors have also reported the spatial variation of saturated permeability values of the soil layers, which has been attributed to the variation in soil compaction energy.

Krisdani et al. (2006) have conducted column studies on two different capillary barrier models. Gravely sand and a geosynthetic material (Polyfelt Megadrain 2040) were used as the drainage layer in the columns. The SWCC of the soils were determined using Tempe cell and pressure plate tests while the GWCC (Geotextile water characteristic curve) was determined using capillary rise principle. The column setup consisted of the coarse-grained layer sandwiched between two layers of fine sand. Small tip tensiometers and time domain reflectometry (TDR) were installed along the column for measurement of pore

water pressure and volumetric water content respectively (Infiltration column setup same as Yang et al. 2004a). Rapid drawdown tests and simulated rainfall tests were conducted on the columns. The pore water pressure profiles obtained indicated that higher matric suction profiles were developed in the fine layer overlying the geotextile layer. This resulted in lower unsaturated permeability values and more water storage in the fine layer. The results obtained indicate that the geotextile layer acts as a better capillary barrier than the gravelly sand.

Lewis and Sjostrom (2010) have reviewed various techniques involved in the design of soil column and have listed out the best practices for saturated, unsaturated, monolithic, and packed soil columns. Unnatural preferential flow (sidewall flow, macropore flow, and fingering) has been identified as the most critical design issue with unsaturated columns, which occurs due to lack of proper packing or flexing of column walls. The authors have recommended caution for the use of the experimental approach of free drainage, in which soil pore water flows from the base of the soil column under zero tension. Generally, in such cases capillary fringes are formed (up to 90 cm thick) and the unsaturated column operating under free drainage may actually be saturated resulting in unreliable flow data. Reporting of the soil water characteristic curve (SWCC) accounting for hysteresis wasidentified to be crucial for reproducibility of experiments in unsaturated columns.

Sun et al. (2010) have studied the changes in the water balance resulting from the use of geotextile in a lysimeter pan experiment performed in a monolithic alternative landfill cover. The geotextile was used as a plant root barrier for the drainage layer. Laboratory column studies and numerical modelling (using SEEP/W and VADOSE/W) were implemented for studying the effects of the geotextile layer on water balance. Volumetric water sensors were fitted in the columns at specified heights and continuous measurements were recorded. The authors state that the excess water on the surface may result in preferential flow (sidewall flow). The laboratory finding and numerical analysis indicated the formation of a capillary barrier at the geotextile layer. This effect was responsible for storing additional 70 L of water per cubic meter of soil, which can later be potentially removed by evapotranspiration by plants.

2.8 Field study on landfill cover system

Numerous research works were carried out all over the world in last few decades for investigating the performance of different type of cover system. A chronological review

of water percolation studies of cover system in the field is provided in Table 2.5. From the table, it can be noted that the ET and CB cover systems are mostly studied by conducting laboratory column test or numerical simulation. As far as the field studies of landfill cover system are concerned, the efficacy of ET and CB cover systems have been investigated by using lysimeter technique (Choo and Yanful 2000; Albright et al. 2004; Scanlon et al. 2005b). It is noticed that the lysimeter based monitoring is expensive, time-consuming and do not give representative evapotranspiration (Zhang and Sun 2014; Mijares et al. 2012). The effect of vegetation on evapotranspiration of the cover system has been considered in numerical studies as shown in Table 2.5

Benson et al. (2001) conducted a study for the evaluation of final cover performance as part of a five-year study referred to as the alternative cover assessment program (ACAP). Data were collected from 24 final cover test sections located at eleven sites in seven states. Climates ranging from arid to humid/subtropical were represented. Tentative recommendations regarding equivalent percolation rates for conventional covers have been made based on the data. The recommended equivalent percolation rates for covers with composite barriers were 1 mm/yr. for semi-arid and arid climates and 5 mm/yr. for humid climates.

Hauser et al. (2001) discussed innovative vegetative landfill covers that use no barriers. They consist of a layer of soil covered by native grasses to control infiltration as follows: (1) the soil stores infiltrating water; and (2) natural evapotranspiration empties the soil water reservoir. The vegetative cover concept was extensively verified in the field. They proposed that evapotranspiration cover should be associated with correctly designed and constructed vegetative covers.

A site-specific unsaturated flow investigation was undertaken by Zornberg et al. (2003) for the analysis and design of an evapotranspiration (ET) cover system at the Operating Industries, Inc. (OII) Superfund landfill in southern California. The site-specific sensitivity evaluation shows that percolation response to design parameters such as rooting depth, cover thickness, and saturated hydraulic conductivity is highly nonlinear. This facilitated selection of the design parameters in the final cover. The analyses also provide insight into the effect of irrigation, increased natural precipitation, and initial moisture content of the cover soils.

Henken-Mellies and Gurtung (2004) conducted a long-term observation through large-scale field tests, which were conducted in Bavaria, Germany in order to test the effectiveness of landfill cover systems. In their study a simple landfill cover consisting of

a thick layer of loamy sand was placed in one of the large lysimeters; the other lysimeter was filled with a more elaborate cover design (1 m of top soil, a drainage geocomposite, and a GCL). The water balance of the landfill cover system inside each of the lysimeters was measured during a four-year period. The overall results emphasize the importance of a properly designed landfill cover system, including a sufficiently thick re-cultivation layer to regulate the water balance of the surface cover system, an effective drainage layer, and a sealing layer, which keeps its low permeability. The drainage geocomposite and the Ca-GCL proved to be effective elements within the landfill cover system. The approach used in their investigation helped to capture additional uncertainties regarding the effects of degradation mechanisms on long-term cap performance.

Albright et al. (2006a) evaluated hydraulic properties of the compacted clay barrier layer in a final landfill cover in southern Georgia, USA. After four years, the clay barrier was excavated and examined for changes in soil structure and hydraulic conductivity. The in situ and laboratory tests indicated that the hydraulic conductivity increased approximately three orders of magnitude (from $\approx 10^{-7}$ to $\approx 10^{-4}$ cm· s^{-1}) during the service life. The findings also indicate that clay barriers must be protected from desiccation and root intrusion if they are expected to function as intended.

Benson et al. (2007a) studied the post construction changes in the hydraulic properties of water-balance cover soils. In the study hydraulic properties of soils used for water balance covers measured at the time of construction and one to four years after construction are compared to assess how the hydraulic properties of cover soils change over time as a result of exposure to field conditions. Data are evaluated from ten field sites in the United States that represent a broad range of environmental conditions. After two to four years, many water balance cover soils can be assumed to have K_s between 10^{-5} and 10^{-3} cm/ s, θ_s between 0.36 and 0.40, van Genuchten α parameter between 0.002 and 0.2 kPa^{-1}, and van Genuchten *n* between 1.2 and 1.5. The data may be used to estimate changes in hydraulic properties for applications such as waste containment.

McGuire et al. (2009) conducted a case study of a full-scale evapotranspiration cover. In the study the design, construction, and performance analyses of a 6.1 ha evapotranspiration (ET) landfill cover at the semiarid U.S. Army Fort Carson site, near Colorado Springs, Colo. are presented. Favourable hydrologic performance for a 5-year period was documented by lysimeter-measured and Richards'-based calculations of annual drainage that were all < 0.4 mm/ year. Water potential data suggest that ET removed water

that infiltrated the cover and contributed to a persistent driving force for upward flow and removal of water from below the base of the cover.

The water balances and the long-term performance of different landfill cover systems have been measured in situ by Melchoir et al. (2010) in large-scale lysimeters on the landfill Hamburg-Georgswerder, Germany since 1988. The water balance was used to test the applicability of hydrological evaluation of landfill performance (HELP) model. Tensiometers, neutron probes, and time domain reflectometry (TDR) were used to collect soil suction and water content data. The study quantified the irreversible impact of crack formation in cohesive soil barriers and geosynthetic clay barriers due to desiccation, shrinkage, ion exchange, and plant root penetration. The hydraulic conductivity of the cohesive soil barriers increased from 2×10^{-10} to 9×10^{-8} m/s. The composite barriers with geomembranes above cohesive soil barriers performed well, showing no leakage and only very little thermally induced water transport.

A comprehensive study was conducted by Henken-Mellies and Schweizer (2011) to examine the performance and possible changes in the effectiveness of landfill surface covers. The performance of three different landfill cover systems has been monitored in large-scale lysimeter test fields at the municipal solid waste landfill of Aurach, Bavaria (Germany). It was observed that the required long-lasting protection of CCL and GCL against root penetration and desiccation can be provided by an appropriately thick soil cover (possibly 2 to 3 m) or by a geomembrane. The hydraulic conductivity of the compacted clay layer or of the geosynthetic clay liner may increase substantially, if there is no long-lasting protection against desiccation.

A study was conducted Albright et al. (2012) at seven sites across the United States to evaluate the field hydrology of final covers with a composite barrier (a geomembrane over a soil barrier or a geosynthetic clay liner) for final closure of landfills. They found that the percolation from all test covers generally was coincident with high water storage in the surface soil layer and lateral flow in the drainage layer on the surface of the geomembrane barrier. Water balance predictions were made with the hydrologic evaluation of landfill performance model using site-specific input. Surface runoff was over-predicted and evapotranspiration under-predicted when as-built soil hydraulic properties were used as input.

Li et al. (2013) conducted a numerical investigation of the performance of covers with capillary barrier effects (CCBEs) in South China. In their study, several combinations of lean clay, clayed sand, and silty sand with gravel are examined using

saturated/unsaturated seepage analysis. Two contrasting conditions, i.e., a drizzle lasting for a long time and an intense storm lasting for a short time, were applied to the covers. The covers perform well when subject to prolonged small rainfall at an initial maximum suction of 150 kPa. When subject to a short-time heavy rainfall, breakthrough occurred in the cover consisting of clayed sand overlying silty sand with gravel. Of the three covers, a CCBE consisting of lean clay overlying silty sand with gravel performs well under both prolonged light rainfall and short time heavy rainfall conditions.

Zhan et al. (2014) investigated the performance of an inclined three-layer cover with capillary barrier effect (CCBE) comprising silt, sand, and gravel, for usage under humid climatic conditions. Numerical modeling was simulated for a 60 m long inclined CCBE system to investigate the effective length of lateral diversion under a prolonged heavy rainfall. The physical modeling tests demonstrate the effectiveness of the inclined three-layer CCBE system for heavy rainfall up to about 70 mm/h. The capillary barrier at the sand–gravel interface of the system failed and allowed deep percolation when the saturated hydraulic conductivity of the top silt layer was in the order of 5.3×10^{-6} m/s. When the saturated hydraulic conductivity of the top silt layer was reduced by one order to 5.3×10^{-7} m/s, the inclined three-layer CCBE system was successful in laterally diverting all the infiltrated water near the interface.

2.9 Numerical modelling of cover system

Numerical modelling of landfill cover is very essential to understand its complex unsaturated fluid flow system and long-term performance. A variety of modelling tools based on water balance methods or theory of fluid dynamics in unsaturated porous media are available for numerical analysis of the MLCS. They range in complexity from relatively simple empirical correlations to sophisticated computer-based finite difference and finite element models. Table 2.6 summarizes the modelling approaches used for simulating MLCS performance.

Berger et al. (1996) studied the suitability of hydrologic evaluation of landfill performance (HELP) model of the US EPA for the simulation of the water balance of landfill cover systems. HELP model considers gravitational forces as driving forces of water flow only. Therefore, capillary barriers cannot be simulated using HELP. In the study, model results were compared with field data of the water balance, measured in the test conducted on the Georgswerder landfill in Hamburg. The measured and simulated data were found to be in good agreement for lateral drainage, but not for surface runoff.

Khire et al. (1997) conducted a study on water balance modelling of earthen final cover. In the study, the hydrologic data measured from two earthen final cover test sections were compared with predictions made using two water balance models (HELP and UNSAT-H). Hydrologic and meteorological data including precipitation, air temperature, solar radiation, relative humidity, wind speed, and wind direction were collected at each test section for three years. Percolation, overland flow, and soil water content were monitored continuously. Predictions of the water balance were made using HELP and UNSAT-H. Percolation was slightly overestimated in HELP and underestimated in UNSAT-H. However, both models captured the seasonal variations in overland flow, evapotranspiration, soil water storage, and percolation. UNSATH captured these variations more accurately than HELP.

Chang et al. (1999) conducted the water balance evaluation of final closure cover of near surface radioactive waste disposal facility in France under domestic climatic conditions. In the study, it was found that until 100 years after closure of disposal vault, the infiltration flux for the most favourable cover design was negligible even under doubling of the ambient precipitation conditions. When the degradation of asphalt and geomembrane after 100 years of closure was considered, the infiltration flux significantly increased to the design criteria of cover system.

Table 2.6 List of reviewed modelling tools used for the simulation of the landfill cover system

Model (Reference)	Numerical Method			Governing equation			Data required				Simulation of landfill cover					Modelling consideration							Limitation					
	Empirical method	Finite element method	Finite difference method	Water balance equation	Fick's law	Richard's equation	Soil hydraulic data	Vegetation parameter	Climate parameter	Hydraulic evaluation	Vapor flow	Soil heat flow	Landfill gas flow	Hydrologic evaluation	Unsaturated flow	Ground freezing	Lateral drainage	ET estimation	Soil anisotropy	Soil heterogeneity	Non-mechanistic model	One dimensional	unavailability	Limited modelling depth	Highly computational	Fixed time step
SHAW (Flerchinger and Saxton 2000)	X	X	✓	✓	✓	✓	✓	✓	✓	✓	✓	✓	X	✓	✓	X	X	✓	X	✓	X	✓	X	✓	✓	X
UNSAT-H (Fayer and Jones 1990)	X	X	✓	✓	X	✓	✓	✓	✓	✓	✓	✓	X	✓	✓	✓	X	✓	X	✓	X	✓	X	X	✓	✓
LEACHM (Hutson and Wagnet 1992)	X	X	✓	✓	X	✓	✓	X	✓	✓	X	X	X	X	✓	X	X	X	✓	✓	X	✓	X	✓	X	✓
HELP (Shroeder et al. 1994)	✓	X	X	✓	X	X	✓	✓	✓	✓	X	X	X	✓	X	X	✓	✓	X	✓	X	X	X	X	X	✓
SWIM V2 (Verburg et al. 1996)	X	X	✓	X	X	✓	✓	X	✓	✓	X	X	X	X	✓	X	X	X	X	✓	X	✓	✓	X	X	✓
HYDRUS 2D (Šimůnek et al. 1999)	X	✓	X	✓	X	✓	✓	✓	✓	✓	X	X	X	X	✓	X	✓	X	✓	✓	X	X	X	X	✓	X
SoilCover (Geo-Analysis Ltd. 2000)	X	✓	X	✓	✓	✓	✓	✓	✓	✓	✓	✓	X	✓	✓	✓	X	X	X	✓	X	✓	X	X	✓	X
VS2DI (Hsieh et al. 2000)	X	X	✓	X	X	✓	✓	X	X	✓	X	✓	X	X	X	X	X	✓	X	✓	X	X	X	X	X	X
VADOSE/W (GEO-SLOPE 2010)	X	✓	X	✓	✓	✓	✓	✓	✓	✓	✓	✓	✓	✓	✓	✓	✓	✓	✓	✓	X	X	X	X	✓	X
SEEP/W (GEO-SLOPE 2014)	X	✓	X	X	X	✓	✓	X	✓	✓	X	X	X	X	✓	X	✓	X	✓	✓	X	X	X	X	✓	X

Water balance simulations were conducted by Khire et al. (2000) with the unsaturated flow model UNSAT-H to assess how layer thicknesses, unsaturated hydraulic properties, and climate affect the performance of capillary barriers. Simulations were conducted for four locations in semiarid and arid climates. Hydraulic properties of four fine grained and two coarser-grained soils were selected to study how saturated and unsaturated hydraulic properties affect the water balance. Results of the simulations indicate that thickness and hydraulic properties of the surface layer significantly affect the water balance of capillary barriers. See what they have reported on climate and compare with our results.

Scanlon et al. (2002) conducted a study to compare water balance simulation results from seven different codes, HELP, HYDRUS-1D, SHAW, SoilCover, SWIM, UNSAT-H, and VS2DTI, using 1–3-year water balance monitoring data from non-vegetated engineered covers (3 m deep) in warm (Texas) and cold (Idaho) desert regions. Simulation results from most codes were similar and reasonably approximated measured water balance components. Simulation of excess runoff was a problem for all codes. Annual drainage was estimated to within ±64% by most codes. The code comparison study identified important factors for simulating the near-surface water balance of engineered covers.

Zornberg et al. (2003) investigated a site-specific unsaturated flow using LEACHM model for the design of evapotranspirative (ET) cover system at the Operating Industries, Inc. (OII) Superfund landfill in southern California. The study indicated that the percolation control in an ET cover system relies on water storage within the cover soils during the rainy season and on the subsequent release of the stored moisture by evapotranspiration during the dry season.

Noel and Rykaart (2003) conducted a comparative evaluation of a cover design using four different codes (SoilCover, SWIM, HYDRUS-2D and HELP. The data set used for the comparative study is a well calibrated data set that that has been collected over a long period in time and according to strict controls. The authors present the pitfalls of numerical modelling of the surface flux boundary conditions, as well as present guidelines towards appropriate use of these modelling tools.

Preston and Bridge (2004) conducted field-test of the Simultaneous Heat and Water (SHAW) model for its ability to reliably estimate poplar transpiration, volumetric soil water content, and soil temperature of a landfill cover located in southern Ontario, Canada. The model was then used to estimate deep drainage and to ascertain the influence of a young poplar tree systems (PTS) on the soil water balance of the landfill cover. The SHAW model

tended to underestimate poplar transpiration and overestimate volumetric soil water content. The model estimated soil temperature very well, particularly in the upper 1 m of the landfill cover. The SHAW model simulations showed that deep drainage decreased appreciably with the presence of a young PTS largely through increased interception of rainfall.

Yanful et al. (2006) employed SoilCover model to simulate one-dimensional evaporation from hypothetical moisture-retaining cover systems. This helped in evaluating the influence of several cover properties and hydro-geologic parameters on performance. The simulated water content profile and layer porosity were then used to estimate oxygen diffusion coefficients of various cover layers. The oxygen flux through the cover systems was computed by using the oxygen diffusion coefficients.

Brown (2007) investigated evapotranspiration landfill cover to determine the design parameters by using Simultaneous Heat and Water (SHAW) model. SHAW model was calibrated to predict transpiration using the Parameter Estimation Software Tool (PEST). The study indicated the annual deep percolation to be less than 60mm.

Ogorzalek et al. (2008) used LEACHM, HYDRUS, and UNSAT-H to predict surface runoff (R), evapotranspiration (ET), soil–water storage (S), and percolation for simulating hydrology of the water-balance covers. Simulated results were compared with measured water-balance data from a lysimeter employed to monitor a capillary barrier cover profile in a sub humid climate. LEACHM and HYDRUS computed total R with reasonable accuracy within 18 mm. In contrast, UNSAT-H consistently overestimated R by at least 239 mm. All three codes overestimated ET in late winter and early spring and S was underpredicted.

Bashir et al. (2015) presented the results of numerical modelling to investigate the role of hysteresis of soil water characteristic curve (SWCC) on the infiltration characteristic of soil subjected to four different climatic conditions like very dry, dry, neutral, and wet climates, within the Canadian province of Alberta using HYDRUS 1D computer code. The consideration of hysteresis in the SWCC of a soil resulted in the prediction of significantly different infiltration characteristics than those predicted using a non-hysteretic SWCC. It is important to consider hysteresis of SWCC for all climate types ranging from very dry to wet. The greater the degree of hysteresis in a soil's SWCC, the more pronounced the differences between the predictions from hysteretic and non-hysteretic simulations. Regardless of the climatic conditions and the type of soil, the use of wetting hydraulic

parameters results in prediction of increased infiltration and movement of water as compared to the predictions using the drying hydraulic parameters. For soils that exhibit greater degree of hysteresis, it is important to measure both the drying and the wetting branches of the SWCC accurately.

Argunhan-Atalay and Yazicigil (2018) investigated the performance of various cover configurations for limiting water percolation and oxygen into the northern waste rock storage area of the Kışladağ gold mine, in Uşak, Western Turkey. SEEP/W and VADOSE/W codes were employed to model the flow in unsaturated and saturated zones for assessing the performance of various cover systems. The accuracy of input data was checked during calibration for steady-state conditions with SEEP/W. Subsequently, bedrock, waste rock, and three different cover alternatives were modelled under transient conditions for 20 years using daily climatic data.

2.10 Critical appraisal on reviewed literature

The reviewed literature reveals that cover system is an essential component of waste disposal facility (landfill) for minimizing rainwater ingress into the underlying waste. Review of the existing literature exemplifies the complexities and challenges associated with the successful design of cover system for its long-term performance. Based on previous studies it is observed that the suitability of the different cover systems and the design of their individual components depends on many site-specific factors like climatic condition, soil type, plant species, topographic features, and the type of waste at that site. The secondary factors governing the design include aesthetic criteria, ecological criteria, post closure site use criteria and the regulatory requirements. In several reviewed case studies on the test plot of few cover systems under different climatic conditions, it has been observed that the field performance should be monitored to ensure long-term existence of MLCS under adverse weather conditions.

The reviewed field studies indicate that the overall performance of MLCS is superior as compared to the other cover systems. Alternative cover systems (ET covers, capillary barrier covers, and anisotropic barrier) have also shown good performance in dry (arid to semi-arid) climates. However, existing literature indicates that such covers may not be suitable for regions with high rainfall. Thus, it can be concluded that MLCS is preferable in regions with high precipitation over other cover systems for minimizing percolation. Many laboratory studies have been carried out by previous researchers employing the use

of soil columns for understanding the performance behaviour of monolithic or multi layered soil systems under various experimental conditions. Most of these studies have been attempted for soil-geotextile systems or capillary barrier systems. Thereby more studies on MLCS including all the soil layers with the thickness similar to that provided in the field are required for complete understanding percolation characteristics.

Based on reviewed literature on some modelling tools, it is well established that numerical modelling for performance evaluation of cover system is essential for studying different scenarios. Several researchers have carried out comparative studies of the experimental results with numerical modelling results. Water balance models have also been proposed for predicting the long-term performance, which is extremely difficult to be evaluated in field or laboratory studies.

It is noted in the literature survey that the hydraulic performance of a MLCS at a particular site is very specific as there are many site-specific governing criteria. Few well-advanced countries like USA and UK have developed their own design guidelines for various cover systems. For example, after carrying out extensive research works on various issues related to cover system, EPA has developed the design guidelines, which is particularly suitable for USA climate. From detailed review, it is clear that field monitoring and laboratory studies are further needed for developing countries like India as many of the near surface hazardous landfills are reaching its closure stage. Therefore, the hydraulic performance evaluation of cover system is needed for high humid, high rainfall regions like Indian subcontinent.

2.11 Objectives and scopes of the proposed research work

The objective of the research work is hydraulic performance assessment of multi-layered cover system for near surface hazardous waste disposal facility for tropical climatic condition of India.

The scopes of the study are outlined as follows:

(i) Performance evaluation of water content sensors for each soils used in the MLCS.

(ii) Laboratory investigation on MLCS columns under constant water ponding.

(iii) Field investigation on sloped MLCS under natural weather condition.

(iv) Numerical analyses of long-term hydraulic performance efficacy of the MLCS considering climate change impact.

Chapter 3
Materials and Methodology

3.1 General

Various materials that finds its application in multi-layered cover system (MLCS) for landfills were considered for the present study. These materials were subjected to different laboratory tests for their chemical, physical, and geotechnical characterization. The results obtained from these tests are summarized in this chapter. Apart from this, details of the different generic instrument/ sensor used and the methodology adopted are presented. In addition, few important theoretical concepts relevant to this study has also been discussed.

3.2 Material selection

The current study was conducted by employing various indigenous soil, bentonite clay, fly ash and commercially available geosynthetic clay liner (GCL). In the study, Medium sand (MS) was used as the drainage layer (DL) in laboratory columns and field cover system. This material was chosen based on hydraulic conductivity (10^{-5} m/s) that satisfies drainage layer criterion (Landreth et al. 1991). 30% bentonite (BN) was mixed with 70% native soils (red soil: RS or black soil: BS) or fly ash (FA) for constructing the barrier layer (BL). In one case, 1 cm thick GCL was used over the BL as an additional hydraulic barrier. The surface layer (SL) comprised of native soil (RS and BS). In two cases, 50% FA was added in the SL. The source, designation, proportion and combination for their use as different cover layer materials are detailed in Table 3.1.

3.3 Material characterization

The laboratory characterization of materials used in this study was performed in accordance with the procedure reported in ASTM international code or Indian standard code summarized in Table 3.2. The specific gravity was determined using the small density bottle or pycnometer. The hygroscopic water content of soil was determined by standard oven drying method. The consistency limits i.e. liquid and plastic limit of the soil sample were evaluated in the laboratory by Casagrande method. The grain size distribution was obtained based on dry, wet sieve and hydrometer analyses. The classification of the soil samples was decided according to unified soil classification system (USCS). Specific surface area was determined in the laboratory following the EGME method recommended

by Cerato and Lutenegger (2002). Standard Proctor tests of soil was conducted to determine its compaction characteristics. The constant head test was performed for obtaining saturated hydraulic conductivity of sand and fly ash and falling head test was used for low permeable soils (red soil, BARC soil, bentonite and their mixes). For this test the samples were compacted at OMC and MDD. Shrinkage and swelling properties were evaluated for plastic soils. Organic content, pH value and cation exchange capacity were also determined for the chemical characterizations of each soil. Each tests were repeated at least thrice and the average results obtained from these tests are shown in table 3.3. Chemical composition of four original soil materials i.e. red soil, black soil, bentonite and fly ash were determined in the form of major oxides using X-ray fluorescence (Aχios, PANalytical). The result is presented in Table 3.4.

Table 3.1 Details of various materials used in the study

Material	Designation	Source	Used for
Medium sand (MS)	MS	local river sand, Northeast India	DL
Fly ash (FA)	A	thermal power plant, Farakka, Eastern India	SL and BL
Red soil (RS)	RS	local silty clay, Northeast India	SL and BL
Black soil (BS)	BS	Mumbai, Maharashtra, Western India	SL and BL
Bentonite	BN	Barmer, Rajasthan, Western India	BL
Red soil-fly ash mix	RF	mix of 50% red soil and 50% fly ash	SL
Black soil-fly ash mix	BF	mix of 50% black soil and 50% fly ash	SL
Fly ash-bentonite mix	FB	mix of 70% fly ash and 30% bentonite	BL
Red soil-bentonite mix	RB	mix of 70% red soil and 30% bentonite	BL
Black soil-bentonite mix	BB	mix of 70% black soil and 30% bentonite	BL
Geosynthetic clay liner	GCL	Commercially available	BL

Notes: SL, DL and BL are surface layer, drainage layer and barrier layer respectively, of the multi-layered landfill cover system used for this study.

Table 3.2 Various references for basic characterization of materials

Basic characterization	Reference (IS/ASTM code/literature)
Specific gravity	IS 2720 Part 3 (1980)/ASTM D854-14 (2014)
Hygroscopic water content	IS 2720 Part 2 (1973)/ASTM D4959 (2016)
Saturated hydraulic conductivity	IS 2720 Part 17 (1986)/ASTM D2434-68 (2011)
Specific surface area	Cerato and Lutenegger (2002)
Linear shrinkage	IS 2720 Part 20 (1992)/ASTM D4943 (2013)
Free swell index	IS 2720 Part 40 (1977)/ASTM D4546 (2014)
Grain size distribution	IS 2720 Part 4 (19854)/ASTM D6913-17 (2009)
Liquid limit and plastic limit	IS 2720 Part 5 (1985)/ASTM D4318-17 (2010)
Shrinkage limit	IS 2720 Part 6 (1972)/ASTM D427-04 (2008)
USCS classification	ASTM D2487-17 (2006)
Compaction characteristics	IS 2720 Part 7 (1980)/ASTM D698-07 (2007)
Soil pH value	IS 2720 Part 26 (1987)/ASTM D4972-13 (2013)
Percentage of organic matter	IS 2720 Part 22 (1972)/ASTM D2974-14 (2014)
Cation exchange capacity	IS 2720 Part 24 (1976)/ASTM D7503-18 (2014)

Table 3.3 Properties of soil materials used in the study

Properties	Soil Materials									
	MS	**FA**	**RS**	**BS**	**BN**	**RF**	**BF**	**FB**	**RB**	**BB**
General										
Specific gravity (G)	2.69	2.17	2.68	2.61	2.88	2.41	2.38	2.51	2.72	2.69
Hygroscopic water content (%)	2.54	2.63	5.45	9.17	11.6	3.95	5.73	6.85	7.31	9.92
Saturated hydraulic conductivity (m/s)	4×10^{-05}	2×10^{-07}	3×10^{-09}	2×10^{-09}	2×10^{-12}	3×10^{-08}	4×10^{-08}	3×10^{-09}	2×10^{-10}	4×10^{-10}
Specific surface area (m^2/gm)	NA	67	55	89	348	31	48	109	143	167
Linear shrinkage (%)	NA	NA	1.83	1.95	3.22	0.56	1.35	1.32	2.25	3.70
Free swell index (%)	NA	NA	10	12	686	4	5	75	213	214
Grain size distribution (%)										
Gravel > 4.75 mm	0.0	0.0	0.0	0.0	0.0	0.0	0.0	0.0	0.0	0.0
2.00 mm < Coarse sand < 4.75 mm	13.6	0.0	17.2	14.3	0.0	8.3	7.2	0.0	12.0	10.2
0.425 mm < Medium sand < 2.00 mm	69.6	0.0	15.6	15.5	0.0	7.7	8.2	0.0	10.8	10.7
0.075 mm < Fine sand < 0.425 mm	15.4	24.0	16.0	8.2	4.9	20.4	17.3	14.6	12.7	9.2
0.002 mm < Silt < 0.075 mm	1.4	74.0	18.7	22.2	31.3	46.5	47.9	52.5	22.5	23.7
Clay < 0.002 mm	0.0	2.0	32.5	39.8	63.8	17.1	19.4	32.9	42.0	46.2
Atterberg limits										
Liquid limit (%)	NA	NA	42	60	295	33	37	93	117	130
Plastic limit (%)	NA	NA	22	33	42	17	19	20	28	35
Shrinkage limit (%)	NA	NA	21	22	11	16	18	17	18	19
Plasticity Index (%)	NA	NA	20	27	253	16	18	73	89	95
USCS classification	SW	ML	CL	CL	CH	ML	ML	MH	MH	MH
Compaction characteristics										
Optimum moisture content (%)	NA	19	20	29	33	19	24	22	23	32
Maximum dry density (g/cm^3)	NA	1.38	1.68	1.40	1.34	1.63	1.36	1.49	1.57	1.36
Chemical characteristics	NA									
Soil pH value (at 28.5^0 C)	NA	8.23	6.85	6.01	9.15	7.31	7.24	8.47	7.54	6.95
Percentage of organic matter (OM)	NA	NA	0.48	2.95	0.22	0.21	0.96	0.06	0.40	2.43
Cation exchange capacity (meq./100gm)	NA	1.85	8	10	27	3	6	8.32	13.7	15.1

NA: not applicable

Table 3.4 Chemical composition (by % weight) of the material used

Oxide (%)	Materials used				
	RS	**BN**	**BS**	**FA**	**MS**
SiO_2	61.92	49.13	52.23	46.47	NA
Al_2O_3	14.98	12.99	19.06	27.49	
Fe_2O_3	5.16	9.55	15.6	1.06	
MnO	0.101	0.016	0.54	2.93	
MgO	0.09	0.17	1.39	0.06	
CaO	0.02	3.09	1.32	2.84	
Na_2O	2.17	2.19	2.82	0.56	
K_2O	1.45	0.39	1.44	0.84	
TiO_2	0.68	1.6	2.76	6.58	
P_2O_5	0.009	0.025	0.09	5.20	
SiO_2+ Al_2O_3+ Fe_2O_3	82.06	71.67	86.89	75.02	
Loss on ignition	13.52	20.879	2.75	6.17	

3.4 Instrument/ Sensor used in this study

There are two basic parameters that describe the state of water in soil. One is soil water content and the other is soil water potential. 5TM sensor and profile probe were used to measure the volumetric soil water content (θ). A WP4 dew point potentiameter and TEROS21 sensor was used to measure matric soil suction (ψ) or soil water potential in the MLCS. A microclimate monitoring system was used for recording weather parameters in the study area. These instrument are discussed in the following section.

3.4.1 Volumetric water content sensors

Mainly two volumetric water content sensors i.e. 5TM and PR2/6 profile probe have been utilized in this present research study. 5TM sensor is produced by METER Group USA. (formerly Decagon Devices Inc., USA) and another sensor, PR2 profile probe is manufactured by Delta-T Devices Ltd, UK. According to the user manual provided by the manufacturing companies, these sensors indirectly measure volumetric soil water content, θ, via measurement of the dielectric constant of the soil media using capacitance/frequency domain technology. These sensors use an electromagnetic field by supplying oscillating wave of 70MHz to 100 MHz frequency to measure the dielectric constant of soil medium to determine its volumetric water content.

3.4.1.1 5TM Sensor

The 5TM determines θ by measuring the dielectric constant of the soil (or other porous media) using capacitance/frequency domain technology. Signal filtering minimizes salinity and textural effects, making the 5TM accurate in most soils and soilless media. Factory calibrations are included for mineral soils, potting soils, rock wool, and perlite. The 5TMs small size makes it easy to install in the field and the greenhouse. This robust sensor can be pushed directly into undisturbed soil to ensure good accuracy. The 5TM is installed and plugged into the Em50 data-logger. Fig. 3.1 shows 5TM with three prongs connected to a circuitry head and its compatible data logger. The zone of influence of the sensor is 5 cm around the edge of the prongs and 1 cm from the bottom end of the prong. A thermistor in contact with the prong provides the temperature reading. As 5TM is a digital sensor the output values are in digital. The value for permittivity is the apparent dielectric permittivity multiplied by a value of 50. According to the 5TM operator's manual 2015, the following Topp's equation (Topp et al. 1980) (Eq. 1) is recommended for relating dielectric property to the θ in mineral soils.

$$\theta = 4.3\times10^{-6}\times\varepsilon_a^3 - 5.5\times10^{-4}\times\varepsilon_a^2 + 2.92\times10^{-2}\times\varepsilon_a - 5.3\times10^{-2} \quad (3.1)$$

The range for apparent dielectric constant (ε_a) that can be measured is from 1 (air) to 80 (water) and the accuracy for measurements in θ using generic equation is about ± 3 %. For higher accuracy in measuring the volumetric water content soil specific calibration equation need to be developed for different soils. Few technical specifications of 5 TM sensor are listed in table 3.5.

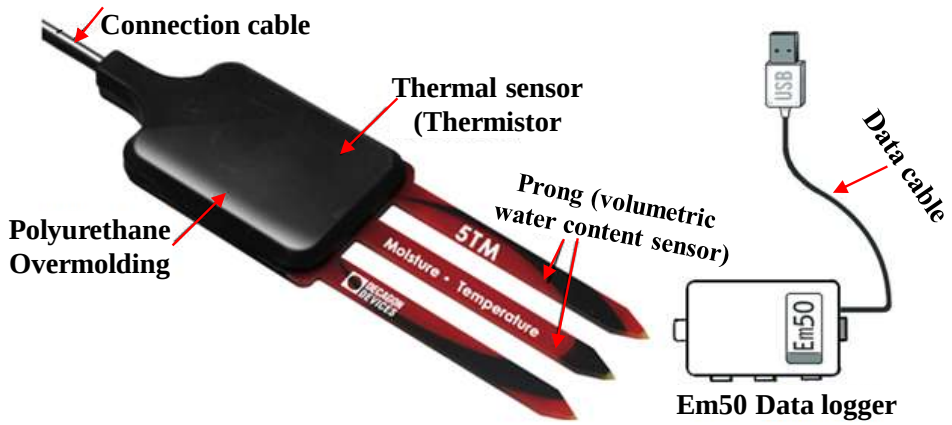

Fig. 3.1 Em50 data logger and components of 5TM sensors (5TM manual, 2015)

Table 3.5 Technical specification of 5TM sensor

Measurement	Volumetric water content (θ), dielectric constant (ε_a) and temperature (T)
Measurement range	θ: 0 to 0.1 m^3/m^3; ε_a: 1 (air) to 80 (water); T: –40 – 60 °C
Accuracy	θ (Using Topp equation): ± 3% (mineral soils that have solution electrical conductivity < 10 dS/m); ± 2% (using medium specific calibration in any porous medium), ε_a: ± 1 (1 – 40) and ± 15% (40 – 80); T: ± 1 °C
Resolution	ε_a: 0.1 (1 – 20), < 0.75 (20 – 80); θ: 0.08% (from 0 to 50% VWC); T: 0.1°C
Volume of influence	715 ml around the sensor
Operating Environment	Temperature: –40 to 60°C
Measurement time	150 ms (millisecond)
Power requirement	3.6 - 15 VDC, 0.3 mA quiescent, 10 mA during 150ms measurement
Output	RS232 or SDI-12
Connection type	3.5mm "stereo" plug, or stripped and tinned lead wires (3)
Cable length	5 m
Compatible data logger	Em50 data logger
Construction material	Vinyl cover filled with polyurethane resin or macromelt
Dimension	10cm×3.2cm×0.7cm

Working principle of 5TM sensors

The basic principle behind the working of the sensors is that the dielectric constant (ε_a), of soil medium changes with its water content. Dielectric permittivity, ε_a is dependent on the capacitance property of the soil mass. The sensors give the output in millivolt (mV) based on the soil capacitance property. The mV output is further converted to θ, based on the calibration equation. For highly saturated and dry soil mass, the value of ε_a would vary between 80 and 4. This broad range of ε_a is used to determine θ of a soil mass. Appropriate calibration equation parameters have been used for soils used in this study by performing laboratory calibration. The sensor comprises of an oscillator working at a frequency of 70 MHz, which generates an electromagnetic (EM) field. The EM field charges the soil around the sensor. This stored charge is measured using copper traces provided on the prongs and is proportional to ε_a and θ. It must be noted that the EM field produced by the sensor decreases with distance from prong surface and hence θ measurement is confined to a zone of 50 mm from edge of the prong.

3.4.1.2 PR2/6 Profile Probe

The PR2/6 Profile Probe (PR2/6-UM-3.0, Delta-T Devices Ltd., UK) as shown in Fig. 3.2 measures θ of the soil medium at 6 different depths up to 100 cm below the ground surface. The probes are inserted into a specially designed access tube with thin-wall tubes, which maximize the penetration of the electromagnetic field into the surrounding soil. Access tubes are manufactured to strict tolerances and are exceptionally strong and durable in the soil. Correct installation is essential requiring the use of specially designed auger equipment. The technical specifications of PR2/6 Profile Probe are listed in the Table 3.6.

Working principle

The PR2 Profile Probe measures θ with minimal influence from either salinity or temperature. It consists of a sealed polycarbonate rod, ~25mm diameter, with electronic sensors (seen as pairs of stainless steel rings) arranged at fixed intervals along its length. The output from each sensor is a simple analogue dc voltage (V). These outputs are easily converted into soil moisture using a general soil calibration (Eq. 3.2).

$$\theta = \frac{\left(1.125 - 5.53V + 67.17V^2 - 234.42V^3 + 413.56V^4 - 356.68V^5 + 121.53V^6\right) - a_0}{a_1} \quad (3.2)$$

where a_0 and a_1 are the calibration coefficients.

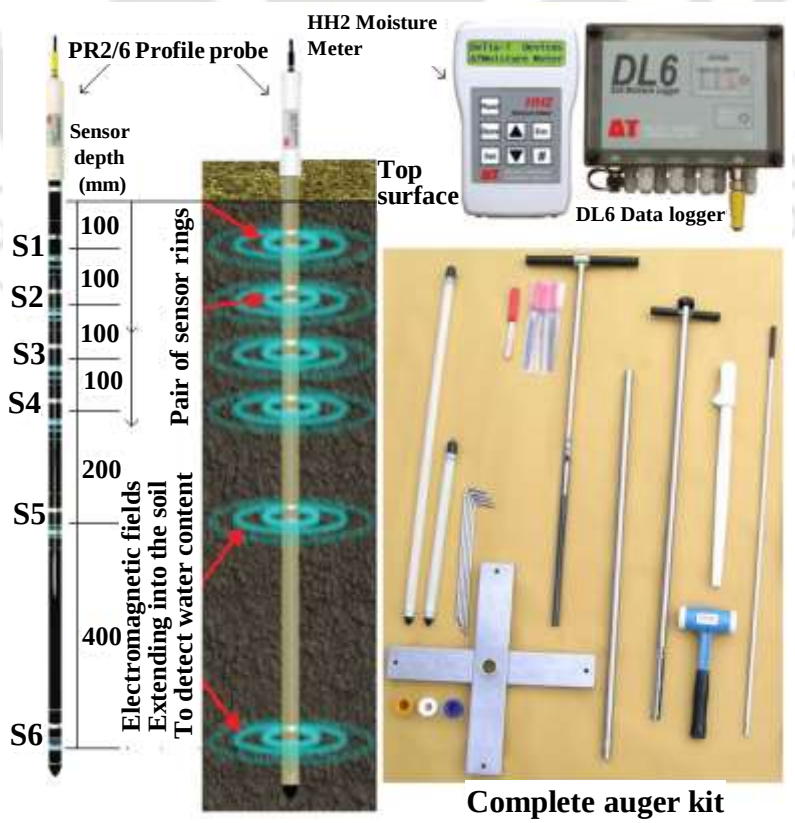

Fig. 3.2 Different components of PR2/6 profile probe and its accessories

Table 3.6 Technical specifications of PR2/6 Profile Probe

Measurement	Volumetric soil moisture content (θ)
Measurement range	0 to 1.0 m^3/m^3
Accuracy	±0.04 m^3/m^3, 0 to 40°C (after soil specific calibration)
	±0.06 m^3/m^3, 0 to 40°C (with generalized calibration)
Volume of influence	Vertically: ~95% sensitivity within ±50 mm of upper ring of each pair.
	Horizontally: ~95% sensitivity within a cylinder of radius 100 mm.
Environment	0 to 40°C for full accuracy, –20 to 60°C full operating range.
Measurement time	Full accuracy achieved within 1s from power-up.
Power requirement	Minimum: 5.5V DC with 2m cable, Maximum: 15V DC. PR2/6 consumption: < 120 mA
Output	For (PR2/6), 6 analogue voltage outputs: ~0 to 1.0V DC corresponding to 0 - 0.6 m^3/m^3 (mineral calibration)
Connection type	8-core screened.
Cable length	2 m
Compatible data logger	DL6 Data logger, Handheld moisture meter
Construction material	25.4mm polycarbonate tube with pairs of stainless steel rings
Dimension	Length: 1350mm and diameter: 25.4 mm
Weight	Weight: 0.95 kg

Handheld moisture meter

HH2 handheld moisture meter is a readout unit for recording θ from the Profile Probe. Readings are displayed on the LCD and can be stored for later download to a PC. Alternately, a DL6 logger (Delta-T Devices Ltd., UK) can be used for continuous monitoring of θ variation with time which provides a cost-effective solution for logging Profile Probes is utilized in this study.

3.4.2 Soil suction sensors

This study uses TEROS21 sensor (METER Group, USA) and WP4 dew point potentiameter (WP4-T, METER Group, USA) for measuring soil suction.

3.4.2.1 TEROS21 sensor

The TEROS21 sensor is a matric water potential sensor that provides long term, maintenance-free soil water potential and temperature readings at any depth without sensitivity to salts. The range of the TEROS21 sensor varies from field capacity to air dry. Its epoxy over-molding can withstand harsh soil environment when buried in the field. The TEROS21 sensor uses a silica based ceramic material that doesn't degrade and doesn't need

replacement or recalibration. The sensor is accurate in salty environments, a variety of soils, and even in locations where the salinity conditions change over time. The TEROS21 sensor is composed of a moisture content sensor and a porous substrate with a known moisture release curve. After the porous material has equilibrated with the surrounding soil, the moisture sensor measures the water content of the porous material, the sensor uses the moisture release curve to translate moisture content into water potential. The sensor's measurement range depends on the pore size distribution wherein wider the range of pore sizes, higher the measurement range. The TEROS21 sensor uses a ceramic interface for higher measurement range. However, a sensor's accuracy depends on how well the moisture release curve characterizes the porous substrate in that particular sensor. Fig. 3.3 shows different components of TEROS21 sensor and the technical specifications are mentioned in Table 3.7.

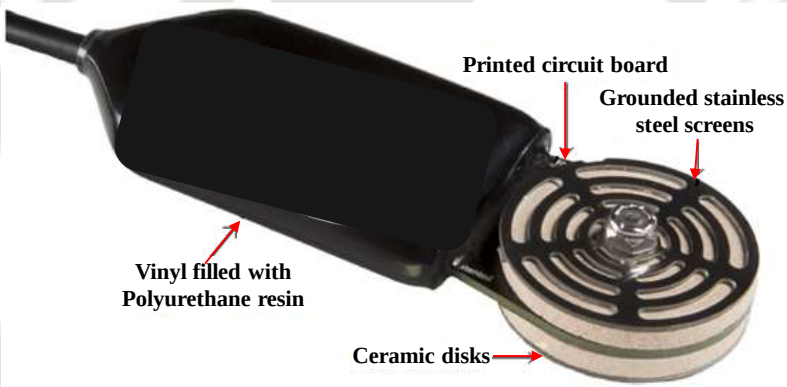

Fig. 3.3 Different components of TEROS21 sensor

Table 3.7 Technical specifications of TEROS21 sensor

Measurement	Soil water potential (ψ), Soil Temperature (T)
Measurement range	ψ: -9 to -100,000 kPa; T: -40° to 60°C
Accuracy	ψ: ±(10% of reading + 2 kPa) from -9 to -100 kPa; T: ± 1°C
Resolution	ψ: 0.1 kPa; T: 0.1°C
Operative environment	-40–60°C (Water potential measurements may be wrong below 0°C)
Measurement speed	150 ms (millisecond)
Equilibrium time	10 min to 1 hour depending on soil water potential
Sensor type	Frequency domain with calibrated ceramic discs, thermistor
Power requirement	3.6 - 15 VDC, 0.03 mA quiescent, 10 mA during 150 ms measurement
Output	RS232 (TTL) with 3.6 volt levels or SDI-12 communication protocol
Connection type	3.5mm "stereo" plug, or stripped and tinned lead wires (3)
Cable length	5 m
Compatible data logger	Em50 Data logger
Construction material	Stainless steel screen, ceramic discs, vinyl cover filled of polyurethane resin
Dimension	9.6 cm (length) x 3.5 cm (breadth) x 1.5 cm (width)

Working principle

TEROS21 sensor uses the same principle as the second law of thermodynamics, which states that connected systems with differing energy levels move towards an equilibrium energy level. When an object comes into hydraulic contact with the soil, the water potential of the object comes into equilibrium with the soil water potential. A wide range of water content measurements can be done by measuring the dielectric permittivity of the ceramic discs.

Water content and water potential are related by a relationship unique to a given material, called the moisture characteristic curve. The ceramic used with the TEROS21 sensor has a wide pore size distribution and is consistent between discs, giving each disc the same moisture characteristic curve. Thus, the water potential can be inferred with the moisture characteristic curve after measuring the water content of the ceramic. Eq. 3.3 represents the component variables for determining total soil water potential (ψ_t):

$$\psi_t = \psi_p + \psi_g + \psi_o + \psi_m \tag{3.3}$$

The subscripts p, g, o, and m are pressure, gravitational, osmotic, and matric, respectively. Of these four components, only ψ_o and ψ_m are significant and often measured in soil. TEROS21 sensor measures the matric potential of the soil ψ_m. A Em50 data logger is used for continuous data logging of suction measured from TEROS21.

3.4.2.2 Dew point potentiameter

A WP4 dew point potentiameter (METER Group; formerly Decagon, USA) shown in the Fig. 3.4 has been used to measure total suction (ψ_t) of the samples. This instrument works on the principle of chilled mirror dew point technique and estimate the relative humidity of the sample. The device consists of a sealed chamber with a cooling fan, a mirror, a photoelectric cell and an infrared thermometer. The soil sample is placed in a plastic or stainless steel container with a diameter of 40 cm. The container is then placed in the tray and moved into the temperature controlled chamber. There the sample specimen gets equilibrated with the chamber environment. A Peltier cooling system is used to reduce the temperature on the surface of the mirror to the dew point temperature. The photoelectric cell detects the first sign of condensation on the mirror and the temperature

at which the moisture appears at the mirror corresponds to the dew point. The temperature of the mirror at that point is measured by a thermocouple. The infrared thermometer measures the temperature of the chamber which is equal to the temperature of the sample at equilibrium condition. The vapour pressure above the soil specimen in the chamber and the saturated vapour pressure at the same temperature are computed using the dew point temperature and the sample temperature. The total suction of the sample is then calculated by Kelvin's equation (Fredlund and Rahardjo 1993). This whole calculation part is performed by the device and the suction value displayed on LED panel along with the temperature of the sample. A cooling fan is used to circulate the air and reduce the equilibration time which is approximately 5-10 min. The only limitation of this instrument is inaccurate measurement of total suction in very low suction range (below 1 MPa depending on the type of soil) and a small change in temperature can affect the suction value in that range.

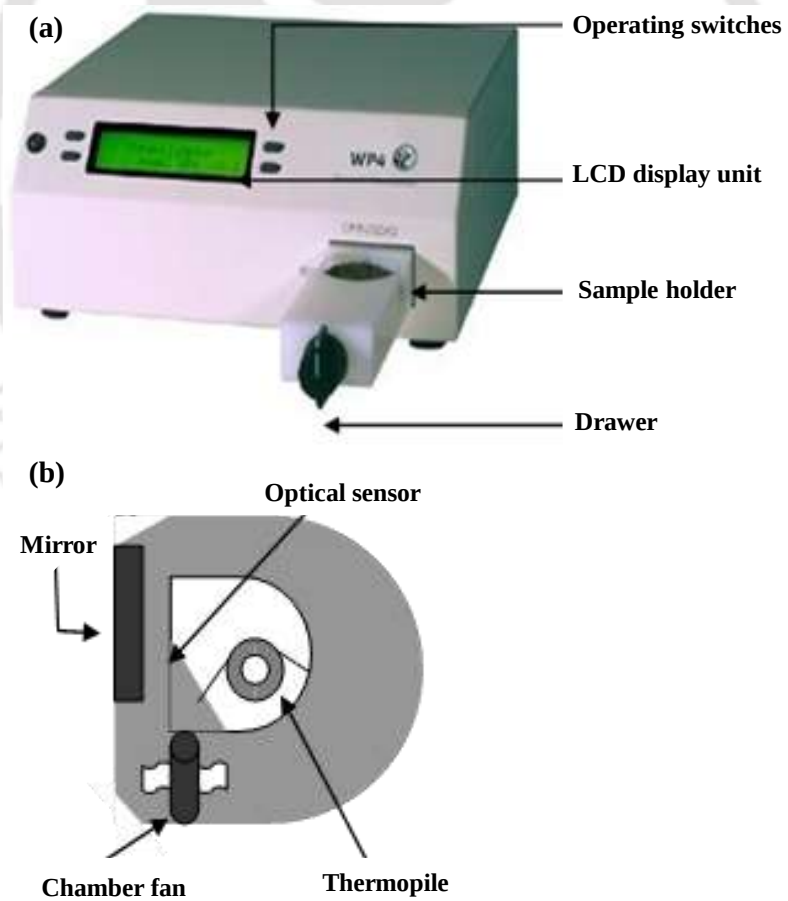

Fig. 3.4 Details of (a) WP4-C potentiameter and (b) block chamber

Calibration

The WP4 instrument need to be calibrated before using it to measure soil suction by a standard solution of 0.5M KCl. The solution should yield a total suction value of 2.19 ± 0.1 MPa at 25°C (WP4-T user manual). This standard solution of 0.5M KCl is provided by the manufacturer. If the measured suction of the solution is more or less than the given value, then the calibration was readjusted.

Sample preparation

Air dried sample was mixed with sufficiently high amount of deionized water and then sealed in disposable plastic packet for 24 hours for maturation. After 24 hours, the sample was filled in a plastic container by a spatula and placed it in the block chamber for suction measurement. The weight of sample was also measured using a high precision balance having accuracy of 0.0001g after each suction measurement. The sample cup was then left for air drying till the next measurement was taken. This whole process was done till high suction value was attained or increase in suction value was very low. At the end of the test, the specimen was placed in a drying oven for 24 hours to get the dry weight of the sample. With the help of dry weight and the wet weight the water content at each suction value was calculated and plotted in graphical form.

3.4.3 Microclimate monitoring system

In the study, a microclimate monitoring system (Meter group, USA) shown in the Fig. 3.5has been installed in the field for measuring the precipitation, temperature, relative humidity and wind speed.

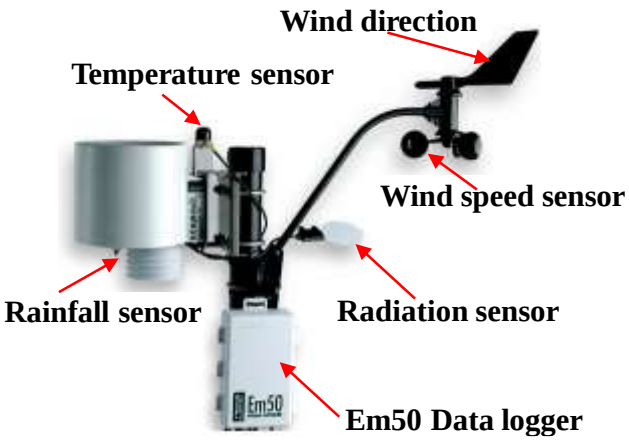

Fig. 3.5 Microclimate monitoring system for measuring climatic data

3.5 Theoretical concepts used in this study

This section represents the brief theoretical background of the current study with an attempt to understand the hydraulic performance of multi-layered cover system. For instance, concept of water flow in unsaturated soil media, hydraulic conductivity function, soil water characteristic curve and water balance have been discussed. Technical description of numerical modelling in HYDRUS 2D has also been presented in the section.

3.5.1 Water flow in unsaturated soil

Darcy's law can be extended to unsaturated flow with modification that conductivity becomes a function of the matric suction head (ψ). The modified equation for unsaturated media is presented as follows.

$$q = -K(\psi) \times \nabla H \tag{3.4}$$

where q is rate of water flow, $K(\psi)$ is hydraulic conductivity function, ∇H is the hydraulic head gradient, which may include both the suction and gravitational components. This equation along with its alternative formulation is known as the *Richards' equation.* The above equation does not account for the hysteretic behaviour of the SWCC. To account for transient flow processes, continuity equation is used as follows:

$$\frac{\partial \theta}{\partial t} = -\Delta.q \tag{3.5}$$

Thus,

$$\frac{\partial \theta}{\partial t} = -\Delta.\left[K(\psi)\Delta H\right] \tag{3.6}$$

The hydraulic head H in general, is the sum of suction head ψ and the gravity head z. The above equation can thus be written as:

$$\frac{\partial \theta}{\partial t} = -\Delta.\left[K(\psi)\Delta(z-\psi)\right] \tag{3.7}$$

Considering only flow along the vertical direction z the above equation transforms into:

$$\left(\frac{\partial \theta}{\partial t}\right) = \frac{\partial}{\partial z}\left[K(\psi)\frac{\partial(z-\psi)}{\partial z}\right] \tag{3.8}$$

$$\left(\frac{\partial \theta}{\partial t}\right) = -\frac{\partial}{\partial z}\left[K(\psi)\frac{\partial \psi}{\partial z}\right] + \frac{\partial K(\psi)}{\partial z} \tag{3.9}$$

This partial differential equation forms the basis of unsaturated flow through a soil system in one direction. This equation is highly non-linear and requires numerical method for solution. This study uses Hydrus 2D for solving this partial differential equation for MLCS.

3.5.2 Soil water characteristic curve (SWCC)

The SWCC is a graphical relationship between water content and suction of a soil. Hydraulically and physically, it means how much equilibrium water a soil can take at a given suction originally. It is also referred to as soil moisture retention curve or water retention curve. The various characteristic features associated with SWCC are shown in Fig. 3.6. Saturated water content (θ_s) is the maximum moisture content which a soil can have. It is moisture content corresponding to very low suction stress (ψ = 0). Initial linear portion of the curve represents saturated water content. Air entry value (ψ_{aev}) corresponds to the value of negative pore-water pressure when air enters the largest pore present in the soil sample. It is a function of the maximum pore size in a soil and is also influenced by the pore-size distribution within a soil. Soils with large, uniformly shaped pores have relatively low ψ_{aev}. The slope of SWCC represents the rate at which the volume of water stored within the soil decreases as the suction increases and vice versa, over a range of values from the air entry value to the pressure at the residual water content. The slope of SWCC determines water storage function. The rate of de-saturation decreases with increasing in slope. Residual suction (ψ_r) corresponds to the suction which corresponds to the residual water content in soils. Residual water content (θ_r) is the water content of a soil at which a further increase in negative pore-water pressure does not produce significant changes in water content. This point can also be expressed in terms of the degree of saturation by dividing the residual water content by the porosity of the soil.

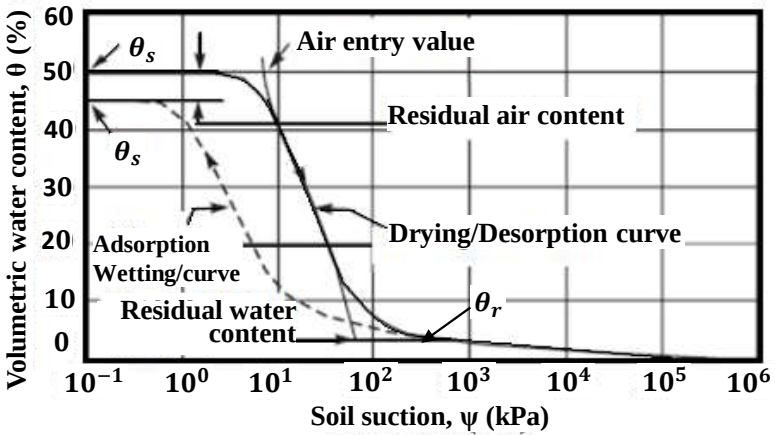

Fig. 3.6 Soil-water characteristic curve showing the regions of de-saturation

3.5.2.1 Equations for SWCC

Several equations have been proposed by the previous researchers for defining soil-water characteristic curves. The most common equations are proposed by Brooks and Corey (1966), van Genuchten (1980), Fredlund and Xing (1994). These equations are presented in terms of gravimetric rather than volumetric water content. Representation of the soil-water characteristic curve in terms of gravimetric water content (w) avoids experimental errors associated with volume change of the soil during drying. However, they can also be represented in terms of volumetric water content (θ). Equation for SWCC proposed by van Genuchten (1980) which can be presented in terms of w (Eq. 3.10) as well as θ (Eq. 3.11) is utilized for the current study.

$$w(\psi) = w_{rg} + (w_s - w_{rg}) \times \left[1 + a_g (\psi)^{n_g}\right]^{-1} \tag{3.10}$$

where a_g is function of the air entry value of the soil (kPa), n_g is function of the rate of water extraction from the soil, once the air entry value has been exceeded, w_s is saturated gravimetric water content, w_r is residual gravimetric water content, and ψ is soil suction (kPa).

$$\theta(\psi) = \theta_r + \frac{\theta_s - \theta_r}{\left[1 + (|\alpha\psi|)^n\right]^m} \tag{3.11}$$

where $\theta(\psi)$ is volumetric water content corresponding to suction, ψ, θ_s is saturated volumetric water content, θ_r is residual volumetric water content; α (related to air entry suction of the soil), n (related to pore size distribution of the soil) and m (related to overall symmetry of the SWCC) are van Genuchten parameters.

3.5.2.2 Hydraulic conductivity function (HCF)

Hydraulic conductivity is measured on the basis of availability of voids which are filled with water and it depends upon the properties of the fluid and the porous medium. In a saturated soil, the hydraulic conductivity is a function of the void ratio (Lambe and Whitman, 1979). In an unsaturated soil, it is significantly affected by combined changes in the void ratio and the degree of saturation (or water content) of the soil. As water flows through the pore space filled with water, the percentage of the voids filled with water become an important factor. As the suction increases or soil become drier air content increases and the hydraulic conductivity decreases. There are various methods by which

we can calculate the hydraulic conductivity of unsaturated soil but in each case the soil pore size distribution forms the basis for predicting the hydraulic conductivity. Previous researchers have proposed models for determining hydraulic conductivity function knowing the SWCC as listed in table 3.8. The present study utilizes the hydraulic conductivity function proposed by Mualem (1976).

Table 3.8 Various models for hydraulic conductivity function

Model	Equation	Fitting Parameters	Model type
Richards (1931)	$k(\psi) = a\psi + b$	a, b	Empirical
Gardner (1958)	$k(\psi) = \frac{k_s}{1 + a\psi^n}$	a, n	Empirical
Brooks and Corey (1966)	$k = \begin{cases} k_s & \psi \le \psi_b \\ k_s \left(\frac{\psi_b}{\psi} \right)^n & \psi > \psi_b \end{cases}$	n	Macroscopic
Campbell (1974)	$k(\theta) = k_s \left(\frac{\theta}{\theta_s} \right)^n$	n	Macroscopic
Mualem (1976)	$k(\psi) = k_s (S_e)^I \left[1 - \left\{ 1 - (S_e)^{\frac{1}{m}} \right\} \right]^2$	m	Statistical

Notes: $S_e = \frac{\theta(\psi) - \theta_r}{\theta_s - \theta_r}$, where S_e is the effective water saturation (0 < Se < 1), I is pore connectivity parameter which was estimated (Mualem, 1976) to be about 0.5 for many soils. $\theta(\psi)$ is volumetric water content (θ) corresponding to ψ suction,. k_s is saturated hydraulic conductivity, θ_s is the saturated volumetric water content, θ_r is the residual volumetric water content, and α, n and m are empirical parameters that depend on the soil type

3.5.3 Water balance model

Water balance is framework for simplifying, describing and quantifying the hydrological budget of water, which is specific to an area and time interval. It is driven by climate based on variations in precipitation, temperature and other local factors (vegetation, soils, land use, seasonality). Inputs, storages, and outputs are all distributed variables and vary with time. Rates of inputs and outputs and many other hydrological relevant properties vary spatially over geographic region. There are various methodologies to measure and calculate the different parameters like infiltration, evaporation, evapotranspiration, but water balance method is easy and applicable among all those measurement methods. In a

water balance analysis, the concept of conservation of water mass is applied to measure the storage, inflow, or outflow of it. For example, the water balance of a landfill cover system shown in Fig. 3.7 can be understood by Eq. 3.12.

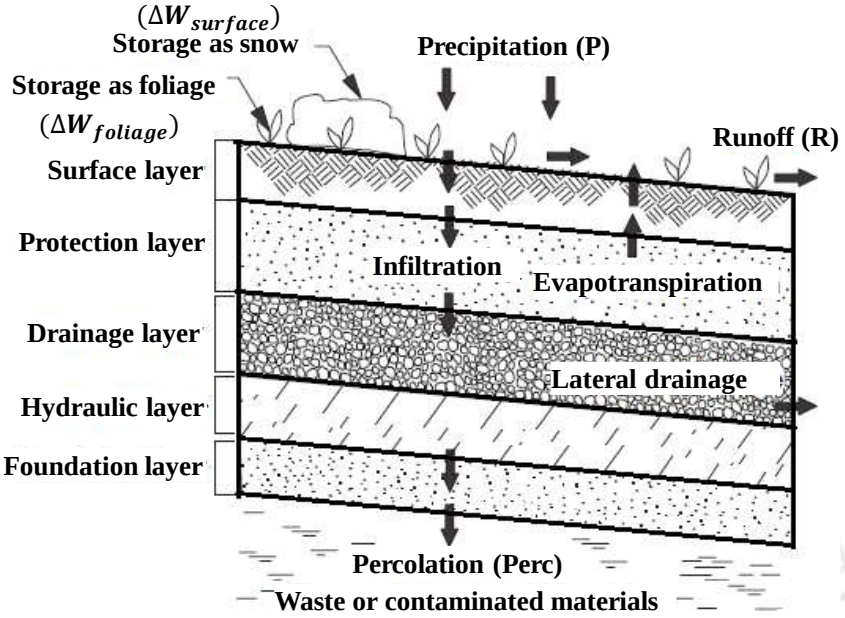

Fig. 3.7 Graphical Representation of water balance concept (Koerner and Daniel, 1997)

$$P = R + ET + \Delta W_{surface} + \Delta W_{foliage} + \Delta W_{soil} + L + PERC \quad (3.12)$$

where P is precipitation (mm/day), R is runoff (mm/day), ET is evapotranspiration (mm/day), $\Delta W_{surface}$ is change in water storage at surface (mm/day), $\Delta W_{foliage}$ is change in water storage on plant foliage (mm/day), ΔW_{soil} is change in water storage in cover system soil (mm/day), L is lateral drainage (mm/day), and $PERC$ is percolation through the cover system (mm/day).

Water is input to the cover system as precipitation in the form of rain or snow and lost from the cover system by runoff, ET, lateral drainage, and percolation. Water is present on the top of cover system as ponded water or snow, on plant foliage, and in cover system soils by capillary action. Infiltrated water which stored in the soil and percolate through its layer get escaped by evaporation and evapotranspiration if plants are there. For most cover systems, infiltration is primarily removed from the cover system by ET. Flow from lateral drainage layers is typically a much smaller component of the water balance than ET. For a cover system after the infiltration, percolation, and erosion are main aspects to worry about after its stability. Even if a relatively small amount of potential lateral flow is left un-drained in a cover system, hydraulic heads can build up over the hydraulic barrier, leading to destabilizing seepage forces on cover system slopes.

3.5.4 Modelling water flow in HYDRUS 2D

HYDRUS 2D is a two-dimensional unsaturated flow model developed by Simunek et al. (Šimůnek et al. 1999). The HYDRUS 2D program numerically solves the Richards's equation for saturated and unsaturated water flow and convection-dispersion type equations for heat and solute transport in horizontal as well as vertical section. Flow equation incorporates a sink term to account for water uptake by plant roots. Lateral flow and anisotropy also can be included. Precipitation and potential evaporation are the soil-atmosphere boundary condition input (climatic inputs) required for modelling.

The input soil properties required are saturated hydraulic conductivity and fitting parameters of soil water retention function. In addition, van Genuchten parameters can be predicted by inputting the percentage of sand, silt and clay, density, field capacity, and/or wilting point water content by neural prediction. Vegetation parameters required include the heads between which transpiration occurs and also the heads between which transpiration is optimal. The water flow part of the model considers prescribed head and flux boundaries, boundaries controlled by atmospheric conditions, free drainage boundary conditions.

Chapter 4

Performance Enhancement of Volumetric Water Content Sensors

4.1 General

An accurate measurement of the volumetric water content (θ) is essential for several geotechnical, geoenvironmental and hydrological projects. There are different electro-magnetic sensors for measuring θ with its inherent advantages and limitations. It is well established that a particular volumetric water content sensor should be specifically calibrated for individual soils for its better accuracy and reliability in measurement. This chapter discusses performance evaluation and improvement of PR2/6 profile probe and 5TM sensor for ten different soils/ geomaterials that has its application in waste containment projects.

4.2 Performance enhancement of profile probe

Profile probe (PP) (Model PR2/6 from Delta-T Devices, UK) is a handy instrument for simultaneously measuring θ at shallow multiple depths in the field. In this study, the accuracy of θ measurement is important for determining moisture migration and water balance associated with multi-layered cover system (MLCS) provided over non-operational landfills. There are no guidelines or controlled procedure for evaluating accuracy of PP for varying layers of MLCS. A simple laboratory setup is developed in this study to evaluate all six sensors of PP simultaneously for a particular soil type and compaction state. The results were used to improve accuracy of PP measurements for the type of soils generally used in MLCS.

4.2.1 Background study on profile probe

Soil water content measurement is necessary for carrying out researches in various geoenvironmental projects such as monitoring the performance of waste containment liners and covers, rainfall induced slope stability and pavements (Bonaparte et al. 2002; Scanlon et al. 2005b; Albright et al. 2006b; Roseen et al. 2012). The gravimetric water content (w) determination is the most precise and reliable method, but needs destructive soil sampling and 24-hours oven drying, making it unsuitable for continuous real-time monitoring. Instantaneous, non-destructive and continuous measurement of θ using probes/ sensors is advantageous for research related to the field of agriculture, forestry, hydrology, soil

science, soil physics, geotechnical and geoenvironmental engineering and waste management (Eller and Denoth 1996; Gardner et al. 1998; Hillel 1998; Bradford et al. 2002; Li et al. 2005; Thompson et al. 2007). Several researchers have correlated θ with physical properties of the porous media such as soil suction, flow, infiltration, volume change and strength (van Genuchten 1980; Bell et al. 1987; Dean et al. 1987; Robinson et al. 1999; Robinson and Friedman 2001; Bradford et al. 2002; Kelleners et al. 2004a and b; Li et al. 2005; Cosh et al. 2005).

Methods were developed in the past for indirect non-destructive measurement of θ based on its correlation with properties such as electromagnetism, electrical resistivity, impedance, dielectric permittivity and capacitance of the porous media (Dean et al. 1987; Cambell 1990; Evett and Steiner 1995; Gaskin and Miller 1996; Paltineanu and Starr 1997; Friedman 1998; Kelleners et al. 2004b). Accordingly, different sensors/ probes emerged based on the concept of neutron scattering, the gamma ray attenuation, time domain reflectometry, frequency domain reflectometry, time domain transmission, capacitance and impedance (Bell et al. 1966; Topp et al. 1980; Ledieu et al. 1986; Bell et al. 1987; Evett and Steiner 1995; Noborio 2001; Friedman 2005; Wraith et al. 2005). Among all the sensors and probes, profile probe (PP) developed by Delta – T Devices Limited is found to be quite handy for measuring θ at multiple shallow depths up to 1 m, simultaneously. It essentially has 6 sensors attached over its length of 1.0 m. PP measures θ as a function of dielectric constant (ε_a) of soil or more specifically to its square root of dielectric constant ($\sqrt{\varepsilon_a}$). These parameters are sensitive to particle size distribution, mineralogy, plasticity characteristics, organic content, density of soil (Friedman 2005; Lukanu and Savage 2006; Saito et al. 2009; Kodešová et al. 2011), salinity and temperature change (Baumhardt et al. 2000; Evett et al. 2006; Merlin et al. 2007; Loiskandl et al. 2010). Hence it is obvious that θ determination based on ε would also get influenced by the aforementioned factors. Therefore, it is important to ascertain whether measured θ by embedded sensors in PP would represent actual water content status present in a particular soil type. It is also expected that all embedded sensors of PP should give identical θ in a homogeneous soil with comparable density.

The apprehensions stated above are mainly related to the appropriateness of calibration equation that converts the measured electrical parameter of the sensor to θ of the soil. This issue becomes more prominent when PP is used for θ measurement in MLCS

where there are different layers of soils within 1m depth. A single general calibration equation as available for PP may not be appropriate for different soils with widely varying properties used in MLCS. For reliable and continuous measurements of θ in the field MLCS, a critical evaluation of PP measurements is required for ascertaining the preciseness of θ measurement by individual sensors and parity among all sensors. There are different studies that deals with calibration of volumetric water content sensors under both laboratory as well as field conditions (Yoder et al. 1998; Morgan et al. 1999; Baumhardt et al. 2000; Kelleners et al. 2004a; Polyakov et al. 2005; Evett et al. 2006). The studies on PP by previous investigators (Huang et al. 2004; Polyakov et al. 2005; Evett et al. 2006) revealed that laboratory calibration was superior to field calibration for ensuring better precision in θ measurement. These studies considered average value of θ measured by six sensors of PP with a presumption that there are no sensor related bias. The experimental procedure reported in past studies was not capable of controlled performance evaluation of each sensors of PP separately.

4.2.2 Materials and method

The PP measurements were performed for ten soils intended to be used in MLCS. The medium plastic red soil (RS) and black soil (BS) which are commonly found in India was used as the surface layer, medium sand (MS) was used as drainage layer and Bentonite (BN) from Barmer, Rajasthan, India was used to construct hydraulic barrier layer. In addition, two soil specimens designated as RF and BF were prepared by blending 50% of recycled fly ash (FA) with 50% of RS and BS respectively. Furthermore, three soil samples were prepared by uniformly mixing red soil, black soil and recycled fly ash (FA) with bentonite in the ratio 70:30 for hydraulic barrier application and designated as RB, BB and FB respectively. It was ensured that the proposed mix qualifies the permeability criterion requirement ($<10^{-9}$ m/s) of hydraulic barrier recommended by USEPA guidelines (Landreth et al. 1991)). The basic physical, geotechnical and chemical properties of all the soils were investigated using standard laboratory procedures reported in the ASTM or IS codes and presented in Table 3.2 of chapter 3.

Fig. 4.1shows the in-house developed experimental setup for the performance evaluation of PP. It consists of a wooden table of height 850 mm with a central hole of 28 mm diameter. A hollow PVC cylinder of 300 mm diameter, 250 mm height and 12 mm wall thickness was mounted on a Plexiglas plate with a central hole of 28 mm diameter.

The hole of Plexiglas plate was adjusted to coincide with the hole of the wooden table. A thin walled access tube (27 mm internal diameter) of PP was inserted through the central hole of the base plate. Total length of access tube is 1.05 m from the surface of soil sample to facilitate the scanning of all 6 six sensors through the soil sample. The access tube was secured at the bottom to maintain vertical position. For measurements, PP was inserted into the access tube which maximize the penetration of electromagnetic field within the surrounding soil mass. The measurement of θ was recorded with the help of a handheld moisture meter. The PP sensors can measure θ in the range 0% to 100% with an accuracy of ±6% and can operate in the temperature range of -20 ºC to +60 ºC (Delta-T Devices Ltd. 2008).

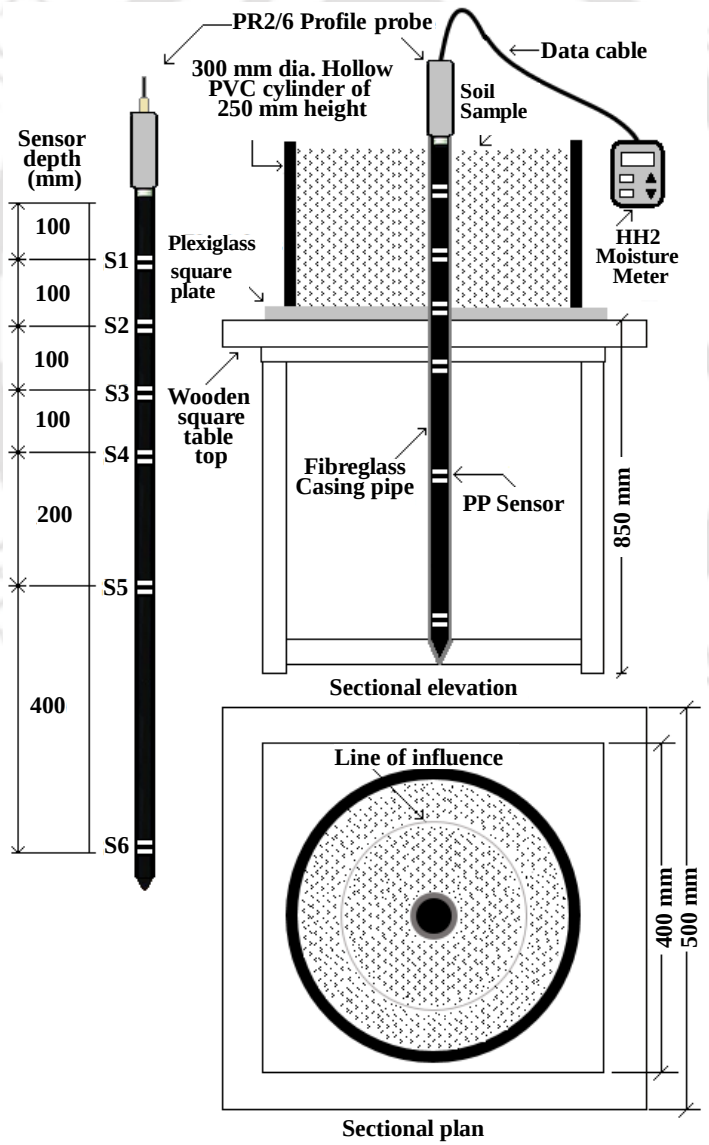

Fig. 4.1 Schematic diagram of the laboratory setup for calibration of PP sensors

Profile probe (PP) works on the principle of frequency domain reflectometry (FDR) and capacitance method (Whalley et al. 1992; Whalley et al. 2004; Czarnomski et al. 2005; Mwale et al. 2005). PP creates a 100 MHz signal to each of the sensors which in turn transmits an electromagnetic field into the soil mass. Radius of generated electromagnetic field is 100 mm from the sensor and each sensor has 50 mm zone of influence on top and bottom measured from the center of the sensor. The probe consists of sealed polycarbonate rod of 25.4 mm diameter and 1350 mm length and houses six embedded electronic sensors (designated as S1 to S6 in Fig. 4.1) along its length for measuring θ at 100 mm, 200 mm, 300 mm, 400 mm, 600 mm and 1000 mm from the top of the probe. PP sensor output is in terms of voltage V (volts). Eq. 4.1 is a 6th order polynomial for estimating square root of dielectric constant ($\sqrt{\varepsilon_a}$) of soil from measured V. It is then used to evaluate θ using linear relationship as shown in Eq. 4.2. (Roth et al. 1992; Kodešová et al. 2011).

$$\sqrt{\varepsilon_a} = 1.125 - 5.53V + 67.17V^2 - 234.42V^3 + 413.56V^4 - 356.68V^5 + 121.53V^6 \quad (4.1)$$

$$\sqrt{\varepsilon_a} = a_0 + a_1\theta \quad (4.2)$$

where, a_0 and a_1 are calibration parameters. Generalized values of parameters a_0 and a_1 are suggested as 1.6 and 8.4 for mineral soil and 1.3 and 7.7 for organic soils for PP measurements.

The soil mixed with required amount of gravimetric water content was compacted in the cylindrical mould in three layers using 2.6 kg rammer. For a particular soil, different initial compaction states were used to evaluate the performance of PP. Measurements of each sensor were performed at the mid location of PVC mould for cross-comparison of six sensor measurements. For each compacted sample, measurement was performed twice, once during insertion and again during removal to observe any inconsistency in the readings. Corresponding density and final water content of the compacted soil was measured after PP measurements by extruding nine undisturbed core samples from three different depths within the influence zone of the PP sensors. For every compaction state of a particular soil, volumetric water content was measured thrice by rotating the PP shaft at an angle of 120° to ensure repeatability and the measured θ is designated as θ_m.

It was observed that the readings of PP were fairly repeatable. For the same compaction state, the computed (theoretical) volumetric water content (θ_c) was determined using Eq. 4.3.

$$\theta_c = \frac{w \times \rho_d}{\rho_w} \tag{4.3}$$

where, w is average gravimetric water content determined based on oven drying method (105°C, 24 hours) by taking three samples from influence zone of PP sensor after measurement, ρ_d is the dry density of soil and ρ_w is the density of water. Performance evaluation of PP was conducted by comparing θ_m and θ_c If the comparison was poor, re-calibration was performed.

The existing field calibration methodology for the PP discussed in Qi and Helmers (2008) is found to be laborious. Their study did not attempt to evaluate individual sensors and hence the parity in sensor measurements were not ascertained. Computed volumetric water content θ_c was determined from soil bulk density and gravimetric water content obtained from undisturbed soil cores extracted at a location 1 m away from the access tube which was far beyond the influence zone of PP (0.2 m from access tube). This would have a significant influence on the performance evaluation of PP making it less representative. Huang et al. (2004) conducted laboratory calibration of PP by erecting soil column of 1.2 m height and 0.25 m diameter for accommodating all the sensors at a time to obtain PP measurements. The method is cumbersome, strenuous, material and time intensive for constructing the soil column and performing calibration. Most importantly, soil compaction will be non-homogeneous and hence the sensor measurements will be density dependent. In the current study, the proposed experimental setup was conceived with a view to circumvent these limitations. About one-fifth of the soil mass used by Huang et al. (2004) was required for the present setup making the compaction less tedious and less time intensive. The main advantage of the proposed experimental setup is that all the sensors of PP measures identical state of the soil (centre of the PVC cylinder), which is not possible while performing PP measurements in the field or in a long cylinder. This procedure is a novel modification of all the existing performance evaluation efforts for PP reported in the literature.

4.2.3 Observations and discussion

Fig. 4.2 depicts comparison of θ_m with θ_c for six sensors measured in six soils considered in this study. From the figure, it can be noted that θ_m marginally deviated from θ_c for soils MS, RS and BS and significantly deviated for soils RB, BB and BN (under prediction for RB and BN and over prediction for BB) necessitating a possible corrective measure for precise PP measurements. In general, deviation in θ_m was found to increase with plasticity and bulk density of soil, which is similar to observations reported in literature (Huang et al. 2004; Evett et al. 2006).

In this study, a two-way calibration was adopted by correlating θ_c to measured raw sensors' outputs in terms of voltage (V) and square root of dielectric constant $\left(\sqrt{\varepsilon_a}\right)$. Figure 4.3 shows the variation of computed θ_c as a function of measured voltage (V) for all the six sensors and six soil types. From the figure, it can be observed that the variation of θ_c follows a non-linear response with V. Hence, polynomial equations of different orders were fitted to the observed variation. For all sensors and different soil types, there is no significant improvement beyond third order polynomial calibration equation represented by Eq. 4.4.

$$\theta = AV^3 - BV^2 + CV - D \tag{4.4}$$

where A, B, C and D are sensor and soil specific calibration parameters summarized in Table 4.1. It is interesting to note that for the same type of embedded sensors, the calibration constants are not same in a particular soil. This aspect is generally not checked and validated for most of the projects involving PP measurements, with a presumption that there is no sensor related uncertainty. Figure 4.4 presents the relationship between θ_c and $\sqrt{\varepsilon_a}$ for all sensors and soils considered in this study. The variation is observed to follow a linear trend presented by Eq. 4.5.

$$\theta = a\sqrt{\varepsilon_a} - b \tag{4.5}$$

where, a and b are the soil specific calibration parameters summarized in Table 4.1.

Table 4.1 Details of soil and sensor specific calibration for all PP sensors

Soil Sample	Probe Sensor	Based on voltage measurement						Based on dielectric constant			
		Parameters				R^2	RMSE (%)	Parameters		R^2	RMSE (%)
		A	B	C	D			a	b		
MS	PPS1	-0.72	-1.68	-0.57	-0.07	0.99	0.35	0.13	0.20	0.99	0.85
	PPS2	0.70	0.45	0.34	0.04	0.96	2.08	0.12	0.18	0.95	2.18
	PPS3	0.14	0.72	0.37	0.08	0.98	1.48	0.13	0.22	0.97	1.73
	PPS4	-0.81	-2.30	-1.19	-0.21	0.98	1.50	0.13	0.21	0.97	1.79
	PPS5	-0.59	-1.91	-0.95	-0.16	0.99	1.02	0.14	0.24	0.99	1.15
	PPS6	0.45	0.27	0.14	0.04	0.95	2.09	0.13	0.22	0.94	2.33
FA	PPS1	3.35	6.21	4.74	1.11	0.98	0.43	0.14	0.21	0.96	1.01
	PPS2	0.78	0.65	0.29	0.03	0.97	1.22	0.12	0.23	0.95	1.56
	PPS3	1.17	2.14	1.72	0.41	0.98	1.15	0.15	0.20	0.94	1.12
	PPS4	2.51	4.32	2.54	0.61	0.97	1.03	0.11	0.21	0.96	1.17
	PPS5	2.52	5.43	3.01	0.71	0.98	1.21	0.13	0.18	0.97	1.53
	PPS6	3.61	7.52	4.32	1.02	0.99	0.56	0.14	0.17	0.96	1.23
RS	PPS1	4.44	8.31	5.72	1.22	0.99	0.55	0.13	0.20	0.99	1.06
	PPS2	0.94	0.55	0.26	0.02	0.99	1.33	0.14	0.25	0.98	1.69
	PPS3	2.13	3.10	1.97	0.37	0.99	1.28	0.13	0.22	0.99	1.13
	PPS4	3.71	6.23	3.84	0.71	0.99	1.01	0.12	0.21	0.99	1.21
	PPS5	3.80	6.47	4.01	0.73	0.99	1.37	0.12	0.17	0.99	1.62
	PPS6	4.80	8.62	5.47	1.06	0.99	0.70	0.12	0.18	0.99	1.15
BS	PPS1	2.95	4.30	2.42	0.42	0.99	1.37	0.14	0.27	0.99	1.91
	PPS2	2.16	2.70	1.38	0.21	0.99	1.08	0.14	0.27	0.99	1.71
	PPS3	3.84	6.28	3.77	0.71	0.99	1.53	0.13	0.25	0.99	2.00
	PPS4	2.59	3.85	2.29	0.42	0.99	0.99	0.13	0.24	0.99	1.28
	PPS5	3.50	5.66	3.42	0.63	0.99	1.13	0.13	0.23	0.99	1.29
	PPS6	5.43	9.79	6.22	1.23	0.99	0.88	0.12	0.22	0.99	1.36
BN	PPS1	2.37	2.87	1.59	0.35	0.98	2.53	0.17	0.40	0.98	2.91
	PPS2	6.12	12.31	9.37	2.46	0.98	2.68	0.17	0.38	0.98	2.96
	PPS3	5.35	10.04	7.14	1.73	0.96	2.24	0.16	0.36	0.98	2.52
	PPS4	-3.61	-11.1	-9.19	-2.39	0.99	2.09	0.16	0.35	0.97	3.47

	PPS5	-1.91	-6.89	-5.59	-1.34	0.98	3.02	0.16	0.38	0.95	4.17
	PPS6	-35.44	-93.6	-79.7	-22.2	0.99	1.48	0.18	0.47	0.95	4.44
RF	**PPS1**	2.32	5.31	3.67	1.07	0.99	0.33	0.16	0.23	0.94	1.21
	PPS2	0.81	0.75	0.23	0.56	0.98	1.33	0.17	0.25	0.96	1.74
	PPS3	1.11	1.13	1.61	0.63	0.99	1.21	0.16	0.24	0.96	1.32
	PPS4	2.42	3.35	2.44	0.71	0.98	1.11	0.13	0.22	0.94	1.74
	PPS5	2.31	4.37	3.23	0.69	0.99	1.32	0.15	0.23	0.96	1.82
	PPS6	2.23	6.46	3.43	1.23	0.99	0.65	0.17	0.27	0.94	1.91
BF	**PPS1**	1.77	3.42	3.35	0.35	0.99	1.52	0.17	0.21	0.98	1.71
	PPS2	3.32	1.36	2.22	0.28	0.99	1.10	0.16	0.23	0.98	1.81
	PPS3	2.35	5.44	4.55	0.78	0.99	1.42	0.14	0.22	0.97	2.07
	PPS4	1.51	2.52	3.31	0.51	0.99	0.88	0.15	0.26	0.98	1.23
	PPS5	2.62	4.65	2.53	0.67	0.99	1.21	0.15	0.24	0.98	1.31
	PPS6	6.33	7.82	5.11	1.11	0.99	0.74	0.14	0.21	0.97	1.29
FB	**PPS1**	1.74	3.59	1.45	2.35	0.98	1.96	0.15	0.38	0.98	2.65
	PPS2	5.22	10.12	8.36	1.36	0.98	2.72	0.13	0.37	0.98	2.81
	PPS3	4.33	9.05	6.23	1.63	0.96	2.32	0.17	0.39	0.98	2.36
	PPS4	3.56	5.12	8.23	2.41	0.99	2.11	0.17	0.32	0.97	3.41
	PPS5	1.72	4.93	4.65	1.45	0.98	3.13	0.19	0.35	0.95	4.15
	PPS6	5.54	5.65	9.62	8.24	0.99	1.81	0.16	0.41	0.95	4.32
RB	**PPS1**	4.45	9.07	6.70	1.53	0.99	0.89	0.11	0.14	0.98	2.06
	PPS2	1.73	3.10	2.55	0.60	0.99	1.38	0.12	0.17	0.98	2.18
	PPS3	0.47	0.63	1.04	0.31	0.98	1.76	0.12	0.18	0.96	2.80
	PPS4	2.95	5.32	3.81	0.83	0.99	1.69	0.13	0.20	0.98	1.92
	PPS5	2.39	4.64	3.72	0.86	0.99	1.27	0.13	0.18	0.97	2.39
	PPS6	5.73	11.25	7.93	1.75	0.99	1.15	0.13	0.21	0.99	1.73
BB	**PPS1**	8.32	16.11	10.54	2.19	0.99	1.20	0.11	0.23	0.98	2.30
	PPS2	6.70	12.55	8.06	1.63	0.98	1.82	0.12	0.23	0.98	2.32
	PPS3	6.54	11.91	7.41	1.45	0.99	1.10	0.12	0.24	0.97	2.43
	PPS4	6.71	12.32	7.73	1.53	0.98	2.22	0.12	0.25	0.96	3.11
	PPS5	4.68	8.16	5.01	0.95	0.99	1.25	0.12	0.21	0.98	1.94
	PPS6	7.87	15.05	9.76	2.00	0.99	1.47	0.12	0.23	0.98	2.33

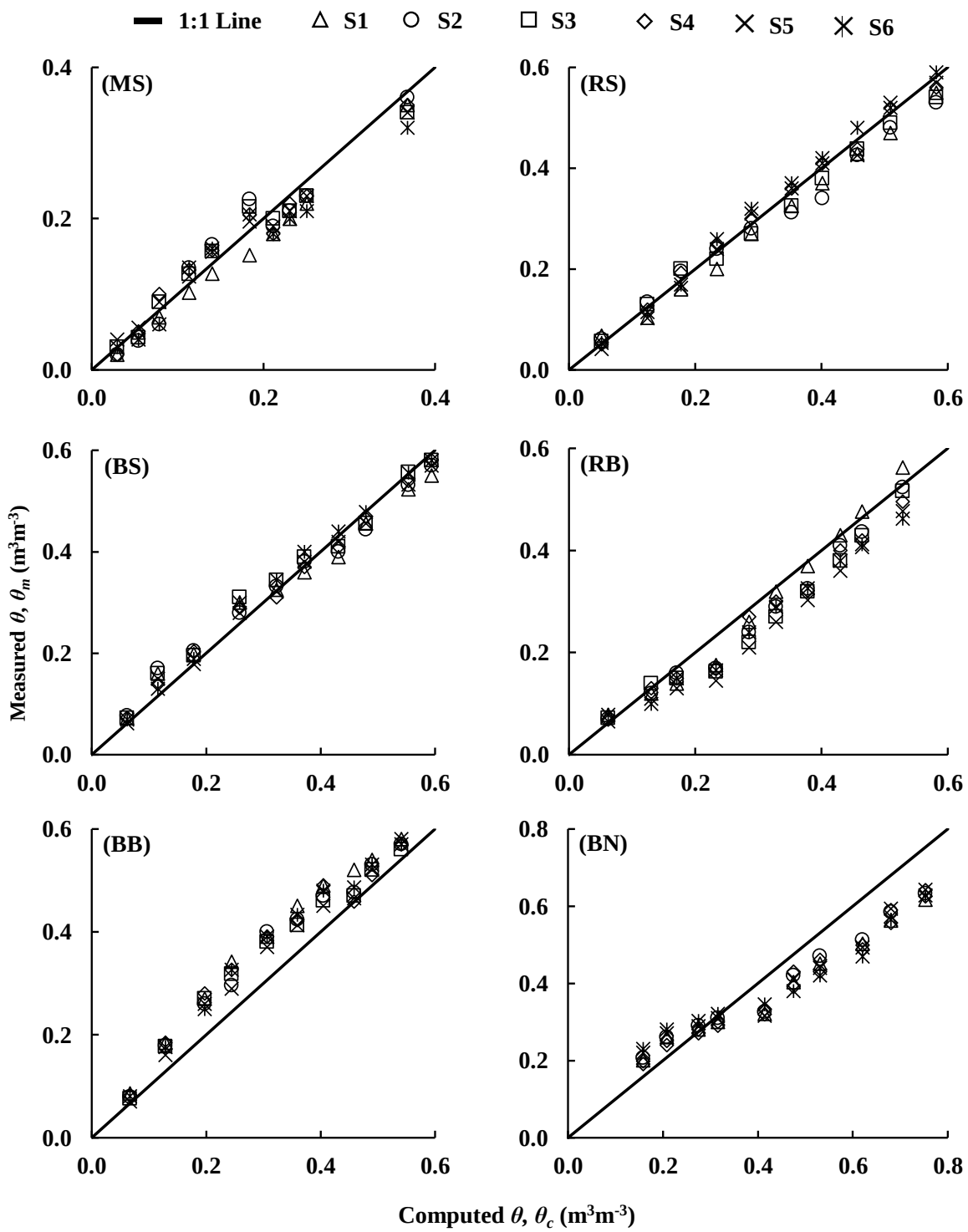

Fig. 4.2 Comparison of PP measurement, θ_m with computed volumetric water content, θ_c

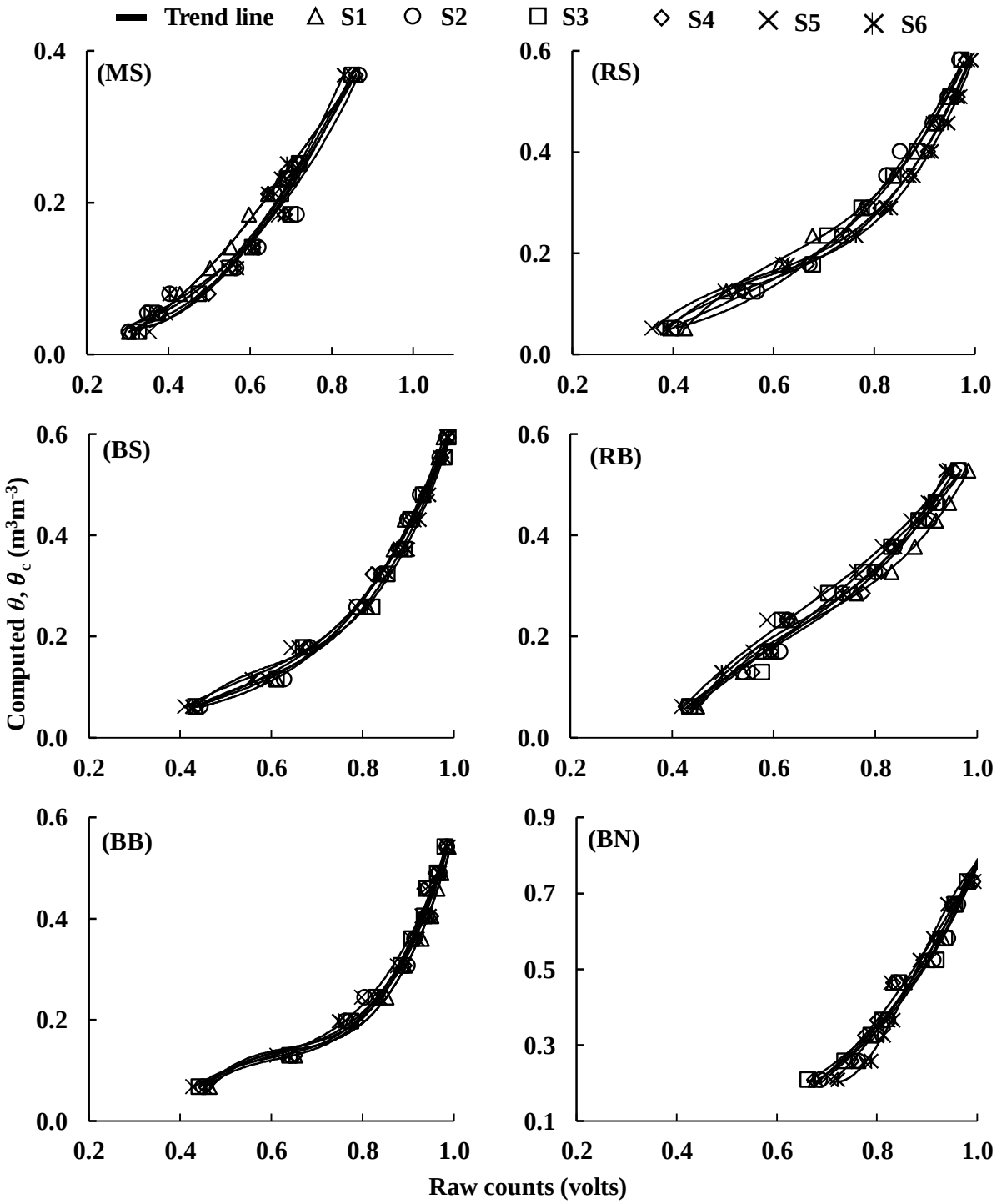

Fig. 4.3 Calibration of PP sensors with respect to measured voltage

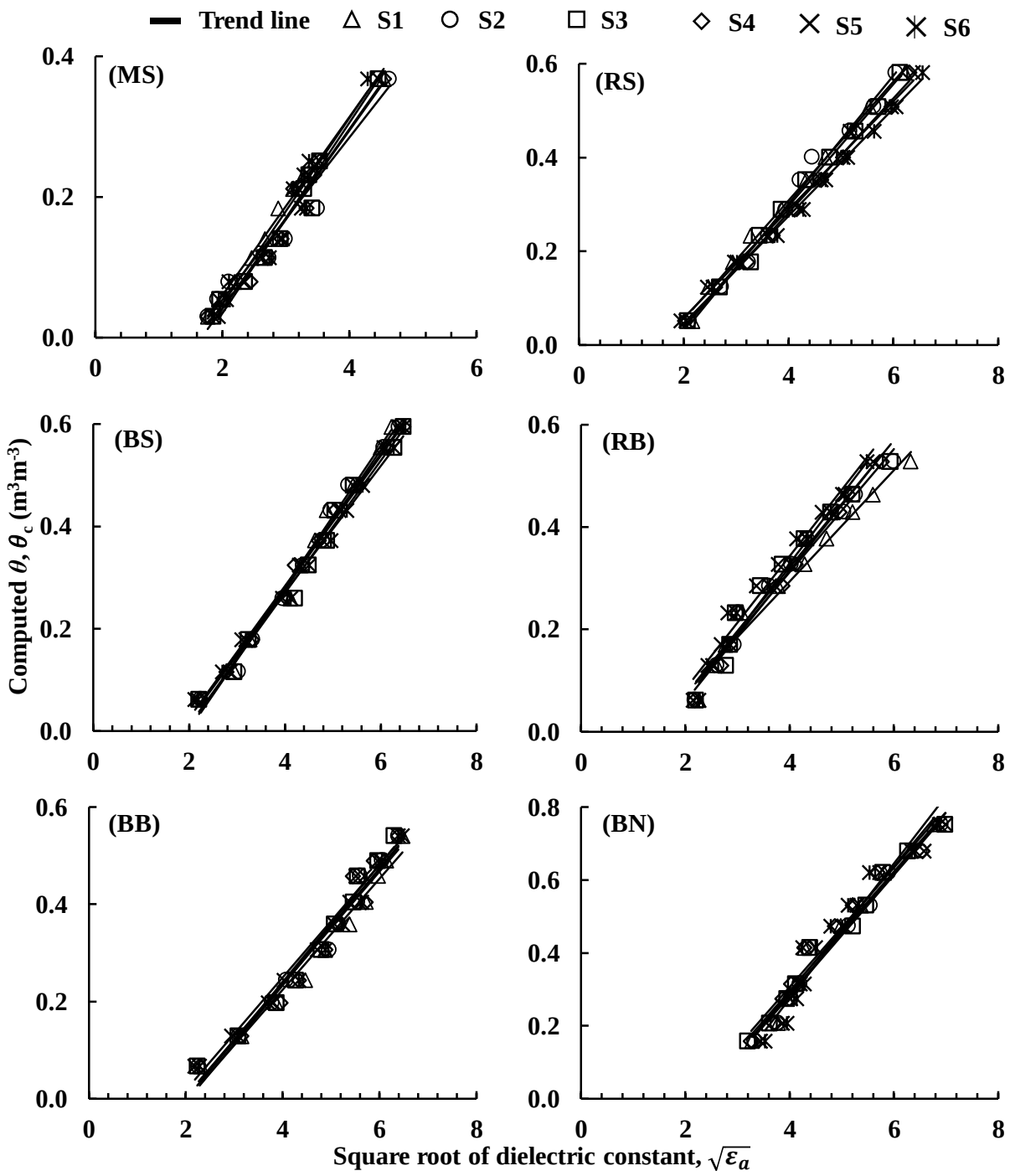

Fig. 4.4 Calibration of PP sensors by considering dielectric constant

The calibration constants reported in Table 4.1 were used to re-calculate θ_m from the known values of voltage V and $\sqrt{\varepsilon_a}$ The re-calculated values of θ_m are designated as θ_{mr}. The θ_{mr} was compared with corresponding θ_c as shown in Fig. 4.5 based on soil and sensor specific calibration equation in terms of $\sqrt{\varepsilon_a}$. For the sake of brevity, the results of θ_{mr} obtained from V is not presented here in. It is quite encouraging to note that there is a significant improvement in the accuracy of PP measurements when a soil and sensor specific calibration is performed using the laboratory setup developed in this study.

For unambiguous validation of newly proposed procedure, a new set of experimental data was generated and compared with θ_c as shown in Figs. 4.6 and 4.7 corresponding to measured V and $\sqrt{\varepsilon_a}$, respectively. From the two figures, it can be noted that θ_m matches well with θ_c for all soils and sensors. It is noteworthy to state that all the sensors gave consistently the same values after following the procedure stated in this study. For clarity, Fig. 4.8 presents the comparison of different sensor readings before and after calibration for the same compaction state for two soils RS and RB. The trends are similar for other soils as well and not presented here for brevity. It can be noted that for the same θ_c (particular compaction state), all the sensors gave different θ_m before adopting the procedure discussed in this study. This aspect is generally overlooked in the literature presuming that all the sensors would yield similar results. After performing sensor and soil specific calibration, the θ_m matched well with θ_c and all the sensors exhibited same values. The results shown in Figs. 4.6 and 4.7 also indicates that polynomial calibration based on measured V is marginally better than $\sqrt{\varepsilon_a}$ based linear calibration. This is further corroborated by marginally improved values of regression coefficient (R^2) and root mean square error (RMSE) for polynomial calibration presented in Table 2. Quantitatively the PP measurement accuracy improved from ±6 % to ±1 % and ±2 % in case of polynomial and linear calibration, respectively. The outcome of this study brings out the possibility of soil and sensor specific calibration errors that can result in improper interpretation of measured results in the field monitoring of projects such as MLCS. Following section aims to demonstrate the implication of improper PP measurements on change in soil water storage determination of different MLCS layers.

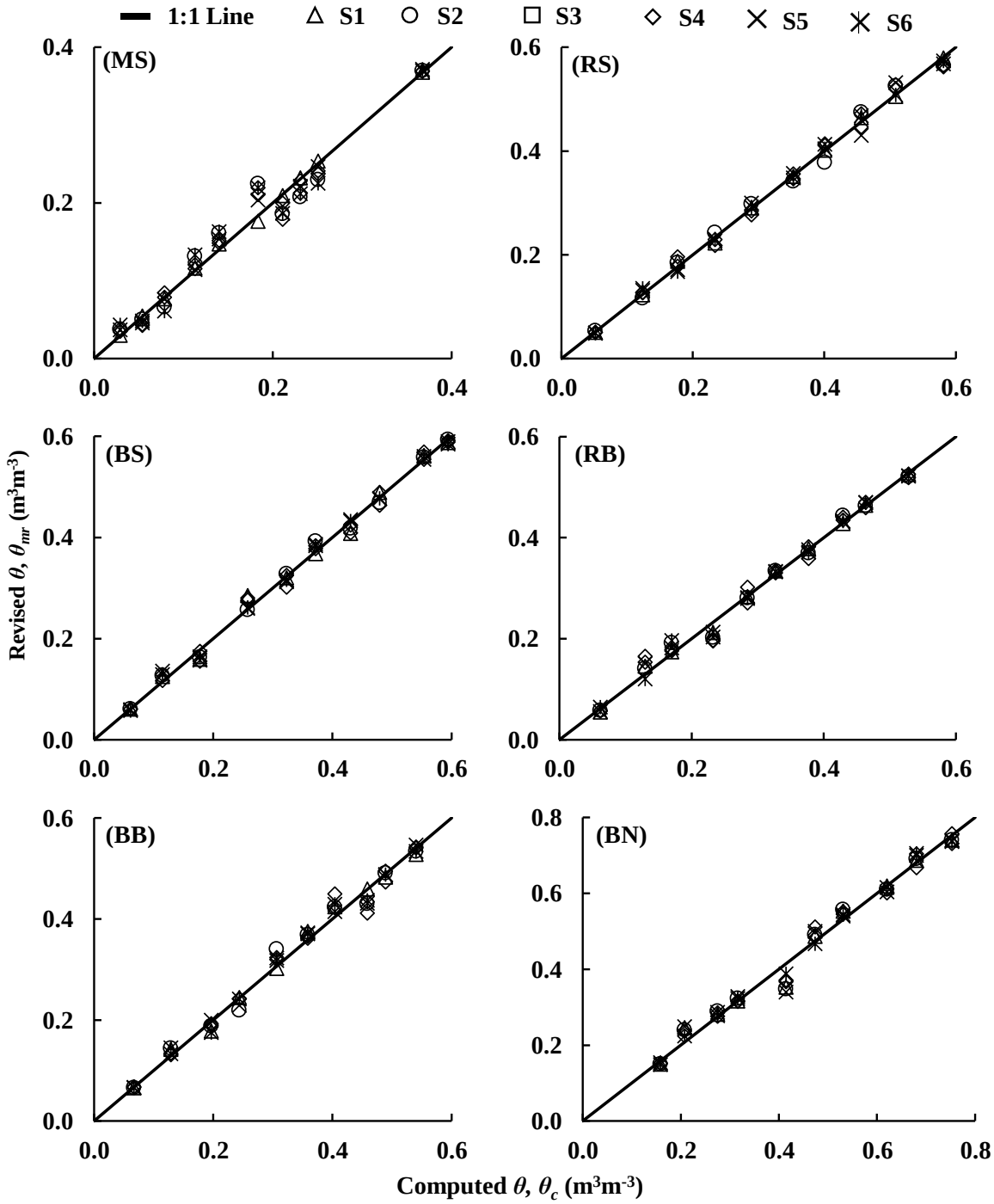

Fig. 4.5 Comparison of re-calculated PP measurements based on modified calibration

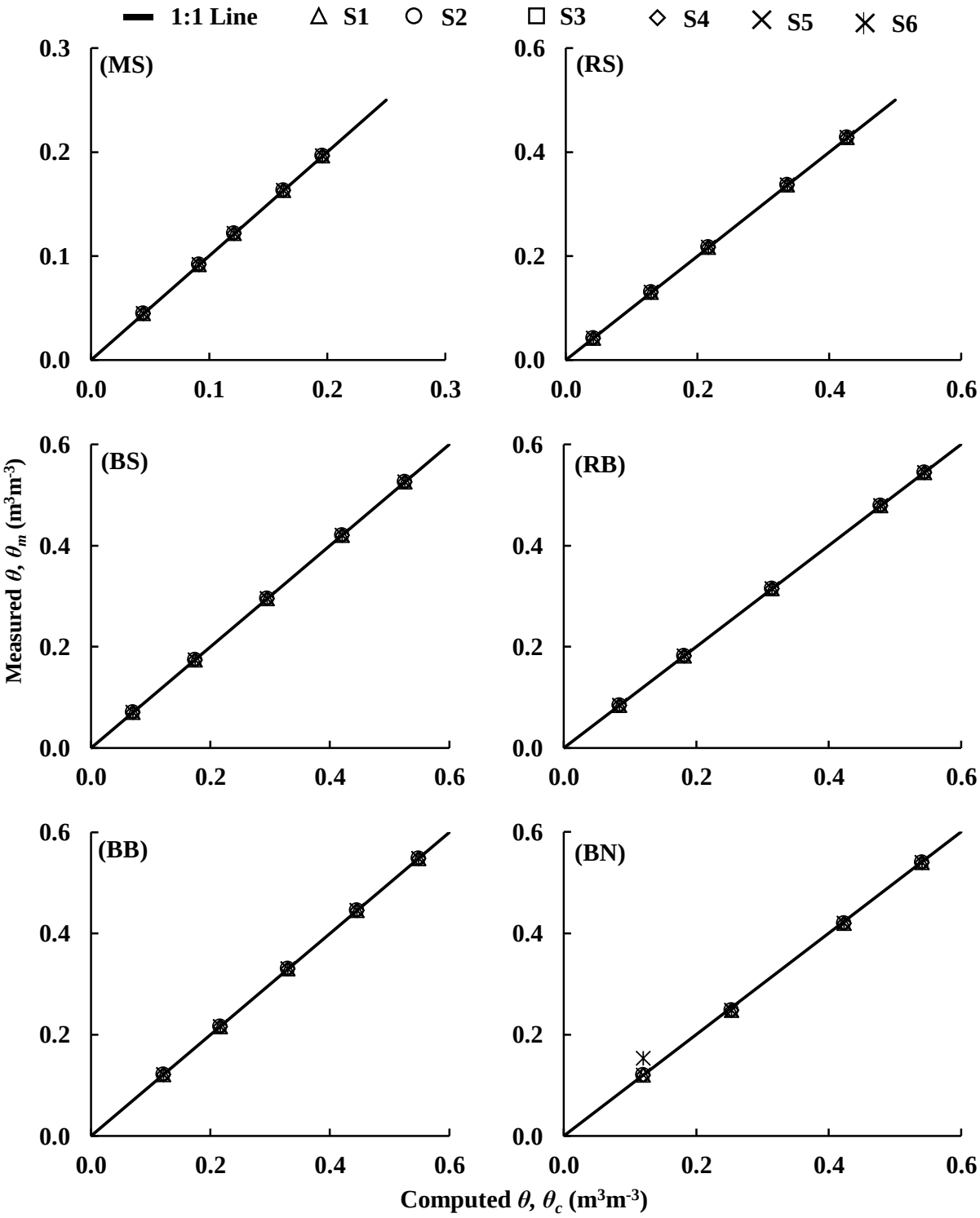

Fig. 4.6 Validation of calibration equation evaluated based on measured voltage

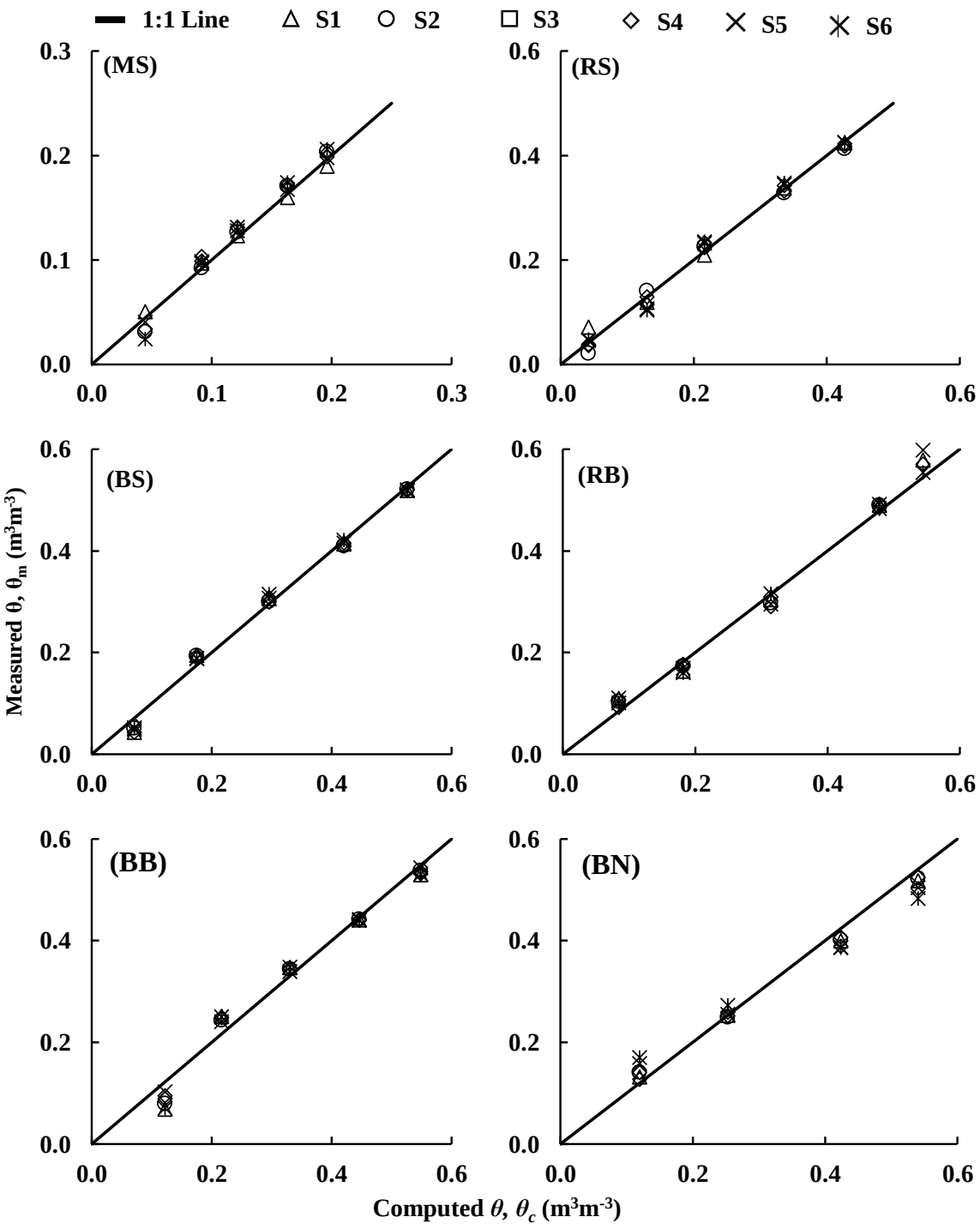

Fig. 4.7 Validation of calibration equation generated based on dielectric constant

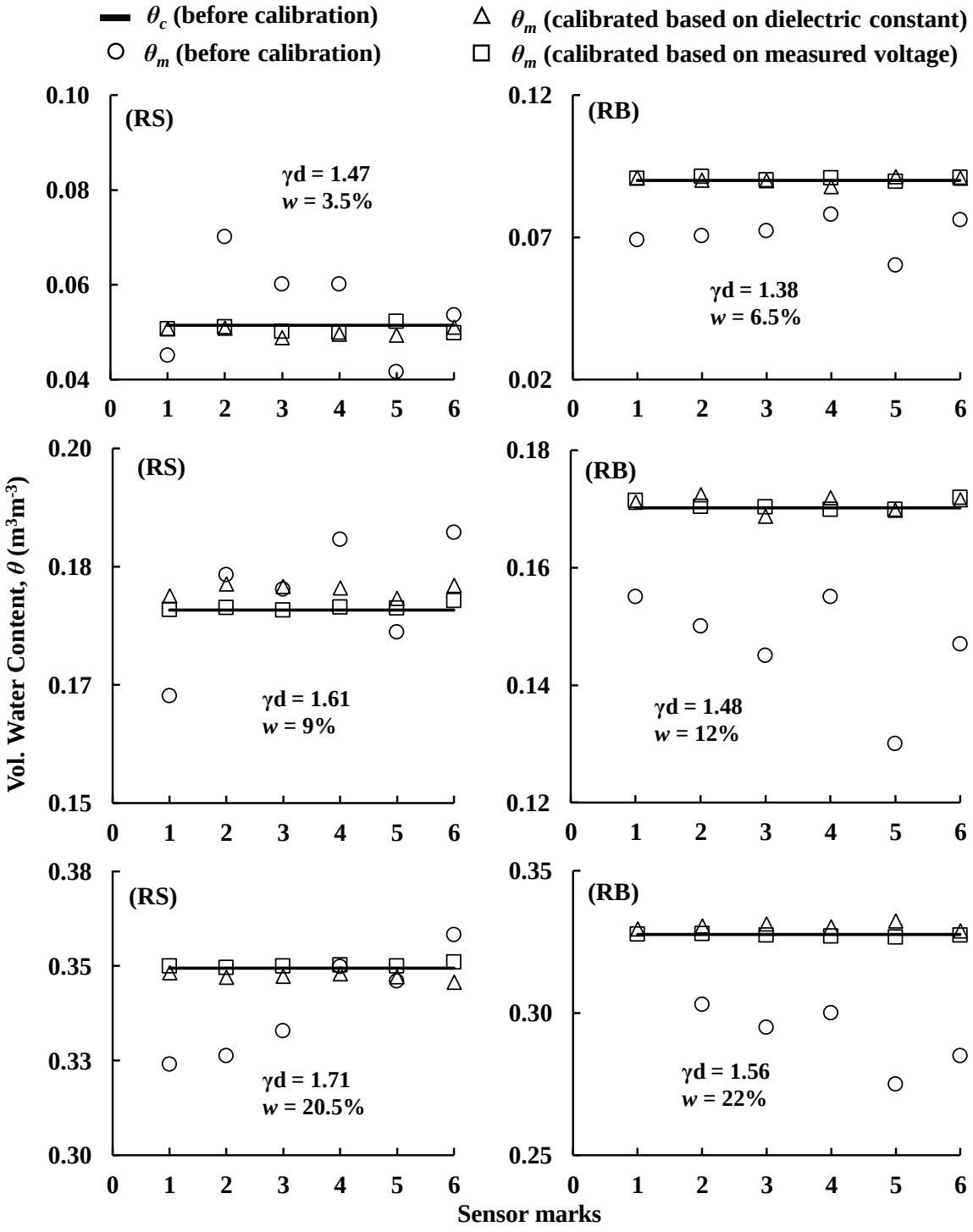

Fig. 4.8PP measurements at three various compaction state in RS and RB

4.2.4 Application of PP measurements

To establish the effectiveness of the proposed procedure, an experimental study was conducted using a cylindrical column replicating three layers of MLCS. The top layer of the column is a surface layer (RS) followed by drainage layer (MS) and a barrier layer (RB). The layered column was subjected to a constant head of 1.5 m of water at the top as illustrated in Figure 4.9 for exploring the hydraulic performance of each layer by monitoring volumetric water content (θ) with time using PP. If a soil mass of known volume is under continuous wetting or drying, Eq. 4.6 can be utilized to determine the change in soil water storage for a specific time duration (Albright et al. 2004). For a certain layer in MLCS, the positive and negative change in soil water storage implies wetting and drying of the soil mass, respectively.

$$\Delta S = V_G \times \left(\theta_f - \theta_i\right) \tag{4.6}$$

where, ΔS is the change in soil water storage for a particular time duration, V_G is the geometric volume of the soil, θ_i is the initial volumetric water and θ_f is the final volumetric water content for a given time duration.

In this study, the trial MLCS column was erected as shown in Fig. 4.9 to determine the change in soil water storage of the three layers using PP measurements. For the MLCS column, θ measurements in surface layer was possible with all the six sensors, in drainage layer by 5th and 6th sensor (Fig. 4.1) and in barrier layer by only 6th sensor. The results of ΔS presented in Fig. 4.10 were determined from θ_m measured using PP by following the calibration equation before and after the procedure proposed in this study. It can be clearly noted that all the sensors gave widely varying results for ΔS in RS (surface layer) before the corrective procedure was adopted. The error in ΔS of the surface layer was more pronounced for 2nd sensor as compared to other sensors. Figure 4.10 also details that ΔS were overestimated both in MS of drainage layer (5th and 6th sensors) and in RB of the barrier layer (6th sensor) before adopting soil and sensor specific calibration procedure. A maximum error of 18 % in the determination of ΔS was noticed for drainage layer. After employing the corrective procedure, ΔS determination obtained from all the sensors matched well. The observations clearly demonstrate the efficacy of laboratory procedure proposed in this study for improving the accuracy of PP measurements. Based on the observation, this study strongly advocates using the soil-specific and sensor specific correction of PP before using it for field monitoring programs associated with MLCS.

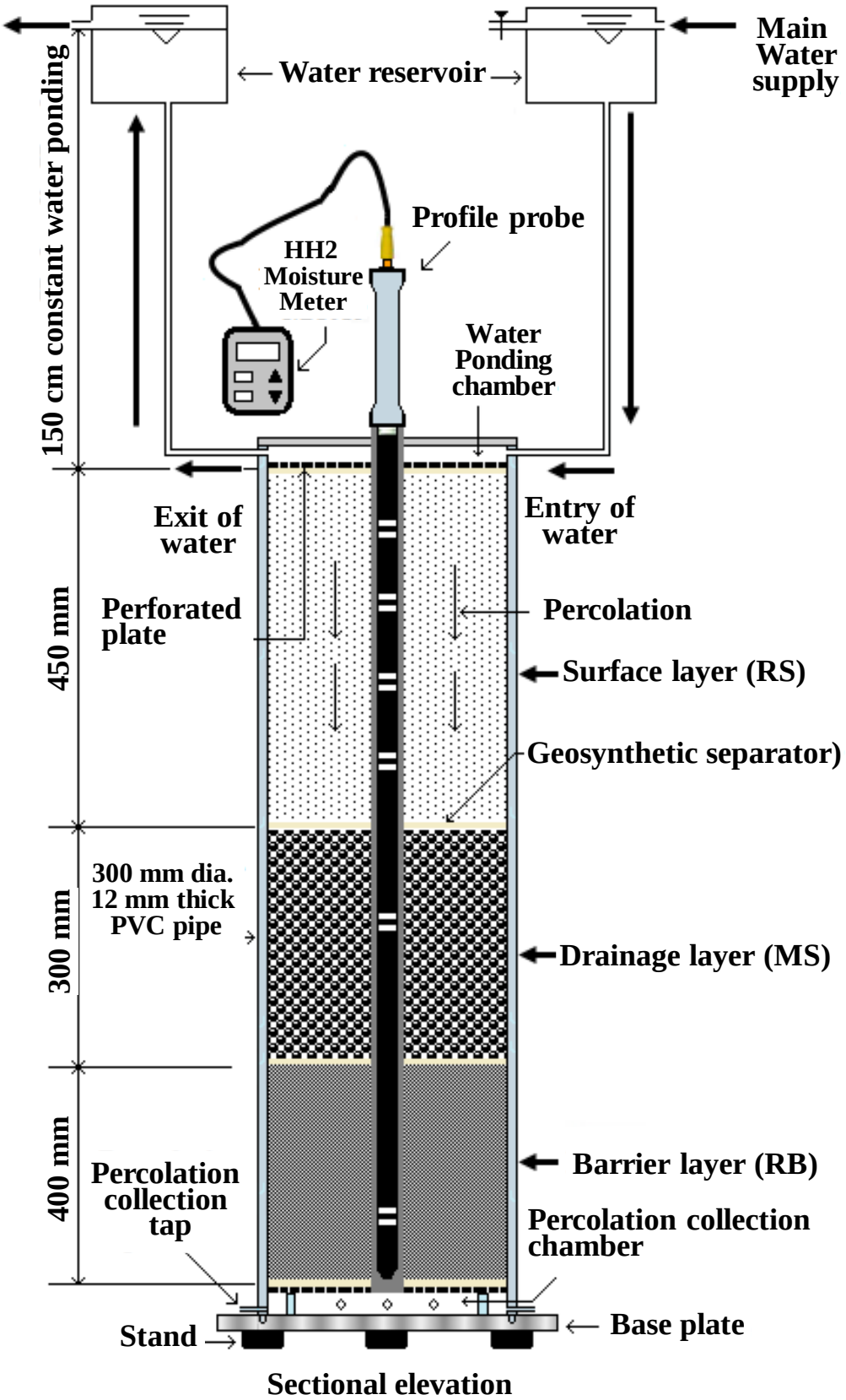

Fig. 4.9 Experimental column setup to assess effectiveness of the corrective procedure for PP measurement

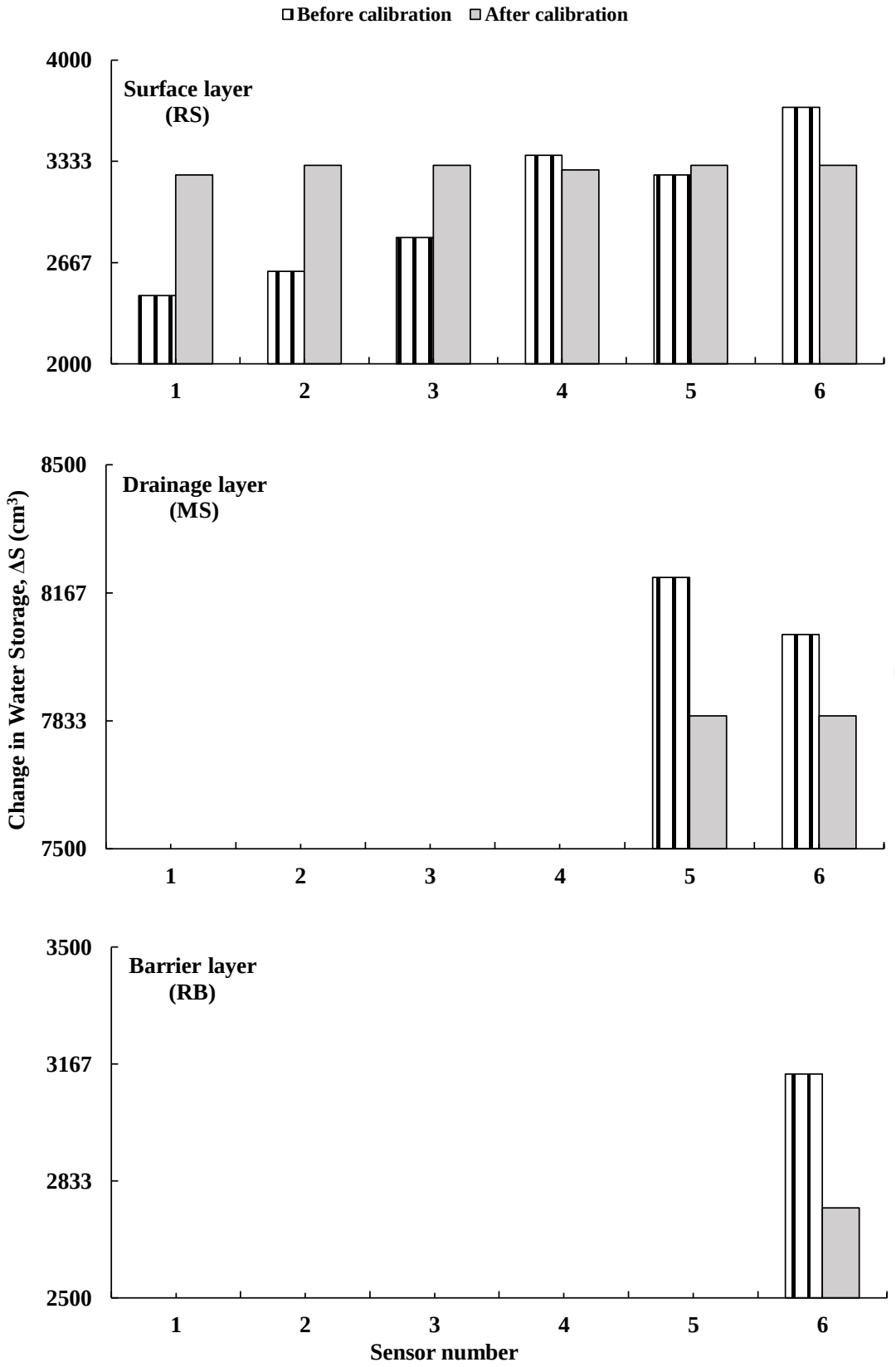

Fig. 4.10 Significance of corrective procedure for PP measurement on change in soil water storage determination

4.3 Performance enhancement of 5TM sensor

This section evaluated the performance of electromagnetic 5TM point sensor for real-time monitoring of θ in MLCS. Since θ governs the hydraulic and mechanical characteristics of geomaterials, its variation is monitored as a function of space and time for evaluating the performance of MLCS. A simple experimental setup was developed in this study for performance assessment of 5TM sensor for ten different soils materials discussed in the previous section. The study would help (i) to assess the appropriateness of factory calibration of 5TM in different types of soil (ii) to adopt a corrective procedure for calibration of 5TM sensors and (iii) to improve its measurement accuracy for monitoring the hydraulic performance of the MLCS.

4.3.1 Background study on 5TM sensor

The amount of water present in a soil, expressed either by gravimetric water content (w) or volumetric water content (θ), controls mechanical and hydraulic behavior of landfill liners and covers, earthen structures, landslides and embankments (Albright et al. 2006b; Norris et al. 2008; Orense et al. 2004; Widomski et al. 2015). Non-destructive θ measurement is preferred to w measurement, which is destructive, time and labour intensive, and restricts real-time monitoring. Several sensors are developed in the recent past for instantaneous and continuous measurement of θ for real-time performance assessment of landfill liners and covers (Bonaparte et al. 2002; Zhang et al. 2009), pavements (Žiliūte et al. 2016), rainfall-induced slope stability (Orense et al. 2004), and concrete structures (Norris et al. 2008). Application of these sensors is also popular in agriculture and irrigation (Sui 2018), water resource and hydrology (Chandler et al. 2017), forestry (Ataka et al. 2014), waste management (Chen et al. 2012), soil physics (Vaz and Hopmans 2001), agronomy and soil science (Jabro et al. 2017). The working of these sensors are based on electromagnetic wave propagation (Bell et al. 1987; Gardner et al. 1998), radiation, neutron scattering, X-ray and the gamma ray attenuation (Evett and Steiner 1995; Gaskin and Miller 1996), time domain reflectometry (TDR) (Jones et al. 2002; Topp and Davis 1985), time domain transmission (TDT) (Harlow et al. 2003), frequency domain reflectometry (FDR) (Minet et al. 2010; Xu et al. 2012), and heat diffusion (Basinger et al. 2003).

The techniques mentioned above measure θ indirectly based on its correlation with properties such as electrical conductivity, electrical resistivity, dielectric constant or

permittivity, impedance or capacitance of the porous media (Cosh et al. 2005; Robinson et al. 1999; Roth et al. 1992; Topp et al. 1980). Several researchers have correlated θ with physical properties of the porous media such as soil suction, infiltration, volume change and strength (Bradford et al. 2002; van Genuchten 1980). From the literature, it is observed that majority of the sensors are electromagnetic sensors (ES) based on capacitance/FDR/TDR/TDT. The ES is economical, reliable, and extensively used for determining the spatio-temporal variation of θ (Perkins et al. 2014; Vereecken et al. 2010). The accuracy of ES measurement depends on factors affecting electromagnetic wave propagation, which includes soil type, salinity, texture, pH, temperature, bulk density, clay content, organic content, mineralogy, installation procedure, measuring technique and measurement range (Baumhardt et al. 2000; Evett et al. 2006; Friedman 2005; Gong et al. 2003).

The ES measures the dielectric constant of surrounding soil mass with a repeated frequency generated by electronic oscillator (Kelleners et al. 2004b; Skierucha and Wilczek 2010) and correlates it to θ by using a suitable calibration equation. Such an equation is developed under controlled laboratory condition mostly using reference minerals. Reviewed literature indicates both underestimation (Czarnomski et al. 2005) and overestimation of θ (Foley and Harris 2007) attributed to improper calibration. Previous studies have shown that the best result can be obtained using site and depth-specific calibration of moisture sensors (Bircher et al. 2016; Huang et al. 2004; McCann et al. 2014; Morgan et al. 1999; Visconti et al. 2014). Several studies have established the significance of soil specific calibration of ES for reliable θ measurements (Bogena et al. 2017; Böhme et al. 2013; Chandler et al. 2005; Cobos and Chambers 2010; Kodešová et al. 2011; Matula et al. 2016; Polyakov et al. 2005; Saito et al. 2009; Vaz et al. 2013; Yoder et al. 1998). These studies have shown that the soil specific calibration can increase the measurement accuracy from ±4% to ±1%. However, there are very few studies (Maqsoud et al. 2017; Parvin and Degré 2016) that investigate the accuracy of 5TM sensors.

This study deals with the performance evaluation of 5TM sensor for real-time monitoring of θ in different layers of a landfill cover system (CS). The CS is an engineered structure constructed over the near surface waste disposal facility to minimize the interaction of rain water with the underlying waste. Based on the previous literature (Landreth et al. 1991; USEPA 1989a and b), it can be stated that a conventional CS generally consists of three main layers (hydraulic barrier layer overlain by surface and

drainage layer). The thickness of these layers is kept at par with site requirements but never less than 30 cm. Surface layer or the top layer of CS is made of compacted silty sand (or loamy soil) having adequate strength and water storage capacity. Apart from resisting rainfall and run-off induced erosion, surface layer also accommodates vegetation growth without compromising its function. It is constructed at 3-5% slope with permeability in the range of 10^{-5} to 10^{-8} m/s. The drainage layer is comprised of granular material (sand) having a permeability greater than 10^{-4} m/s, which drains out the infiltrating water laterally. The hydraulic barrier layer is compacted clayey soil (or native soil amended with bentonite) with permeability less than 10^{-9} m/s to reduce water percolation.

4.3.2 Materials and method

The 5TM sensor shown in Fig 4.11 is 10cm×3.2cm×0.7cm in dimension with measuring prongs of 5.5 cm length. The sensor can work in the temperature range of – 40 ºC to 60 ºC and measure θ in the range of 0% to 100% with the accuracy of ± 3% using generalized calibration proposed by the manufacturer. When electric power is applied to the 5TM sensor, it creates an oscillating wave of 70 MHz frequency to each sensor prong. It transmits an electromagnetic field in the surrounding soil mass that charges according to the dielectric constant of the soil material. This electronic charge is proportional to the soil dielectric constant and therefore to the soil water content. The 5TM microprocessor measures the charge and outputs a value of dielectric constant in terms of unprocessed raw values having units of $\varepsilon_a \times 50$. Factory calibration of the 5TM sensor enables to measure dielectric constant (ε_a) accurately in the range of 1 (air) to 80 (water). There are different equations to convert raw dielectric constant data measured by 5TM into θ. The following Topp's equation (Eq. 4.7) (Topp et al. 1980) which converts raw dielectric constant into θ for mineral soil, is the most popular equation.

$$\theta = 4.3\times10^{-6}\times\varepsilon_a^3 - 5.5\times10^{-4}\times\varepsilon_a^2 + 2.92\times10^{-2}\times\varepsilon_a - 5.3\times10^{-2} \quad (4.7)$$

In this study, air-dried soil samples sieved through 2 mm sieve were used to prepare ten different soil-water mixes (mixed with distilled water), from dry to relatively wet. The mixed soil sample was kept in polythene cover and preserved in a desiccator for uniform water distribution for at least 24 hours. Soil sample was then packed to a specific bulk

density (ρ_b) into a cylindrical polyvinyl chloride (PVC) container of 30 cm internal diameter and 25 cm height (dimensions were so chosen to maintain influence zone criterion of the sensor) as shown in Fig. 4.11. To ensure uniform ρ_b during packing, the container volume was divided into three equal parts, and the soil sample in three equal portions was compacted uniformly with 2.6 kg rammer. Further, the 5TM sensor (along with 1 cm length of cable connected to the sensor) was inserted vertically at the center of the uniformly compacted soil column. A dummy guide insertion blade was used to facilitate easy insertion of 5TM. After insertion, Em50 data logger was connected to the sensor, and θ measurement designated as θ_m along with unprocessed raw data (R_w) was acquired. All measurements were repeated thrice and average results were considered in this study. Gravimetric water content (w) of the soil sample collected from the sensor influence zone was determined by oven drying (105°C, 24 hours) after 5TM measurements and converted into computed volumetric water content (θ_c) using Eq. 4.3.

The measured θ_m and computed θ_c (true value for any soil sample) were then compared to evaluate the accuracy of the 5TM sensor. If the deviation was unsatisfactory, then the corrective procedure stated below was performed to evolve a new calibration equation for 5TM sensor corresponding to the soils used in CS. For this purpose, the θ_c was plotted against measured raw counts (electronic signal of the sensor) or dielectric constant and the relationship was quantified. This relationship gives appropriate new calibration equation for different soil materials used in CS. The betterment of corrective procedure was confirmed by marginally improved values of regression coefficient (R^2) and root mean square error ($RMSE$) calculated using Eq. 4.8, and reported in Table 4.2. Independent data was generated for validating the appropriateness of the new calibration equation.

$$RMSE = \sqrt{\frac{\sum_{i=1}^{n}\left(\theta_{mi} - \theta_{ci}\right)^2}{n}} \tag{4.8}$$

where, θ_{mi} is i^{th} θ_m measured by the 5TM sensor, θ_{ci} is corresponding i^{th} θ_c computed based on oven dry method and n is the number of total measurements.

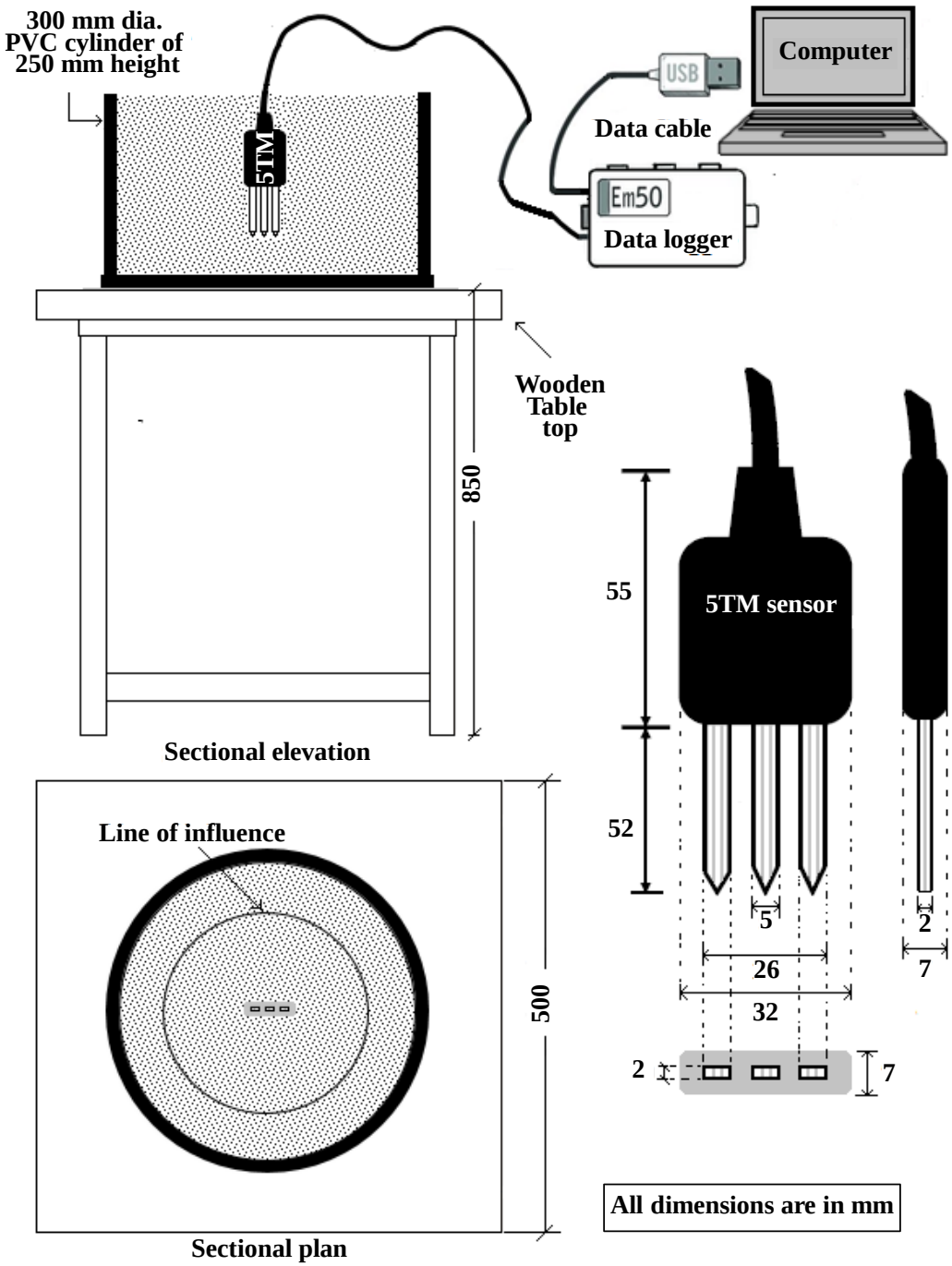

Fig. 4.11 Schematic diagram of the laboratory setup for calibration of 5TM sensor

4.3.3 Observations and discussion

Figure 4.12 portrays the comparison of measured θ_m with computed θ_c for ten different soil materials used in CS. The figure shows that default calibration of 5TM sensor underestimates θ measurements for all the soil samples used in the study except for a higher

range of θ for BB. The figure also indicates a significant deviation of θ_m from θ_c in dry and wet range. Deviation in θ_m was noticed to increase with an increase in clay content and bulk density for BS, RB, BB and BN, which is similar to the observations reported in the literature (Cobos and Chambers 2010; Ju et al. 2010). The deviation was pronounced due to the presence of a higher percentage of coarser particles for MS and RF. Such trends were also reported in previous literature (Vaz et al. 2013). Observations from figure 4.12 strongly suggest the necessity of a corrective procedure to minimize error in 5TM measurements. In this study, a soil specific re-calibration was performed using the setup shown in Figure 4.11. Re-calibration was performed in two ways: (i) linear calibration (LC) illustrated in Figure 3 by correlating θ_c to measured raw outputs (R_w) and (ii) polynomial calibration (PC) presented in Figure 4 by correlating θ_c to dielectric constant (ε_a).

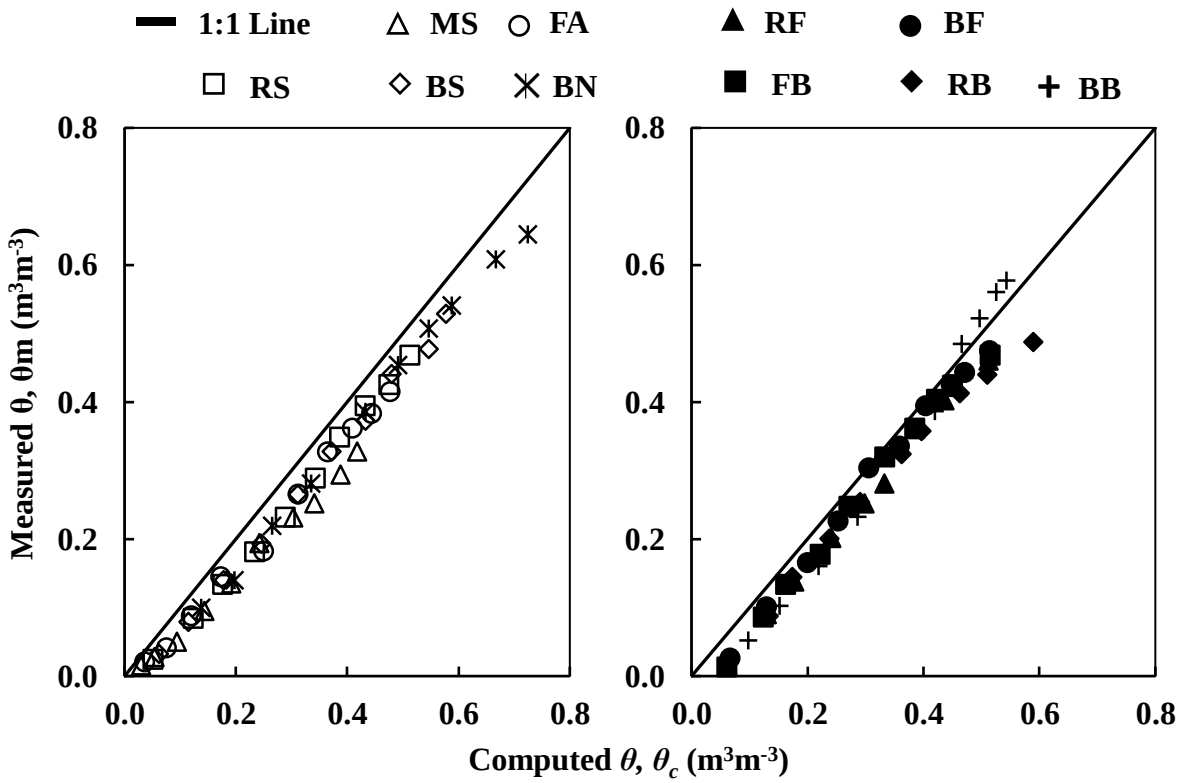

Fig. 4.12 Comparison between measured and computed volumetric water content

Figure 4.13 presents the relationship between θ_c and R_w for each soil material considered in this study. The variation is observed to follow a linear trend represented as Eq. 4.9.

$$\theta = aR_w + b \tag{4.9}$$

where a and b are soil specific calibration parameters summarized in Table 4.2. Figure 4.14 depicts the variation of computed θ_c as a function of ε_a for the soil materials. From the figure, it can be observed that the variation of θ_c follows a non-linear response with ε_a. Hence, polynomial equations of different orders were fitted to the observed variation. For all soil types, there is no significant improvement beyond the third order polynomial equation represented by Eq. 4.10 which is similar to Topp equation (Topp et al. 1980).

$$\theta = A\varepsilon_a^3 - B\varepsilon_a^2 + C\varepsilon_a - D \tag{4.10}$$

where *A, B, C and D* are soil-specific calibration parameters of 5TM sensor listed in Table 4.2.

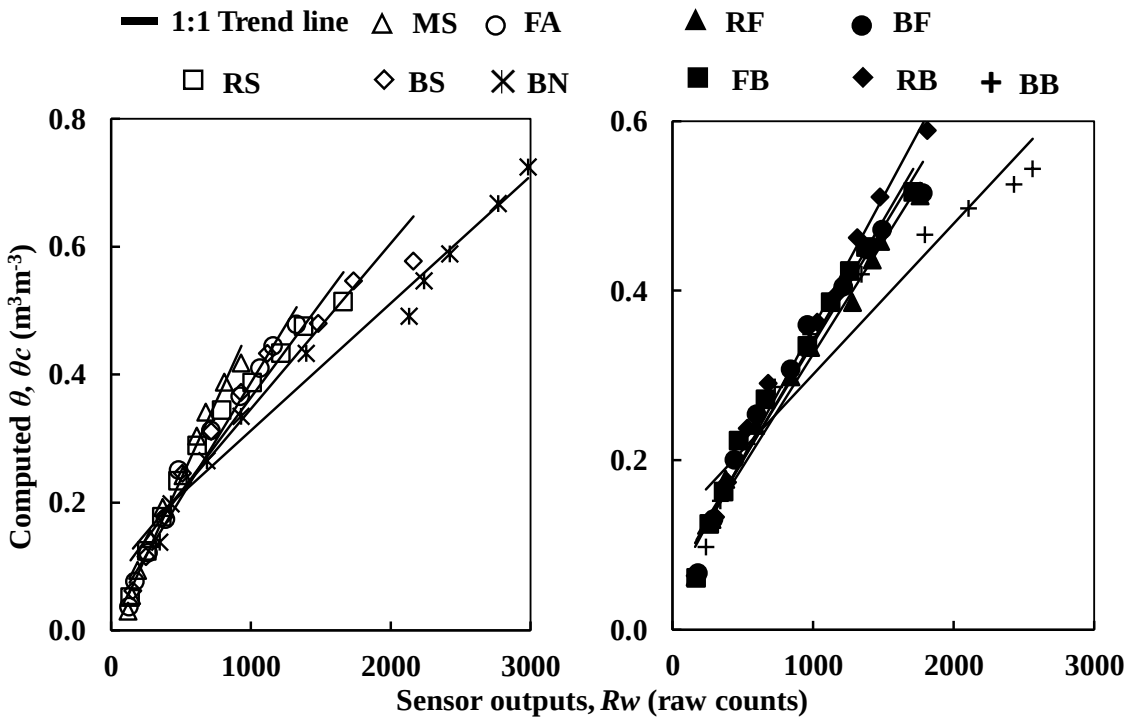

Fig. 4.13 Calibration of 5TM sensor based on raw counts by linear fit

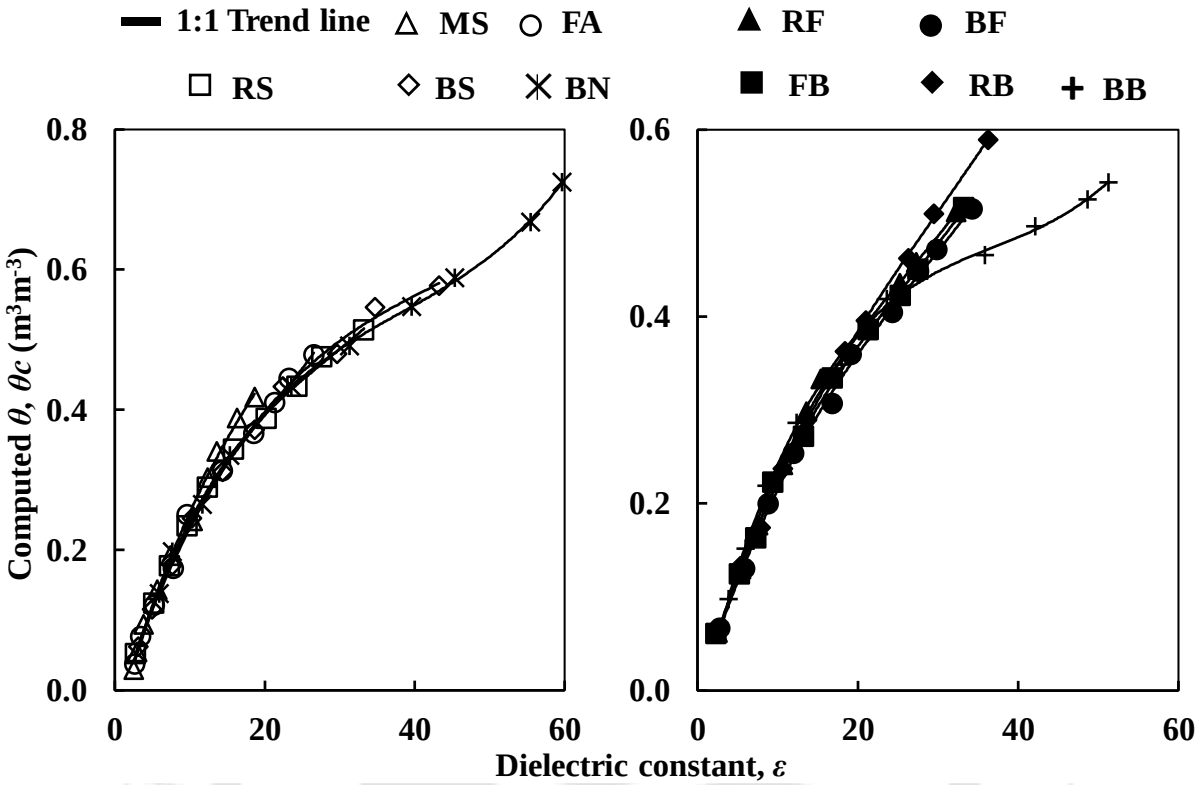

Fig. 4.14 Calibration of 5TM sensor based on dielectric constant by polynomial fit

Table 4.2 Details of soil specific calibration for 5TM sensor in various soils

Soil Sample	Evaluation based on raw count by linear fit				Evaluation based on dielectric constant by polynomial fit					
	Calibration parameters		Statistical parameters		Calibration parameters				Statistical parameters	
	a	b	R^2	RMSE (%)	A	B	C	D	R^2	RMSE (%)
MS	0.0005	-0.0043	0.98	2.15	0.00001	0.0009	0.038	0.049	0.99	0.16
FA	0.0004	0.0271	0.98	2.44	0.00002	0.0013	0.041	0.058	0.99	1.04
RS	0.0003	0.0684	0.95	7.65	0.00001	0.001	0.038	0.045	0.99	0.43
BS	0.0003	0.0876	0.94	3.84	0.000005	0.0006	0.032	0.028	0.99	0.54
BN	0.0002	0.1134	0.98	4.04	0.000006	0.0007	0.032	0.019	0.99	0.89
RF	0.0003	0.0596	0.98	2.57	0.00001	0.0008	0.032	0.018	0.99	0.00
BF	0.0003	0.0632	0.97	2.97	0.000007	0.0006	0.027	0.007	0.99	0.71
FB	0.0003	0.0574	0.98	1.72	0.000009	0.0007	0.029	0.008	0.99	0.89
RB	0.0003	0.0482	0.98	2.52	0.000005	0.0005	0.027	0.003	0.99	0.90
BB	0.0002	0.1232	0.93	7.07	0.000007	0.0008	0.033	0.016	0.99	0.54

The calibration parameters reported in Table 4.2 were used to re-calculate θ_m designated as θ_{mr} from known values of R_w and ε_a. The θ_{mr} calculated based on soil specific calibration equations in terms of R_w and ε_a were compared with the corresponding θ_c as shown in Figs. 4.15 and 4.16, respectively. The data indicates that there was a significant improvement in the precision of θ measurements when the proposed soil-specific calibrations were followed. For validation, a new set of experimental data was generated and compared with θ_c as shown in Fig. 4.17 and 4.18 corresponding to measured R_w and ε_a, respectively. From the figures, it can be noted that θ_m matches well with θ_c for all the soils used in this study. It is noteworthy to state that the 5TM sensor consistently gave accurate θ measurement after following the procedure stated in this study. Results as shown in figures 4.17 and 4.18 also indicates that the polynomial calibration (PC) based on measured ε_a is marginally better than R_w based linear calibration (LC). Quantitatively the 5TM measurement accuracy improves from $\pm 8\%$ to $\pm 1\%$ and $\pm 2\%$ in the case of PC and LC, respectively. The following section intends to show the effect of improper 5TM measurements on soil water storage determination of different CS layers.

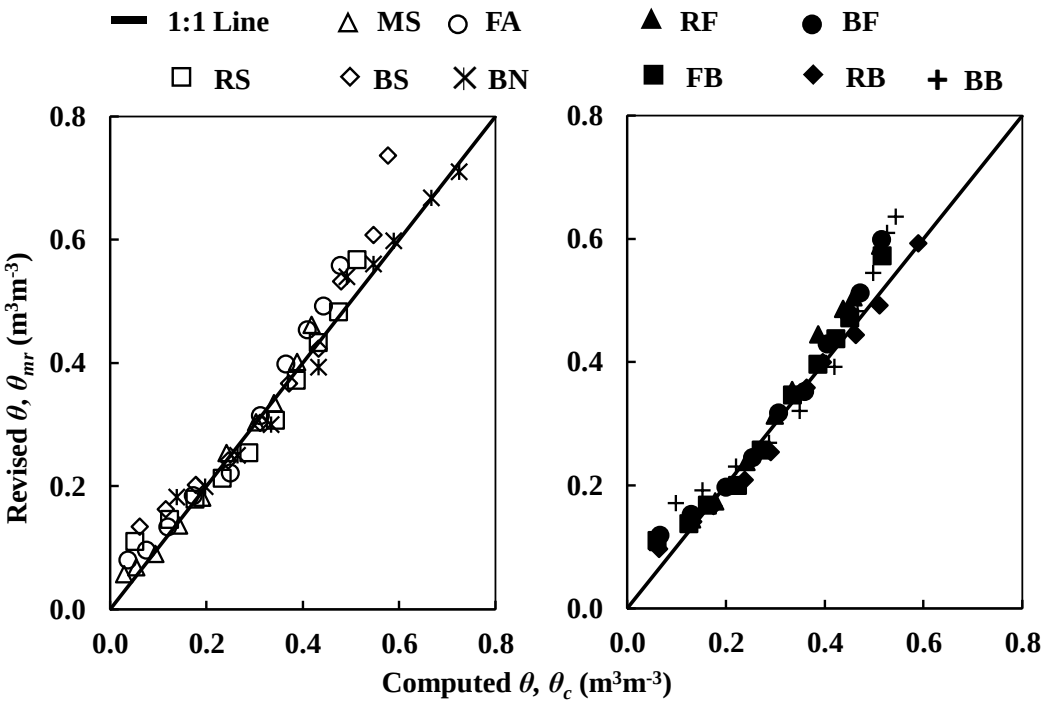

Fig. 4.15 Comparison of re-calculated 5TM measurements using modified linear calibration

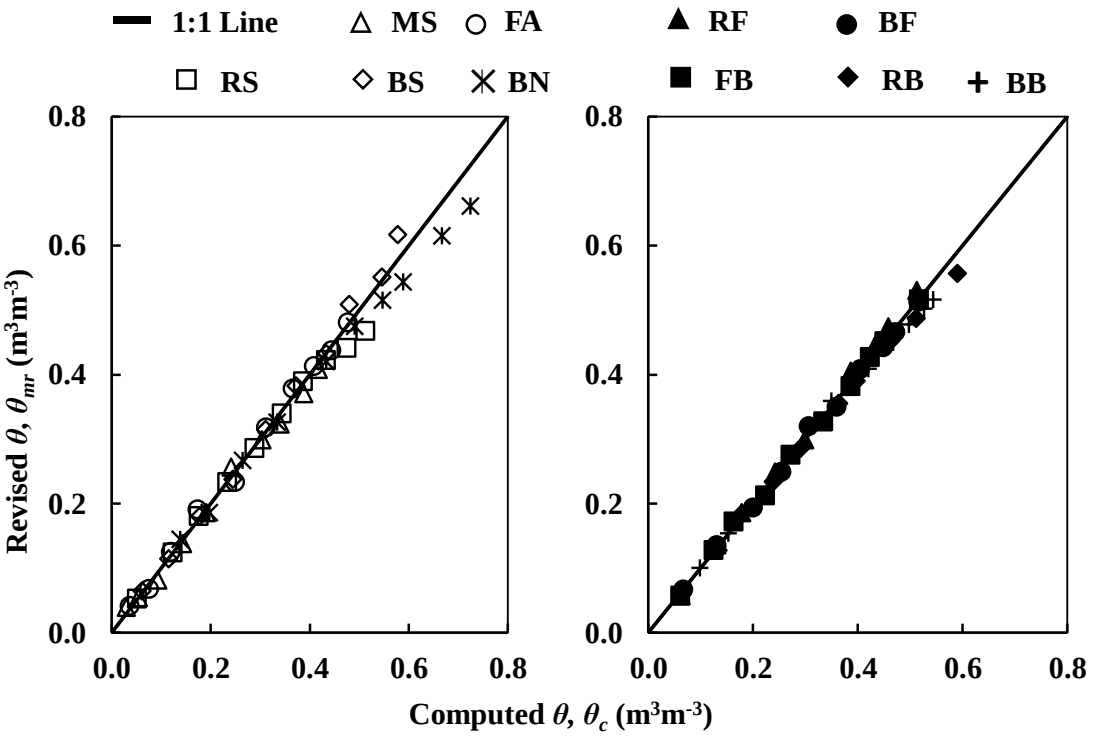

Fig. 4.16 Comparison of re-calculated 5TM measurements using modified polynomial calibration

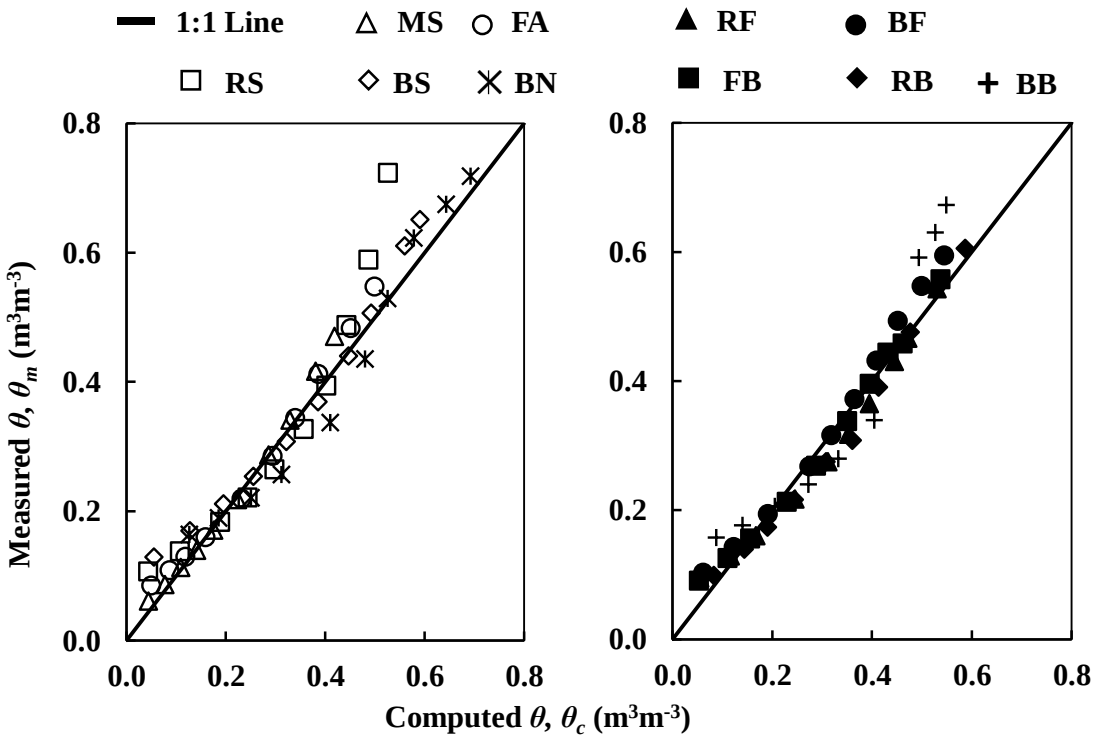

Fig. 4.17 Validation of linear calibration evaluated based on raw counts

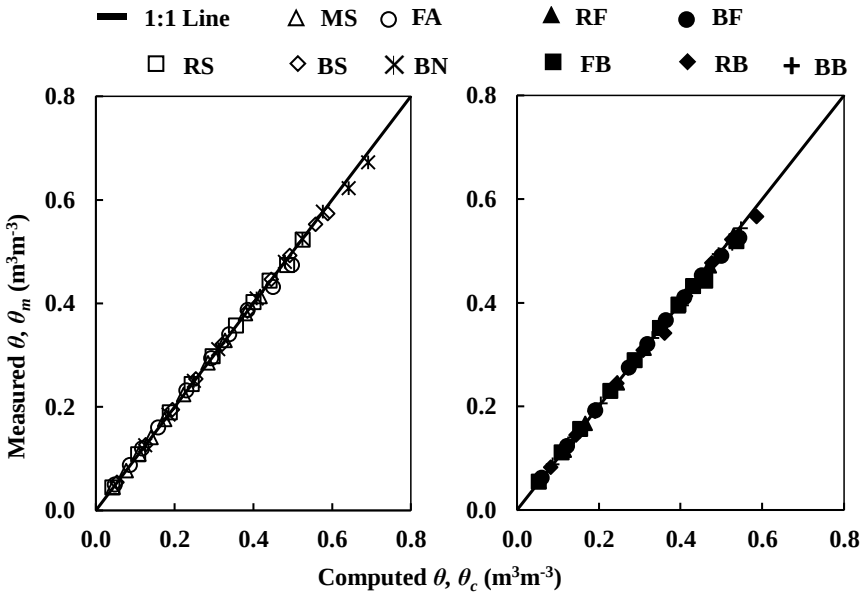

Fig. 4.18 Validation of polynomial calibration evaluated based on dielectric constant

4.3.4 Application of 5TM measurements for soil water storage determination

An experimental study on a cylindrical column replicating three layers of CS was carried out under constant ponding of water causing progressive saturation of cover layers, to establish the effectiveness of the proposed procedure. The top layer of the column is a surface layer composed of red soil (RS) followed by a drainage layer (MS) and a barrier layer (RB) successively. In the study, the layered column was subjected to a constant ponding depth of 1.5 m of water at the top as shown in Figure 4.19 for exploring the hydraulic performance by monitoring θ with time using the 5TM sensor. The θ measured by 5TM sensor becomes constant at saturated water content (θ_s) of the soil mass of known volume (V). The θ_s of each soil layer can also be determined theoretically by using Eq. 4.11 from the known value of specific gravity (G) and dry density (ρ_d) reported in Table 3.2 of chapter 3, and density of water (ρ_w). Further, Eq. 4.12 can be utilized to determine soil water storage (S_w) at saturated state of each layer either by using calculated or measured θ_s.

$$\theta_s = 1 - \frac{\rho_d}{G\rho_w} \tag{4.11}$$

$$S_w = V \times \theta_s \tag{4.12}$$

In this study, 5TM measurements from the trial MLCS column was used to determine the S_w of individual layers. For each layer, S_w determined based on θ_s before and after calibration was compared with theoretical calculation, as shown in Figure 4.20. An absolute error of 13 %, 15 % and 7 % was noticed in the determination of S_w in surface, drainage and barrier layer, respectively, before calibration. The corresponding error of respective layers was reduced to 7%, 10% and 2% by following LC and to 0.4%, 0.6% and 0.4% for PC. Observations from the figure reveal the usefulness of the proposed laboratory procedure for enhancing the accuracy of θ measurements by the 5TM sensor. This study strongly recommends conducting soil specific calibration of the 5TM sensor by considering dielectric constant before employing it for field monitoring programs associated with important projects such as MLCS.

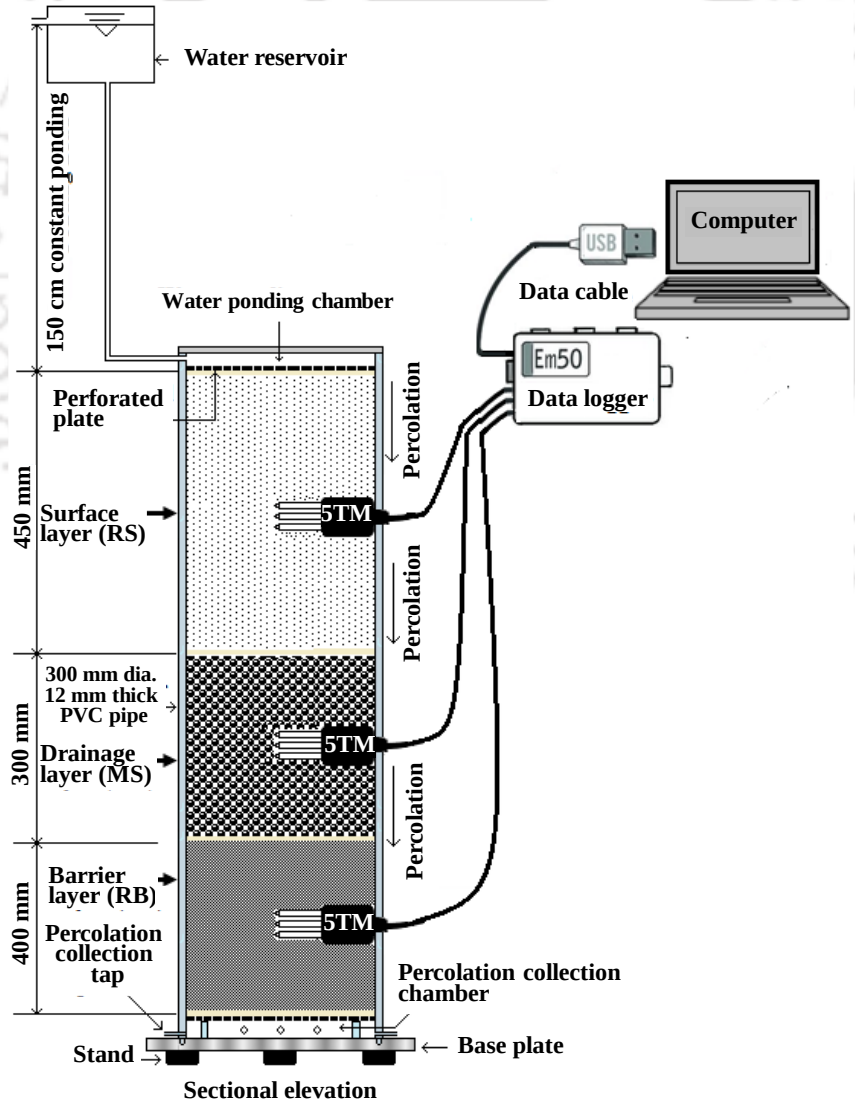

Fig. 4.19 Experimental column setup to assess the effectiveness of the corrective procedure for 5TM measurement

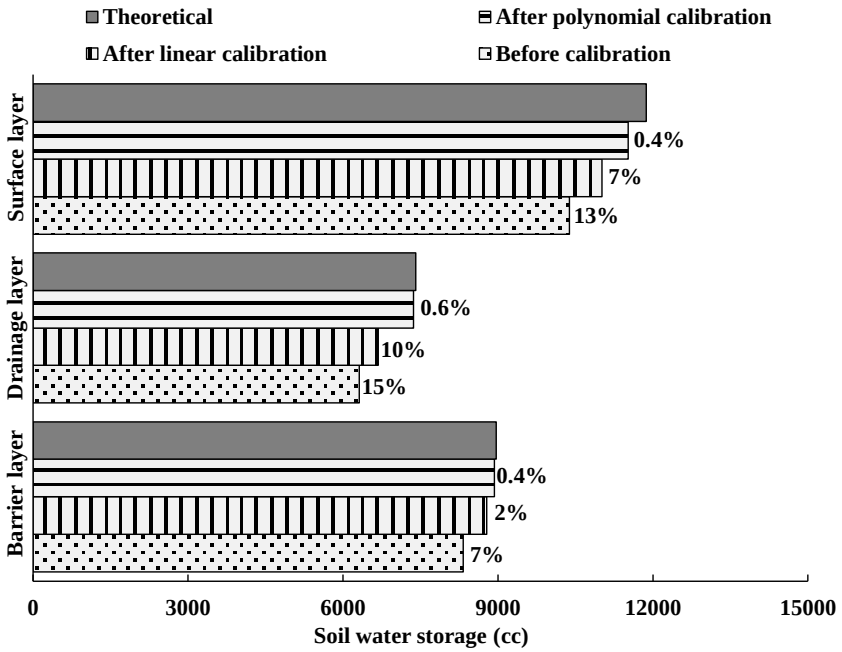

Fig. 4.20 Significance of corrective procedure for 5TM measurement on soil water storage determination

4.4 Summary

4.4.1 Profile probe

The study presented in the current chapter deals with the performance evaluation and improving the accuracy of profile probe (PP) used for measuring depth varying volumetric water content θ in the field for a multi-layered cover system (MLCS). A laboratory setup was developed for evaluating all the sensors of PP simultaneously in a compacted soil mass, which is not reported in the literature earlier. The performance evaluation of PP indicated that the measured θ (θ_m) was different from theoretically computed θ (θ_c) and each of the embedded sensors gave widely varying results for the same measurement location in the soil mass. The deviation in observed results was found to increase with an increase in soil plasticity, which is consistent with the observations in the literature. Based on the proposed laboratory procedure in this study, a new soil specific and sensor specific calibration equations were developed for the soils used in different layers of MLCS. The new calibration parameters improve the accuracy of θ measurement from ±6% to ±1%. The usefulness of the proposed method was demonstrated by using a MLCS column. The implication of inaccurate measurements of PP on determining the change in soil water storage in different layers of MLCS column was studied. It was noted that there was an error of 18% when PP measurement was performed without correction.

Also, the sensors measured widely varying results before adopting the corrective procedure for PP measurements. All the sensor measurements gave identical change in soil storage in different layers of MLCS after adopting the correction procedure. Based on the encouraging observations, this study strongly advocates the use of proposed laboratory procedure for accurate measurements of θ using PP before employing it for field monitoring programs for important projects such as MLCS.

4.4.2 5TM sensor

The study also deals with the improvement in accuracy of 5 TM sensor which is a low-cost volumetric water content (θ) sensor for real-time monitoring of θ in MLCS. It was noted that by adopting a general calibration for different soils would underestimate θ measurements. Significant deviation of measured θ (θ_m) from computed θ (θ_c) in the drier and wetter range was noticed for all soil samples used in the study, except in higher range of θ for a black soil-bentonite mix (BB). Increase in deviation can be attributed to the increase in clay content, bulk density and to the higher percentage of coarser particles of soil samples. A well-structured calibration program was demonstrated in this study for the type of soils used in MLCS. A significant improvement in the precision of θ measurements was noted when two proposed methods (linear calibration, LC and polynomial calibration, PC) was adopted for soil-specific calibration. Quantitatively 5TM measurement accuracy improves from ±8 % to ±1 % for PC and ±2 % for LC. The results indicated that PC is marginally superior to LC. A study on a cylindrical column replicating three layers of MLCS was also conducted to establish the effectiveness of the proposed procedure by evaluating layer specific soil water storage (S_w). The absolute error of 13 %, 15 % and 7 % in the determination of S_w was noticed in surface, drainage and barrier layer, respectively, for 5TM measurements without calibration. This corresponding layer-wise absolute error minimized to 7%, 10% and 2% by following LC, and to 0.4%, 0.6% and 0.4% by adopting PC. The observations of the study revealed the usefulness of the corrective laboratory procedure for enhancing the accuracy of θ measurements by the 5TM sensor with a view to improving its performance efficiency, and it also suggested PC to be used in preference to LC. Thus the study strongly recommends conducting soil specific calibration of the 5TM sensor before employing it for real-time field monitoring programs associated with important projects like MLCS.

Chapter 5

Percolation Assessment of MLCS under Constant Water Ponding

5.1 General

Multi-layered cover system (MLCS) constructed over a landfill minimizes water percolation into underlying waste to prevent leachate formation and groundwater contamination. The main objective of this chapter is to assess the progressive saturation of four different MLCS configurations under constant water ponding. The four column configurations varied based on layer specific materials. Volumetric water content was recorded as a function of time at different depths for 900 days to observe percolation. All results obtained from the column test were finally compared with numerical simulation considering three different approaches. The study aims to understand the saturation rate of different layers of MLCS and hence evaluate the adequacy of different layer material and configuration.

5.2 Background study

Hazardous waste from industries and nuclear sector (low level) are secured in engineered landfill having a liner system at the bottom (Aldaeef and Rayhani 2015; Hamdi and Srasra 2013; Rowe 2011) and a cover system on the top (Apiwantragoon et al. 2015; Landreth et al. 1991). The cover system is constructed after the landfill reaches its full capacity for minimizing percolation of rainwater into the underlying waste (Rowe 2005). Based on the literature listed in Table 2.5, it was noted that different types of cover system have evolved over the last few decades mainly based on two mechanisms known as evapotranspiration (ET) and capillary barrier (CB) action. The ET and CB cover system are suitable for arid and semi-arid regions where the average annual rainfall ranges from 100 mm to 600 mm (Aljaradin and Persson 2015; Bohnhoff et al. 2009). For supporting vegetation growth, the ET cover system utilizes its water storage capacity to store the infiltrated rainwater until it is removed by soil evaporation and plant transpiration (Barnswell and Dwyer 2012; Blight 2009; Schnabel et al. 2012). The CB cover system comprised of a vegetated fine-grained soil layer overlying a coarse-grained soil layer (Zhan et al. 2014). In addition to evapotranspiration, the CB cover system relies on the capillary barrier action between the two layers to minimize water percolation (Subedi et al. 2013). However, these two type of cover system was found to be inadequate for humid regions with average annual rainfall more than 1000 mm (Ng et al. 2015; Zhang and Sun 2014).

Due to low water holding (or removing) capacity, these cover system performs poorly under the humid climate which may also be attributed to preferential water flow through the roots (Khapre et al. 2017; Song et al. 2017) and the desiccation cracks (Hoor and Rowe 2013; Sinnathamby et al. 2014; Vallejo 2009).

Previous researchers (Ng et al. 2016, 2019a and b) have advocated MLCS for regions with humid climate.. The multi-layer cover system is obtained by introducing a low permeable compacted clay layer (CCL) as the hydraulic barrier beneath a CB layer system (Rowe 2005). The bottom CCL is advantageous to impede the ingress of water percolated from the upper CB layer. A chronological review of the previous studies on percolation through the cover system is summarized in Table 2.5 to highlight the importance of various methodologies adopted for the investigation. The table also focuses on the inclusion of geosynthetic clay liner (GCL) and different recycled materials in cover system. Most of the laboratory investigations employ artificial rainfall simulator or constant head method to carry out the percolation studies.

Furthermore, one-dimensional column studies have been conducted to understand the water infiltration in different cover system under varying boundary conditions. However, no studies exist for catastrophic scenarios of flood wherein the cover system was inundated by water for an extended period. This is essential in view of recent cases of extreme floods occurring due to climate change (Kundzewicz et al. 2013). Such situations are evidently seen in northeast India where there is the overflow of the Brahmaputra river, resulting in constant ponding condition in some areas for a few months (Dhar and Nandargi 2000). Very recently, other western states of India, Kerala, and Maharashtra, have also experienced constant water ponding due to heavy rainfall for hours (Francis and Gadgil 2006). In addition to this, investigations are required for exploring the suitability of utilizing the alternate materials like fly ash, asphalt concrete in cover system for specific applications.

5.3 Materials and methods

5.3.1 Testing materials

The current study was conducted by employing various indigenous soil, bentonite clay, fly ash and commercial geosynthetic clay liner (GCL). The source, designation, and the proportion and combination for their use as different cover layer are detailed in Table 3.1. The soil mix proportions were decided based on layer specific criteria of hydraulic

conductivity (10^{-5}-10^{-8} m/s for surface layer (SL) and less than 10^{-9} m/s for barrier layer (BL)) reported in previous literature (Landreth et al. 1991; USEPA 1989a and b). Medium sand (MS) was used as the drainage layer (DL) in all constructed columns due to its high hydraulic conductivity (10^{-5} m/s). The basic physical, geotechnical and chemical properties of all the soils were investigated using standard laboratory procedures reported in the relevant code of Indian standard (IS) or international American society of testing and materials (ASTM) and are presented in Table 3.3.

5.3.2 Testing equipment

Profile probe (PR2/6-UM-3.0, Delta-T Devices Ltd., UK) housing six embedded sensors at different depths were utilized in the study for monitoring the variation in volumetric water content (θ) with time and depth. A handheld moisture meter was used for recording the θ from each PPS. Each PPS can measure θ ranging from dry state (0%) to saturated state (θ_s) with an accuracy of ±6% for an operating temperature range of -20 ºC to +60 ºC. However, the accuracy of PPS measurements was further improved up to ±1% based on its soil specific calibration conducted in house which is described in details in the previous chapter.

5.3.3 Column construction

The four test columns designated as C1, C2, C3, and C4, were fabricated using polyvinyl chloride (PVC) cylindrical container of 30 cm internal diameter and 120 cm height. Every container has four separable parts of 30 cm height to facilitate the soil packing. Each part was combined with the successive part by half-lap joint, and suitable sealant was applied to prevent water leakage. The top 2.5 cm portion of each column container was kept empty for applying a constant water ponding on the CS column using an overhead tank. The bottom 2.5 cm portion was used as a percolation collection chamber. The remaining 115 cm was utilized for constructing the CS column. Each CS column comprised of three layers; the hydraulic barrier layer (BL), drainage layer (DL), and surface layer (SL) of height 40, 30 and 45 cm respectively. Column dimensions were so selected based on the influence zone criterion (10 cm radius and 105 cm depth) of the profile probe (Users' guide, Delta-T Devices Ltd.) and layer heights were kept at par with the field requirements (USEPA 1989a and b). Schematic diagram of the laboratory setup of four columns is presented in Fig. 5.1 and the details of layer materials are listed in Table 5.1.

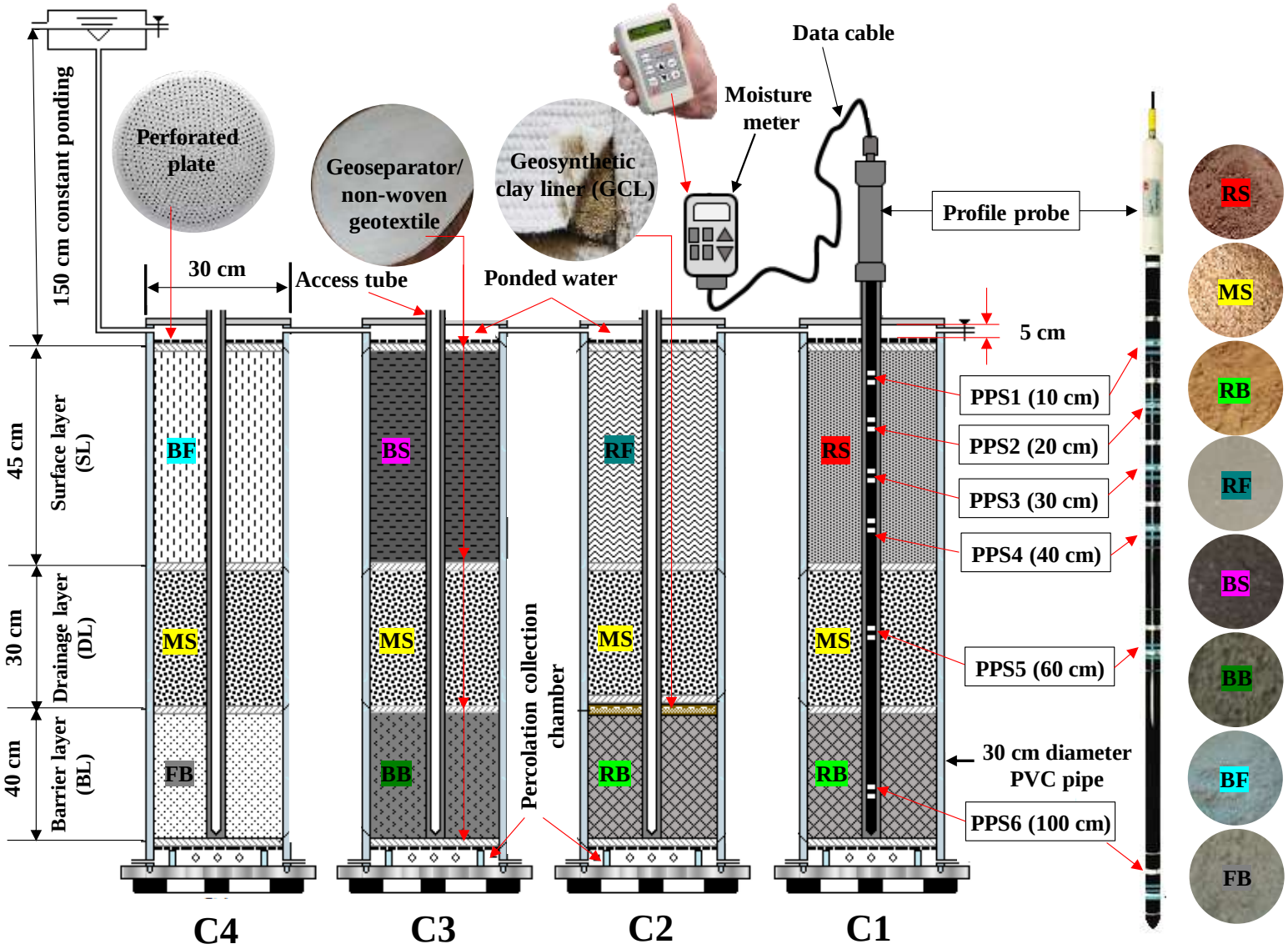

Fig. 5.1 Schematic diagram of experimental setup of four MLCS columns

Table 5.1 Details of layer materials used in test columns for the study

Test column	Cover system	Layer (designation)	Soil material (designation)
C1	Three-layered cover system	Surface layer (SL)	Red soil (RS)
		Drainage layer (DL)	Medium sand (MS)
		Barrier layer (BL)	Red soil-bentonite mix (RB)
C2	Four-layered cover system	Surface layer (SL)	Red soil-fly ash mix (RF)
		Drainage layer (DL)	Medium sand (MS)
		Additional barrier layer	Geosynthetic clay liner (GCL)
		Barrier layer (BL)	Red soil-bentonite mix (RB)
C3	Three-layered cover system	Surface layer (SL)	Black soil (BS)
		Drainage layer (DL)	Medium sand (MS)
		Barrier layer (BL)	Black soil-bentonite mix (BB)
C4	Three-layered cover system	Surface layer (SL)	Black soil-fly ash mix (BF))
		Drainage layer (DL)	Medium sand (MS)
		Barrier layer (BL)	Fly ash-bentonite mix (FB)

The BL, DL, and SL were packed uniformly with their respective soil successively from bottom to top into each CS column based on the mass-volume method. The dry soil mass was mixed with required water (distilled) and kept for maturation before compacting it. The BL of each CS column was placed by compacting the respective soil mix uniformly

by 2.6 kg rammer to its maximum dry density (MDD) and optimum moisture content (OMC) as reported in Table 3.3. The DL was constructed on top of BL by compacting air dried MS at approximately 50% of its maximum relative density by calibrating the height of fall. This was overlain by the SL compacted uniformly to MDD and OMC similar to BL. In each CS column, a porous geosynthetic separator was used at each layer interface for isolating different layer mass. An additional non-woven geotextile was utilized at the interface between SL and DL to prevent the clogging of porous drainage materials due to the ingress of fine soil particles from the upper layer. A 1 cm thick GCL was employed as the additional hydraulic barrier layer in column C2 wherein 50% fly ash (FA) was used in SL. 50% and 70% of fly ash were also utilized in SL and BL, respectively for column C4 to investigate its potentials as a sustainable alternate material in CS for landfill applications. A profile probe access tube was embedded in each CS column vertically along the central axis of the packed mass of CS layers during the erection and compaction process. A thin layer of sealant was applied at the interface between the access tube and the surrounding soil mass. Similar care was taken for the inside boundary of the column to minimize the preferential flow of water. The same constant water ponding of 150 cm depth was applied at the top of all four CS columns by interconnecting the top reservoirs to an elevated water supply tank. Figure 5.2 represents the pictorial view of the construction steps, placement of various materials, and fully erected CS column setup.

The profile probe was inserted into the access tube for scanning θ at the depths of 10, 20, 30, and 40 cm in SL, 60 cm in DL and 100 cm in BL of each CS column. The θ measurements were performed thrice in a day, and their average was considered as measured daily θ. In the study, θ measured at 10, 20, 30, 40, 60 and 100 cm depths of any column is designated as θ_{10}, θ_{20}, θ_{30}, θ_{40}, θ_{60} and θ_{100} respectively. For any individual column depth, the time taken for the θ to deviate from its initial state (θ_i) is considered as the time for deviation (t_d) and the total time duration taken from the initial condition to the saturation is designated as the time for saturation (t_s) in this study. The time interval or difference between t_s and t_d ($t_s - t_d$), is defined as the transition period (TP). The TP of θ_{10}, θ_{20}, θ_{30}, θ_{40}, θ_{60} and θ_{100} measured in any CS column are designated as TP_{10}, TP_{20}, TP_{30}, TP_{40}, TP_{60}, and TP_{100}, respectively. The variation of θ in each column layer subjected to progressive saturation under constant ponding of water was monitored as the function of depth and time for 900 days.

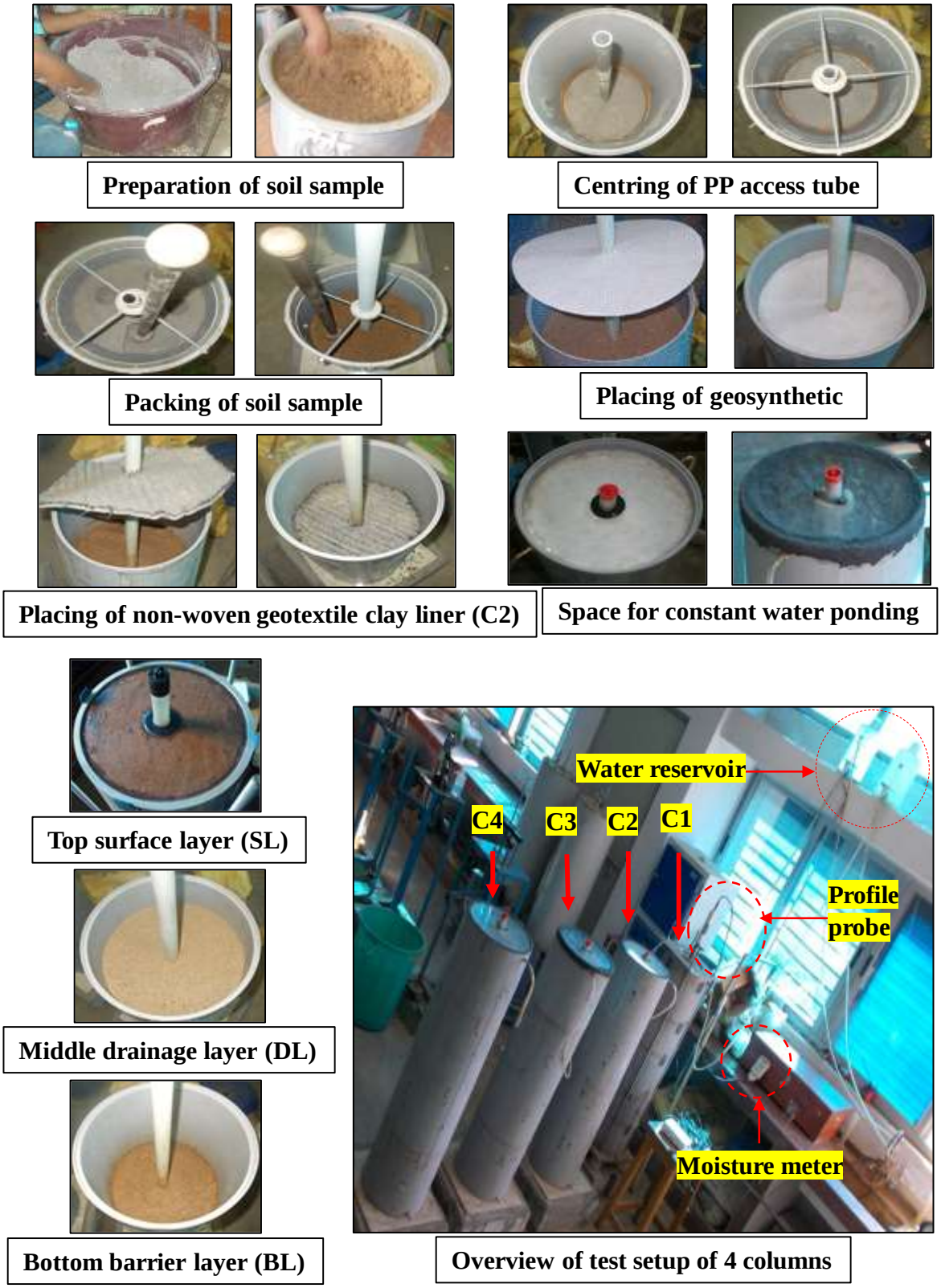

Fig. 5.2 Pictorial view of construction of test columns

5.3.4 Numerical analyses

The vertical water movements through the experimental CS columns for 900 days were numerically modelled using HYDRUS 2D software code (Šimůnek et al. 1999). The computer code solves modified Richard's equation (Richards 1931) (Eq. 5.1) of water flow through saturated or unsaturated soil media by finite-element (FE) approach (McDougall et al. 1996).

$$\frac{\partial \theta}{\partial t} = \frac{\partial}{\partial x_i}\left[k\left(k_{ij}^{A} \frac{\partial h}{\partial x_j} + k_{iz}^{A} \right) \right] - S \tag{5.1}$$

where, θ is the volumetric water content (L^3L^{-3}), h is the pressure head (L), S is a sink term (T^{-1}), x_i (i = 1, 2) are the spatial coordinates (L), t is time (T), k_{ij}^{A} are components of a dimensionless anisotropy tensor k^A and k is unsaturated hydraulic conductivity function (LT^{-1}) given by

$$k\left(h, x, y, z\right) = k_s\left(x, y, z\right) k_r\left(h, x, y, z\right) \tag{5.2}$$

where k_r is relative hydraulic conductivity and k_s is saturated hydraulic conductivity.

Figure 5.3 presents the geometry, boundary conditions, shape, and size of FE mesh for the CS column. Figure 5.4 shows mesh convergence study with the variation of θ at 40 cm depth of Column C1 with time for triangular FE mesh of different sizes from 1.5 cm to 15 cm. The figure indicates that FE mesh size of less than 3 cm has no significant effect on the results. Therefore, a triangular FE mesh of size 3 cm was considered for subsequent numerical analyses. Hydraulic parameters of individual soil layer of each CS column were evaluated to serve as input parameters for numerical analyses. These parameters include residual volumetric water content (θ_r), saturated volumetric water content (θ_s), van Genuchten parameters α and n, saturated hydraulic conductivity (k_s), and pore connectivity parameters (I). The k_s was determined in the laboratory by falling head permeability test (ASTM D5084). Pore connectivity parameter (I) was assumed to be 0.5 for all soil materials based on previous literature (Mualem 1976).

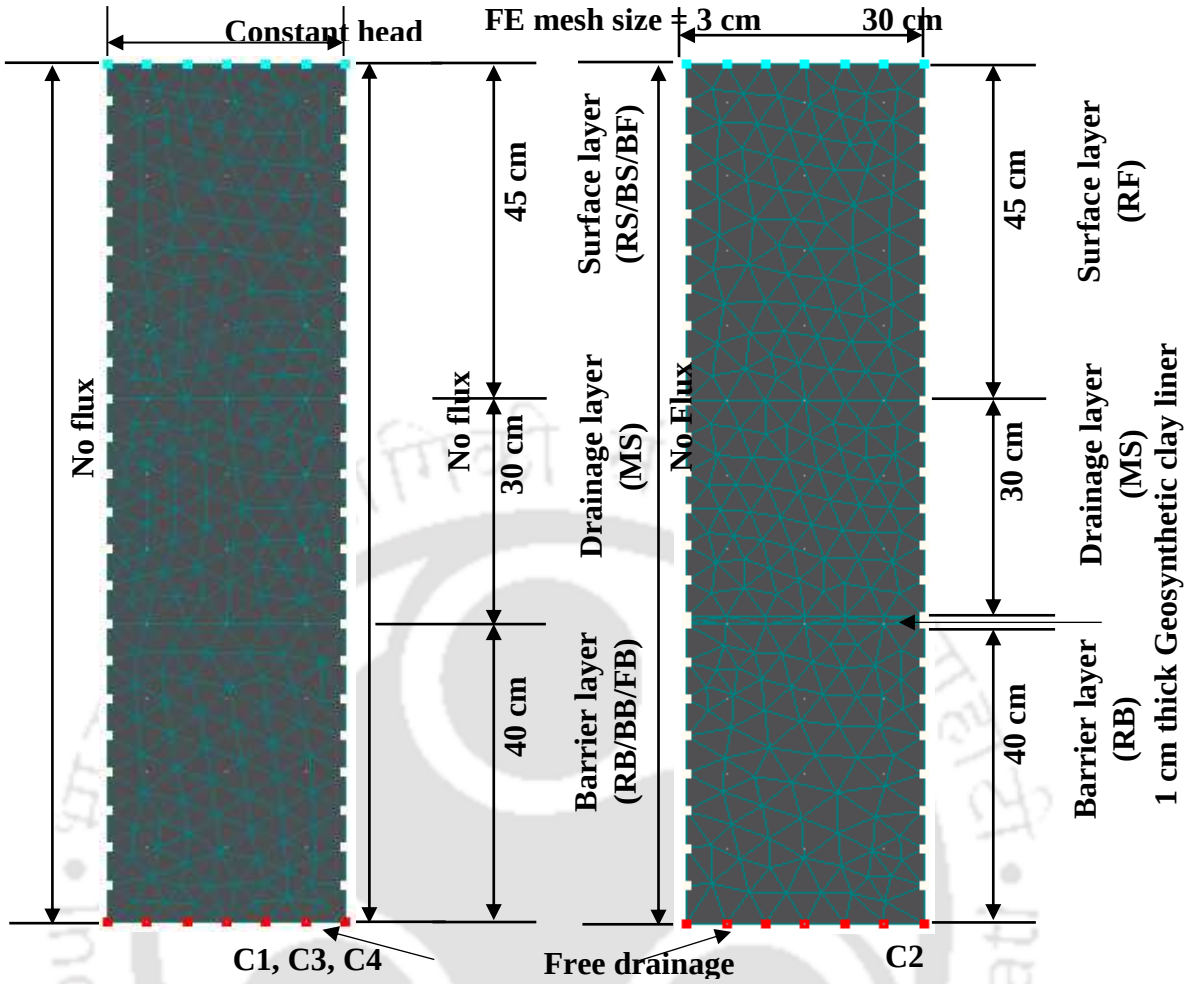

Fig. 5.3 Geometry, boundary conditions used for numerical modelling

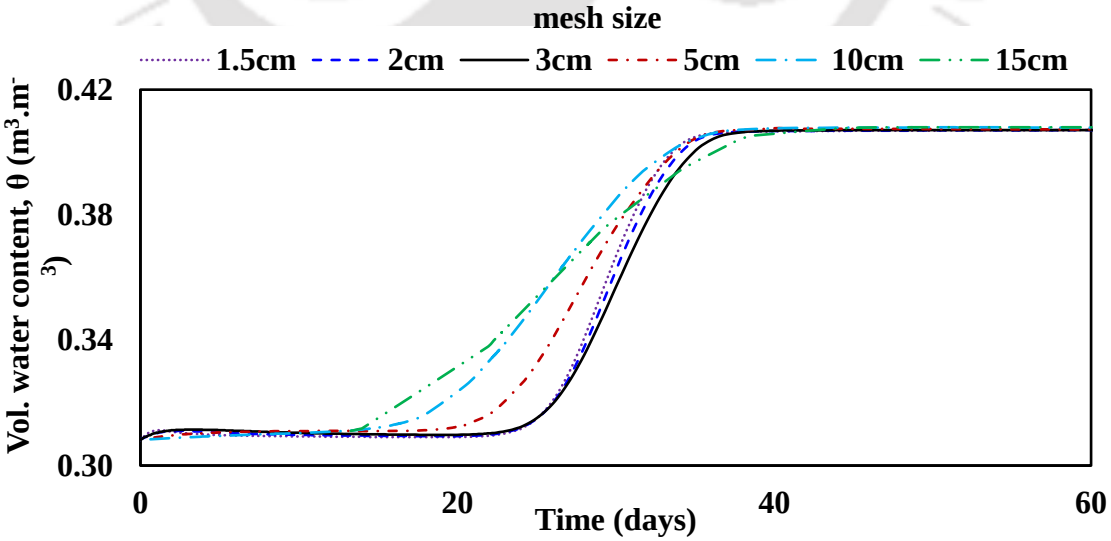

Fig. 5.4 Convergence study of finite element mesh size used for numerical modelling

The soil hydraulic parameters θ_r, θ_s, α, and n were determined by fitting van Genuchten equation (Eq. 5.3) to soil-water characteristic curves (SWCC) obtained from three different approaches. The first approach used neural network prediction (Rosetta Lite V. 1.1 2003) based on soil textural properties (Wosten et al. 1999). The second approach computed hydraulic parameters from drying SWCC measured by 5TM, TEROS 21 sensors and dew point potentiameter (WP4-T, Decagon Devices Inc., USA). The last approach included hydraulic parameters from wetting SWCC obtained from 5TM and TEROS 21 sensors (METER Group, USA) during water infiltration (Malaya 2011). The details of the three SWCCs (predicted, drying and wetting) of soil materials are presented in Fig. 5.5. These hydraulic parameters are designated as PHP, DHP and WHP for predicted, drying and wetting hydraulic properties respectively. The parameters estimated for each layer material of four CS columns are reported in Table 5.2. Only, the hydraulic parameters of GCL were adopted based on the data available in the literature (Benson et al. 2007b). Table 5.2 also presents the initial θ (θ_i) of each column layer, which was considered as initial conditions in the numerical simulations. A constant ponding head of 150 cm was applied at the top of each CS column. No flux boundary condition was chosen for vertical sides of the column. A free drainage boundary condition was selected at the base of the column model. The numerical flow simulation estimates θ variation with depth and time for the abovementioned initial and boundary conditions, which was compared with the measured test results obtained from the column study. The accuracy of the test measurements was improved by performance enhancement of PP based on in-house calibration.

$$\theta(\psi) = \theta_r + \frac{\theta_s - \theta_r}{\left[1 + \left(|\alpha\psi|\right)^n\right]^m} \tag{5.3}$$

where, $\theta(\psi)$ is volumetric water content corresponding to suction, ψ, θ_s is saturated volumetric water content, θ_r is residual volumetric water content; α (related to air entry suction of the soil), n (related to pore size distribution of the soil) and m (related to overall symmetry of the SWCC) are van Genuchten parameters.

Table 5.2 Hydraulic characteristics of all soil materials used in numerical simulation

Soil column	Layer (Material)	Designation	θ_r	θ_s	α	n	k_s	I	θ_i
C1	Surface layer (RS)	WHP	0.061	0.406	0.0010	1.24	3E-9	0.5	0.308
		DHP	0.062	0.419	0.0005	1.31	3E-9	0.5	0.308
		PHP	0.076	0.404	0.0023	1.30	3E-9	0.5	0.308
	Drainage layer (MS)	WHP	0.039	0.369	0.0498	1.78	4E-5	0.5	0.060
		DHP	0.040	0.381	0.0408	1.81	4E-5	0.5	0.060
		PHP	0.049	0.379	0.0259	2.06	4E-5	0.5	0.060
	Barrier layer (RB)	WHP	0.076	0.421	0.0004	1.21	2E-10	0.5	0.330
		DHP	0.077	0.438	0.0003	1.23	2E-10	0.5	0.330
		PHP	0.086	0.436	0.0011	1.28	2E-10	0.5	0.330
C2	Surface layer (RF)	WHP	0.0584	0.381	0.00057	1.61	3E-8	0.5	0.287
		DHP	0.0586	0.392	0.00047	1.67	3E-8	0.5	0.287
		PHP	0.0585	0.406	0.00145	1.57	3E-8	0.5	0.287
	Drainage layer (MS)	WHP	0.039	0.369	0.0498	1.78	4E-5	0.5	0.060
		DHP	0.040	0.381	0.0408	1.81	4E-5	0.5	0.060
		PHP	0.049	0.379	0.0259	2.06	4E-5	0.5	0.060
	GCL (Benson et al. 2007b)		0.068	0.6	0.001	2.00	6E-11	0.5	0.115
	Barrier layer (RB)	WHP	0.076	0.421	0.0004	1.21	2E-10	0.5	0.330
		DHP	0.077	0.438	0.0003	1.23	2E-10	0.5	0.330
		PHP	0.086	0.436	0.0011	1.28	2E-10	0.5	0.330
C3	Surface layer (BS)	WHP	0.0711	0.447	0.00053	1.30	6E-9	0.5	0.333
		DHP	0.0713	0.456	0.00025	1.42	6E-9	0.5	0.333
		PHP	0.0852	0.431	0.00162	1.28	6E-9	0.5	0.333
	Drainage layer (MS)	WHP	0.039	0.369	0.0498	1.78	4E-5	0.5	0.060
		DHP	0.040	0.381	0.0408	1.81	4E-5	0.5	0.060
		PHP	0.049	0.379	0.0259	2.06	4E-5	0.5	0.060
	Barrier layer (BB)	WHP	0.0851	0.478	0.00017	1.38	4E-10	0.5	0.358
		DHP	0.0853	0.491	0.00011	1.49	4E-10	0.5	0.358
		PHP	0.0903	0.453	0.001	1.27	4E-10	0.5	0.358
C4	Surface layer (BF)	WHP	0.0606	0.418	0.00118	1.33	4E-8	0.5	0.286
		DHP	0.0607	0.427	0.00111	1.29	4E-8	0.5	0.286
		PHP	0.0628	0.412	0.0021	1.43	4E-8	0.5	0.286
	Drainage layer (MS)	WHP	0.039	0.369	0.0498	1.78	4E-5	0.5	0.060
		DHP	0.040	0.381	0.0408	1.81	4E-5	0.5	0.060
		PHP	0.049	0.379	0.0259	2.06	4E-5	0.5	0.060
	Barrier layer (FB)	WHP	0.0812	0.409	0.00037	1.29	3E-9	0.5	0.322
		DHP	0.0813	0.413	0.00031	1.27	3E-9	0.5	0.322
		PHP	0.0881	0.417	0.00065	1.39	3E-9	0.5	0.322

Note: WHP = wetting hydraulic parameters, DHP = drying hydraulic parameters, PHP = predicted hydraulic parameters, θ_r = residual volumetric water content ($m^3.m^{-3}$); θ_s = saturated volumetric water content ($m^3.m^{-3}$); α (cm^{-1}) and n = van Genuchten parameters; k_s = saturated hydraulic conductivity (m/s); I = pore connectivity parameter; θ_i = initial volumetric water content ($m^3.m^{-3}$)

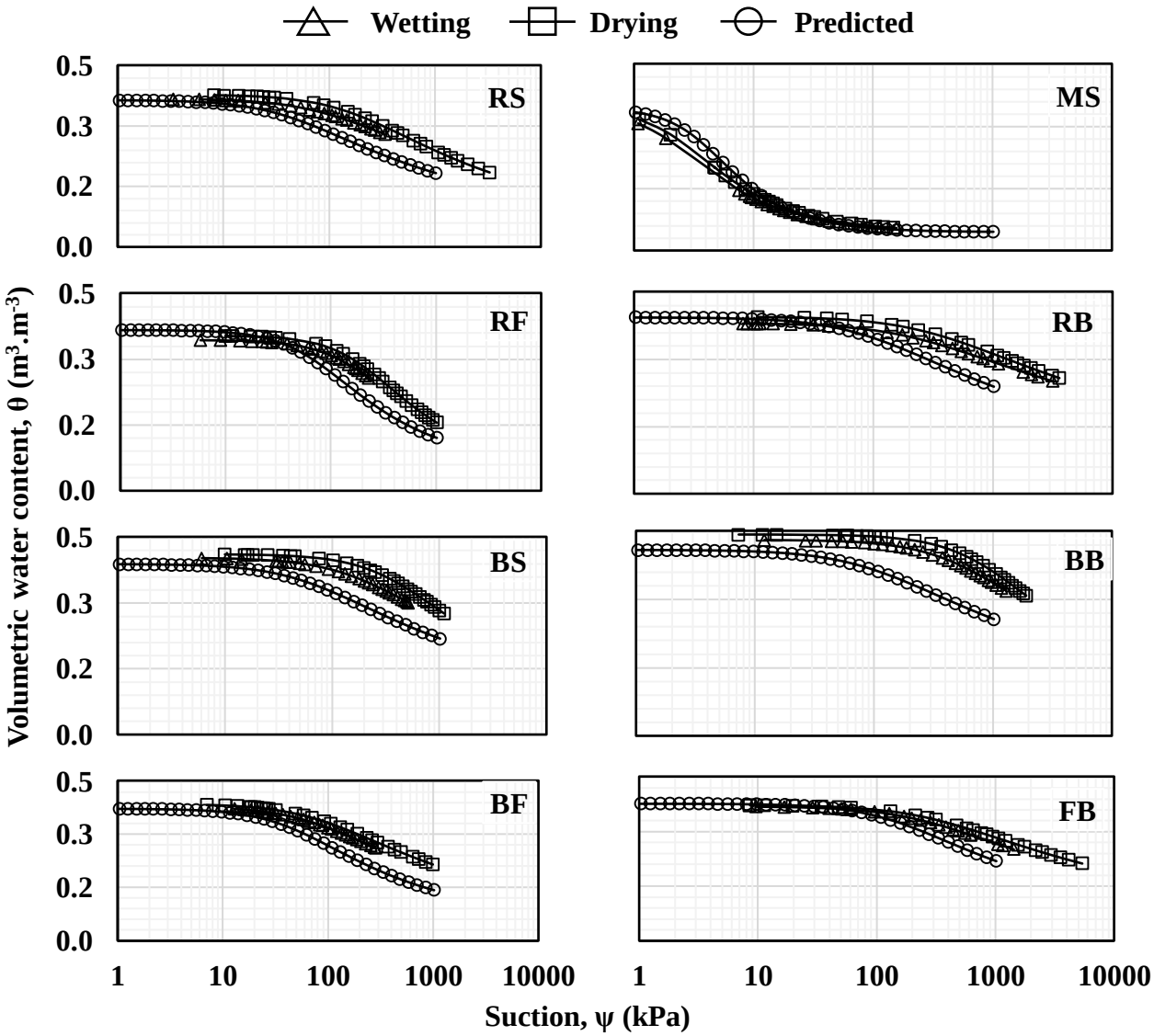

Fig. 5.5 Predicted, drying and wetting SWCCs of various layer materials

5.4 Results and discussion

5.4.1 Surface layer performance

The θ versus time response measured at 20, 30 and 40 cm depths (variation of θ_{20}, θ_{30} and θ_{40} with time) in the SL of the four CS columns are presented in Fig. 5.6. The figure shows an increase in θ from θ_i when waterfront reaches the sensor influence zone and ultimately reaches to saturated θ indicated by a constant value. Based on the data reported in Table 5.3, TP_{20}, TP_{30}, TP_{40} of any CS column can be arranged in the order $TP_{20} < TP_{30} < TP_{40}$. This inferred that the rate of saturation diminished with depth for SL. This may be due to the progressive difficulty in replacing air pockets by the percolating water (Touma

et al., 1984). It can also be derived from Fig. 5.6 that for any depth of SL, the TP varies in the order TP(C2) < TP(C4) < TP(C3) < TP(C1). It can be deduced that the SL of C2, which used 50% FA and 50% RS mix performed poorly in minimizing water percolation. The SL of C4 with 50% FA-50% BS performed marginally better than C2. The SL of C1 and C3, composed of RS and BS, respectively, performed almost four times better in restricting the percolation. It demonstrates that FA inclusion in the SLs of Column C2 and C4 resulted in their quick saturation within a short time (3 to 7 days). The SL performance thus deteriorated rapidly due to FA addition due to an increase in permeability of the surface layer. However, the SLs of C1 and C3, saturate in 32 to 35 days, which is at a much slower rate as compared to C2 and C4. In the context of three numerical inputs for water retention parameters (PHP, DHP, and WHP), the WHP input was found to predict the percolation in SLs for all the four columns better. This is expected as the water infiltration through a MLCS column is a gradual wetting phenomenon. Based on Table 5.3, the average percentage error in TP for different numerical inputs was computed at various depth considering all four columns and summarized in Table 5.4. It can be noted from the table that the percentage error decreases with the increase of column depth. The WHP based simulations result in less average error compared to DHP and PHP based simulations. However, the difference in percentage error is minimal for WHP and DHP. This indicates that the error incurred by considering DHP (easy to determine) instead of WHP for a continuous wetting phenomenon is marginal.

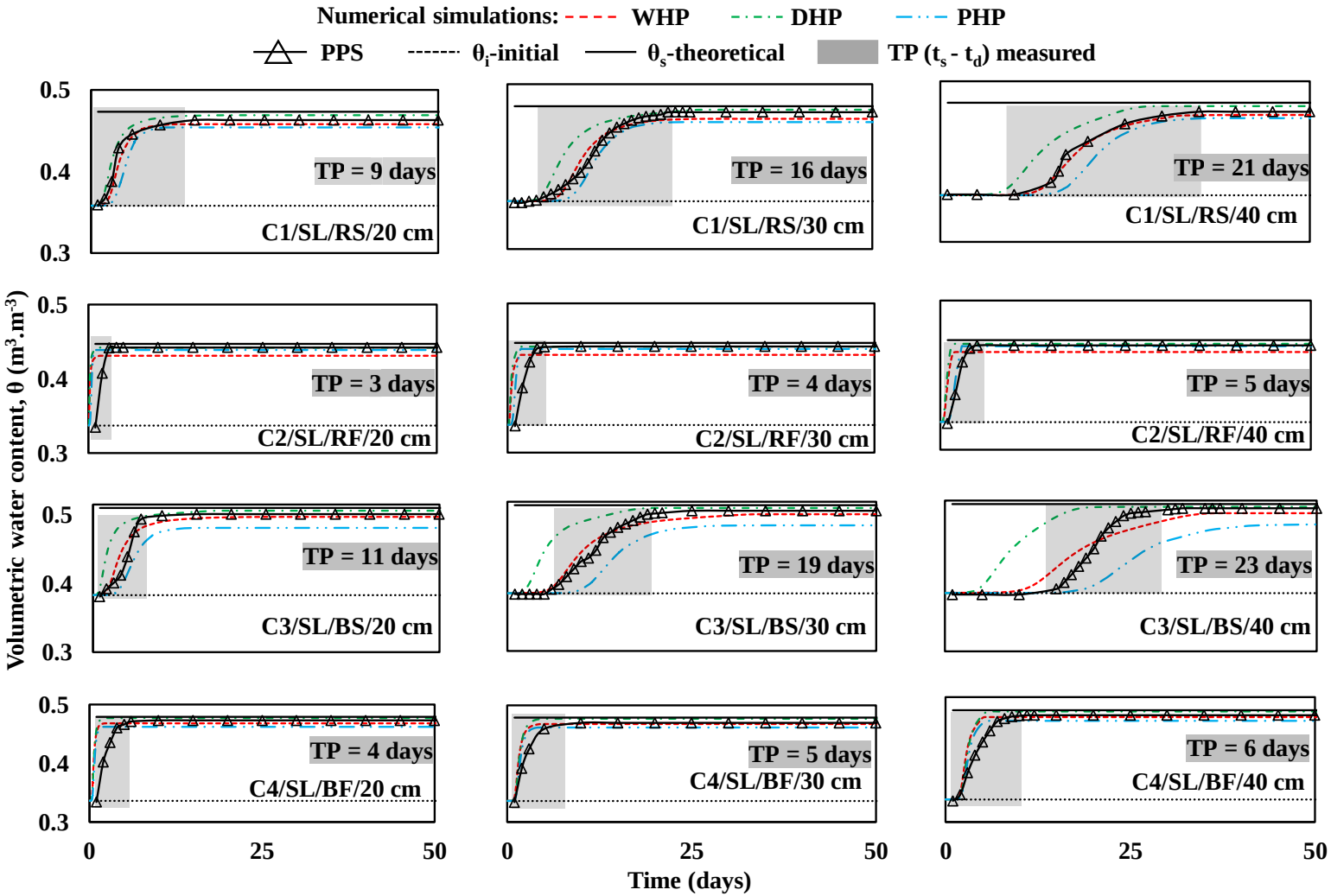

Fig. 5.6 Variation of volumetric water content at various depths of surface layer

Table 5.3 Time of deviation and time to saturation of θ at various depths of 4 columns

Layer	Depth	Based on	C1			C2			C3			C4		
			t_d	t_s	TP	t_d	t_s	TP	t_d	t_s	TP	t_d	t_s	TP
SL	10 cm	PPS	0.4	5	4.6	0.21	2.6	2.39	0.5	7	6.5	0.21	2.78	2.7
		WHP	0.3	3	2.7	0.17	1.1	0.83	0.3	5	4.7	0.17	0.75	0.2
		DHP	0.2	4	3.8	0.04	0.7	0.66	0.1	4.2	4.1	0.01	0.08	0.1
		PHP	0.6	2	1.4	0.08	0.4	0.32	0.5	3	2.5	0.01	0.43	0.4
	20 cm	PPS	1	10	9	0.35	3.37	3.02	1.3	12	10.7	0.37	4.1	3.8
		WHP	1	11	10	0.13	1.7	1.6	1.3	15	13.7	0.21	2.2	1.9
		DHP	1.2	13	11.8	0.1	1.6	1.5	1.1	16	14.9	0.18	1.3	1.1
		PHP	2.3	11	8.7	0.23	0.8	0.6	3	14.5	11.5	0.23	2.2	1.9
	30 cm	PPS	3	19	16	0.65	4.88	3.73	7	26	19	1.84	6.85	4.9
		WHP	4	24	20	0.27	2.4	2.1	5.8	29	23.2	0.95	4.6	3.6
		DHP	3.2	26	22.8	0.23	2.2	2.0	3	20	17	0.85	5.3	4.4
		PHP	6.5	24	17.5	0.72	1.8	1.08	9	32	23	1.05	4.2	3.2
	40 cm	PPS	8	29	21	1.14	5.74	4.8	11	34	23	2.26	8.2	6
		WHP	9	33	24	0.53	2.9	2.4	9.3	37	27.7	1.77	5.2	3.4
		DHP	7	29	22	0.47	3	2.5	5.3	24	18.7	1.79	6.1	4.3
		PHP	11	35	24	1.37	3.3	1.9	19	51	32	1.59	5.6	4.0
DL	60 cm	PPS	50	223	173	8.55	22	13.4	55	341	286	9.25	24.5	15.3
		WHP	50	225	175	5.36	21	15.6	49	332	283	7.86	26.5	18.6
		DHP	49	234	185	4.62	19.5	15	42	312	270	9.56	30	20.4
		PHP	47	226	179	6.21	21.3	15.1	55	272	217	9.17	29.3	20.2
GCL	75 cm	PPS	_	_		_	_		_	_		_	_	
		WHP	_	_		62	223	161	_	_		_	_	
		DHP	_	_		96	223	127	_	_		_	_	
		PHP	_	_		87	233	146	_	_		_	_	
BL	100 cm	PPS	182	327	145	283	730	447	171	296	125	41	134	93
		WHP	172	312	140	279	711	432	156	277	121	46	136	90
		DHP	130	273	143	176	543	367	103	221	139	38	144	106
		PHP	160	290	130	238	692	454	172	357	185	24	42	18

Note: θ = volumetric water content ($m^3.m^{-3}$); t_s = time to saturation (days); t_d = time to deviation from initial condition (days); PPS = profile probe sensor, simulations based on WHP = wetting hydraulic properties, DHP = drying hydraulic properties, PHP = predicted hydraulic properties

Table 5.4 Average percentage error in TP for different numerical inputs

Layer	Depth	% error based on numerical inputs		
		WHP	DHP	PHP
SL	10 cm	56	57	76
	20 cm	34	35	48
	30 cm	27	29	34
	40 cm	25	32	37
DL	60 cm	10	14	18
BL	100 cm	3	11	35

Notes: The average percentage error was computed by considering the percentage error of all four columns

5.4.2 Drainage layer performance

Figure 5.7 presents the θ vsersus time profile recorded at 60 cm depth (θ_{60} variation with time) in the middle of DLs (MS in all the columns). In the figure, θ_{60} approached saturation very rapidly in C2 and C4. The saturation of θ_{60} was gradual in C1. Rate of saturation of θ_{60} in C3 followed three different ways; moderate at the initial stage, very slow at the intermediate stage and then again moderated at the final stage. This might be due to presence of organic matter (OM; 2.93%) in upper SL consisting of less permeable BS. The OM may affect pore size distribution by modifying the soil structure to create very tortuous and thin pathways for water to percolate (Nemes et al., 2005). From Table 5.3, 4 columns can be ordered as C2 (13 days) < C4 (15 days) < C1 (173 days) < C3 (286 days) based on the TP_{60} required for θ_{60} saturation in DL. It implies that the DLs of C2 and C4, wherein 50% FA was mixed with RS and BS respectively in the above SL, took sufficiently less time than the DL of C1 and C3. This observation is in line with those reported in the previous section. The saturation of θ_{60} in the DLs of C1 and C3 took relatively longer duration attributed to low permeable (10^{-9} m/s) SL. This might also be due to CB effect at the interface between SL and BL (Abdolahzadeh et al. 2011; Parent and Cabral 2006), which works till the saturation of the overlying SL. Furthermore, it might be explained based on the previous study, which investigated the water flow mechanism for saturating a vertical sand column erected inside a cylindrical container (Kuang et al., 2011). According to Kuang et al. (2011), the percolated water which arrived at the middle of the DL, commenced the saturation (θ_{60}) but before its full saturation some amount of water migrated downward due to very high permeability (10^{-5} m/s) and less water holding capacity of MS.

Since there was no provision for lateral drainage, the water accumulated in the DL due to highly impermeable hydraulic BL (10^{-10} m/s) beneath DL. This results in progressive saturation of DL from bottom to top. While comparing TP_{60} of C1 and C3, it can be noted that the saturation of θ_{60} in C3 took 113 days (refer Table 5) additionally, even though permeability of the upper SLs was of the same order. This might be due to the downward flow of percolated water through the preferential paths (created by the decomposition of OM (2.43%)) in BL before the saturation of DL (Boyle et al. 1989). The measurements from all the CS columns except C3 were commensurable with all three numerical approaches which were adopted to simulate DL percolation. This might be because of low hysteresis in the SWCCs of MS (Yang et al. 2004b) presented in Fig.5.5. In C3, only WHP based numerical simulation matched well with the measured variation of θ_{60} with time.

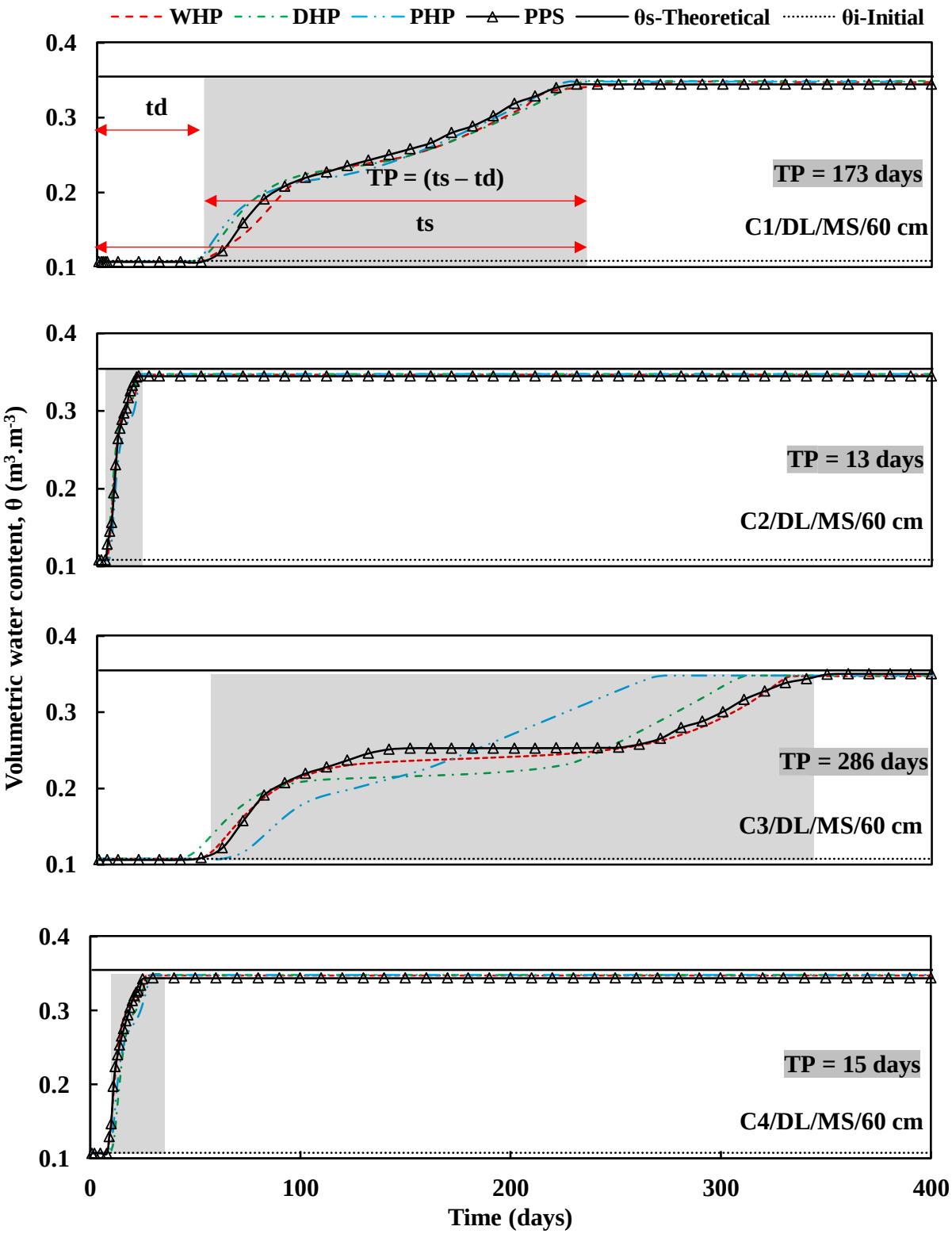

Fig. 5.7 Variation of volumetric water content at 60 cm depth in drainage layer

5.4.3 Barrier layer performance

Figure 5.8 shows the variation of θ_{100} with time measured in BL of all 4 columns and TP_{100} (days) required for θ_{100} saturation summarized in Table 5.3. Based on the table, 4 columns can be arranged in an ascending order of TP_{100} as C4 (93) < C3 (125) < C1 (145) < C2 (447). This implies that the θ_{100} in C4 saturates faster due to a highly percolating FA in both SL (50% FA) and BL (70% FA). It demonstrates that the FA addition in SL drastically deteriorated the hydraulic performance of subsequent layers of a CS. Although the permeability of SL (10^{-9} m/s), DL (10^{-5} m/s) and BL (10^{-10} m/s) in both C1 and C3 were of the same order, the intermediate TP_{100} for their BL was not of the same magnitude. TP_{100} in C3 was found to be 20 days less than the TP_{100} in C1, plausibly due to water flow increase in BL through the pores generated by decomposition of OM (Boyle et al. 1989). In case of C2, even though 50% FA was added in SL, the TP_{100} for saturation of θ_{100} in BL was found as 447 days, which is the longest duration among all 4 CS columns. This is evidently due to the inclusion of low permeable GCL (10^{-11} m/s reported in Table 5.2) as an additional hydraulic barrier layer on the top of the BL. These observations strongly advocate GCL inclusion in the landfill cover system for reducing water percolation into the underlying waste. It also endorses the need for a well-designed SL for the percolation performance of bottom layers.

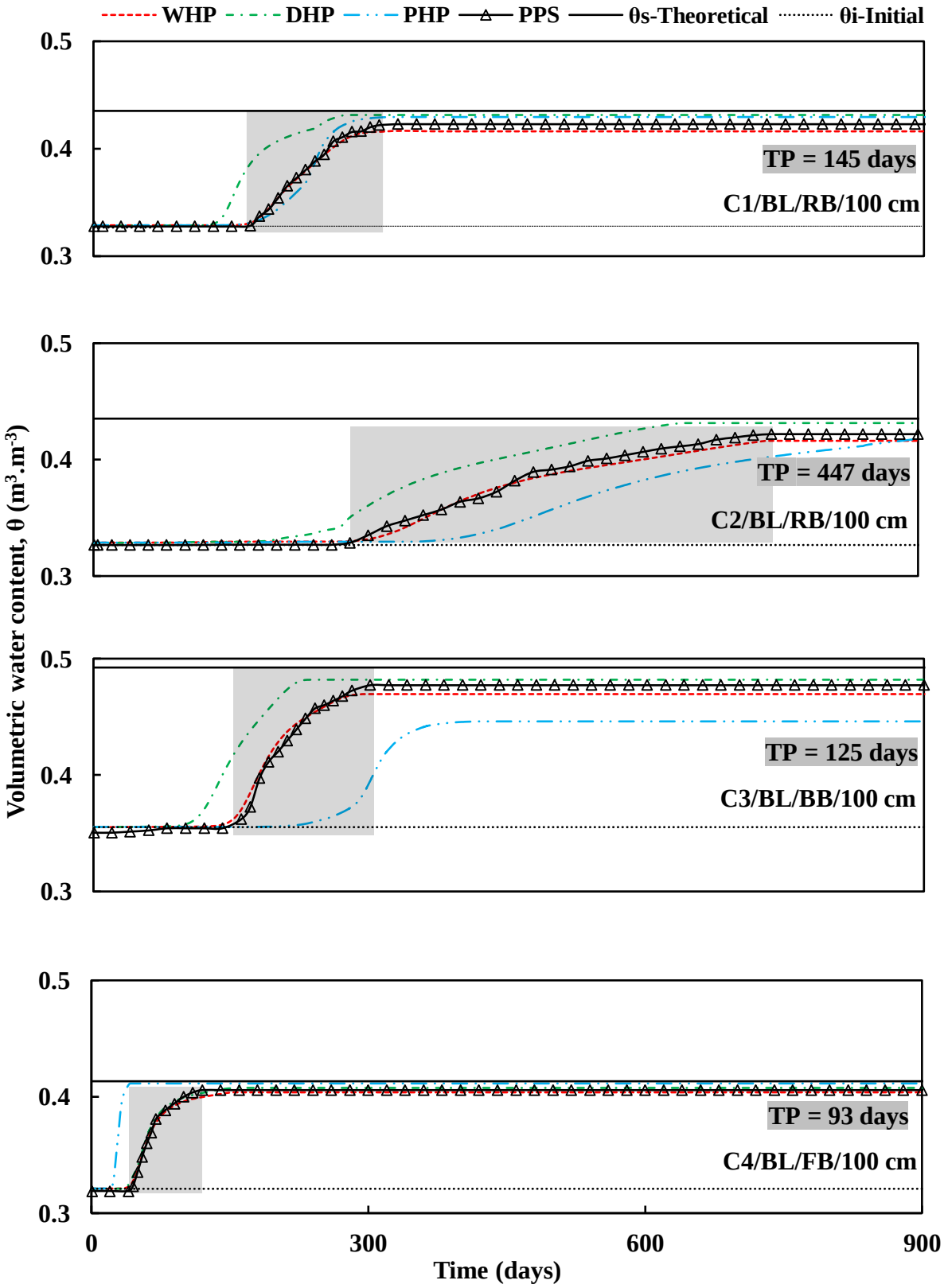

Fig. 5.8 Variation of volumetric water content at 100 cm depth in barrier layer

5.4.4 Overall performance of MLCS based on column study

It can be noticed from the Figs. 5.6 to 5.8 that the soil specific θ_s measured by PPS in SL, DL and BL of each CS column were slightly lesser than their respective theoretical values. The theoretical θ_s is equal to porosity computed from the measured mass-volume relationship given by Eq. 4.11. The simulated results of θ_s were comparable with measured θ_s and also marginally lesser than theoretical θ_s. This was expected due to the presence of entrapped air (Wang et al. 1997). Once the PPS measurement reached θ_s in a column layer, it remained the same for the entire duration of the study as each and every column underwent progressive wetting under constant water ponding. t_d and t_s at various depths obtained from PPS measurement and WHP based simulation are portrayed in Fig. 5.9. The figure depicts the layer-specific hydraulic performance of all CS columns by referring to t_d and t_s along with the depth. Figure 5.10 depicted the t_d and t_s at 100 cm depth in the BLs of 4 columns. The figure also shows the TP_{100} ($t_s - t_d$ at 100 cm depth) for all the columns. These results were acquired from measurement by PPS and simulation using WHP. The figure furnished a clear understanding of overall percolation performance of 4 various MLCS under constant water ponding. The figure clearly identified 4 CS columns to be organized in the order as C4 < C3 < C1 < C2 based on experimental as well as numerical analyses of TP_{100}.

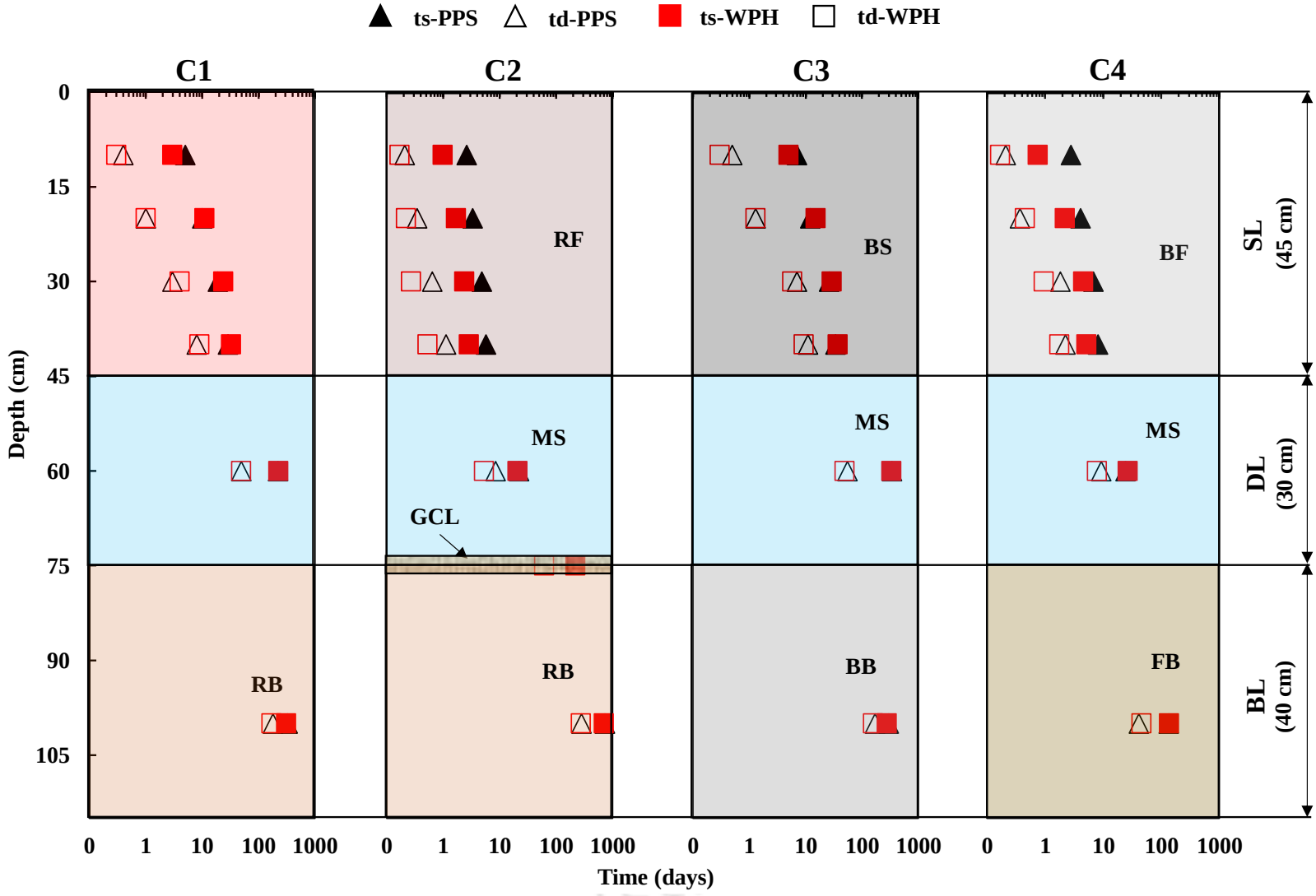

Fig. 5.9 Time duration before deviation and to saturation of different column depths

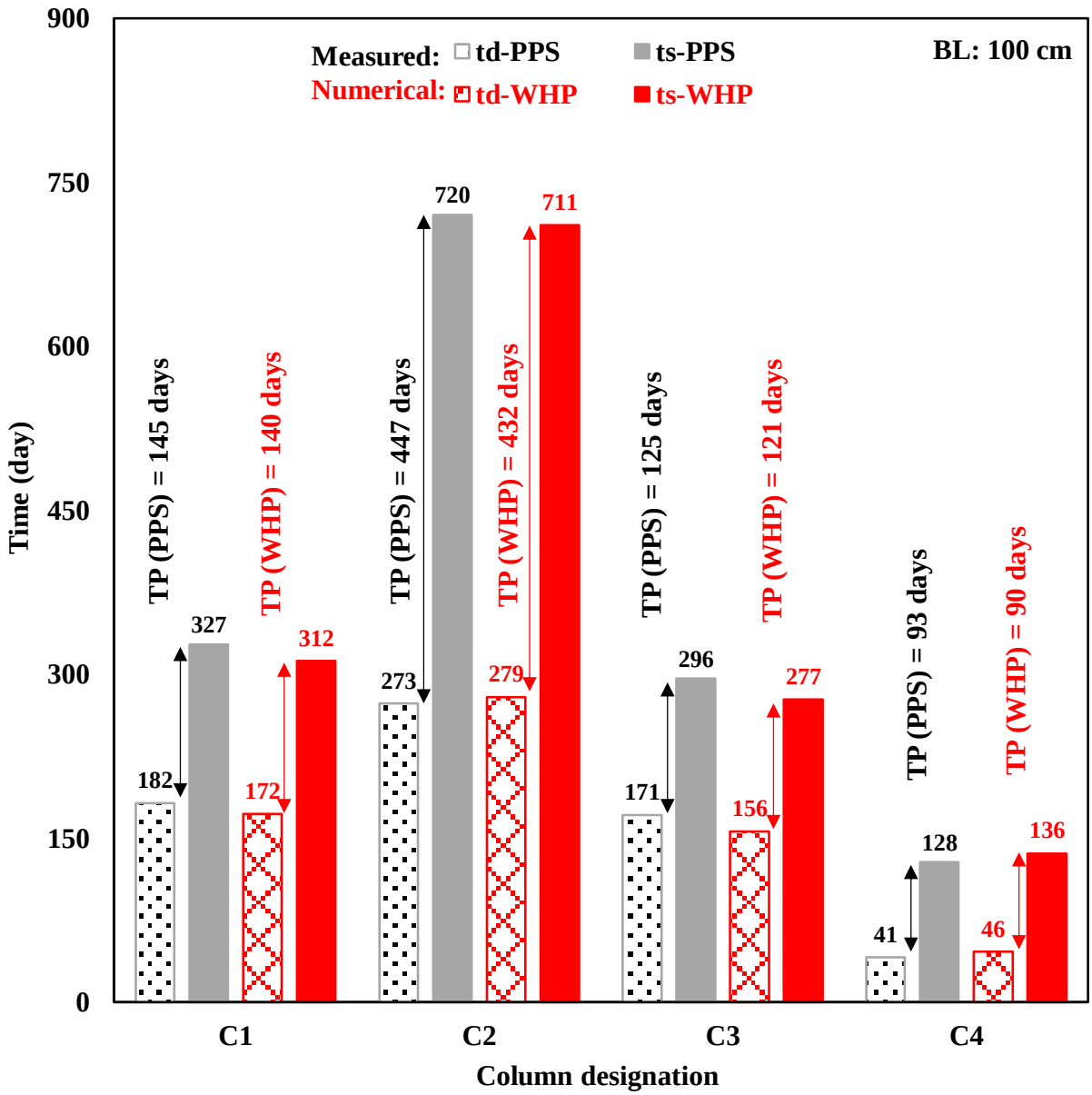

Fig. 5.10 Time duration before deviation and to saturation of 100 cm column depth

5.4.5 Cost analysis

The cost-effectiveness of using GCL in the pilot CS columns was investigated based on the numerical results obtained from this study. A simple analysis was carried out for evaluating bentonite cost saved due to the inclusion of GCL in the CS columns to achieve the same hydraulic performance which was attained in the absence of GCL. The time to saturation of full height of a particular CS column was predicted based on the most favourable numerical input (WHP) when GCL was not used. Corresponding to that time, the wetting depth of BL was determined for the case when the GCL was used. For the same

hydraulic performance, the remaining depth of bentonite in BL was saved due to GCL incorporation. The cost saved due to GCL inclusion was estimated by Eq. 5.5 for each case based on the cost of materials only (bentonite or GCL or both). For instance, Figure 5.11 illustrates the cost estimation adopted for materials used in C2. The cost of the only bentonite used in the CS column wherein GCL was not included, was computed based on equation 5.6. For another case, the cost of both bentonite and GCL was evaluated based on equation 5.7.

$$C = \left(\frac{C_B - C_{B+G}}{C_B} \times 100 \right)\% \tag{5.5}$$

$$C_B = \frac{\pi}{4} d^2 h \times D \times P \times R_B \tag{5.6}$$

$$C_B = \frac{\pi}{4} d^2 h \times D \times P \times R_B + \frac{\pi}{4} d^2 \times R_G \tag{5.7}$$

where C is the percentage of cost-benefit, C_B is cost of bentonite when GCL is not used, C_{B+G} is cost of both GCL and bentonite when the GCL is used, $\pi = 3.14$, d is inside diameter of column container wherein BL or GCL was placed, h is saturated height of BL, D is density of BL material, P is percentage of bentonite used for BL ($P = 30\% = 0.3$), R_B is bentonite price, R_G is GCL price. The results of the cost-benefit analyses of 4 CS columns were summarized in Table 5.5. GCL inclusion saved approximately 63%, 74%, 69% and 87% bentonite clay in BLs of C1, C2, C3, and C4 respectively. Accordingly, the cost-benefit of 36% in C1, 47% in C2, 38% in C3 and 59% in C4 were achieved by which the columns can be arranged in the order C4 < C2 < C3 < C1. Moreover, the installation of GCL during the construction of CS is quite easy as compared to the conventional approach of constructing compacted BL, which is laborious, time-consuming and expensive (Simon and Müller 2004).

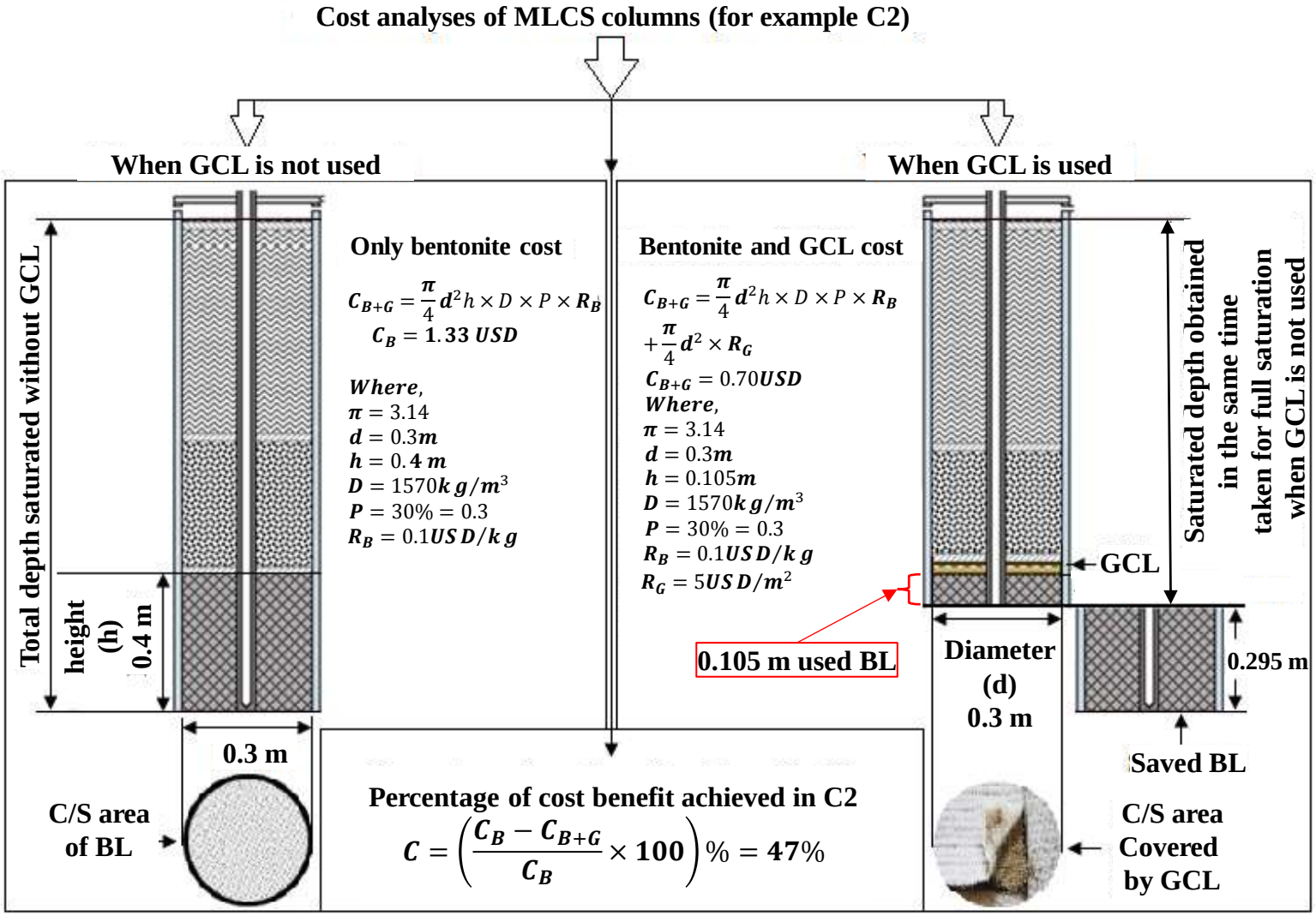

Fig. 5.11 Cost analysis of GCL and bentonite used for test columns

Table 5.5 Material cost analysis of geosynthetic clay liner (GCL) and bentonite used in hydraulic barrier layer

Column /layer	Soil mix used	Use of GCL	C/S area (m^2)	Density (kg/m^3)	Height (m)	Volume (m^3)	Bentonite mass (kg)	Bentonite cost (USD)	GCL cost (USD)	Total cost (USD)	Bentonite saving	Cost Benefit
						{[4]×[6]}	{0.3×[5]×[7]}	{0.1×[8]}	{5×[4]}	{[9]+[10]}		
[1]	[2]	[3]	[4]	[5]	[6]	[7]	[8]	[9]	[10]	[11]	[12]	[13]
C1/BL	70% red soil + 30% bentonite	without GCL	0.071	1570	0.400	0.0283	13.32	1.33	0	1.33	–	
		with GCL	0.071	1570	0.155	0.0106	5.0	0.50	0.35	0.85	63%	36%
C2/BL	70% red soil + 30% bentonite	without GCL	0.071	1570	0.400	0.0283	13.32	1.33	0.0	1.33	–	
		with GCL	0.071	1570	0.105	0.0074	3.50	0.35	0.35	0.70	74%	47%
C3/BL	70% black soil + 30% bentonite	without GCL	0.071	1360	0.400	0.0283	11.54	1.15	0	1.15	–	
		with GCL	0.071	1360	0.125	0.009	3.61	0.36	0.35	0.71	69%	38%
C4/BL	70% fly ash + 30% bentonite	without GCL	0.071	1490	0.400	0.0283	12.64	1.26	0	1.26	–	
		with GCL	0.071	1490	0.050	0.004	1.58	0.16	0.35	0.51	87%	59%

Notes: Price (rate) of bentonite = 0.1 USD/kg (https://www.statista.com/statistics/248186/average-bentonite-price, accessed on 3rd April, 2019). Price (rate) of GCL = 5 USD/m^2 (https://www.globalsources.com/manufacturers/Geosynthetic-Clay-Liner.html, accessed on 3rd April, 2019). Installation and transportation cost were not considered.

5.5 Summary

This chapter investigates the hydraulic performance efficiency of different configurations of the multi-layered cover system (CS) suitable for high humid, heavy rainfall areas. The four configurations of CS columns (denoted as C1, C2, C3, and C4) consisted of surface layer (SL), drainage layer (DL) and barrier layer (SL) successively from top to bottom. Only the column C2 had 1 cm thick geosynthetic clay liner (GCL) over the BL as an additional hydraulic barrier layer. C2 and C4 used recycled fly ash (FA) along with the traditional CS soils. Component material was thus different for individual CS layer whose thickness was decided the same as the field layers. Percolation test of these CS columns was conducted under constant water ponding condition. Volumetric water content (θ) was measured as a function of depths and time for each CS column for 900 days to assess the rate of saturation. The numerical assessment of water percolation was carried out for all the columns based on drying, wetting and predicted water retention characteristics.

It was noticed that the numerical analysis performed with wetting hydraulic parameter matched well with the test results. However, the comparison of simulated results between wetting and drying hydraulic characteristics indicated marginal difference demonstrating the possibility of using the latter for a continuous wetting phenomenon. The study showed that the saturation rate diminished with the measurement depth of an individual CS layer. The addition of fly ash (FA) by 50% in SL and 70% in BL of CS column deteriorated its hydraulic performance efficiency by almost 25%. However, the inclusion of geosynthetic clay liner (GCL) enhanced the overall performance efficiency of the CS column by around two times despite the addition of 50% FA in its SL. The study thus advocated the advantage of GCL and disadvantage of FA as the MLCS materials for landfill application. Moreover, GCL inclusion was found to attain a cost-benefit of at least 36% for the configuration of MLCS used for high humid regions. Further investigations are required to understand the adverse effects of local weather conditions and climate on the MLCS constructed in the field.

Chapter 6

Hydraulic Performance of MLCS under Natural Weather Condition

6.1 General

Evapotranspiration and capillary barrier cover systems are utilized as an engineered multi-layered cover system (MLCS) for arid and semi-arid regions. However, previous studies advocate a three-layer hydraulic barrier cover system for high humid climatic regions where the average annual precipitation is more than 1000 mm. North-east India is one of the world's high humid regions receiving average annual precipitation close to 2500 mm. The functioning of the three-layered cover system has been rarely explored for such high humid sites considering natural weather conditions. This chapter evaluated the hydraulic performance of a three-layered hydraulic barrier cover system in high humid regions. A pilot three-layer cover system was constructed close to (5 km) a local landfill site and exposed to natural weather conditions. The weather parameters (precipitation, solar radiation, wind, temperature, and humidity) were measured using a microclimate monitoring system installed adjacent to the constructed cover. The cover system was instrumented for real-time monitoring of volumetric water content or (θ) and matric suction (ψ) with depth. The monitoring was conducted for 800 days from 10th May 2016 to 18th July 2018. The numerical analysis of water flow through the MLCS setup was carried out by a finite element package HYDRUS 2D. The simulations were performed based on the evapotranspiration models from the weather data, measured drying and wetting soil-water characteristic curves (SWCC) for each soil layer and allied parameters. Field measurements were ultimately used to identify the appropriate input hydraulic parameters as well as evapotranspiration models. The natural vegetation development and desiccation cracks on the surface layer were also measured using non-intrusive image analysis. The percolation performance of the MLCS was also evaluated for high precipitation and drought events.

6.2 Background study

The advent of the urban population boom in the 21st century has exacerbated the generation of municipal and hazardous (industrial and nuclear) waste (Guerrero et al. 2013; Inglezakis and Moustakas 2015; Laner et al. 2012; Shivam et al. 2017). The hazardous wastes are disposed into landfills having an engineered bottom hydraulic liner (Aldaeef and Rayhani 2015; Hamdi and Srasra 2013; Rowe 2011; Yidong et al. 2012). A MLCS needs

to be constructed over the waste layer after the landfill reaches its full capacity to minimize the rainwater migration (percolation) into the underlying wastes (Apiwantragoon et al. 2015; Landreth et al. 1991). As presented in Table 2.5, the evapotranspiration (ET) cover system and capillary barrier (CB) cover system was utilized as MLCS for arid and semi-arid regions. The ET cover system use vegetated soil layers for storing water in individual layer until it is either evaporated through the soil surface or transpired through plants (Barnswell and Dwyer 2012; Schnabel et al. 2012; Zhang et al. 2017). The CB cover system contains two soil layers: a coarse-grained soil layer underlying a vegetated fine-grained soil layer; and apart from evapotranspiration, additionally rely on the capillary barrier effect (Harnas et al. 2014; Li et al. 2013; Rahardjo et al. 2016; Subedi et al. 2013; Zhan et al. 2014) between the two layers to minimize water percolation. Both these cover systems have found to be suitable for use in arid and semi-arid regions where annual precipitation is relatively low or moderate (average annual rainfall of 100-600 mm) (Aljaradin and Persson 2015; Bohnhoff et al. 2009; Sadek et al. 2007). For humid regions (with average annual rainfall more than 1000 mm)(Ng et al. 2015; Zhang and Sun 2014) these two cover systems were not found to be adequate to stop water percolation due to low water holding capacity, preferential flow through roots and desiccation cracking (Hoor and Rowe 2013; Khapre et al. 2017; Sinnathamby et al. 2014; Song et al. 2017) .

A novel three-layered cover system was proposed by Ng et al. (2016) which is suitable for sites having a humid climate. A three-layer cover system is obtained by adding a compacted soil-clay barrier layer beneath a CB cover configuration. The additional advantage of a three-layer cover system is that infiltrated water through the CB layer can be intercepted and reduced by the bottom soil-clay barrier layer. Furthermore, the bottom soil-clay barrier layer is protected by the CB layer from any desiccation cracks during dry seasons by minimizing exposure to atmospheric variants (Ng et al. 2016). In literature, the effect of vegetation induced transpiration on the moisture dynamics has been accounted for in the numerical analysis based on assumed leaf area index (LAI) values (Ogorzalek et al. 2008). Several studies have captured the complex moisture dynamics in the cover systems by instrumenting the cover layers to obtain measured suction and water content profiles. A historical review on studies done for water percolation in cover system has been done in a later section to highlight the methodologies used in previous studies.

The field assessment of three-layer cover system has not been done for extremely humid conditions where average annual rainfall can be more than 1500 mm. The

subcontinent of India experiences an average annual rainfall ranging from 1500 to 2700 mm (Kothawale and Rajeevan 2017) along the north-eastern states. The neighbouring areas of Cherapunjee and Mawsynram (25.18°N, 91.35°E) in north-east India are widely known as the wettest places on earth with an annual average rainfall of 11,430 mm. The Guwahati city (26.18°N, 91.40°E), which is close (about 70 km) to these places also experience average annual rainfall of more than 2,000 mm (Jhajharia et al. 2007). The landfill sites (Goel and Kalamdhad 2017) located in Guwahati city are expected to reach its full capacity soon. Also, there are shallow disposal facilities located on the western part of India (especially Mumbai city) for containment of low-level nuclear waste, which receives equally high rainfall. There is a need to construct a cover system that can mitigate water percolation into the waste disposal facilities for such high humid regions.

6.3 Critical appraisal of previous research

Table 2.5 presented in chapter 2 provides a chronological review of water percolation performance in the cover system. From the table, it can be inferred that the majority of the studies have investigated ET and capillary barrier cover systems. In most of the field studies, these two cover systems were preferable to resist water flow into waste layer when they are subjected to annual precipitation less than 700 mm (Khire et al. 2000; Mccartney and Zornberg 2002). The use of clay barrier layer as the surface layer has also been investigated based on the permeability criterion (10^{-9} m/s, USEPA) with percolation limit of 30 mm/year with continuous wetting and unit hydraulic gradient (Melchior 1997). However, unprotected clay barriers have been prone to desiccation cracking (Melchior 1997; Albright et al. 2006a) which increases the permeability by three order (Li et al. 2016). In a three-layer cover system, the bottom clay layer is protected by the upper two soil layers from desiccation during dry seasons (Ng et al. 2016).

The field efficacy of the ET and capillary barrier cover systems have been measured by the evapotranspiration and drainage rate using lysimeters (Choo and Yanful 2000; Albright et al. 2004; Scanlon et al. 2005b). However, lysimeter based monitoring is expensive, time-consuming and do not give representative evapotranspiration. This is due to the geomembrane at the bottom of lysimeter which cut off the moisture and heat flux to lower layers (Zhang and Sun 2014). Field data using corresponding moisture sensor and lysimeter installation along the profile depth revealed that soil water storage and percolation measured by a lysimeter is relatively less than actual field conditions (Mijares et al. 2012). The numerical studies of Mijares et al. (2012) also support these findings. The

effect of vegetation on evapotranspiration of the cover system has been considered in numerical studies as shown in Table 2.5. However, the vegetation cover on surface soil or LAI (one-sided green leaf area per unit ground area) has been mostly assumed, and the effect of individual species type is primarily ignored (Ogorzalek et al. 2008); Khire et al. 2000; Dwyer 2003; Scanlon et al. 2005a; Zhang et al. 2016). Thus, an integrated lab-field-numerical study considering real-time instrumented sections, local weather conditions, vegetation cover, and desiccation potential needs to be undertaken to understand the moisture dynamics in hydraulic barrier cover system subjected to high precipitation.

6.4 Materials and Methodology

6.4.1 Testing materials

Medium plastic red soil (RS), non-plastic medium sand (MS), and high plastic bentonite (BN) were used in the current study to construct a three-layer cover system. RS was collected locally from the hilly area of Guwahati city. It is a medium plastic silty soil and qualifies the requirement of surface soil layer in the cover system (Landreth et al. 1991; USEPA 1989a and b). The MS satisfies the drainage layer criterion specified for the cover layer. The BN used in the study was procured from Barmer, Rajasthan, India. The hydraulic barrier layer was designated as RB with its composition of 70% of RS and 30% of BN by dry weight. RB qualifies the permeability criterion requirement ($<10^{-9}$ m/s) of the hydraulic barrier layer for a three-layer cover system (Landreth et al. 1991; USEPA 1989a and b). The basic physical, geotechnical and chemical properties of all the soils are presented in Table 3.3 of chapter 3.

6.4.2 Testing equipment

Profile probe was utilized for measuring θ at 10 cm, 20 cm, 30 cm, 40 cm, 60 cm, and 100 cm depths of soil cover. 5TM and TEROS 21 sensor was used to measure θ and ψ respectively at the depths of 30 cm, 60 cm and 100 cm. sensor was used to measure. Microclimate monitoring system was employed for measuring daily precipitation, temperature, relative humidity, solar radiation, and wind speed. Em50 data loggers were employed for real-time monitoring of the data from 5TM and TEROS 21 sensors and the microclimate monitoring system.

6.4.3 Construction and instrumentation of cover setup

A reduced scale MLCS with 5% slope (USEPA 1989a and b) was developed inside a masonry structure at a site in Guwahati city of north-east India and was exposed to field weather conditions. The layer materials and configuration of this field MLCS was same as that of laboratory column C1. Field monitoring was performed on the constructed MLCS as proposed by Ng et al. (2016). The MLCS was instrumented to monitor θ and ψ as a function of space and time. Schematic diagram of the entire field setup has been shown in the Fig. 6.1. The mass-volume method was followed to compact the bottom barrier layer (BL) with RB, middle drainage layer (DL) with MS and the top surface layer (SL) with RS, with a thickness of 40, 30 and 45 cm, respectively. These thicknesses are comparable to the field RCRA subtitle C cover system (USEPA 1989a and b). The dimensions of individual cover are depicted in plan and elevation indicated in Fig. 6.1. Soils, RB and RS, were compacted uniformly with a rammer (2.6 kg) at their respective maximum dry density (MDD) and optimum moisture content (OMC) as reported in Table 3.3 in chapter 3. Required quantity of water was mixed uniformly with RB and RS in a separate airtight container to obtain homogeneity. Air dried MS was compacted at approximately 50% of its maximum relative density by calibrating the height of fall. The actual and achieved soil mass density was noticed to vary within ±2%. Each layer was compacted at a 5% mild slope to comply the cover system requirements (Landreth et al. 1991).

During packing of the cover material, three thin-walled access tube of 27 mm internal diameter and 120 cm height was placed vertically with a spacing of 30 cm along the slope. The sensor placements are shown in the Fig. 6.1 as toe section (Tsec) near the cover toe, mid-section (Msec) at cover centre and crest section (Csec) at top of cover. A thin layer of vacuum grease was applied to the outer surface of the access tube to minimize the occurrence of the preferential path of downward water flow. The access tubes embedded were then utilized for inserting the PP to measure θ at different depth. A handheld moisture meter (Delta-T Devices Ltd., UK) was used for measuring and storing the data from the PPS. The θ measurements from PPS were performed thrice in a day, and their average was considered for daily variation of θ. Along one side of the longitudinal centreline of cover setup, three 5TM point sensors were embedded in each of the three cover layers at 30, 60 and 100 cm depth outside the influence zone of the PP. Similarly, TEROS 21 sensors were employed on the opposite side (sectional plan shown in Fig. 6.1) for measuring soil suction. Both 5TM and TEROS 21 sensor were placed in the central vicinity of each cover layer.

All the sensors were connected to Em50 data loggers for continuously monitoring θ and ψ. A personal computer was employed for configuring sensor settings and downloading their stored data with the help of ECH$_2$O utility software provided by the manufacturer.

The whole experimental cover setup was exposed to natural weather conditions for 800 days from 10 May 2016 to 18th July 2018. Figure 6.2 (A, B, C, D) illustrates the pictorial view of the construction and instrumentation of the pilot field cover system. A microclimate monitoring system was installed in the field near the MLCS setup for measuring daily weather data such as precipitation, temperature, relative humidity, solar radiation and wind speed. A transparent fiberglass (Fig. 6.2 C) was also kept along each longitudinal side of the masonry structure for visualizing water front and inspect if any boundary leakage was taking place. A thin plastic sheet (Fig. 6.2 C) was secured to the outer edge of the masonry structure to prevent the occurrence of preferential water flow. Table 6.1 summarizes the details of sensors installed in different cover layer.

The vegetation cover and desiccation cracking were measured after 25 days from the start of the monitoring period. The vegetation density (top view of vegetation) was measured by using the threshold colour technique (Bordoloi et al. 2018) to select the green coloured vegetation pixels. The vegetation density was obtained by dividing the vegetation pixel area by the total area of the cover (refer Fig. 6.3 A). The shoot length was measured by a meter scale and averaged to represent the vegetation growth in elevation. The average shoot length and vegetation density give a 3-D representation of the vegetation cover growth during the monitoring period (Fig. 6.3 A). The vegetation growth observed in the monitoring period was entirely natural (by way of wind transport), and hence significant growth was observed after one year of cover construction. The surface desiccation crack (Fig. 6.3 A) was analysed using the crack intensity factor (CIF) parameter (Gadi et al. 2017), which is the ratio of the crack area (white portion) to the total area of the soil considered (black and white). The same threshold technique was used to segregate the desiccation cracks, and any overlap (i.e., profile probe cap) was selected, and their pixel was calculated. Thus, the only pixel accounted in the desiccation crack area is selected for CIF calculation. The desiccation crack was not continued after 350 days from monitoring as there was growth in grass cover restricting the image analysis of cracks (Fig. 6.3 B).

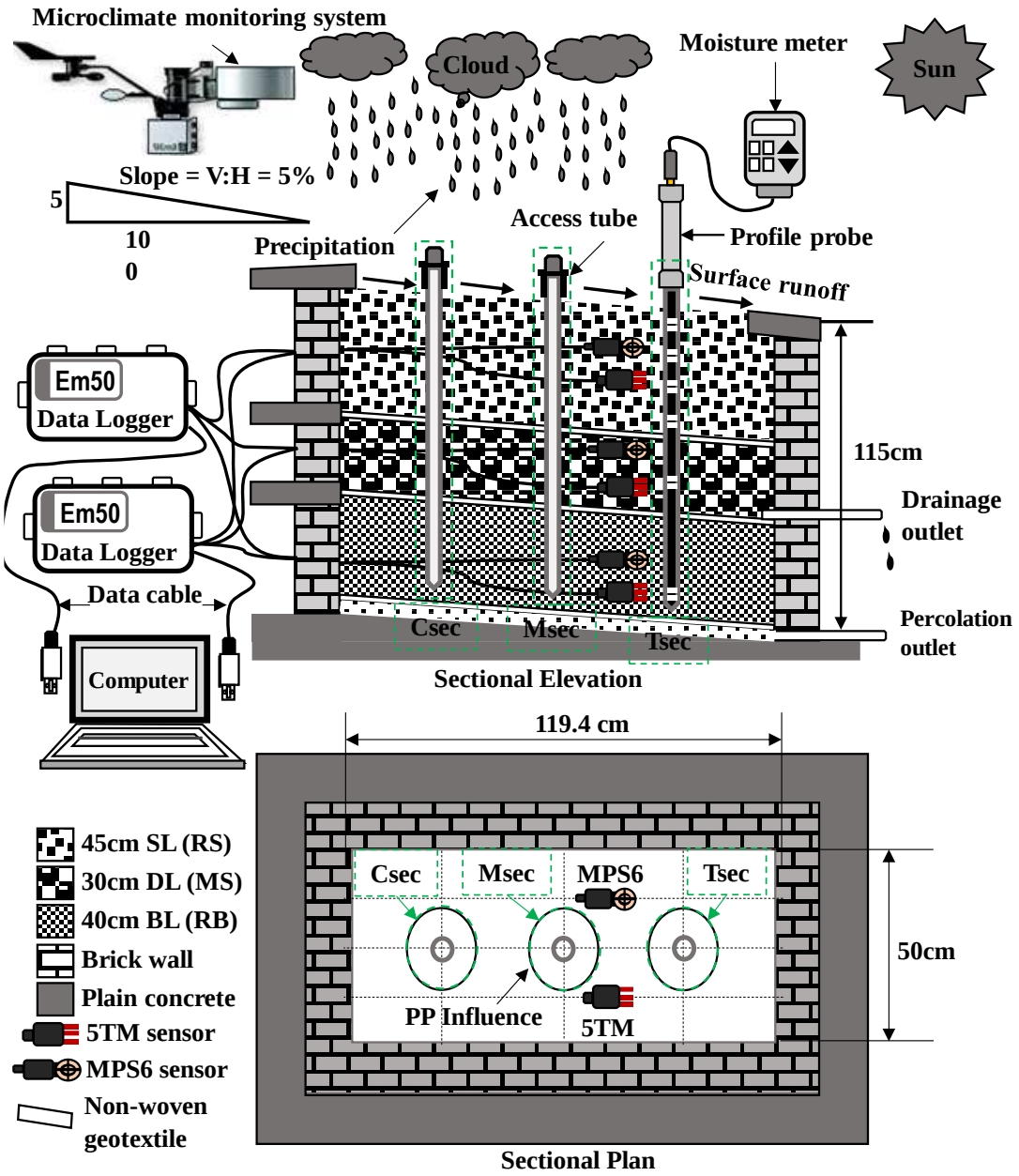

Fig. 1 Schematic diagram of experimental field cover system

Fig. 6.1 Schematic diagram of experimental field cover system

Table 6.1 Details of instrumentation of constructed cover system

Cover Layer (thickness)	Layer material (designation)	Sensor device employed (depth in cm)
SL (45 cm)	Red soil (RS)	PPS1(10), PPS2(20), PPS3(30), PPS4(40), 5TM(30) and TEROS21(30)
DL (30 cm)	Medium sand (MS)	PPS5(60), 5TM(60) and TEROS21(60)
BL (40 cm)	Red soil-bentonite mix (RB)	PPS6(100), 5TM(100) and TEROS21(100)

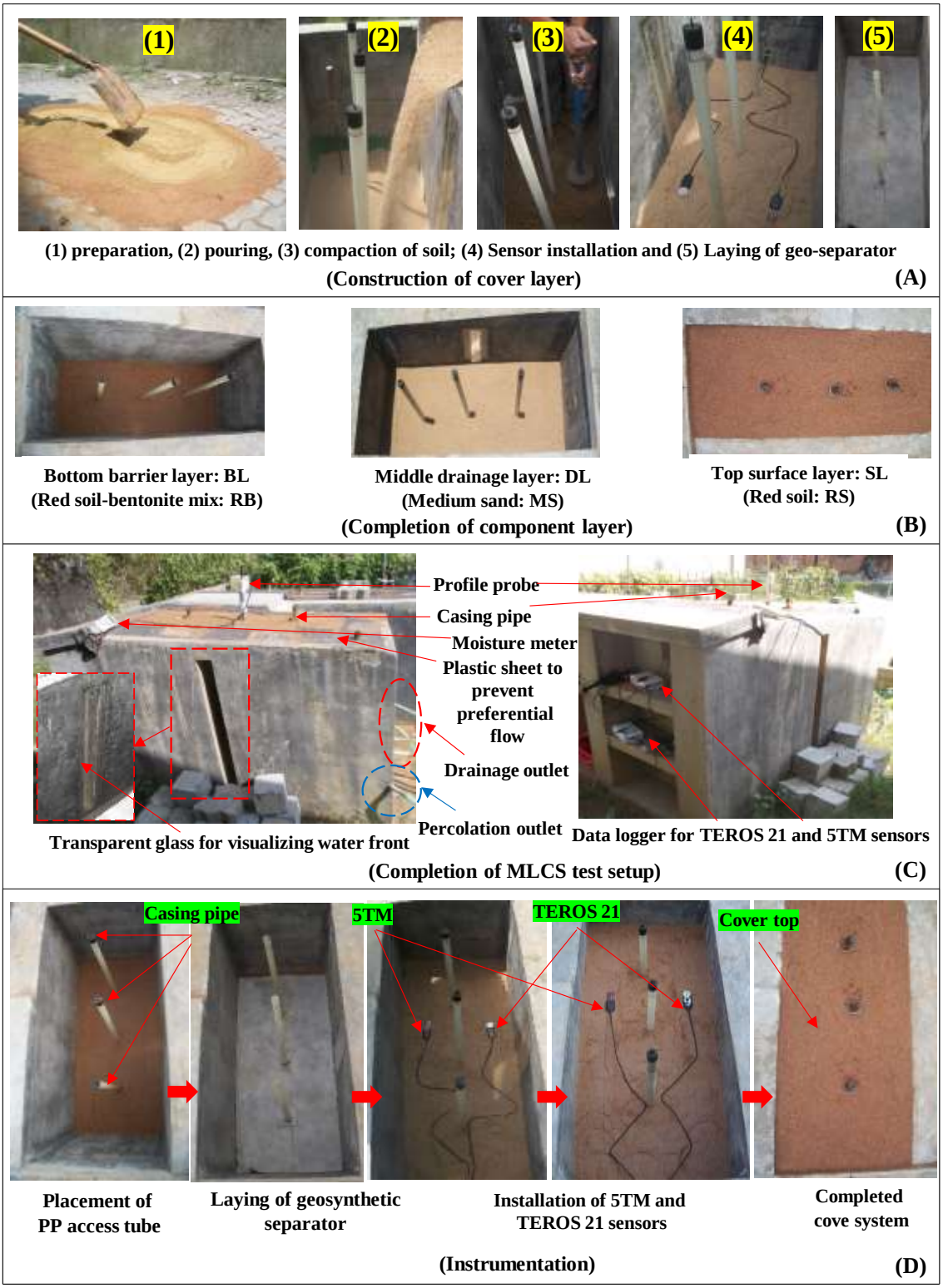

Fig. 6.2 Pictorial view of construction and instrumentation of field cover system

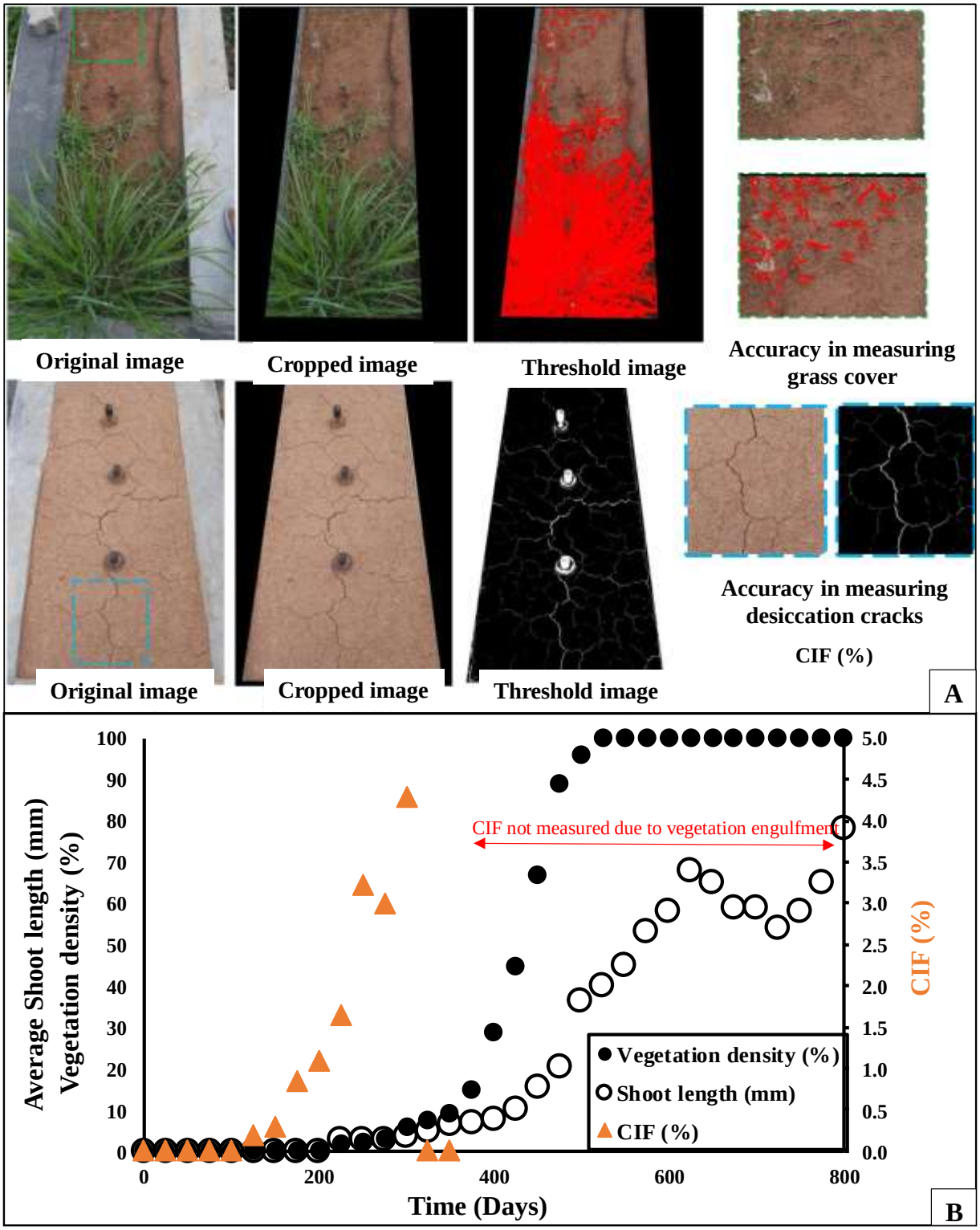

Fig. 6.3 (A) sequential process of measuring vegetation density and crack intensity factor (CIF); and (B) change in vegetation density, shoot length and CIF for the monitored period.

6.4.4 Numerical analysis

Variation of θ and ψ in all three layers of field cover due to environmental conditions for 800 days was simulated using HYDRUS 2D computer code (Šimůnek et al. 1999). The code performed the analysis by solving the modified Richard's equation (Eq. 5.1) (Richards 1931) of water flow through saturated or unsaturated soil media by the finite-element approach.

Figure 6.4 presents the geometry, boundary conditions, shape, and size of finite element (FE) mesh of the MLCS. Figure 6.5 shows mesh convergence study with the variation of θ at 400 mm cover depth with time for triangular FE mesh of different sizes from 5 cm to 25 cm. The figure demonstrates that FE mesh size of less than 10 cm has no significant effect on the results. Hence, triangular FE mesh of size 10 cm was considered for subsequent numerical analyses. Hydraulic parameters of individual soil layer of the field MLCS were same as that of laboratory MLCS column C discussed in section 5.3 of the previous chapter to serve as input parameters for numerical analyses of this chapter. For better understanding, the SWCCs (predicted, drying and wetting) of RS, MS and RB are specially portrayed in Fig. 6.6 and hydraulic parameters estimated from these SWCCs were presented in Table 6.2.

Measured daily weather data are shown in Fig. 6.7 A. Figure 6.7 B presents the values of daily evapotranspiration which were computed based on the daily weather data by using 5 well-known evapotranspiration models as listed in Table 6.3. Thus, 5 different sets of atmospheric or time variable boundary condition were considered on the top of the surface layer in the numerical modelling. No flux boundary conditions were considered for the vertical sides of the cover domain except for drainage face at the toe end. This drainage face was set as free drainage boundary condition to simulate draining out of water percolated from upper surface layer. Bottom face of the cover system was also considered as free drainage boundary condition, which simulates the downward movement of percolated water as anticipated in the field. Initial boundary condition presented in Table 6.2 was assigned in terms of initial θ (θ_i) measured by water content sensors separately in each layer of the test cover. The numerical code thus estimates θ and ψ with depth and time for the abovementioned initial and boundary conditions, which was compared with field measurements from respective sensors installed in the test cover.

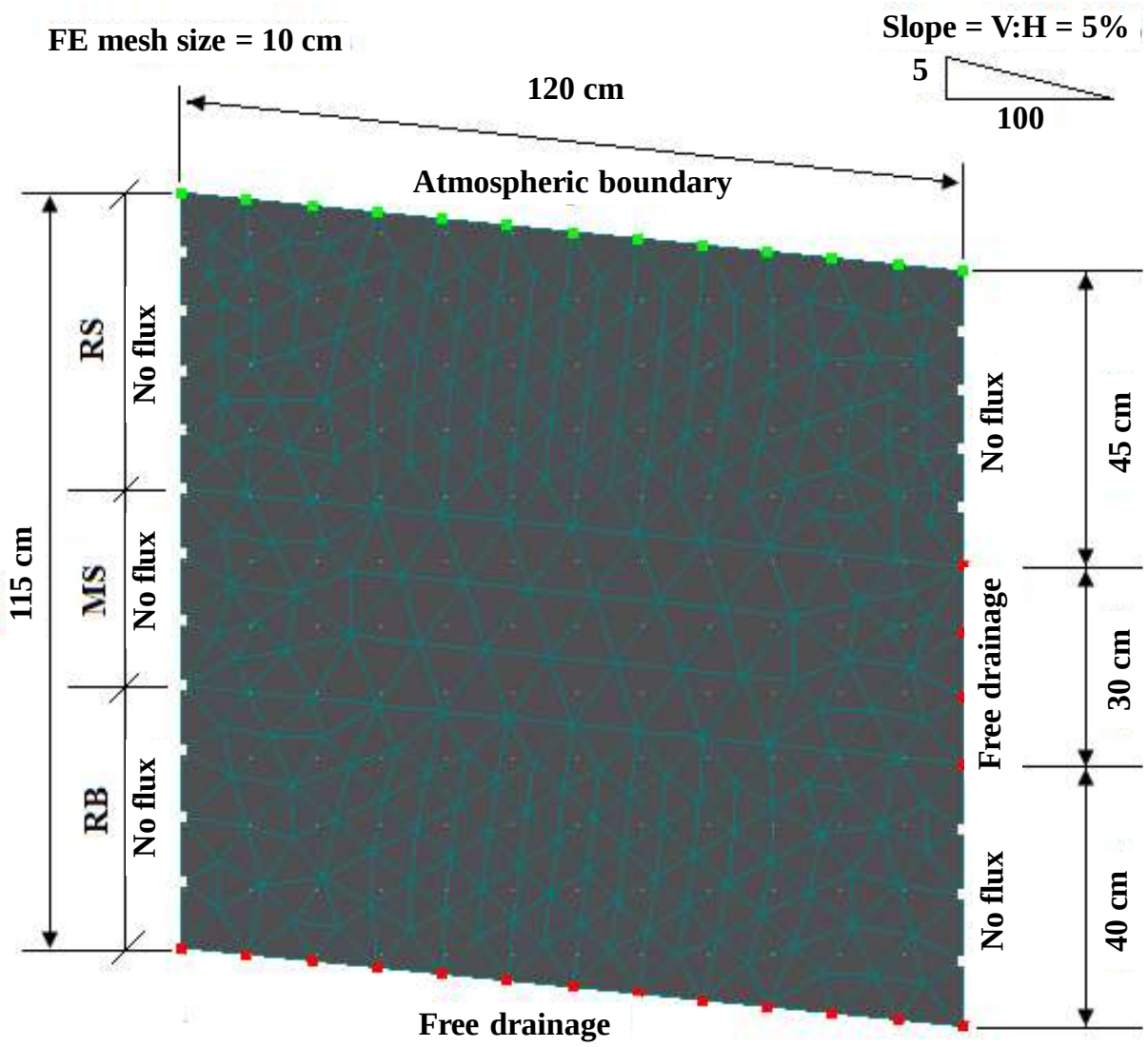

Fig. 6.4 Geometry and boundary conditions used in numerical analysis

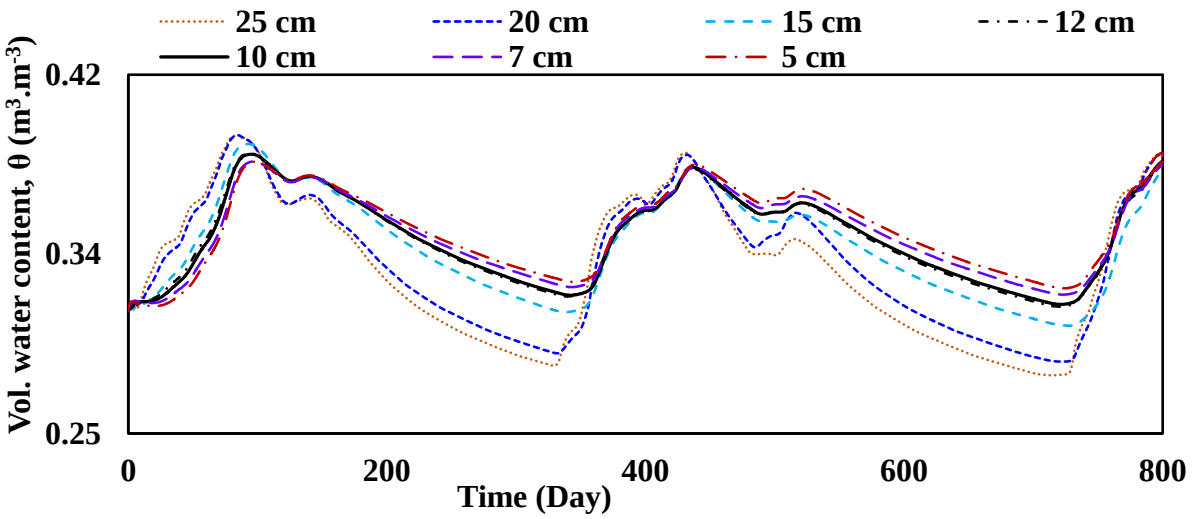

Fig. 6.5 Convergence study of FE mesh size

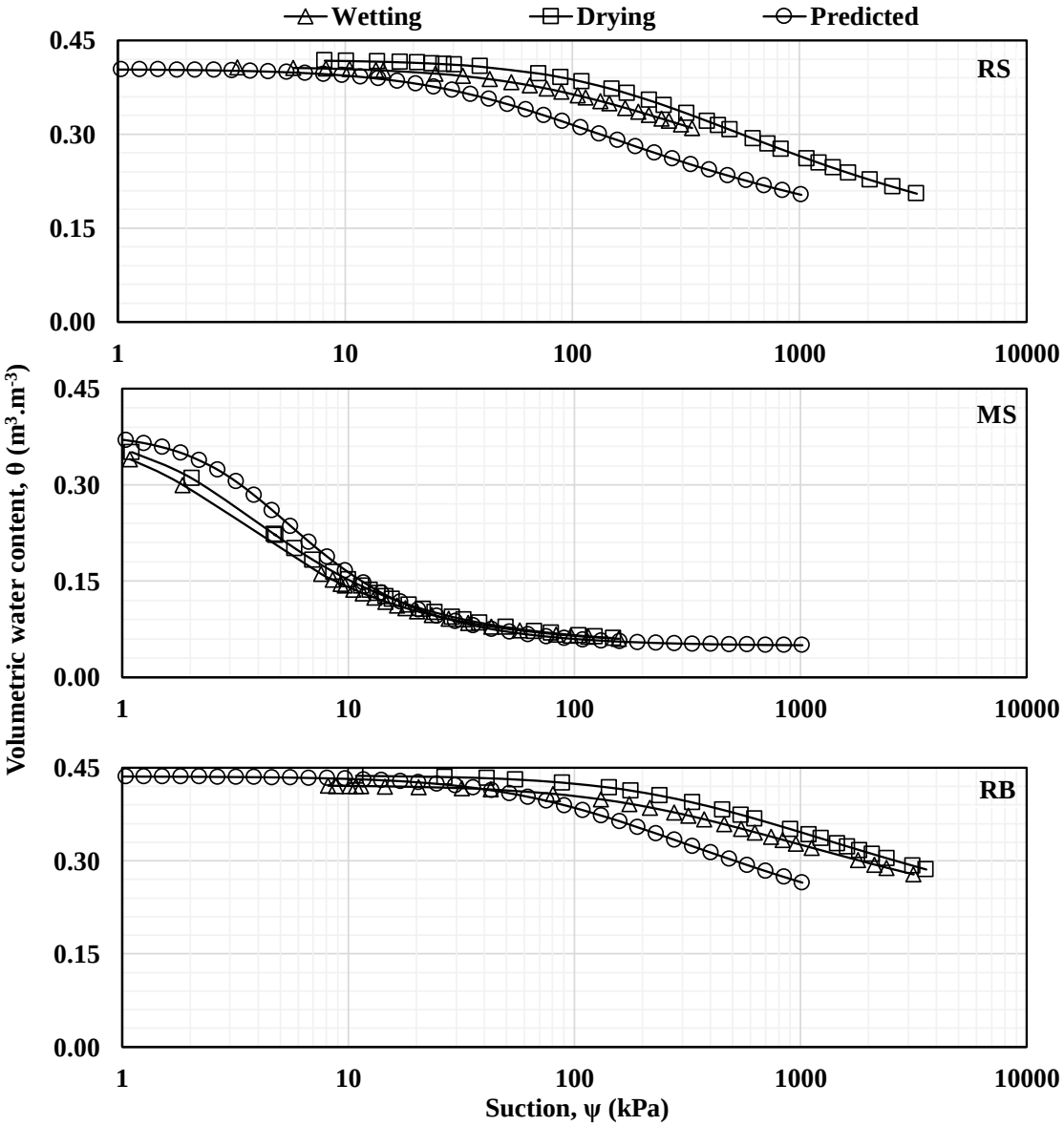

Fig. 6.6 Predicted, drying and wetting SWCCs for RS, MS and RB

Table 6.2 Hydraulic parameters of materials assigned in numerical analyses

Layer (Material)	Designation	Hydraulic parameters						θ_i
		θ_r	θ_s	α	n	k_s	I	
SL (RS)	WHP	0.061	0.406	0.0010	1.24	3E-9	0.5	0.308
	DHP	0.062	0.419	0.0005	1.31	3E-9	0.5	0.308
	PHP	0.076	0.404	0.0023	1.30	3E-9	0.5	0.308
DL (MS)	WHP	0.039	0.369	0.0498	1.78	4E-5	0.5	0.060
	DHP	0.040	0.381	0.0408	1.81	4E-5	0.5	0.060
	PHP	0.049	0.379	0.0259	2.06	4E-5	0.5	0.060
BL (RB)	WHP	0.076	0.421	0.0004	1.21	2E-10	0.5	0.330
	DHP	0.077	0.438	0.0003	1.23	2E-10	0.5	0.330
	PHP	0.086	0.436	0.0011	1.28	2E-10	0.5	0.330

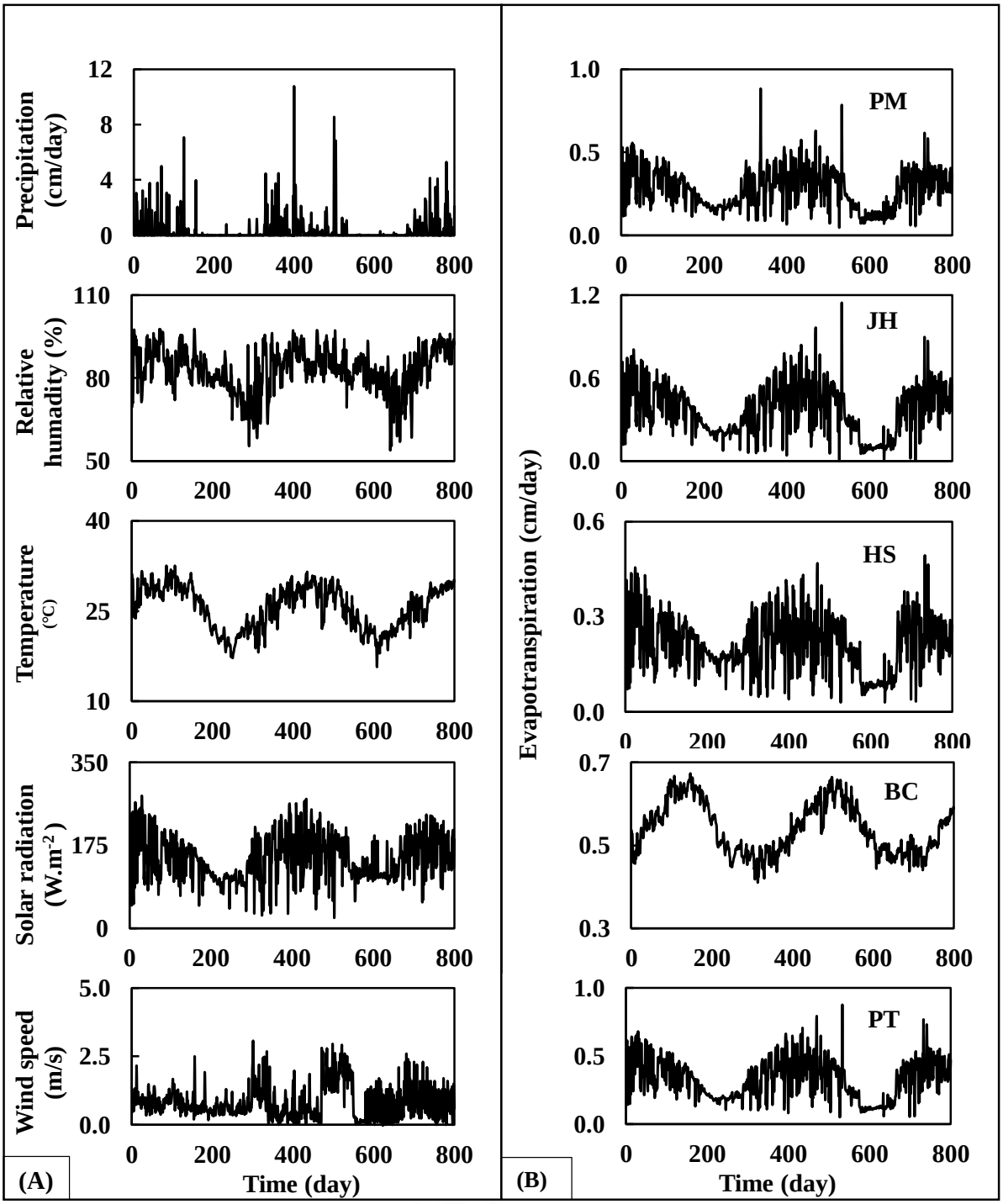

Fig. 6.7 (A) Measured weather data of Guwahati in northeast India and (B) evapotranspiration computed by Penman-Monteith (PM), Jensen-Haise (JH), Hargreaves-Samani (HS), Blaney-Criddle (BC) and Preistley-Taylor (PT) models

Table 6.3 Various Models for computing evapotranspiration (ET) as a part of time variable boundary condition for numerical analyses

Equation computing evapotranspiration (*ET*)	Required weather data	Reference	Designation
$ET = \frac{\Delta(R_n - G) + \rho_a c_p (\delta e) g_a}{\left\{\Delta + \gamma\left(1 + \frac{g_a}{g_s}\right)\right\} L_v}$	Daily mean temperature, wind speed, relative humidity and solar radiation	Penman, 1948; Monteith, 1981; Allen et al., 1998	PM
$ET = \frac{C_t (T_a - T_x) R_s}{L}$	Daily mean temperature and solar radiation	Jensen and Haise, 1963; Grace and Quick, 1988	JH
$ET = \frac{0.0023(T_a + 17.8)\sqrt{(T_{\max} - T_{\min}) R_s}}{\gamma}$	Solar radiation, maximum, minimum and mean daily temperature	Hargreaves and Samani, 1985; Subburayan et al., 2011	HS
$ET = p(0.45T_a + 8.128)$	Daily mean temperature	Blaney and Criddle, 1950; Fooladmand, 2011	BC
$ET = \frac{Ls(R_n - G)a}{\gamma}$	Solar radiation and daily mean temperature	Priestley and Taylor, 1972; Fernandes et al., 2012	PT

Different terminologies: Δ = rate of change of saturation specific humidity with air temperature (MJm^{-3}), R_n = net solar radiation (Wm^{-2}), G = ground heat flux (Wm^{-2}), ρ_a = dry air density (kgm^{-3}), c_p = specific heat capacity of air ($Jkg^{-1}K^{-1}$), δe = specific humidity (Pa), g_a = atmospheric conductance (ms^{-1}), g_s = surface conductance (ms^{-1}), γ = psychrometric constant (PaK^{-1}), γ = volumetric latent heat of vaporization (MJm^{-3}), C_t = temperature coefficient (K^{-1}), R_s = daily solar radiation (Wm^{-2}), T_a = daily mean temperature (°C), $T_{\max}$ = daily maximum temperature(°C), $T_{\min}$ = daily minimum temperature (°C), T_x = constant for a given area, L = latent heat of vaporization (cal/g), p = mean daily percentage of annual daytime hours (%), Δ = slope of the saturation vapour pressure-temperature relationship ($kPa.°C^{-1}$), a = Priestley-Taylor coefficient

6.5 Results and Discussion

6.5.1 Calibration of water content sensors

Figure 6.8 shows θ variation measured by PPS with time at depths of 10, 20 and 40 cm in SL at three different vertical sections (Csec, Msec, and Tsec) as shown in the sectional plan of Fig. 6.1. Measurements of θ before (BC) and after calibration (AC) of the PPS showcase that there is relatively a low variation (1-3%) in readings based on specific drying and wetting stages.

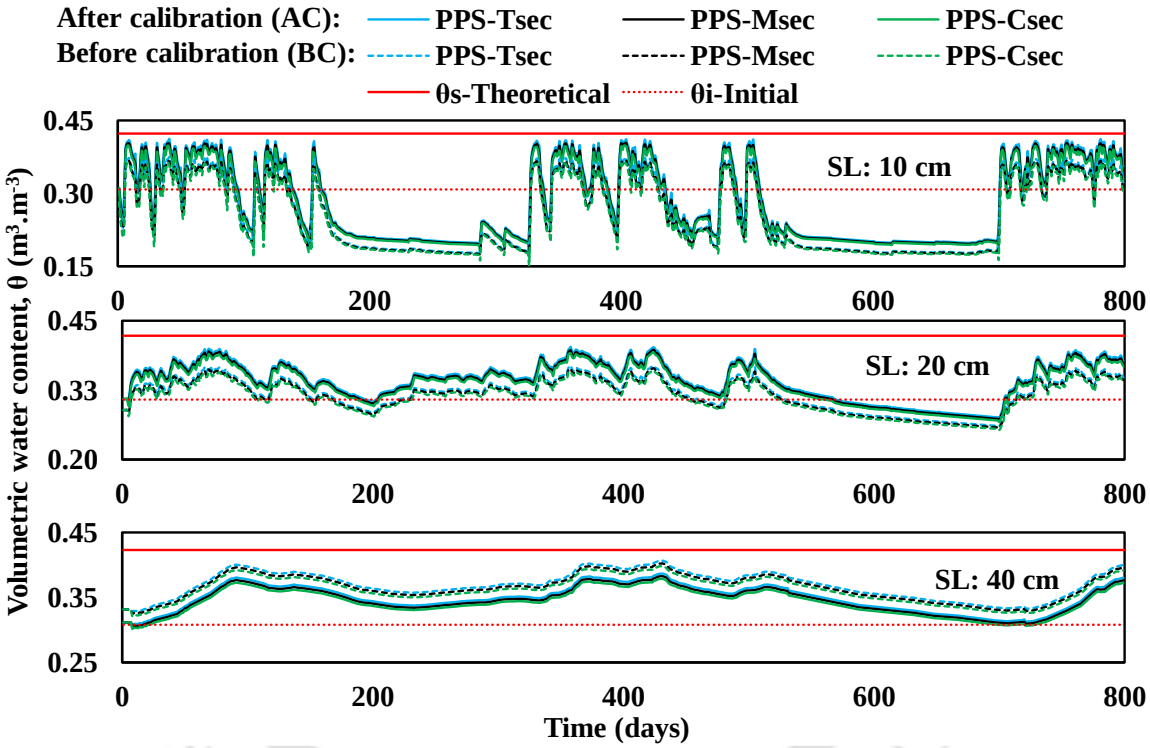

Fig. 6.8 Profile probe measurements at various depths of surface layer

Figure 6.9 juxtaposes θ measured by 5TM and PPS at Msec at three depths (30 cm in SL, 60 cm in DL and 100 cm in BL). From the figure, it can be inferred that non-calibrated θ measured by 5TM underestimates the actual θ by around 5-7% during the monitoring period. Thus, the reading of PPS was found to be more reliable than 5TM if no calibration is done. The absence of calibration procedure can lead to error in data interpretation and deriving conclusions. Hence, the corrected measurements of 5TM and PPS readings were considered for further comparative analysis with simulated results.

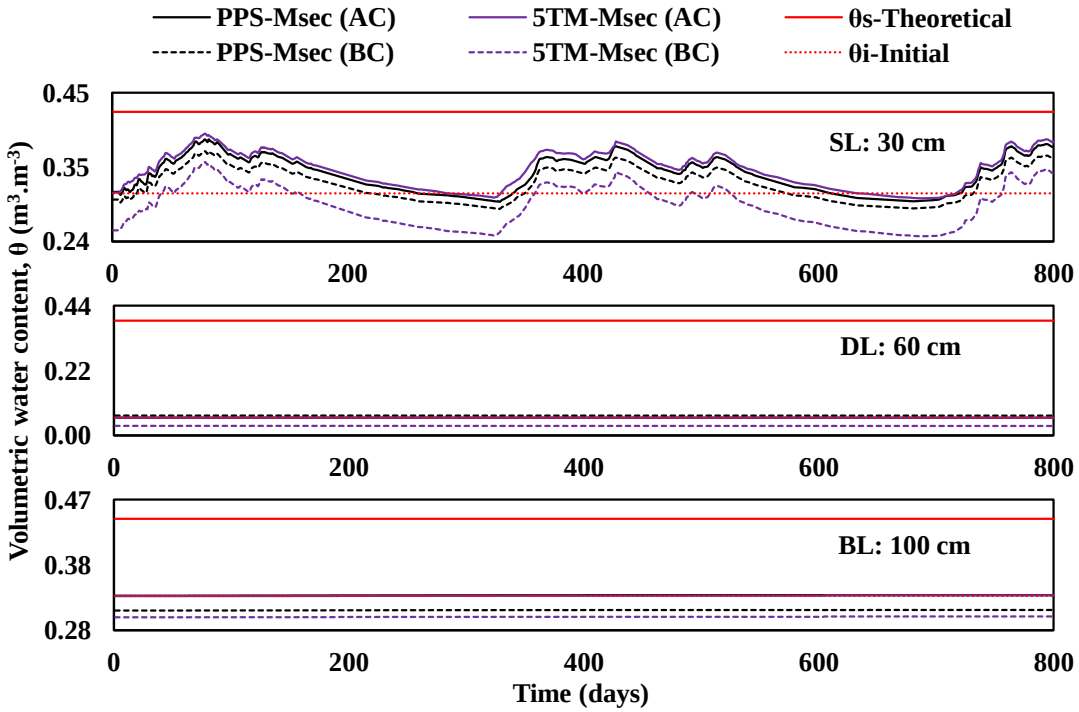

Fig. 6.9 Comparison of PPS and 5TM measurements in SL, DL and BL

6.5.2 Numerical analysis of field cover system

The θ and ψ at 30 cm depth along mid-section of the cover system was simulated by considering 15 different input scenarios based on various evapotranspiration models and hydraulic parameters. Results of these 15 simulations for θ and ψ are depicted in Fig. 6.10 (a, b, c) and 6.11 (a, b, c), respectively. The results indicate the influence of five sets of time variable boundary conditions (corresponding to PM, JH, HS, BC, and PT) for each of the three sets of hydraulic parameters (PHP, WHP and DHP). Figure 6.10 (a, b, c) compares all the simulated θ with 5TM and PPS measurements for 800 days captured at 30 cm depth along mid-section of the cover setup. The figure revealed the PM model (which considers all data from microclimate system) to be most appropriate in replicating the observed field behaviour when drying SWCC (DHP) hydraulic parameter was used. Use of other evapotranspiration models highly underestimated the field measurements of water contents and can be attributed to the non-consideration of wind speed, relative humidity for ET computation. On the other hand, it can be noted that the numerical results obtained using PHP have a significant deviation from field observations in comparison to those obtained using measured WHP and DHP. It is worth mentioning here that, even though field measurements included both wetting and drying spells, the numerical simulation results obtained using DHP exhibited a better match with the measured results.

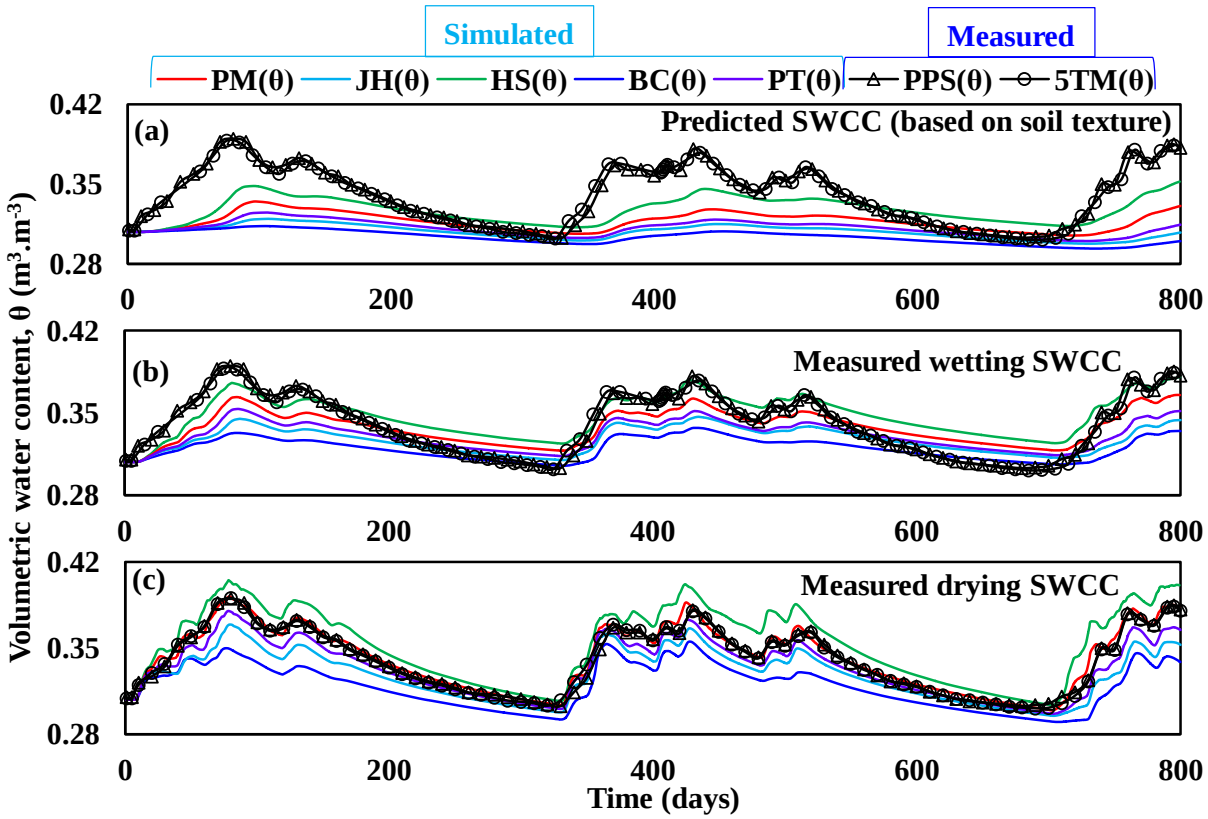

Fig. 6.10 Comparison of volumetric water content (measured at 30 cm depth of mid-section) with simulations obtained based on various approaches

Similarly, Fig. 6.11 (a, b, c) compares simulated ψ with TEROS21 measurements which were recorded at 30 cm depth along mid-section of the test cover. This advocated the accuracy of HS model in simulating ψ with TEROS21 measurements when DHP was considered in the analyses. Other evapotranspiration models poorly computed ψ for capturing its field observations. Besides, PHP based numerical results were not in good agreement with the measured results compared to WHP or DHP based simulations (Fig. 6.11 (c)). The numerical investigation bring out the appropriateness of DHP for simulating the hydraulic performance of the MLCS by considering either PM for capturing θ measurements or HS model for replicating the ψ measurements. On the other hand, most of the measurements of this study are in terms of θ. Hence, DHP and PM based numerical analysis was considered as the most favourable numerical approach for investigating the hydraulic performance of the MLCS. The ψ based measurements were not further considered in the study due to measurement limitation of TEROS 21 for ψ < 10 kPa.

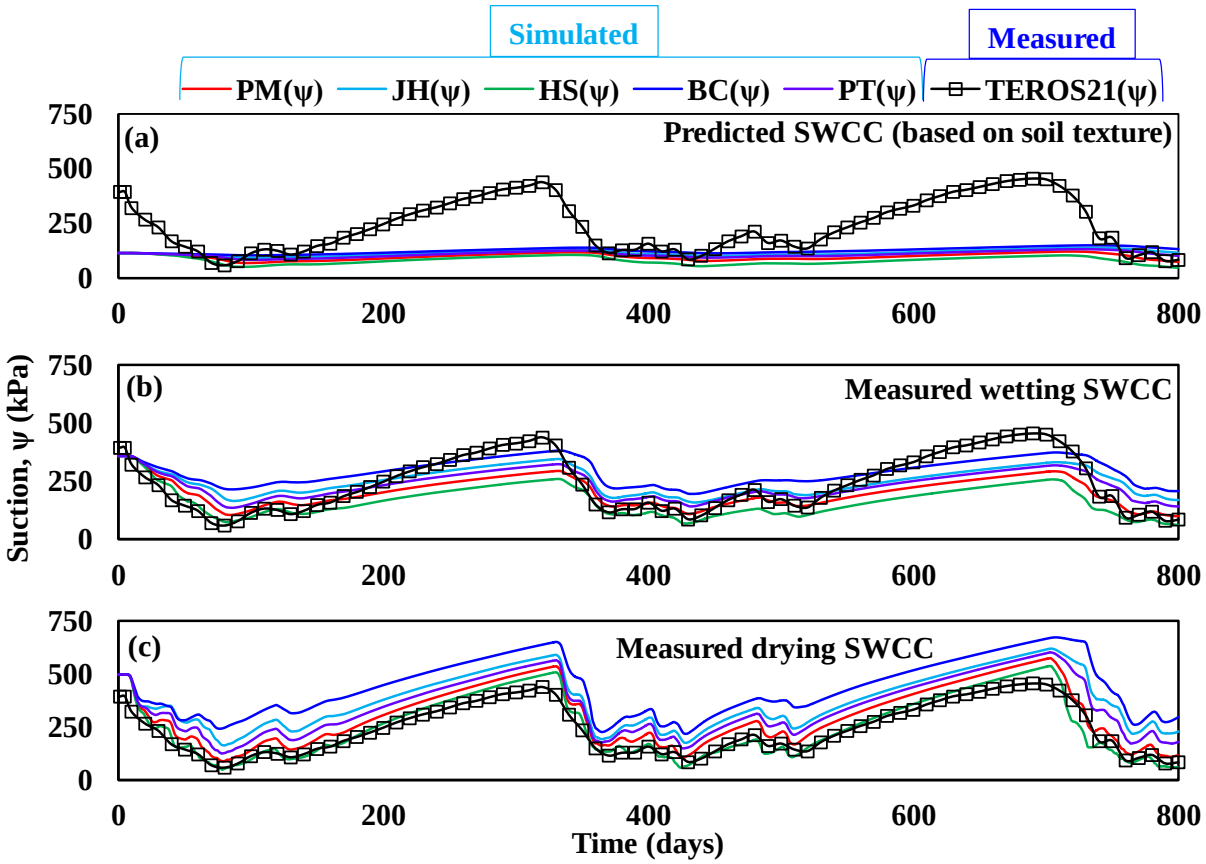

Fig. 6.11 Comparison of measured and simulated suction (measured at 30 cm depth of mid-section) based on different input parameters

6.5.3 Hydraulic performance of cover system

Figure 6.12 demonstrates the comparisons of field measurements of θ at 10, 20, 30 and 40 cm depths in SL at three vertical sections (Csec, Msec, and Tsec) with simulated results. It also shows the moisture status of the drainage (60 cm) and barrier (100 cm) layers. The figure shows that θ in SL varies between maximum (θ_{max}) and minimum (θ_{min}) values of θ (refer Table 6.4) for considered depths within the monitoring period. It can be noted that the numerical simulation satisfactorily captured the periodic variation in θ caused due to wetting-drying phenomena under seasonal weather changes. The figure demonstrates that the upper portion (first 10 cm) of SL exhibited high moisture dynamics due to the evapotranspiration compared to the lower sections.

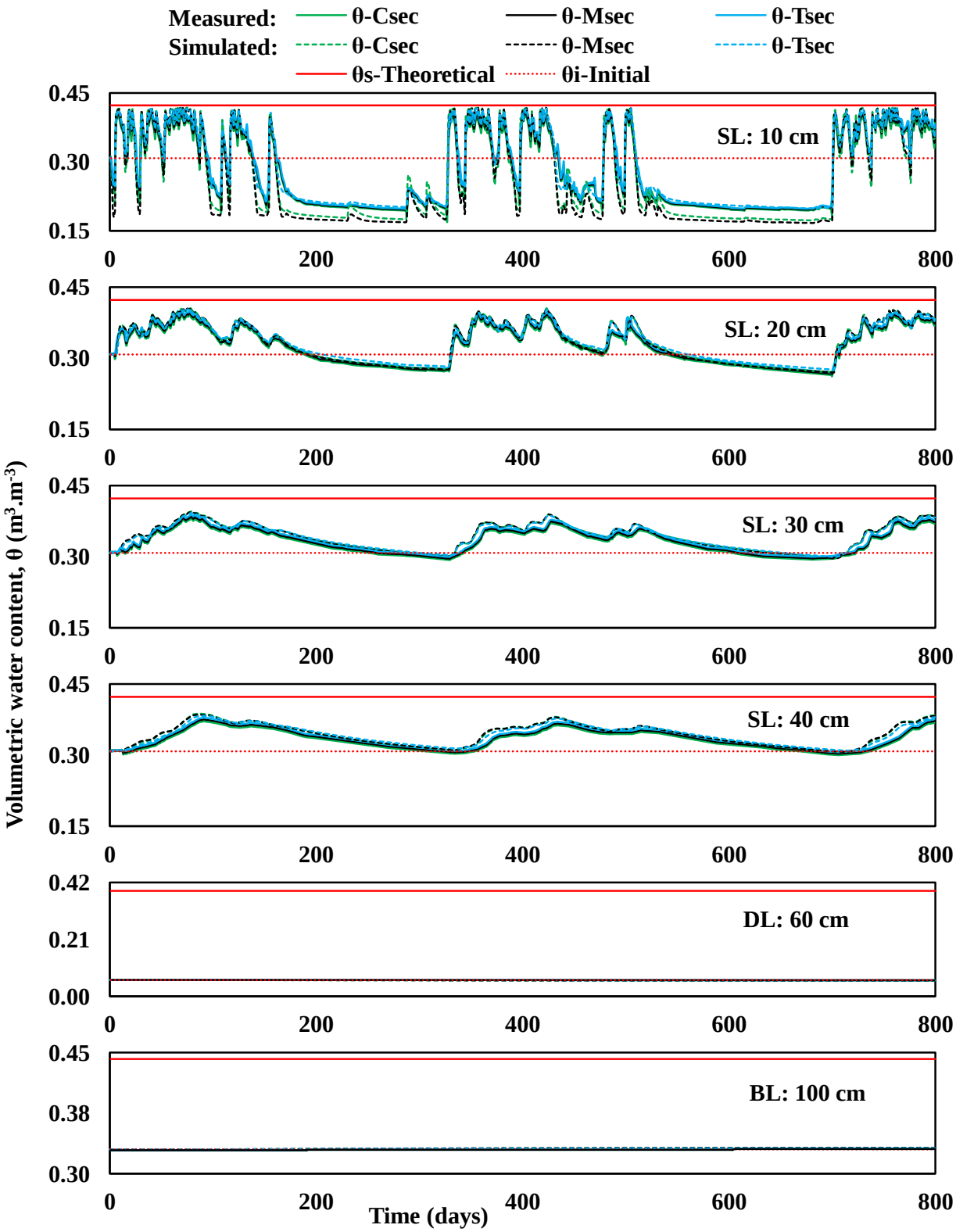

Fig. 6.12 Comparison of measured and simulated volumetric water content obtained based on Penman-Monteith model and drying hydraulic parameters

Table 6.4 Comparison of measured θ_{max} and θ_{min} with numerical simulations

Cover layer	Depth (cm)	Maximum volumetric water content, θ_{max} ($m^3.m^{-3}$)						Minimum volumetric water content, θ_{min} ($m^3.m^{-3}$)					
		Csec		Msec		Tsec		Csec		Msec		Tsec	
		Measured	Simulated	Measured	Simulated	Measured	Simulated	Measured	Simulated	Measured	Simulated	Measured	Simulated
SL	10	0.399	0.418	0.404	0.418	0.411	0.417	0.171	0.172	0.195	0.167	0.197	0.198
	20	0.391	0.406	0.396	0.405	0.401	0.403	0.262	0.271	0.267	0.269	0.270	0.276
	30	0.380	0.395	0.384	0.394	0.389	0.392	0.293	0.297	0.296	0.296	0.299	0.299
	40	0.371	0.388	0.375	0.385	0.379	0.383	0.299	0.307	0.303	0.30	0.306	0.308
DL	60	0.060	0.060	0.060	0.060	0.060	0.060	0.059	0.058	0.059	0.058	0.059	0.059
BL	100	0.330	0.332	0.330	0.332	0.330	0.332	0.329	0.330	0.329	0.330	0.329	0.330

Note: Simulated θ_{max} or θ_{min} were obtained based on numerical simulation performed using drying hydraulic parameters (DHP) and Penman-Monteith (PM) evapotranspiration model

From Fig.6.12, the θ_{max} and θ_{min} observed during the entire monitoring period (or at the end of the period) was plotted along the SL depth in Fig. 6.13 A. Numerically simulated data for the corresponding measured data is presented in Fig. 6.13 B. It indicates that the range of θ variation became gradually narrower as the depth increases. The θ_{max} was noted to reduce as the depth increases, which demonstrates slow downward movement of infiltrated water and diminishing effects of rainfall at lower depths. θ_{min} was found to increase with depth, which indicates the gradual accumulation of infiltrated rainwater with decreasing effects of evaporation as the depth from the surface increases. This may also due to a gradual reduction of the influence of soil-atmosphere boundary (evapotranspiration variations) with depth. From the figure, it can also be observed that θ_{max} never reaches its saturated theoretical value even though it was subjected to sufficiently high rainfall (1873 mm/year). This shows the efficacy of the three-layered cover system as a hydraulic barrier for hazardous wastes.

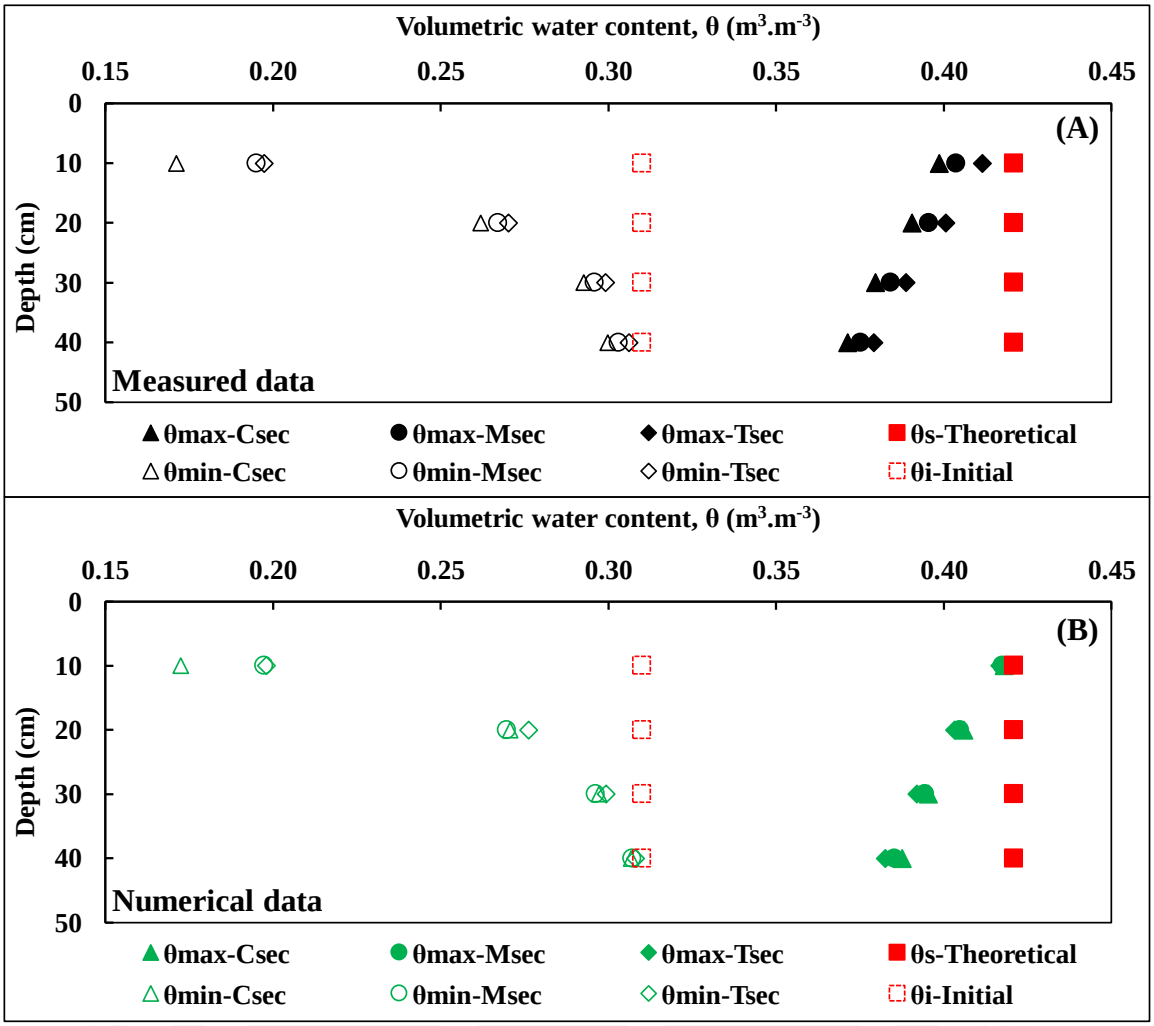

Fig. 6.13 Spatial variation of maximum and minimum volumetric water content in surface layer based on (A) field measurements and (B) numerical analyses at the end

Figure 6.14 illustrates the θ profile along mid-section of the MLCS during extreme drought and heavy rainfall events. Referring to Fig.6.7, θ profile at 210th and 560th day was considered to represent the extreme drought condition, while the 400th and 500th day represents the extreme rainfall condition. Based on the measured and simulated θ profiles shown in Fig. 6.14, it can be noted that even during the days of prolonged heavy rainfall, no percolation was observed in barrier as well as a drainage layer. Vegetation (grass) cover in the 500th day was almost triple than the 400th day. The effect of vegetation was seen in the near saturated water content observed at 10 to 20 cm for extreme rainfall events. The θ was seen to approach saturation (higher water content) for the 500th day with respect to 400th day due to the possible water percolation along the preferential pathway along

grassroots (Liu et al. 1994). The effect of desiccation (CIF is 2% on the 210th day) on the water percolation was not found to be significant (refer Fig 6.14) when compared with the 560th day (covered with 70% vegetation). CIF, which is expected to be in the same range (1.4-2%) for grass species (at around 70% vegetation cover) for compacted conditions (Bordoloi et al. 2018), makes no difference in the moisture profile of the surface layer. Furthermore, the local grass species (*Axonopus compressus* and *Cynodon dactylon*) observed in the current study have a meagre transpiration rate as compared to plant species based on their measured stomatal conductance values (Bordoloi et al. 2018). Thus low transpiration would have resulted in comparable moisture profiles for vegetated phase and no vegetation condition at the beginning of monitoring period.

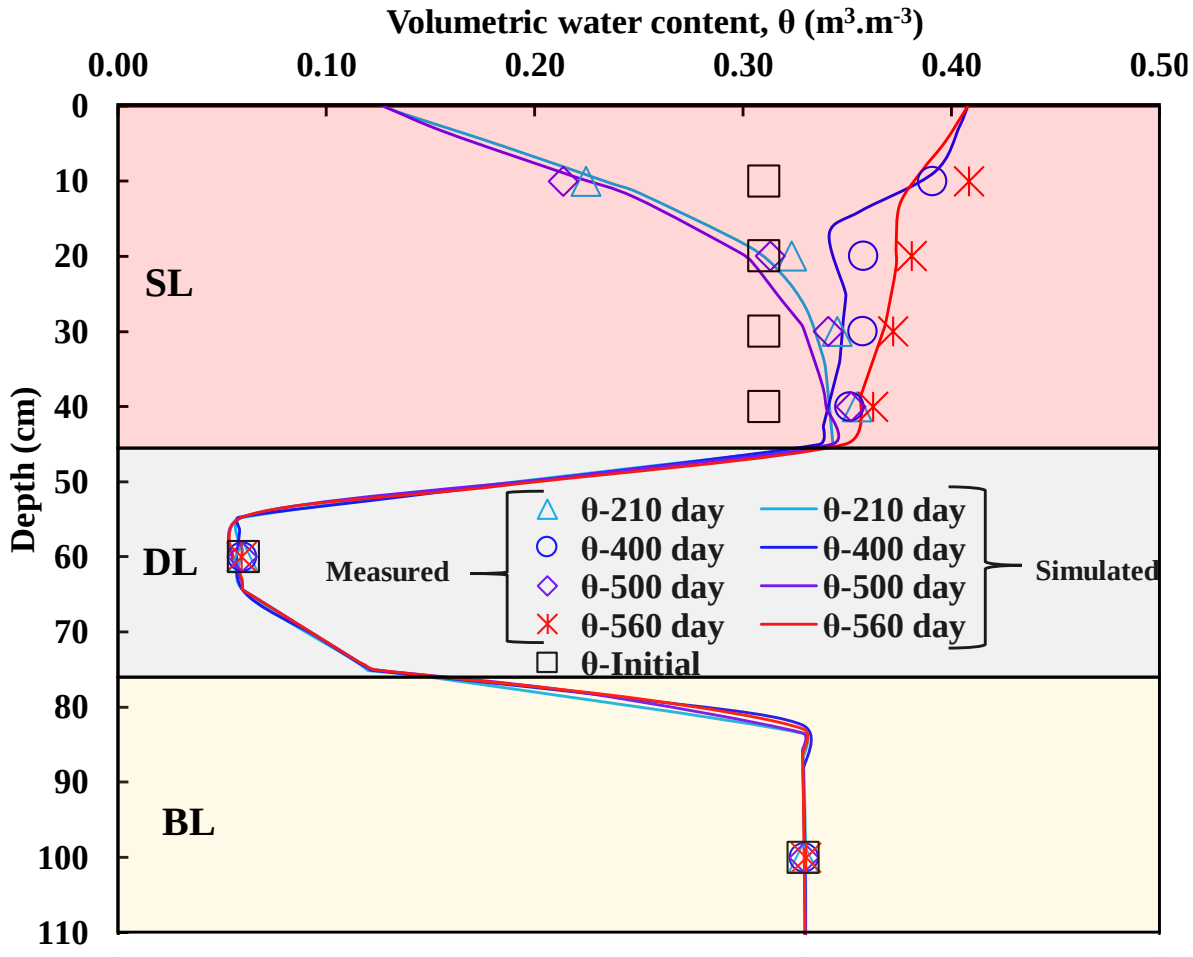

Fig. 6.14 Measured and simulated water content profile for extreme dry period (210th day and 560th day) and extreme rainfall period (400th day and 500th day)

6.6 Summary

In this chapter, the hydraulic performance of a multi-layered cover system (MLCS) for hazardous waste containment was studied based on an instrumented cover system constructed in the field. The site in consideration (North-east India) falls among the highest rainfall zone in the world. The constructed cover was subjected to natural weather conditions for 800 days from 10th May 2016 to 18th July 2018 considering extreme dry and wet spell. Instrumentation was installed for volumetric water content (θ) and matric soil suction (ψ) measurements along the depth of the cover system. Field weather data was recorded by a microclimate monitoring system deployed in the field adjacent to the pilot MLCS. The field observations were compared with the results of numerical simulation performed in HYDRUS 2D code by considering the measured soil-atmospheric boundary conditions based on field monitoring. The numerical analyses investigate the appropriateness of different soil atmospheric boundary conditions based on evapotranspiration models such as Penman-Monteith, Jensen-Haise, Hargreaves-Samani, Blaney-Criddle, and Priestley-Taylor. Three sets of hydraulic parameters obtained from drying, wetting and predicted soil water characteristic curve were also evaluated based on the comparison of numerical results with the field observations.

The observations revealed that numerical simulation performed by considering drying hydraulic properties and evapotranspiration estimated by the Penman-Monteith model matched well with observed results. Based on the observed variation in suction measurements, it was also noted that evapotranspiration computed by Hargreaves-Samani model also gave simulation results comparable with the field observations. The cyclic variation of θ and ψ attributed to precipitation and drying was found to be excessive for the surface layer indicating significantly high soil-atmosphere interaction. There was marginal and no impact of soil-atmosphere changes on drainage and the hydraulic barrier layer, respectively, for the time duration considered in this study. Fluctuation range of θ and ψ in the layer gradually became narrower as observed depth increases. This demonstrates the efficacy of a well-designed surface layer for prolonging the design life of the barrier layer of MLCS for a very humid site. Effect of grass growth and desiccation did not significantly affect the temporal variation of moisture profiles in near surface depth. However, this would impact the results of soil erosion, which has not been incorporated in this study and need to be investigated further.

Chapter 7

Climate Change Impact on Hydraulic Performance of MLCS

7.1 General

The complex moisture dynamics in unsaturated MLCS and its long-term hydraulic efficiency were rarely studied for extremely humid conditions. The main objective of this chapter is to explore the impact of long-term climate change on the hydraulic performance of a MLCS for humid Indian conditions. The previous chapter identified drying hydraulic parameters (DHP) and Penman-Montieth evapotranspiration (PM) for numerically simulating the hydraulic performance of a pilot field MLCS. This information is used in this chapter to study the long-term hydraulic performance of the MLCS by considering climate data of 87 years for two different humid regions (north-east and western coast) of India. The numerical simulations are conducted with and without consideration of material performance deterioration.

7.2 Background study

The functioning of MLCS is dependent on the contrasting unsaturated hydraulic properties of fine-grained and coarse-grained soil (Divya et al. 2012; Khire et al. 2000; Leoni et al. 2004; Li et al. 2013; Ogorzalek et al. 2008; Rahardjo et al. 2012; Yang et al. 2004a, 2006, Zornberg et al. 2003, 2010). Among the various MLCS, a three-layered barrier cover system has been proposed for humid climatic regions (Albright et al. 2006b; Ng et al. 2015, 2016; Zhang et al. 2016; Zhang and Sun 2014). The expected design life of these MLCS is more than 100 years. This necessitate understanding the hydraulic performance of MLCS for an extended period under soil-atmosphere climatic boundary condition. The studies reported in the literature deals with the hydraulic performance assessment of MLCS conducted in laboratory with column experiments (Ibrahim et al. 2014; Indrawan et al. 2007; Ng et al. 2016; Yang et al. 2006) and sloped flume tests (Iryo and Rowe 2005; Melchior et al. 2010; Ng et al. 2015; Nyhan et al. 1997; Parent and Cabral 2006). All the laboratory studies have limitations pertaining to conditions of having either a flat surface (Krisdani et al. 2006; Yang et al. 2006), instrumentation limitations (Bussière et al. 2003; Ibrahim et al. 2014) or controlled ponding conditions (Indrawan et al. 2007). Based on the literature of field studies of the MLCS (discussed in section 6.2 of the previous chapter) it can be noted that there is a dearth of real time field data for an extended period

of time, which incorporates the effect of natural climatic changes, surface desiccation and vegetation for high humid regions.

Increasing greenhouse gases due to rapid urbanization have substantial implications for climate at global and regional scales (Wilby and Dawson 2007). The effect of climate change on the functioning of MLCS has been rarely investigated from the purview of geotechnical engineering. This is essential as the changing climate will directly affect the evapotranspiration from the surface cover layer and the rainfall extremes. Owing to the high design life of MLCS (100 years), it is essential to evaluate its performance under climate change scenarios. There are no studies that deals with the deterioration of material properties with time for the materials used in MLCS. For an extended period of 100 years' design period, it is expected that the material performance would not remain the same. To take this into account, numerical simulations were performed by considering long-term climatic data (87 years) as soil-atmosphere boundary condition and with and without deterioration in hydraulic characteristics.

7.3 Materials and methodology

7.3.1 Cover configuration and numerical approach

The geomaterials used in the field study of MLCS described in the previous chapter, were considered for performing numerical analyses of climate change impact on MLCS. Their basic physical, geotechnical and chemical properties are detailed in in Table 3.3 of chapter 3**.** The layer configuration of MLCS model considered in numerical analyses was also same as the field MLCS setup discussed in section 6.4. Figure 7.1 presents a conceptual diagram of the MLCS model when GCL (also used in C2 for MLCS column study discussed in chapter 5) was included. The details of this figure in context of the field study was discussed in section 6.4.

This chapter also employed the commercial package HYDRUS 2D. This was previously used in chapter 5 and 6 for validation of the experimental observations. Numerical simulation of hydraulic performance of the MLCS setup under natural weather condition for 800 days was conducted in the chapter 6 to check the adequacy and suitability of various input parameters. The numerical approach which gave most comparable results with the test measurements was considered to be most favourable for the study of this chapter. Hence, it was further adopted in the study for the assessment of climate change impacts on hydraulic performance efficiency of landfill cover system. However, all these

specific details are briefly discussed for better understanding of the study in this chapter. Figure 7.2 A presents the geometry, boundary conditions, shape and size of the finite element (FE) mesh of the MLCS model with the GCL. Figure 7.2 B illustrate the convergence study of FE mesh size corresponding to this MLCS model. Table 7.1 summarizes the drying hydraulic parameters obtained from the Fig. 7.3 assigned in numerical analyses. The atmospheric boundary condition was assigned in the simulations based on daily evapotranspiration which were evaluated by Penman-Monteith model using forecasted climate. The details of the climate forecasting are demonstrated in the following section. Initial and other boundary conditions were considered same as to the field MLCS.

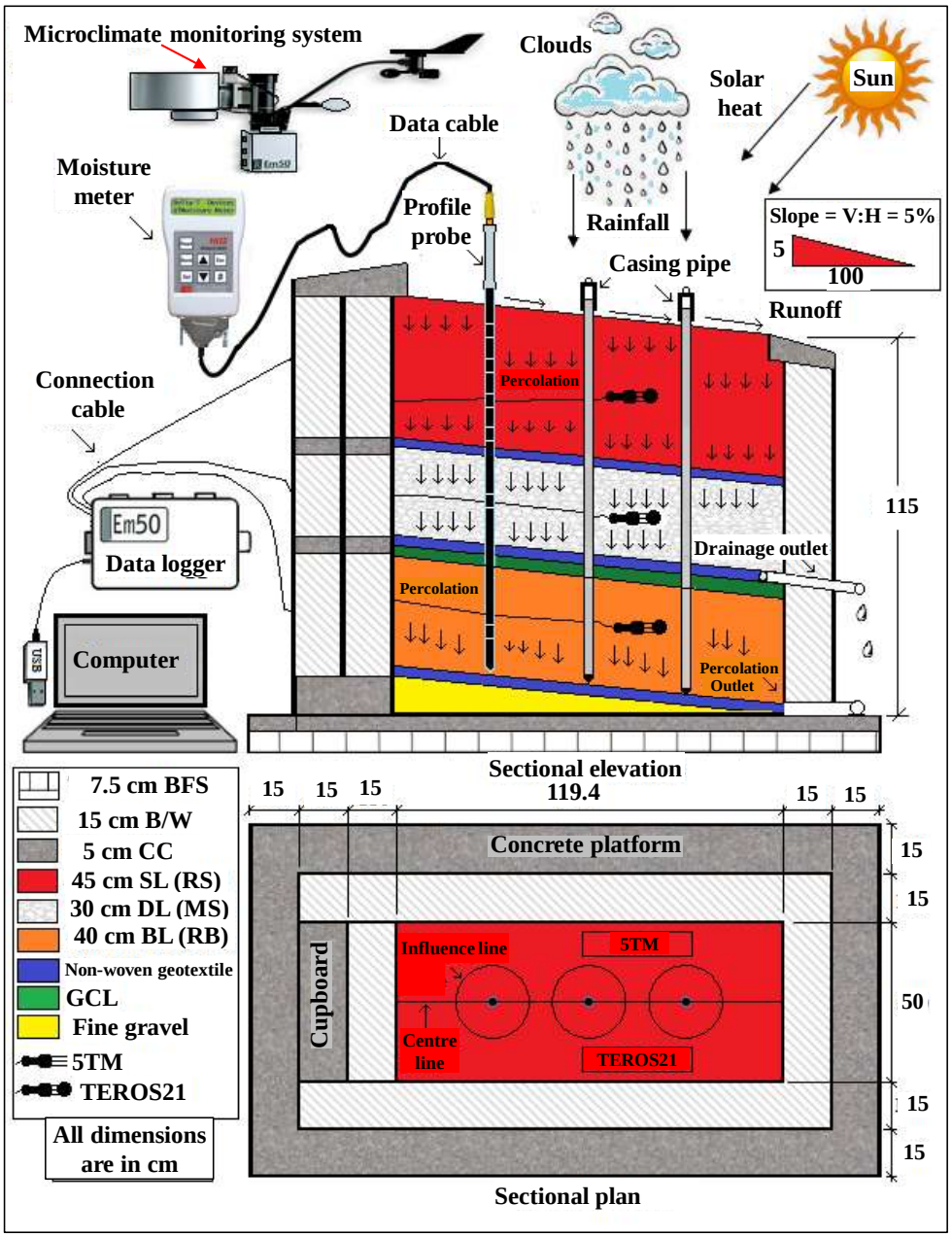

Fig. 7.1 Conceptual diagram of field MLCS when GCL was included

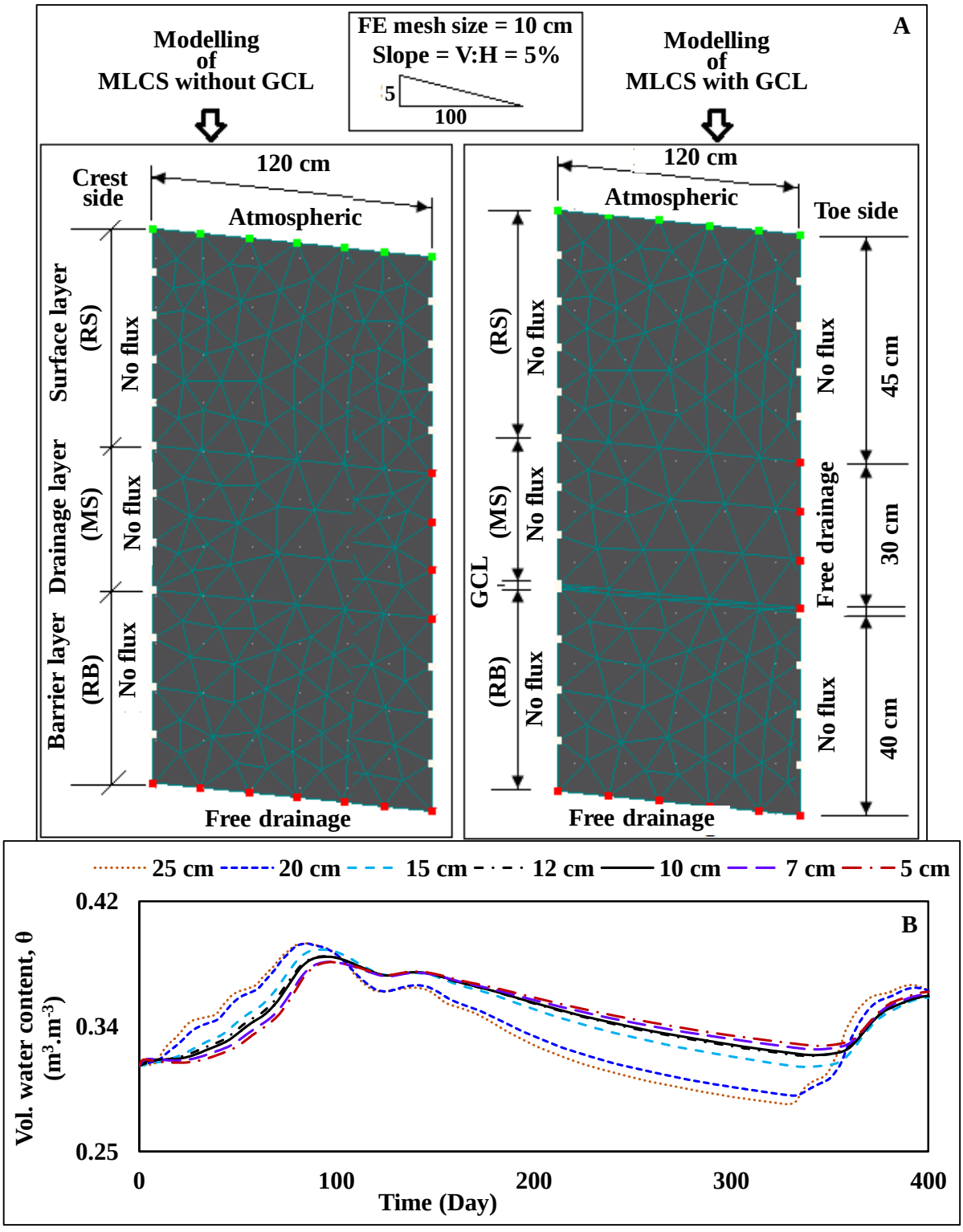

Fig. 7.2 (A) Geometry, boundary conditions used in numerical analysis (B) Convergence study for optimization of FE mesh size

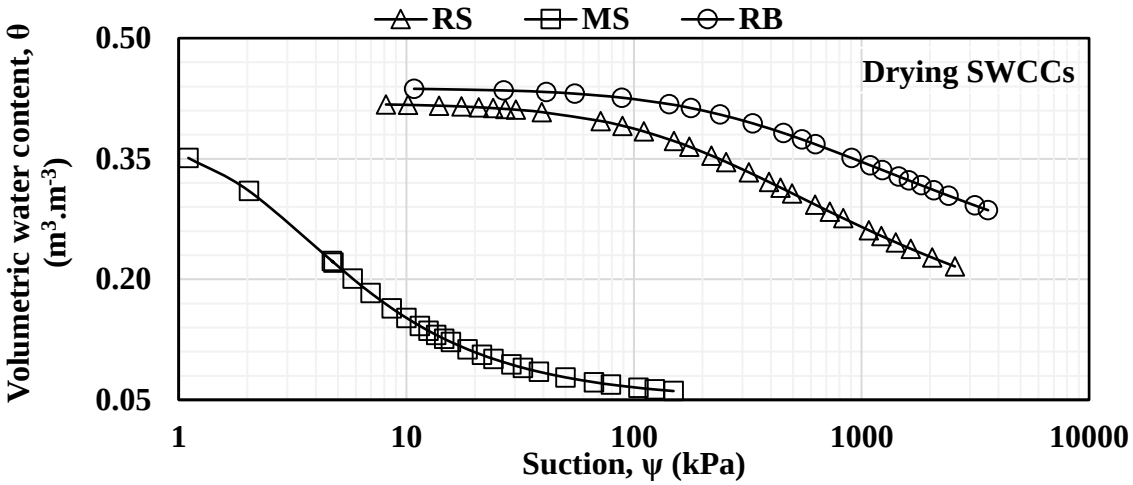

Fig. 7.3 Measured drying soil water characteristic curves used for simulation

Table 7.1 Hydraulic parameters of various materials assigned in numerical analyses

Layer (Material)	Material hydraulic parameters						θ_i
	θ_r	θ_s	α	n	K_s	I	
Surface layer (RS)	0.062	0.419	0.0005	1.31	3E-9	0.5	0.308
Drainage layer (MS)	0.040	0.381	0.0408	1.81	3E-5	0.5	0.060
Geosynthetic clay liner (GCL)	0.068	0.600	0.001	2.00	6E-11	0.5	0.115
Barrier layer (RB)	0.077	0.438	0.0003	1.23	2E-10	0.5	0.330

Notes: These hydraulic parameters were used for the same MLCS configuration either with or without GCL for simulating climate change impact.

7.3.2 Forecasting of futuristic climate

To obtain the forecasted climate data for the selected regions (Guwahati in north-east India and Mumbai in west coast of India) shown in Fig. 7.4**,** Statistical Down Scaling Model (SDSM) technique was adopted. The SDSM determines multiple or single-site scenarios of daily weather variables under current and future regional climate forecasting (Wilby and Dawson 2007). The theoretical considerations, limitations and detailed downscaling methodology have been discussed in literature (Giorgi and Mearns 1991; Wilby and Wigley 1997). The SDSM minimizes the task of statistically downscaling daily weather series through four discrete stages (Wilby et al. 2002). They are (1) screening of predictor variables; (2) calibration of model to be used; (3) synthesis of observed data; and (4) generation of climate change scenarios to provide futuristic data. These are presented

by a flow chart in Fig. 7.5. In the current study, the predictors considered based on previous literature (Dorji et al. 2017; Shivam et al. 2017; Bajracharya et al. 2018) for assessment of futuristic climate data of Guwahati and Mumbai are listed in Table 7.2. It is to be noted that SDSM methodology has been previously used in literature to forecast the climate data for the two selected cities (Rana et al. 2014; Shivam et al. 2017; Vinnarasi and Sarma 2011). The futuristic climate parameters of 87 years forecasted by SDSM technique are presented in Fig. 7.6 (a – e) and used for estimating evapotranspiration (refer Fig. 7.6 f). These were considered as time variable soil-atmosphere boundary condition in numerical analyses for studying the impact of climate change on MLCS. These analyses were performed by considering drying hydraulic parameters (DHP) and Penman-Monteith evapotranspiration model identified based on the comparison of numerical analysis with measured results of field MLCS setup (section 6.5).

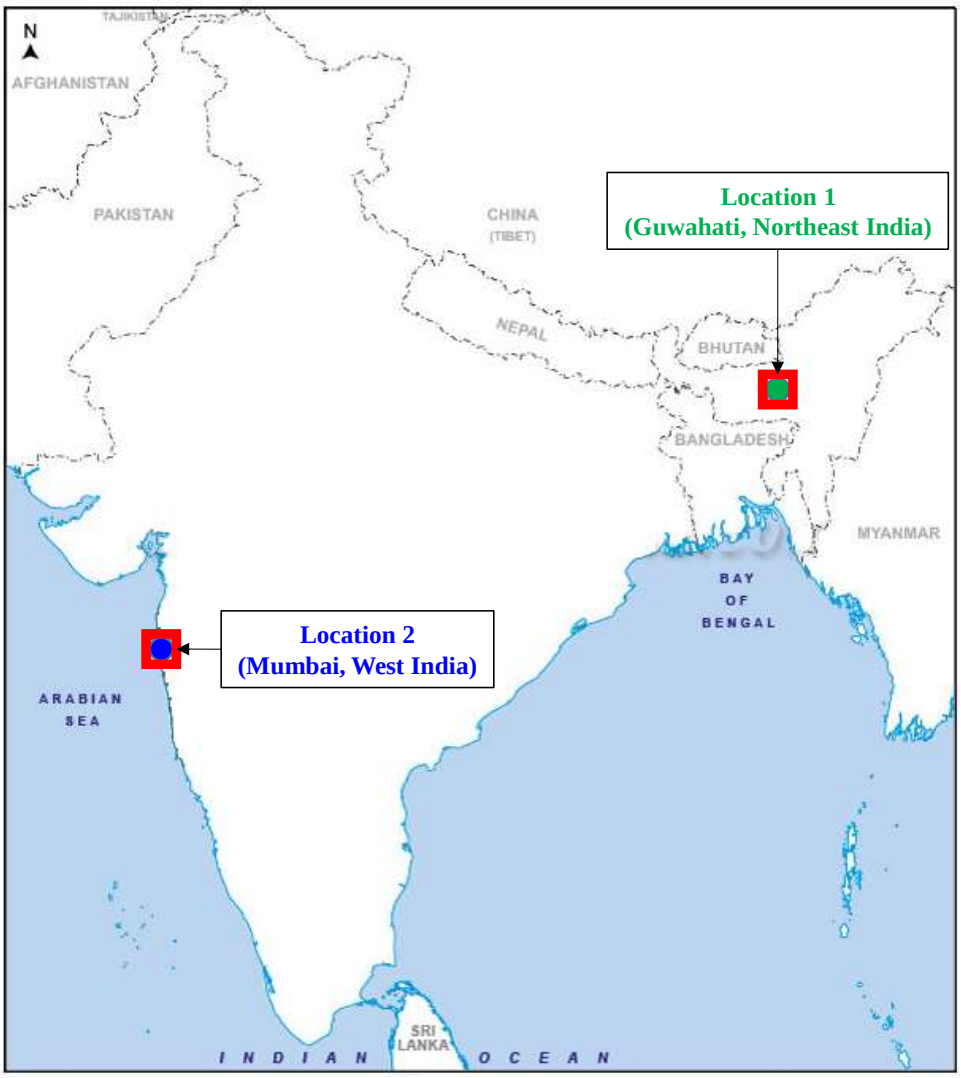

Fig. 7.4 Two different regions in India for the study

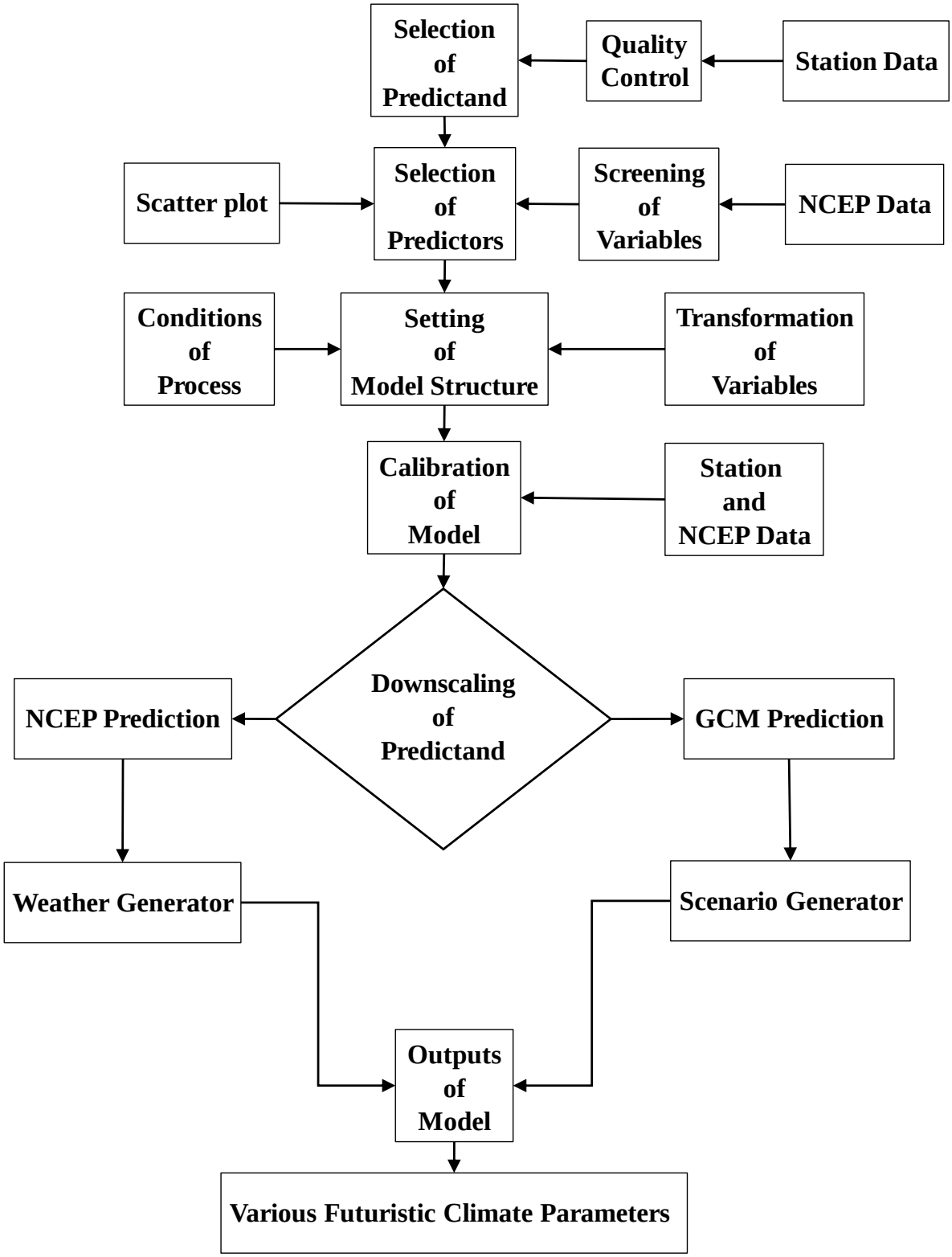

Fig. 7.5 SDSM climate scenario generation process (Wilby et al. 2002)

Table 7.2 List of selected predictors for forecasting various climate parameters (based on Dorji et al. 2017; Shivam et al. 2017; Bajracharya et al. 2018)

Description of Predictor variables	Code	Guwahati (26.18°N, 91.40°E)						Mumbai (19.08°N, 72.88°E)					
		Tx	Tn	Pp	Ws	Rh	Sr	Tx	Tn	Pp	Ws	Rh	Sr
mean sea level pressure	mslp					✓		✓		✓	✓	✓	
surface air flow strength	p_f			✓	✓					✓	✓		✓
surface zonal velocity component	p_u	✓			✓				✓			✓	
surface meridional velocity component	p_v		✓			✓					✓		
surface vorticity	p_z	✓					✓	✓		✓			✓
surface wind direction	p_th		✓		✓					✓			
surface divergence	p_zh					✓						✓	
500 hPa air flow strength	p5_f	✓						✓			✓		
500 hPa zonal velocity component	p5_u			✓	✓				✓				✓
500 hPa meridional velocity component	p5_v					✓						✓	
500 hPa vorticity	p5_z			✓			✓	✓			✓		
500 hPa wind direction	p5_th	✓		✓	✓					✓			✓
500 hPa divergence	p5_zh		✓					✓			✓		
850 hPa air flow strength	p8_f						✓		✓			✓	
850 hPa zonal velocity component	p8_u		✓		✓						✓		
850 hPa vorticity	p8_z	✓						✓	✓				✓
surface precipitation	prcp			✓		✓				✓		✓	
specific humidity at 500 hPa height	s500		✓	✓									
surface specific humidity	shum	✓				✓				✓			
surface mean temperature	temp	✓	✓		✓		✓	✓	✓		✓	✓	✓
500 hPa geopotential height	p500	✓				✓	✓		✓				✓

Notes: Tx = Maximum temperature, Tn = Minimum temperature, Pp = Precipitation, Ws = Wind speed, Rh = Relative humidity, Sr = Solar radiation,

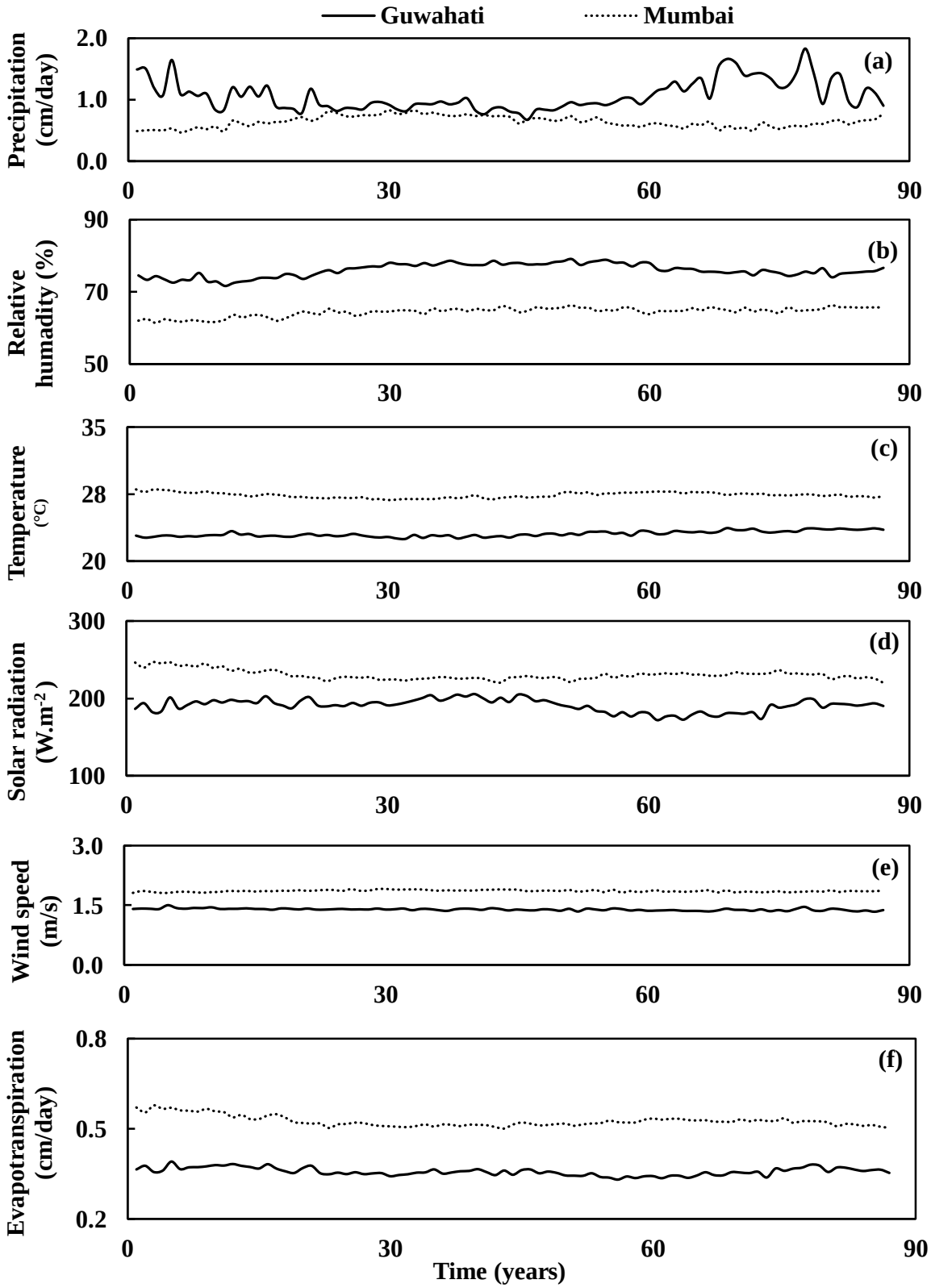

Fig. 7.6 Representation of forecasted climate data for 87 years (a – e) and evapotranspiration computed by Penman-Monteith (PM) model (f)

7.3.3 Climate change impact

Climate is expected to significantly affects the cover system design and performance. Heavy rainfall for a prolonged period leads to increase in rainwater infiltration and erosion of MLCS. Drier climate results in shrinkage and desiccation cracks in the surface layers of MLCS. Cracks may also develop due to the effects of freeze-thaw cycles in cold regions. Repeated cycles of wetting and drying can induce fatigue stress in the geomaterials thereby deteriorating its performance. As a result, hydraulic conductivity may increases in SL because of cracks and root growth (Sinnathamby et al. 2014), hydraulic conductivity of DL may reduce due to clogging of porous drainage materials by the ingress of fine particles from upper layer (Reddy et al. 2010). The BL and GCL may also lose its impermeability over a period of time (Rowe 2012).

The climatic factors affect the types of vegetation that grows on the surface layer of MLCS. Climatic criteria for the design consideration of a cover system may include the quantity and seasonal distribution of precipitation, intensity and duration of specific storm events, seasonal temperature variations, depth of frost penetration, quantity of snow melt, wind speed and direction, solar radiation and humidity (Bonaparte et al. 2002; Jarvis et al. 2013). Unlike laboratory model (chapter 5), field MLCS setup (chapter 6) were subjected to changes in natural weather condition and can undergo erosion, cracking, plant growth as shown in Figure 7.7. Due to a lot of factors contributing to uncertainties, it is difficult to take into account the deterioration of material properties in the long-term numerical modelling. However, this was considered by assigning, one order of change in hydraulic conductivity for the soils considered in this study. As an approximation, hydraulic conductivity was increased to 10^{-8} m/s from 10^{-9} m/s in SL, from 10^{-11} m/s to 10^{-10} m/s in GCL, from 10^{-10} m/s to 10^{-9} m/s in BL and decreased to 10^{-6} m/s from 10^{-5} m/s in DL. All other input parameters were kept same as the case where deterioration was not considered.

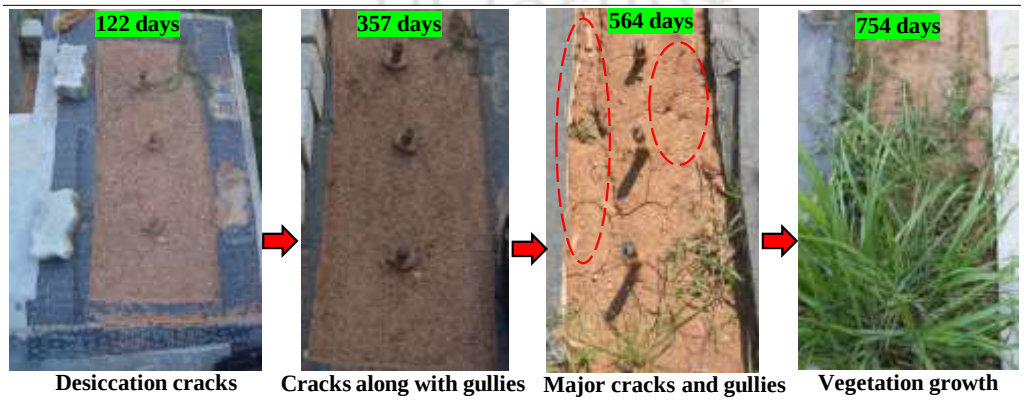

Fig. 7.7 Formation of desiccation cracks, erosion gullies and vegetation on surface layer

7.4 Results and Discussion

The numerical analyses were performed for long-term hydraulic performance of the field MLCS with and without considering GCL between DL and BL. The numerical simulation was performed with and without considering deterioration of material performance. The layer specific results of the analyses are described in the following subsections.

7.4.1 Surface layer efficiency

Figure 7.8 summarises the yearly variations of average, minimum and maximum values of θ (designated as θ_{avg}, θ_{min} and θ_{max} respectively) simulated at 10 cm in SL of field MLCS influenced by climatic variations of Guwahati and Mumbai city in India. Simulated results with and without deterioration of layer material for 87 years are presented in the figure. In both the cases, the cyclic variation in θ_{avg} was found to be within θ_{min} and θ_{max}. The θ_{min} in the SL was found to be below its initial θ (θ_i) for most of the duration, which is mainly due to the higher evaporation from SL during the dry season. In both cases (with and without the consideration of material deterioration), the θ_{max} approached theoretical θ_s. It is clearly noted that the depth of SL considered attains saturation several times for both the climatic conditions of Guwahati and Mumbai region. The inclusion of GCL showcased almost identical profiles with the presented figures for both Guwahati and Mumbai region.

7.4.2 Drainage layer efficiency

Figure 7.9 presents the annual θ profiles of θ_{avg}, θ_{min}, θ_{max} for drainage layer at a depth of 60 cm (i.e. middle) considering two selected locations with and without GCL. In DL, the θ_{avg}, θ_{min} and θ_{max} followed a cyclic variation and noted to be always above its θ_i. It might be due to less influence of evaporation due to the protective SL above the DL. The θ_{max} was well below its theoretical θ_s in both the cases with and without deterioration. The figure clearly indicates that the DL never reaches saturation in the forecasted period regardless of the use of GCL. It may be due to the lateral outflow of infiltrated rain water through the high permeable sloped drainage pathway before attaining saturation. The inclusion or exclusion of GCL doesn't majorly change the water content profile of DL.

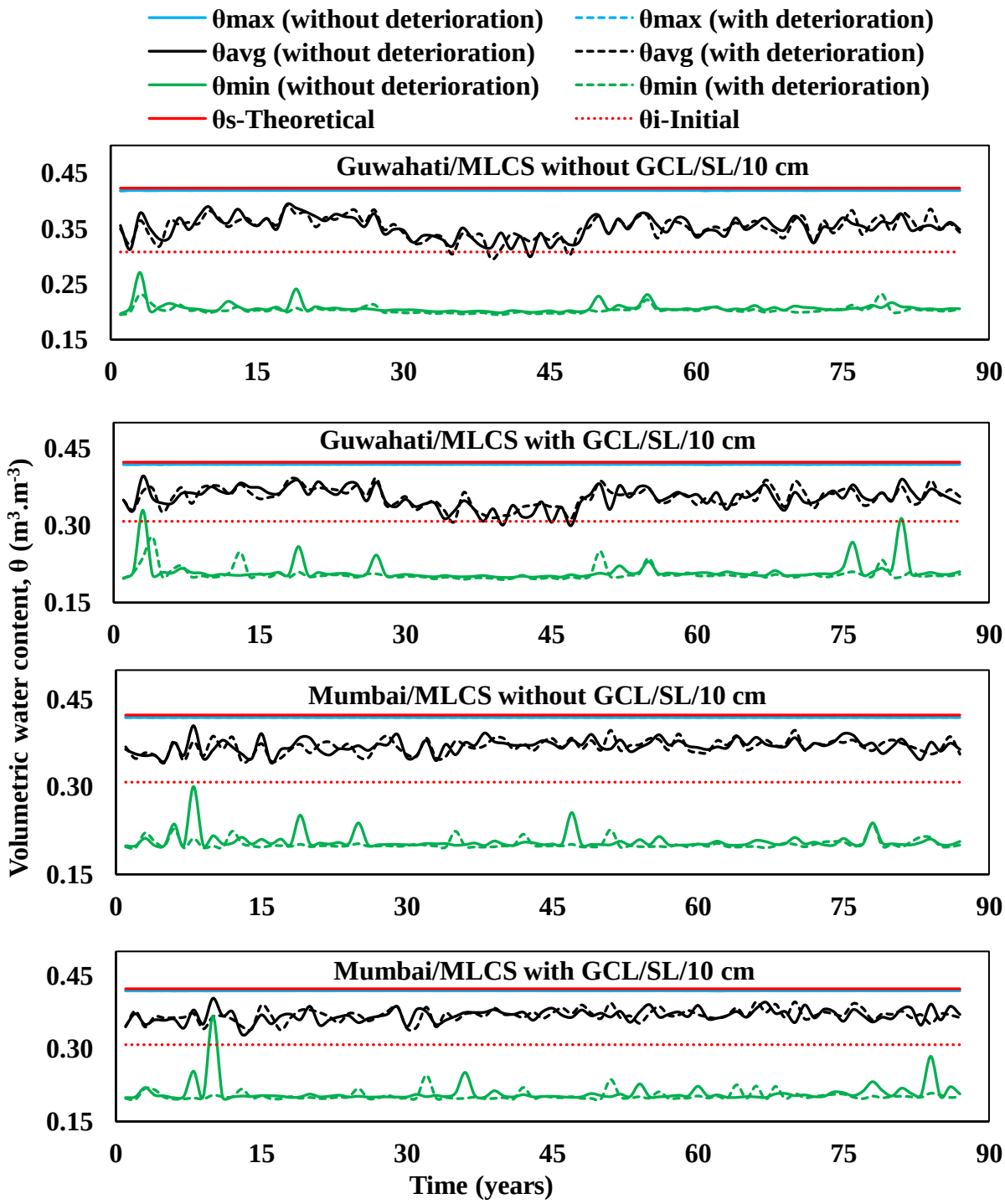

Fig. 7.8 Simulated volumetric water content at 10 cm in surface layer (SL) of MLCS by considering climate change

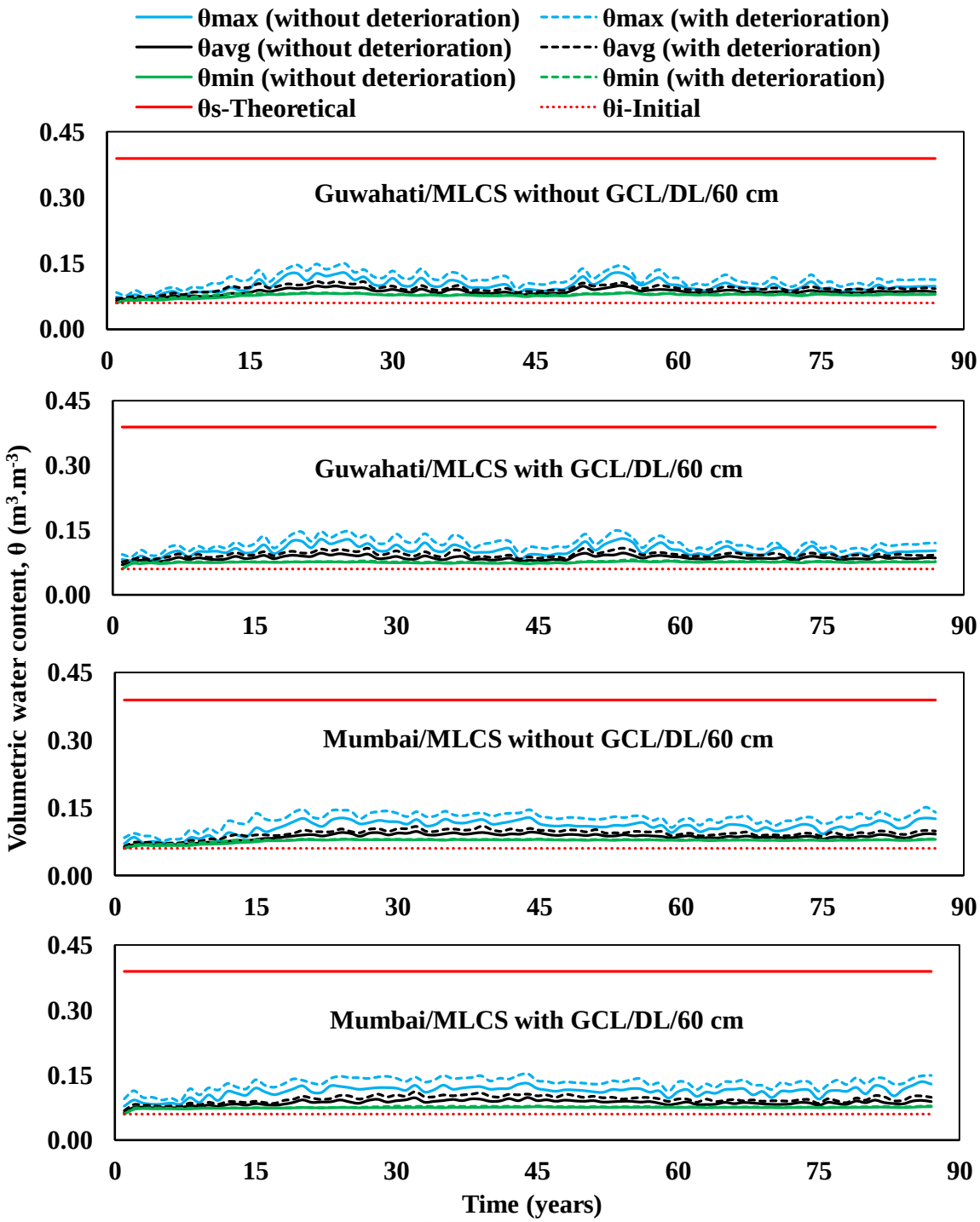

Fig. 7.9 Simulated volumetric water content at 60 cm in drainage layer (DL) of MLCS by considering climate change

7.4.3 Barrier layer efficiency

Figure 7.10 illustrates the annual variations of θ_{avg} predicted at 100 cm depth (i.e. 15 cm above waste layer) in BL. The results are presented in the figure from simulations with and without the effect of material deterioration for both climatic inputs. Both in Guwahati and Mumbai region, the θ_{avg} in BL increases gradually to its saturation and were observed to be always below its theoretical $\theta_{s,}$ attributed to the entrapment of micro air pockets (Touma et al. 1984). Even though barrier layer (10^{-10} m/s) and GCL layer (10^{-11} m/s) have very low permeability, the built up of head at the drainage-barrier layer interface will gradually increase water percolation.

For better understanding, time to saturation in BL was obtained from Fig. 7.10 for all the cases and presented in Fig. 7.11. The θ_{avg} at 100 cm approached saturation in 25 and 28 years for Guwahati and Mumbai city, respectively when GCL was provided and material deterioration was considered in the simulations. Correspondingly, these were 42 and 44 years without considering material deterioration. Similarly, it can be seen from the figure that annual θ_{avg} will ultimately reach saturation by 18 and 20 years in MLCS without GCL for Guwahati and Mumbai regions, respectively without material deterioration. However, the consideration of material deterioration reduces the time of saturation to 13 and 14 years for Guwahati and Mumbai regions, respectively. With reference to climate change for two different geographical settings of Indian subcontinent, the inclusion of GCL will forbid water percolation into the waste layer by at least 25 and 42 years, with and without material deterioration effect, respectively.

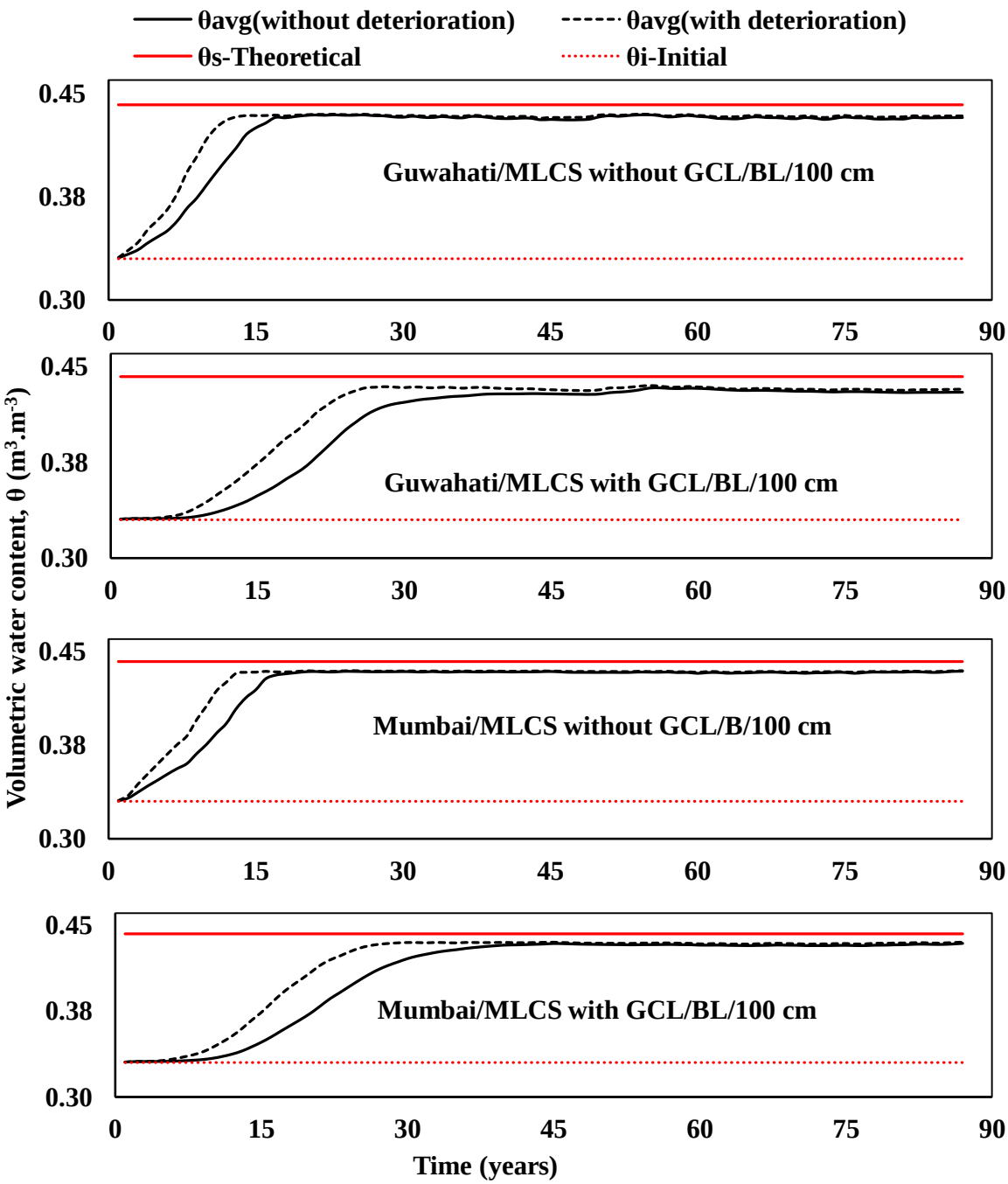

Fig. 7.10 Simulated volumetric water content at 100 cm in barrier layer (BL) of MLCS by considering climate change

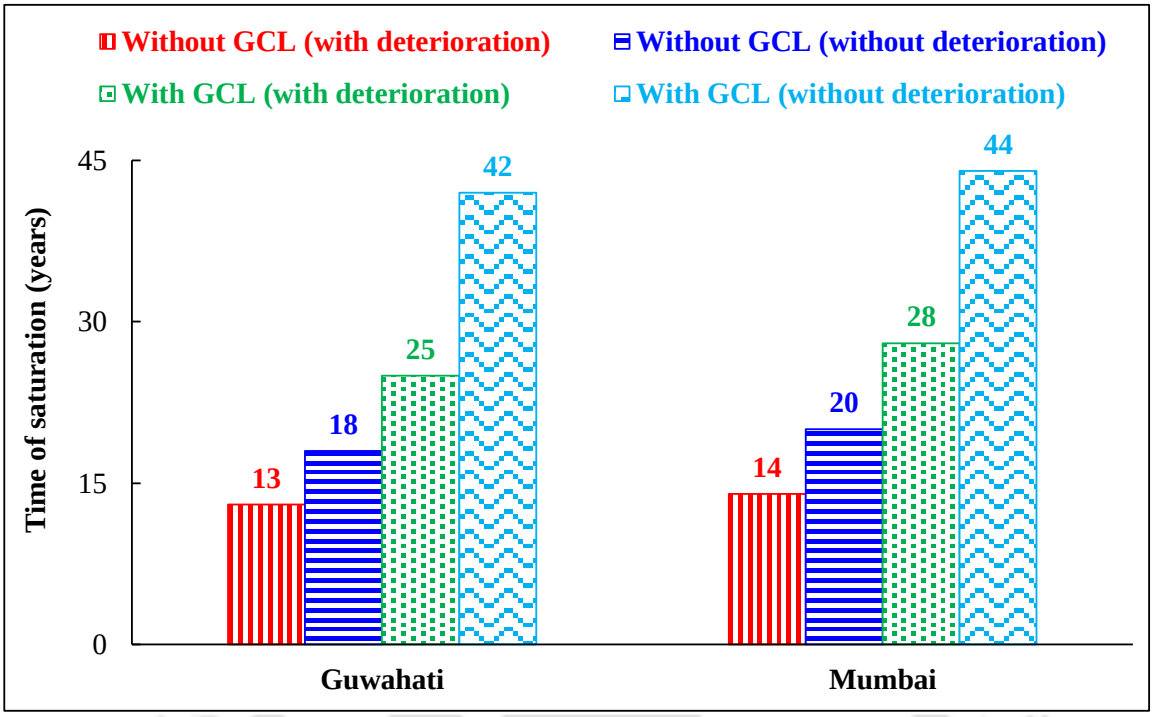

Fig. 7.11 Time to saturation up to the depth of 1000 mm in barrier layer of MLCS

7.5 Summary

The long-term climate change impact on field MLCS was performed by considering the climatic data of north-east and western India for 87 years as input. The simultaneous effect of deterioration of material performance and climate change on the hydraulic performance of MLCS was studied. It was noted that the SL undergoes cyclic wetting and drying for the entire duration denoting a high sensitivity to climatic changes. Under the regional climate of northeast or western India, the SL undergoes saturation for several times in forecasted period of 87 years. The DL never reach saturation in the forecasted period regardless of GCL use. GCL inclusion or exclusion slightly changes the water content profile of DL. Thus, based on global climate change for these two locations, the entire MLCS reaches saturation by 13 and 18 years from the time of cover completion with and without material deterioration, respectively. However, the GCL inclusion in MLCS can resist water interaction with the underlying waste layer by at least 25 and 42 years with and without deterioration, respectively.

Chapter 8

Conclusions and Future Scope of Work

8.1 General

This study deals with the hydraulic performance assessment of the multi-layered landfill cover system (MLCS) for a near surface hazardous waste disposal facility. The study is divided into three sections: (i) controlled laboratory study for understanding the percolation characteristics of MLCS under constant water ponding conducted for 900 days (ii) a pilot hydraulic performance assessment of MLCS exposed to field weather conditions for 800 days (iii) numerical analyses to simulate laboratory and field MLCS followed by the study of climate change impact on hydraulic performance of the MLCS. The conclusions derived from this study are summarized in this chapter followed by major contributions of this study and future scope of work.

8.2 Conclusions from this study

- Measurement accuracy of volumetric water content sensors was enhanced by conducting soil-specific calibration for the generic soils type used in different layers of MLCS. The accuracy enhanced from ±6% to ±1% for profile probe sensors (PPS) and from ±8% to ±1% for 5TM sensor.
- The disparity in the measurements of six sensors housed different depths of profile probe was removed by calibrating it under controlled compaction conditions using an in-house laboratory fabricated setup.
- Percolation study was conducted for four different configurations of MLCS in the laboratory under constant water head boundary conditions for 900 days. Among the four MLCS configurations, the one with geosynthetic clay liner (GCL) performed efficiently despite fly ash addition to its surface layer.
- The MLCS with the fly ash added to its surface and barrier layer underperforms in the absence of GCL.
- The GCL inclusion in the MLCS can save at least 36% bentonite cost to achieve the same performance efficiency where GCLs were not considered.
- Numerical simulation of the laboratory column MLCS (continuous wetting) considering wetting soil-water characteristic curve (SWCC) matched well with the measured results as compared to drying and predicted SWCC.

- A pilot MLCS was constructed in the field and exposed to natural weather conditions for 800 days. At the end of observation period, surface layer (SL) was subjected to high weather impacts. The effects of natural weather on the drainage and barrier layer was observed to be minimal, for the given configuration of surface layer.
- For the entire field observation, barrier layer (BL) was unaffected by percolating water.
- The vegetation growth and desiccation cracks on the SL hardly affected the moisture dynamics in the BL for the entire duration of field observation.
- The numerical simulation of field MLCS matched well with the observations when Penman-Montieth evapotranspiration (ET) boundary condition and drying SWCC was used as input.
- The long-term climate change impact on field MLCS was performed by considering the climatic data of north-east and western India for 87 years as input. It was noted that the SL undergoes cyclic wetting and drying for the entire duration denoting a high sensitivity to climatic changes.
- If the material performance deterioration was considered in the numerical analysis, the MLCS restricts water percolation into the waste by at least 13 years without GCL and 25 years with GCL.
- If material performance deterioration was ignored in the numerical simulation, the MLCS would forbid water percolation into the underlying waste by at least 18 years without using GCL and 42 years with using GCL.

8.3 Major contributions from this study

- Demonstrated the utility of soil-specific calibration in improving the accuracy of volumetric water content sensors used in this study.
- Developed a simple novel calibration setup for simultaneously calibrating the six sensors housed in a profile probe.
- Laboratory evaluation of four different configurations of MLCS suited for high humid, high rainfall regions for a duration of 900 days.
- Field evaluation of a pilot field MLCS instrumented with volumetric water content sensors and soil suction sensors for a period of 800 days.
- Numerical modeling of both laboratory and field MLCS to identify the appropriateness of input functions and boundary conditions used for simulating MLCS.

- Explored the impact of climate change on the hydraulic performance of MLCS by considering 87 years of simulated climate data for two different geographical regions of Indian subcontinent.
- The simultaneous effect of deterioration of material performance and climate change on the hydraulic performance of MLCS was studied.

8.4 Limitations

- Effect of erosion of the surface layer of the pilot field MLCS was not incorporated in the numerical simulation.
- The deterioration in material performance was considered to be constant throughout the time duration of numerical simulation, which may not be representative.
- Hysteresis in SWCC was not considered in the numerical simulations.

8.5 Future scope

- Further studies need to be conducted to investigate the effects of erosion on the hydraulic performance of the MLCS.
- The effect of considering hysteresis models for SWCC for numerical simulation of MLCS need to be studied further.
- Develop and use a reasonable material deterioration model for simulating long-term hydraulic evaluation of MLCS under climate change.
- The MLCS field studies need to be extended for different configurations and varying climatic scenarios.
- Investigate the role of non-woven geotextile in landfill cover performance.

भारतीय प्रौद्योगिकी संस्थान गुवाहाटी
Indian Institute of Technology Guwahati

REFERENCES

1. Abdolahzadeh, A. M., Vachon, B. L., and Cabral, A. R. (2011). "Evaluation of the effectiveness of a cover with capillary barrier effect to control percolation into a waste disposal facility." Canadian Geotechnical Journal, 48(7), 996–1009.

2. Abichou, T., Musagasa, J., Yuan, L., Chanton, J., Tawfiq, K., Rockwood, D., and Licht, L. (2012). "Field performance of alternative landfill covers vegetated with cottonwood and eucalyptus trees." International Journal of Phytoremediation, 14(1), 47–60.

3. Albright, W. H., Benson, C. H., and Apiwantragoon, P. (2012). "Field hydrology of landfill final covers with composite barrier layers." Journal of Geotechnical and Geoenvironmental Engineering, 139(1), 1–12.

4. Albright, W. H., Benson, C. H., Gee, G. W., Abichou, T., Tyler, S. W., and Rock, S. A. (2006a). "Field performance of a compacted clay langfill final cover at a humid site." Journal of Geotechnical and Geoenvironmental Engineering, 132(11), 1393–1403.

5. Albright, W. H., Benson, C. H., Gee, G. W., Abichou, T., Tyler, S. W., and Rock, S. A. (2006b). "Field performance of three compacted clay landfill covers." Vadose Zone Journal, 5, 1157–1171.

6. Albright, W. H., Benson, C. H., Gee, G. W., Roesler, A. C., Abichou, T., Apiwantragoon, P., Lyles, B. F., and Rock, S. A. (2004). "Field water balance of landfill final covers." Journal of Environmental Quality, 33(6), 2317–2332.

7. Aldaeef, A. A., and Rayhani, M. T. (2015). "Hydraulic performance of compacted clay liners under simulated daily thermal cycles." Journal of Environmental Management, 162, 171–178.

8. Aljaradin, M., and Persson, K. M. (2015). "Numerical evaluation of different landfill daily cover in semiarid areas-Jordan." International Journal of Environment and Waste Management, 16(2), 95–111.

9. Allen, A., and Taylor, R. (2006). "Waste disposal and landfill: control and protection." Protecting groundwater for health: managing the quality of drinking-water sources, 631–652.

10. Allen, R. G., Pereira, L. S., Raes, D., and Smith, M. (1998). "Crop evapotranspiration - Guidelines for computing crop water requirements." Irrigation and Drainage Paper, 56, 1–15.

11. Apiwantragoon, P., Benson, C. H., and Albright, W. H. (2015). "Field Hydrology of Water Balance Covers for Waste Containment." Journal of Geotechnical and Geoenvironmental Engineering, 141(2), 04014101–20.

12. Argunhan-Atalay, C., and Yazicigil, H. (2018). "Modeling and Performance Assessment of Alternative Cover Systems on a Waste Rock Storage Area." Mine Water and the Environment, Springer Berlin Heidelberg, 37(1), 106–118.

13. ASTM International. (2006). "Standard Practice for Classification of Soils for Engineering Purposes (Unified Soil Classification System)." ASTM D2487-17, 1-10, West Conshohocken, PA, USA.

14. ASTM International. (2007). "Standard Test Methods for Laboratory Compaction Characteristics of Soil Using Standard Effort." The Annual Book of ASTM Standards, ASTM D698-07, pp. 1-11, West Conshohocken, PA, USA.

15. ASTM International. (2008). "Standard Test Method for Shrinkage Factors of Soils by the Mercury Method." ASTM D427-04, pp. 1-4, West Conshohocken, PA, USA.

16. ASTM International. (2009). "Standard Test Methods for Particle-Size Distribution (Gradation) of Soils Using Sieve Analysis." ASTM D6913-17, pp. 1-34, ASTM, West Conshohocken, PA, USA.

17. ASTM International. (2010). "Standard Test Methods for Liquid Limit, Plastic Limit, and Plasticity Index of Soils." ASTM D4318-17, pp. 1-20, West Conshohocken, PA, USA.

18. ASTM International. (2011). "Standard Test Method for Permeability of Granular Soils (Constant Head)." ASTM D2434-68, pp. 1-6, ASTM, West Conshohocken, PA, USA.

19. ASTM International. (2013a). "Standard Test Method for Shrinkage Factors of Soils by the Wax Method." ASTM D4943-08, pp. 1-5, West Conshohocken, PA, USA.

20. ASTM International. (2013b). "Standard Test Method for pH of Soils." ASTM International, ASTM D4972-13, pp. 1-4, West Conshohocken, PA, USA.

21. ASTM International. (2013c). "Standard Test Methods for One-Dimensional Swell or Collapse of Cohesive Soils." ASTM D4546 − 14, pp. 1-9, West Conshohocken, PA, USA.

22. ASTM International. (2014a). "Standard Test Method for Measuring the Exchange Complex and Cation Exchange Capacity of Inorganic Fine - Grained Soils." ASTM D7503-18. pp. 1-5, West Conshohocken, PA, USA.

23. ASTM International. (2014b). "Standard Test Methods for Specific Gravity of Soil Solids by Water Pycnometer." ASTM D854 − 14, pp. 1-8, West Conshohocken, PA, USA.

24. ASTM International (1994) "Test Method for Measurement of Hydraulic Conductivity of Saturated Porous Materials Using a Flexible-Wall Permeameter." ASTM D5084, West Conshohocken, PA, USA.

25. ASTM International. (2014c). "Standard test methods for moisture, ash, and organic matter of peat and other organic soils." ASTM International, ASTM D2974-14, pp. 1-4, West Conshohocken, PA, USA.

26. ASTM International. (2016). "Standard Test Method for Determination of Water (Moisture) Content of Soil by Direct Heating." ASTM D4959-16, 1-6, West Conshohocken, PA, USA.

27. Ataka, M., Kominami, Y., Miyama, T., Yoshimura, K., Jomura, M., and Tani, M. (2014). "Using capacitance sensors for the continuous measurement of the water content in the litter layer of forest soil." Applied and Environmental Soil Science, 2014(627129), 1–5.

28. Bajracharya, A. R., Bajracharya, S. R., Shrestha, A. B., and Maharjan, S. B. (2018). "Climate change impact assessment on the hydrological regime of the Kaligandaki Basin, Nepal." Science of the Total Environment, Elsevier B.V., 625, 837–848.

29. Barnswell, K. D., and Dwyer, D. F. (2012). "Two-year performance by evapotranspiration covers for municipal solid waste landfills in northwest Ohio." Waste Management, Elsevier Ltd, 32(12), 2336–2341.

30. Barnswell, K., and Dwyer, D. (2011). "Assessing the performance of evapotranspiration covers for municipal solid waste landfills in Northwestern Ohio." Journal of Environmental Engineering, 137(4), 301–305.

31. Bashir, R., Sharma, J., and Stefaniak, H. (2015). "Effect of hysteresis of soil-water characteristic curves on infiltration under different climatic conditions." Canadian Geotechnical Journal, 53(2), 273–284.

32. Basinger, J. M., Kluitenberg, G. J., Ham, J. M., Frank, J. M., Barnes, P. L., and Kirkham, M. B. (2003). "Laboratory Evaluation of the Dual-Probe Heat-Pulse Method for Measuring Soil Water Content." Vadose Zone Journal, 2, 389–399.

33. Baumhardt, R. L., Lascano, R. J., and Evett, S. R. (2000). "Soil Material, Temperature, and Salinity Effects on Calibration of Multisensor Capacitance Probes." Soil Science Society of America Journal, 64(6), 1940–1946.

34. Bell, J. P., and Mcculloch, J. S. G. (1966). "Soil Moisture Estimation by the Neutron Scattering Method in Britain." Journal of Hydrology, 4, 254–263.

35. Bell, J. P., Dean, T. J., and Hodnett, M. G. (1987). "Soil moisture measurement by an improved capacitance technique, part II. Field techniques, evaluation and calibration." Journal of Hydrology, 93(3), 79–90.

36. Bennett, G. F. (2007). Waste Management Practices: Municipal, Hazardous, and Industrial. Journal of Hazardous Materials.

37. Benson, C. H., and Khire, M. V. (1995). "Earthen cover for semi-arid and arid climates." Geotechnical Special Publication, Madison.

38. Benson, C. H., and Othman, M. A. (1993). "Hydraulic conductivity of composite clay frozen and thawed in situ." Journal of Geotechnical and Geoenvironmental Engineering, 119(2), 276–294.

39. Benson, C. H., Kucukkirca, I. E., and Scalia, J. (2010). "Properties of geosynthetics exhumed from a final cover at a solid waste landfill." Geotextiles and Geomembranes, Elsevier Ltd, 28(6), 536–546.

40. Benson, C. H., Sawangsuriya, A., Trzebiatowski, B., and Albright, W. H. (2007a). "Postconstruction Changes in the Hydraulic Properties of Water Balance Cover Soils." Journal of Geotechnical and Geoenvironmental Engineering, 133(4), 349–359.

41. Benson, C. H., Thorstad, P. A., Jo, H. Y., and Rock, S. A. (2007b). "Hydraulic performance of geosynthetic clay liners in a landfill final cover." Journal of Geotechnical and Geoenvironmental Engineering, 133(7), 814–827.

42. Benson, C., Abichou, T., Albright, W., Gee, G., and Roesler, A. (2001). "Field evaluation of alternative earthen final covers." International Journal of Phytoremediation, 3(1), 105–127.

43. Berger, K., Melchior, S., and Miehlich, G. (1996). "Suitability of hydrologic evaluation of landfill performance (HELP) model of the US Environmental Protection Agency for the simulation of the water balance of landfill cover systems." Environmental Geology, 28(4), 181–189.

44. Bircher, S., Andreasen, M., Vuollet, J., Vehviläinen, J., Rautiainen, K., Jonard, F., Weihermüller, L., Zakharova, E., Wigneron, J. P., and H Kerr, Y. (2016). "Soil moisture sensor calibration for organic soil surface layers." Geoscientific Instrumentation, Methods and Data Systems, 5(1), 109–125.

45. Blaney, H. F., and Criddle, W. D. (1950). "Determining water requirements in irrigated areas from climatological and irrigation data, USDA SCSTP- 96." US Department of Agriculture, Washington, DC.

46. Blight, G. (2009). "Solar heating of the soil and evaporation from a soil surface." Géotechnique, 59(4), 355–363.

47. Boardman, B. T., and Daniel, D. E. (1996). "Hydraulic Conductivity of Desiccated Geosynthetic Clay Liners." Journal of Geotechnical Engineering, 122(3), 204–208.

48. Bogena, H. R., Huisman, J. A., Schilling, B., Weuthen, A., and Vereecken, H. (2017). "Effective calibration of low-cost soil water content sensors." Sensors (Switzerland), 17(1), 1–12.

49. Böhme, B., Becker, M., and Diekkrüger, B. (2013). "Calibrating a FDR sensor for soil moisture monitoring in a wetland in Central Kenya." Physics and Chemistry of the Earth, 66, 101–111.

50. Bohnhoff, G. L., Ogorzalek, A. S., Benson, C. H., Shackelford, C. D., and Apiwantragoon, P. (2009). "Field data and water-balance predictions for a monolithic cover in a semiarid climate." Journal of Geotechnical and Geoenvironmental Engineering, 135(3), 333–348.

51. Bonaparte, R., Daniel, D. E., and Koerner, R. M. (2002). Assessment and Recommendations for Improving the Performance of Waste Containment Systems. United States Environmental Protection Agency, Office of Research and Development, National Risk Management Research Laboratory, Cincinnati, OH 45268.

52. Bordoloi, S., Hussain, R., V.K., G., H., B., L., S., R., K., Garg, A., and S., S. (2018). "Monitoring soil cracking and plant parameters for a mixed grass species." Geotechnique Letters, 8, 1–7.

53. Bouazza, A., Zornberg, J. G., and Adam, D. (2002). "Geosynthetics in Waste Containment Facilities: Recent Advances." 7th International Conference on Geosynthetics, 445–507.

54. Bowders, J. J., Daniel, D. E., Wellington, J., and Houssidas, V. (1997). "Managing Desiccation Cracking in Compacted Clay Liners Beneath Geomembranes." Geosynthetics '97 Conference Proceedings, Industrial Fabrics Association International, St. Paul, 527–540.

55. Boyle, M., Frankenberger, W. T., and Stolzy, L. H. (1989). "The Influence of Organic Matter on Soil Aggregation and Water Infiltration." Journal of Production Agriculture, 2(4), 290–299.

56. Brachman, R. W. I., and Gudina, S. (2008). "Gravel contacts and geomembrane strains for a GMB/CCL composite liner." Geotextiles and Geomembranes, Elsevier Ltd, 26(6), 448–459.

57. Brachman, R. W. I., and Sabir, A. (2010). "Geomembrane puncture and strains from stones in an underlying clay layer." Geotextiles and Geomembranes, Elsevier Ltd, 28(4), 335–343.

58. Bradford, S. A., Yates, S. R., Bettahar, M., and Simunek, J. (2002). "Physical factors affecting the transport and fate of colloids in saturated porous media." Water Resources Research, 38(12), 63-1-63–12.

59. Brooks, R. H., and Corey, A. T. (1966). "Properties of porous media affecting fluid flow." Journal of the Irrigation and Drainage Division, 61–88.

60. Brown, D. W. (2007). "Determination of Evapotranspiration Landfill Cover System Design Parameters Using the Simultaneous Heat and Water (SHAW) Model." MS Thesis, Department of Environmental Resources and Forest Engineering, State University of New York.

61. Bussière, B., Aubertin, M., and Chapuis, R. P. (2003). "The behavior of inclined covers used as oxygen barriers." Canadian Geotechnical Journal, 40(3), 512–535.

62. Caldwell, J. A., and Reith, C. C. (1993). Principles and Practice of Waste Encapsulation. Lewis Publishers, Chelsea, Michigan.

63. Campbell, G. S. (1974). "A simple method for determining unsaturated conductivity from moisture retention data." Soil Science, 117(6), 311–314.

64. Cerato, A. B., and Lutenegger, A. J. (2002). "Determination of Surface Area of Fine-Grained Soils by the Ethylene Glycol Monoethyl Ether (EGME) Method." Geotechnical Testing Journal, 25(3), 1–7.

65. Chandler, D. G., Seyfried, M. S., McNamara, J. P., and Hwang, K. (2017). "Inference of Soil Hydrologic Parameters from Electronic Soil Moisture Records." Frontier in Earth Science, 5(25), 1–17.

66. Chandler, D. G., Seyfried, M., Murdock, M., and McNamara, J. P. (2005). "Field Calibration of Water Content Reflectometers." Soil Science Society of America Journal, 68(4), 1501–1507.

67. Chang, K., Park, J. W., Yoon, J. H., Choi, H. J., and Kim, C. L. (1999). "Water Balance Evaluation of Final Closure Cover of Near Surface Radioactive Waste Disposal Facility." Journal of the Korean Nuclear Society, 32(3), 274–282.

68. Chen, R., Chen, Y., Chen, W., and Chen, Y. (2012). "Time Domain Reflectometry for Water Content Measurement of Municipal Solid Waste." Environmental Engineering Science, 29(6), 486–493.

69. Choo, L.-P., and Yanful, K. (2000). "Water flow through cover soils using modeling and experimental methods." Journal of Geotechnical and Geoenvironmental Engineering, 126(4), 324–334.

70. Christopher, B. R. (1991). "Geotextiles in landfill closures." Geotextiles and Geomembranes, 10(5–6), 459–470.

71. Cobos, D. R., and Chambers, C. (2010). "Calibrating ECH2O Soil Moisture Sensors." Decagon Devices Inc., <http://www.decagon.com/Education/Calibrating-Ech2O-Soil-Moisture-Sensors-13393-04-an/> (Jul. 25, 2018).

72. Comer, A. I., Huan, Y. G., and Sculli, M. L. (1995). Freeze Thaw Cycling and Cold Temperature Effects on Geomembrane Sheets and Seams. Agency, U S Environmental Protection, Virginia.

73. Coo, J. L., So, P. S., Chao, Z., Chen, B., and Ng, C. W. W. (2016). "Feasibility study of a new unsaturated three-layer landfill cover system." E3S Web of Conferences, 9, 1–6.

74. Corser, P., and Cranston, M. (1991). "Observations on Long -Term Performance of Composite Clay Liners and Covers." Proceedings, Geosynthetic Design and Performance, Vancouver Geotechnical Society, Vancouver, BC.

75. Corser, P., Pellicer, J., and Cranston, M. (1992). Observation on Long-Term Performance of Composite Clay Liners and Covers. Geotechnical Fabrics Report, Industrial Fabrics Association International, St. Paul.

76. Cosh, M. H., Jackson, T. J., Bindlish, R., Famiglietti, J. S., and Ryu, D. (2005). "Calibration of an impedance probe for estimation of surface soil water content over large regions." Journal of Hydrology, 311(4), 49–58.

77. Czarnomski, N. M., Moore, G. W., Pypker, T. G., Licata, J., and Bond, B. J. (2005). "Precision and accuracy of three alternative instruments for measuring soil water content in two forest soils of the Pacific Northwest." Canadian Journal of Forest Research, 35(8), 1867–1876.

78. Daniel, D. E. (University of T. A., Shan, H. Y. (University of T. A., and Anderson, J. D. (Gundle L. S. I. (1993a). "Effects of partial wetting on the performance of the bentonite component of a geosynthetic clay liner." Geosynthetics 93, Industrial Fabrics Association International, St. Paul, 1483–1496.

79. Daniel, D. E., and Wu, Y. K. (1993b). "Compacted Clay Liners and Covers for Arid Sites." Journal of Geotechnical Engineering, 119(2), 223–237.

80. Daniel, D. E., Koerner, R. M., and Bonaparte, R. (2002). "Assessment and Recommendations for Improving the Performance of Waste Containment Systems." 02/99(December), 1–1039.

81. Daniel, D. E., Koerner, R. M., and Carson, D. A. (1993a). "Quality Assurance and Quality Control for Waste Containment Facilities." (September), 328.

82. Dean, T. J., Bell, J. P., and Baty, A. J. B. (1987). "Soil moisture measurement by an improved capacitance technique, Part I. Sensor design and performance." Journal of Hydrology, 93(3), 67–78.

83. Decagon Devices Inc. (2013). "WP4 Dew Point PotentiaMeter for Measuring Soil Water Potential." Operator's User Manual, Decagon Devices Inc., Pullman, WA, United States of America (USA).

84. Delta-T Devices Ltd. (2011). "DL6 Data Logger for Scanning and Storing Readings from Profile Probe." Operator's User Manual, Delta-T Devices Ltd., Cambridge, United Kingdom (UK).

85. Delta-T Devices Ltd. (2012). "PR2/6 Profile Probe for Measuring Volumetric Water Content." Operator's User Manual, Delta-T Devices Ltd., Cambridge, United Kingdom (UK).

86. Delta-T Devices Ltd. (2013). "HH2 Moisture Meter for Scanning Readings from Profile Probe." Operator's User Manual, Delta-T Devices Ltd., Cambridge, United Kingdom (UK).

87. Dhar, O. N., and Nandargi, S. (2000). "A study of floods in the Brahmaputra basin in India." International Journal of Climatology, 20(7), 771–781.

88. Divya, P. V., Viswanadham, B. V. S., and Gourc, J. P. (2012). "Influence of geomembrane on the deformation behaviour of clay-based landfill covers." Geotextiles and Geomembranes, 34, 158–171.

89. Dorji, S., Herath, S., and Mishra, B. (2017). "Future Climate of Colombo Downscaled with SDSM-Neural Network." Climate, 5(1), 24.

90. Dwyer, S. F. (1997). "Large - Scale Field Study of Landfill Covers at Sandia National Laboratories." Conference Proceedings: Landfill Capping in the Semi-Arid West: Problems, Perspectives, and Solutions, Grand Teton National Park, Wyoming, Sandia National Laboratories, Albuquerque, 87–107.

91. Dwyer, S. F. (1998). "Alternative Landfill Covers Pass the Test." Civil Engineering, ASCE, 68(9), 50–52.

92. Dwyer, S. F. (2001). "Finding a Better Cover." Civil Engineering, ASCE, 71(1), 58–63.

93. Dwyer, S. F. (2003). "Water balance measurements and computer simulations of landfill covers." Ph.D. Thesis, Civil Engineering Department, The University of New Mexico.

94. Eller, H., and Denoth, A. (1996). "A capacitive soil moisture sensor." Journal of Hydrology, 185(4), 137–146.

95. Evett, S. R., and Steiner, J. L. (1995). "Precision of Neutron Scattering and Capacitance Type Soil Water Content Gauges from Field Calibration." Soil Science Society of America Journal, 59(4), 961.

96. Evett, S. R., Tolk, J. A., and Howell, T. A. (2006). "Soil Profile Water Content Determination: Sensor Accuracy, Axial Response, Calibration, Temperature Dependence, and Precision." Vadose Zone Journal, 5(3), 894–907.

97. Fayer, M. J., and Jones, T. L. (1990). "UNSAT-H Version 3.0: Unsaturated Soil Water and Heat Flow Model: Theory, User Manual, and Examples." Model Manual, US Department of Energy, Pacific Northwest National Laboratory Richland, Washinton.

98. Fayer, M. J., Rockhold, M. L., and Campbell, M. D. (1992). "Hydrologic Modeling of Protective Barriers: Comparison of Field Data and Simulation Results." Soil Science Society of America Journal, 56(3), 690–700.

99. Flerchinger, G. N., and Saxton, K. E. (2000). "The Simultaneous Heat and Water (SHAW) Model: Technical Documentation." US Geological Survey, Northwest Watershed Research Center USDA Agricultural Research Service Boise, Idaho.

100. Foley, J. L., and Harris, E. (2007). "Field calibration of ThetaProbe (ML2x) and ECHO probe (EC-20) soil water sensors in a Black Vertosol." Australian Journal of Soil Research, 45(3), 233–236.

101. Fooladmand, H. R. (2011). "Evaluation of some equations for estimating evapotranspiration in the south of Iran." Archives of Agronomy and Soil Science, 57(7), 741–752.

102. Forman, A. D., and Anderson, J. E. (2005). "Design and Performance of Four Evapotranspiration Caps." Practice Periodical of Hazardous, Toxic and Radioactive Waste Management, 9(4), 263–272.

103. Francis, P. A., and Gadgil, S. (2006). "Intense rainfall events over the west coast of India." Meteorology and Atmospheric Physics, 94(1), 27–42.

104. Francisca, F. M., and Glatstein, D. A. (2010). "Long term hydraulic conductivity of compacted soils permeated with landfill leachate." Applied Clay Science, Elsevier B.V., 49(3), 187–193.

105. Fredlund, D. G., and Rahardjo, H. (1993). "Soil mechanics for unsaturated soils." John Wiley & Sons.

106. Fredlund, D. G., and Xing, A. (1994). "Equations for the soil-water characteristic curve." Canadian Geotechnical Journal, 31(6), 1026–1026.

107. Friedman, S. P. (1998). "A saturation degree-dependent composite spheres model for describing the effective dielectric constant of unsaturated porous media." Water Resources Research, 34(11), 2949–2961.

108. Friedman, S. P. (2005). "Soil properties influencing apparent electrical conductivity: A review." Computers and Electronics in Agriculture, 46(1), 45–70.

109. Gadi, V. K., Bordoloi, S., Garg, A., Sahoo, L., Berretta, C., and Sekharan, S. (2017). "Effect of shoot parameters on cracking in vegetated soil." Environmental Geotechnics, 17(13), 1–16.

110. Gardner, C. M. K., Dean, T. J., and Cooper, J. D. (1998). "Soil Water Content Measurement with a High-Frequency Capacitance Sensor." Journal of Agricultural Engineering Research, 71(4), 395–403.

111. Gardner, W. R. (1958). "Some steady-state solutions of the unsaturated moisture flow equation with application to evaporation from a water table." Soil science, 85(4), 228-232.

112. Gaskin, G. J., and Miller, J. D. (1996). "Measurement of Soil Water Content Using a Simplified Impedance Measuring Technique." Journal of Agricultural Engineering Research, 63, 153–159.

113. GEOSLOPE International. (2012). "Seepage Modeling with SEEP / W." GEOS-LOPE International Ltd, Calgary, Alberta, Canada.

114. GEOS-LOPE International. (2014). "Vadose Zone Modeling with VADOSE / W." GEOS-LOPE International Ltd, Calgory, Alberta, Canada.

115. Giorgi, F., and Mearns, L. O. (1991). "Approaches to the Simulation of Regional Climate Change: A Review." Review of Geophysics, 29(90), 191–216.

116. Giroud, J. P. (1994). "Quantification of Geosynthetics Behavior." Proceeding of the Fifth International Conference on Geotextiles, Geomembranes, and Related Products, Singapore, 1249–1273.

117. Goel, G., and Kalamdhad, A. S. (2017). "Degraded municipal solid waste as partial substitute for manufacturing fired bricks." Construction and Building Materials, 155, 259–266.

118. Gong, Y., Cao, Q., and Sun, Z. (2003). "The effects of soil bulk density, clay content and temperature on soil water content measurement using time-domain reflectometry." Hydrological Processes, 17(18), 3601–3614.

119. Grace, B., and Quick, B. (1988). "A Comparison of Methods for the Calculation of Potential Evapotranspiration Under the Windy Semi-arid Conditions of Southern Alberta." Canadian Water Resources Journal, 13(1), 9–19.

120. Gray, D. H., and Sotir, R. B. (1996). Biotechnical and Soil Bioengineering Slope Stabilization: A Practical Guide for Erosion Control. John Wiley & Sons, New York.

121. Gross, B. A. (2003). "Landfill Cover Design and Operation USEPA Workshop on Bioreactor Landfills." USEPA Workshop on Bioreactor Landfill, Washington DC, 1–20.

122. Gross, B. A., Bonaparte, R., and Giroud, J. P. (2002). Waste containment systems: problems and lessons learned. Appendix F in Assessment and Recommendations for Optimal Performance of Waste Containment Systems. US Environmental Protection Agency, National Risk Management Research Laboratory, Cincinnati, OH, 213.

123. Gross, B. A., Bonaparte, R., and Othman, M. A. (1997). "Inferred Performance of Surface Hydraulic Barriers from Landfill Operational Data." International Containment Technology Conference, St. Petersburg, 374–380.

124. Guerrero, L. A., Maas, G., and Hogland, W. (2013). "Solid waste management challenges for cities in developing countries." Waste Management, 33(1), 220–232.

125. Hamdi, N., and Srasra, E. (2013). "Hydraulic conductivity study of compacted clay soils used as landfill liners for an acidic waste." Waste Management, 33(1), 60–66.

126. Hargreaves, G. H., and Samani, Z. A. (1985). "Reference crop evapotranspiration from temperature." Applied Engineering in Agriculture, 1(2), 96–99.

127. Harlow, R. C., Burke, E. J., Ferre, T. P. A., Bennett, J. C., and Shuttleworth, W. J. (2003). "Measuring Spectral Dielectric Properties Using Gated Time Domain Transmission Measurements." Vadose Zone Journal, 2(3), 424–432.

128. Harnas, F. R., Rahardjo, H., Leong, E. C., and Wang, J. Y. (2014). "Experimental study on dual capillary barrier using recycled asphalt pavement materials." Canadian Geotechnical Journal, 51(10), 1165–1177.

129. Hauser, V. L., Gimon, D. M., Bonta, J. V., Howell, T. A., Malone, R. W., and Williams, J. R. (2005). "Models for hydrologic design of evapotranspiration landfill covers." Environmental Science and Technology, 39(18), 7226–7233.

130. Hauser, V. L., Weand, B. L., and Gill, M. D. (2001). "Natural covers for landslide and buried waste." Journal of Environmental Engineering, 127(9), 768–775.

131. Henken-Mellies, W. U., and Schweizer, A. (2011). "Long-term performance of landfill covers - Results of lysimeter test fields in Bavaria (Germany)." Waste Management and Research, 29(1), 59–68.

132. Hewitt, R. D., and Daniel, D. E. (1997). "Hydraulic conductivity of geosynthetic clay liners after freeze-thaw." Journal of Geotechnical and Geoenvironmental Engineering, 123(4), 305–313.

133. Hillel, D. (1998). Environmental Soil Physics. Academic Press San Diego, California, USA.

134. Holtz, R. D., Kovacs, W. D., and Sheahan, T. C. (1981). An Introduction to Geotechnical Engineering. (R. D. Holtz, W. D. Kovacs, and T. C. Sheahan, eds.), Pearson, Ne Jersery.

135. Hoor, A., and Rowe, R. K. (2013). "Potential for Desiccation of Geosynthetic Clay Liners Used in Barrier Systems." Journal of Geotechnical and Geoenvironmental Engineering, 139(10), 1648–1664.

136. Hsieh, P. a., Wingle, W., and Healy, R. W. (2000). "VS2DI — A Graphical Software Package for Simulating Fluid Flow and Solute or Energy Transport in Variably Saturated Porous Media." US Geological Survey.

137. Hsuan, Y. G., and Koerner, R. M. (1998). "Antioxidant Depletion Lifetime in High Density Polyethylene Geomembranes." Journal of Geotechnical and Geoenvironmental Engineering, 124(6), 532–541.

138. Huang, Q., Akinremi, O. O., Sri Rajan, R., and Bullock, P. (2004). "Laboratory and field evaluation of five soil water sensors." Canadian Journal of Soil Science, 84(4), 431–438.

139. Hutson, J. L., and Wagnet, R. J. (1992). "leaching estimation and chemistry model: description and user's guide." The Flinders University of South Austtralia, Adelaide.

140. IAEA. (2001). "Performance of engineered barrier materials in near surface disposal facilities for radioactive waste." (IAEA-TECDOC-1255), 1–50.

141. Ibrahim, A., Mukhlisin, M., and Jaafar, O. (2014). "Rainfall infiltration through unsaturated layered soil column." Sains Malaysiana, 43(10), 1477–1484.

142. Indian Standard 2720: Part 3. (1980). "Methods of test for soils, determination of specific gravity, fine, medium and coarse grained soils.", Bureau of Indian Standards, New Delhi, India.

143. Indian Standard 2720: Part 2. (1973). "Determination of water content of soil." Bureau of Indian Standards, New Delhi, India.

144. Indian Standard 2720: Part 17. (1986). "Methods of test for soils, laboratory determination of permeability." Bureau of Indian Standards, New Delhi, India.

145. Indian Standard 2720: Part 20. (1992). "Laboratory determination of linear shrinkage." bureau of indian standards, New Delhi, India.

146. Indian Standard 2720: Part 40. (1977). "Methods of test for soils: determination of free swell index of soils." Bureau of Indian Standards, New Delhi, India.

147. Indian Standard 2720: Part 4. (1985). "Methods of test for soils: determination of grain size analysis of soil." Bureau of Indian Standards, New Delhi, India.

148. Indian Standard 2720: Part 5. (1985). "Methods of test for soils, determination of liquid and plastic limit of soils." Bureau of Indian Standards, New Delhi, India.

149. Indian Standard 2720: Part 6. (1972). "Methods of test for soils: determination of shrinkage factors." Bureau of Indian Standards, New Delhi, India.

150. Indian Standard 2720: Part 7. (1980). "Methods of tests for soils: determination of water content—dry density relation of soil using light compaction." Bureau of Indian Standards, New Delhi, India.

151. Indian Standard 2720: Part 22. (1972). "Methods of tests for soils: determination of organic matter." Bureau of Indian Standards, New Delhi, India.

152. Indian Standard 2720: Part 26. (1987). "Methods of tests for soils: determination of pH value." Bureau of Indian Standards, New Delhi, India.

153. Indian Standard 2720: Part 24. (1976). "Methods of tests for soils: determination of cation exchange capacity." Bureau of Indian Standards, New Delhi, India.

154. Indrawan, I. G. B., Rahardjo, H., and Leong, E.-C. (2007). "Drying and wetting characteristics of a two-layer soil column." Canadian Geotechnical Journal, 44(1), 20–32.

155. Inglezakis, V. J., and Moustakas, K. (2015). "Household hazardous waste management: A review." Journal of Environmental Management, 150, 310–321.

156. Iryo, T., and Rowe, R. K. (2005). "Hydraulic behaviour of soil – geocomposite layers in slopes." Geosynthetics International, 12(3), 145–155.

157. ITRC. (2003). Technical and Regulatory Guidance Technical and Regulatory Guidance for Design , Installation , and Monitoring of Alternative Final Landfill Covers. Interstate Tehcnology and Regulatory Council, Washington DC.

158. Jabro, J. D., Stevens, W. B., and Iversen, W. M. (2017). "Field performance of three real-time moisture sensors in sandy loam and clay loam soils." Archives of Agronomy and Soil Science, Taylor & Francis, 1–9.

159. Jacobson, J. J., Heydt, H., Piet, S., Sehlke, G., Soto, R., and Visser, J. (2005). "Dynamic Modeling of an Evapotranspiration Cover." Practice Periodical of Hazardous, Toxic, and Radioactive Waste Management, 9(4), 223–236.

160. Jaisi, D. P., Glawe, U., and Bergado, D. T. (2005). "Hydraulic behaviour of geosynthetic and granular landfill drainage materials in the Sa Kaeo landfill, Thailand." Geotextiles and Geomembranes, 23(3), 185-204.

161. James, A. N., Fullerton, D., and Drake, R. (1997). "Field Performance of GCL under Ion Exchange Conditions." Journal of Geotechnical and Geoenvironmental Engineering, 123(10), 897–901.

162. Jarvis, N., Koestel, J., Messing, I., Moeys, J., and Lindahl, A. (2013). "Influence of soil, land use and climatic factors on the hydraulic conductivity of soil." Hydrology and Earth System Sciences, 17(12), 5185–5195.

163. Jensen, M., and Haise, H. (1963). "Estimating Evapotranspiration from Solar Radiation." American Society of Civil Engineers Proceedings, Journal of Irrigation and Dainage Division, 89(IR4), 15–41.

164. Jesionek, K. S., and Dunn, R. J. (1995, October). Landfill final covers: a review of California practice. In Landfill Closures: Environmental Protection and Land Recovery, ASCE, 51-61.

165. Jhajharia, D., Shrivastava, S. K., Tullu, P. S., and Sen, R. (2007). "Rainfall analysis of drought proneness at Guwahati." Indian Journal of Soil Construction, 35(2), 163–165.

166. Jones, S. B., Wraith, J. M., and Or, D. (2002). "Time domain reflectometry measurement principles and applications." Hydrological Processes, 16(1), 141–153.

167. Ju, Z., Liu, X., Ren, T., and Hu, C. (2010). "Measuring soil water content with time domain reflectometry: An improved calibration considering soil bulk density." Soil Science, 175(10), 469–473.

168. Kampf, M., and Montenegro, H. (1997). "On the performance of capillary barriers as landfill covers." Hydrology and Earth System Sciences, 4, 925–929.

169. Kelleners, T. J., Soppe, R. W. O., Ayars, J. E., & Skaggs, T. H. (2004a). Calibration of capacitance probe sensors in a saline silty clay soil. Soil Science Society of America Journal, 68(3), 770-778.

170. Kelleners, T. J., Soppe, R. W. O., Robinson, D. A., Schaap, M. G., Ayars, J. E., and Skaggs, T. H. (2004b). "Calibration of Capacitance Probe Sensors using Electric Circuit Theory." Soil Science Society of America Journal, 68(2), 430–439.

171. Khapre, A., Kumar, S., and Rajasekaran, C. (2017). "Phytocapping: an alternate cover option for municipal solid waste landfills." Environmental Technology, Taylor & Francis, 6, 1–8.

172. Khire, M. V., Benson, C. H., and Bosscher, P. J. (1997). "Water Balance Modeling of Earthen Final Covers." Journal of Geotechnical and Geoenvironmental Engineering, 123(8), 744–754.

173. Khire, M. V., Benson, C. H., and Bosscher, P. J. (1999). "Field data from a capillary barrier and model predictions with UNSAT-H." Journal of Geotechnical and Geoenvironmental Engineering, 125(6), 518–527.

174. Khire, M. V., Benson, C. H., and Bosscher, P. J. (2000). "Capillary barriers: Design variables and water balance." Journal of Geotechnical and Geoenvironmental Engineering, 126(8), 695–708.

175. Kodešová, R., Kodeš, V., and Mráz, A. (2011). "Comparison of two sensors ECH2O EC-5 and SM200 for measuring soil water content." Soil and Water Research, 6(2), 102–110.

176. Koerner, G. R., and Koerner, R. M. (1995). "Temperature Behavior of Field Deployed HDPE Geomembranes." Geosynthetics '95 Conference Proceedings, St. Paul, 921–937.

177. Koerner, R. M. (1998). Designing with Geosynthetics. International Organization, Prentice Hall, New Jersery.

178. Koerner, R. M., and Daniel, D. E. (1997). Final covers for solid waste landfills and abandoned dumps. Thomas Telford, ASCE Press, Reston, Virginia.

179. Koerner, R. M., Soong, T. Y., and Koerner, G. R. (2002). Behavior of Waves in HDPE Geomembranes. U.S. Environmental Protection Agency, National Risk Management Research Laboratory, Cincinnati, OH.

180. Kothawale, D. R., and Rajeevan, M. (2017). Monthly, Seasonal and Annual Rainfall Time Series for All-India Homogeneous Regions and Meteorological Subdivisions: 1871-2016. Report No. 138, Indian Institute of Tropical Meteorology, Pune.

181. Kraus, J. F., Benson, C. H., Erickson, A. E., and Chamberlain, E. J. (1997). "Freeze-thaw cycling and hydraulic conductivity of bentonite barriers." Journal of Geotechnical and Geoenvironmental Engineering, 123(3), 229–238.

182. Krisdani, H., Rahardjo, H., and Leong, E.-C. (2006). "Experimental Study of 1-D Capillary Barrier Model using Geosynthetic Material as the Coarse-Grained Layer." Unsaturated soils, 1683–1694.

183. Kuang, X., Jiao, J. J., Wan, L., Wang, X., and Mao, D. (2011). "Air and water flows in a vertical sand column." Water Resources Research, 47(4), 1–12.

184. Kundzewicz, Z. W., Kanae, S., Seneviratne, S. I., Handmer, J., Nicholls, N., Peduzzi, P., Mechler, R., Bouwer, L. M., Arnell, N., Mach, K., Muir-Wood, R., Brakenridge, G. R., Kron, W., Benito, G., Honda, Y., Takahashi, K., and Sherstyukov, B. (2013). "Flood risk and climate change: global and regional perspectives." Hydrological Sciences Journal, Taylor & Francis, 59(1), 1–28.

185. LaGatta, M. D., Boardman, B. T., Cooley, B. H., and Daniel, D. E. (1997). "Geosynthetic Clay Liners Subjected to Differential Settlement." Journal of Geotechnical and Geoenvironmental Engineering, 123(5), 402–410.

186. Lamb, D. T., Venkatraman, K., Bolan, N., Ashwath, N., Choppala, G., and Naidu, R. (2014). "Phytocapping: An alternative technology for the sustainable management of landfill sites." Critical Reviews in Environmental Science and Technology, 44(6), 561–637.

187. Lambe, T. W., and Whitman, R. V. (1979). Soil Mechanics. Wiley and Sons, New York.

188. Landreth, R. E., and Carson, D. A. (1991). "RCRA Cover Systems for Waste Management Facilities." Geotextiles and Geomembranes, 10, 383–391.

189. Landreth, R. E., Daniel, D. E., Koerner, R. M., Schroeder, P. R., and Richardson, G. N. (1991). Design and construction of RCRA-CERCLA final covers. Seminar Peblication, Washington DC.

190. Ledieu, J., De Ridder, P., De Clerck, P., and Dautrebande, S. (1986). "A method of measuring soil moisture by time-domain reflectometry." Journal of Hydrology, 88(5), 319–328.

191. Laner, D., Crest, M., Scharff, H., Morris, J. W., and Barlaz, M. A. (2012). A review of approaches for the long-term management of municipal solid waste landfills. Waste management, 32(3), 498-512.

192. Leoni, G. L. M., Almeida, M. D. S. S., and Fernandes, H. M. (2004). "Computational modelling of final covers for uranium mill tailings impoundments." Journal of Hazardous Materials, 110(1–3), 139–149.

193. Lewis, J., and Sjöstrom, J. (2010). "Optimizing the experimental design of soil columns in saturated and unsaturated transport experiments." Journal of contaminant hydrology, 115(1-4), 1-13.

194. Li, J. H., Du, L., Chen, R., and Zhang, L. M. (2013). "Numerical investigation of the performance of covers with capillary barrier effects in South China." Computers and Geotechnics, 48, 304–315.

195. Li, X., Lei, T., Wang, W., Xu, Q., and Zhao, J. (2005). "Capacitance sensors for measuring suspended sediment concentration." Catena, 60(3), 227–237.

196. Li, J. H., Li, L., Chen, R., and Li, D. Q. (2016). Cracking and vertical preferential flow through landfill clay liners. Engineering Geology, 206, 33-41.

197. Lin, L. C., and Benson, C. H. (2000). "Effect of wet-dry cycling on swelling and hydraulic conductivity of GCLs." Journal of Geotechnical and Geoenvironmental Engineering, 126, 40–49.

198. Liu, I.-W. Y., Waldron, L. J., and Wong, S. T. S. (1994). "Application of Nuclear Magnetic Resonance Imaging to Study Preferential Water Flow Through Root Channels." Tomography of soil water root processes, (36), 135–148.

199. Loiskandl, W., Buchan, G., Sokol, W., Novak, V., and Himmelbauer, M. (2010). "Calibrating electromagnetic short soil water sensors." Journal of Hydrology and Hydromechanics, 58(2), 114–125.

200. Luellen, J. R., and Brydges, J. M. (2005). "Long-term hydraulic performance evaluation for a multilayer closure cap." Practice Periodical of Hazardous, Toxic and Radioactive Waste Management, 9, 237–244.

201. Lukanu, G., and Savage, M. J. (2006). "Calibration of a frequency-domain reflectometer for determining soil-water content in a clay loam soil." Water SA, 32(1), 37–42.

202. MacDonald, N. W., Rediske, R. R., Scull, B. T., and Wierzbicki, D. (2008). "Landfill Cover Soil, Soil Solution, and Vegetation Responses to Municipal Landfill Leachate Applications." Journal of Environment Quality, 37(5), 1974.

203. Madalinski, K. L., Gratton, D. N., and Weisman, R. J. (2003). "Evapotranspiration covers: An innovative approach to remediate and close contaminated sites." Remediation, 14(1), 55–67.

204. Malaya, C. (2011). "A Study on Measuring Methodologies and Critical Parameters Influencing Soil Suction-Water Content Relationship." PhD Dissertation, Indian Institute of Technology Guwahati, India.

205. Maqsoud, A., Bussière, B., Aubertin, M., Chouteau, M., and Mbonimpa, M. (2011). "Field investigation of a suction break designed to control slope-induced desaturation in an oxygen barrier." Canadian Geotechnical Journal, 48(1), 53–71.

206. Maqsoud, A., Gervais, P., Bussière, B., and Borgne, V. L. E. (2017). "Performance evaluation of equipment used for volumetric water content measurements." WSEAS TRANSACTIONS on ENVIRONMENT and DEVELOPMENT, 13, 27–32.

207. Matula, S., Bát'ková, K., and Legese, W. L. (2016). "Laboratory performance of five selected soil moisture sensors applying factory and own calibration equations for two soil media of different bulk density and salinity levels." Sensors (Switzerland), 16(11), 1–22.

208. McCann, I. R., Fraj, M. B., and Dakheel, A. (2014). "Evaluation of the Decagon ® 5TE Sensor as a Tool for Irrigation and Salinity Management in a Sandy Soil." Proceedings of International Conference on Agricultural Engineering, 153–160.

209. Mccartney, J. S., and Zornberg, J. G. (2002). "Design and Performance Criteria for Evapotranspirative Cover Systems." Proceedings of the Fifth International Conference on Environmental Geotechnics, Rio de Janeiro, Brazil, 195–200.

210. McCartney, J. S., and Zornberg, J. G. (2010). "Effects of infiltration and evaporation on geosynthetic capillary barrier performance." Canadian Geotechnical Journal, 47(11), 1201–1213.

211. McDougall, J. R., Sarsby, R. W., and Hill, N. J. (1996). "A numerical investigation of landfill hydraulics using variably saturated fow theory." Geotechnique, 46(2), 329–341.

212. McGuire, P. E., Andraski, B. J., and Archibald, R. E. (2009). "Case study of a full-scale evapotranspiration cover." Journal of Geotechnical and Geoenvironmental Engineering, 135(3), 316–332.

213. Melchior, S. (1997). "In-situ Studies on the Performance of Landfill Caps." Proceedings, International Containment Technology Conference, St. Petersburg, 365–373.

214. Melchior, S., Berger, K., and Miehlich, G. (1994). Multilayered Landfill Covers: Field Data on the Water Balance and Liner Performance. In-Situ Remediation: Scientific Basis for Current and Future Technologies, G.W. Gee and N.R. Wing (eds.), Battelle Press, Columbus, OH, Part 1.

215. Melchior, S., Sokollek, V., Berger, K., Vielhaber, B., and Steinert, B. (2010). "Results from 18 years of in situ performance testing of landfill cover systems in Germany." Journal of Environmental Engineering, 136(8), 815–823.

216. Merlin, O., Walker, J. P., Panciera, R., Young, R., Kalma, J. D., and Kim, E. J. (2007). "Calibration of a Soil Moisture Sensor in Heterogeneous Terrain." MODSIM 2007 International Congress on Modelling and Simulation, 2604–2610.

217. METER Group. (2015). "Em50 Data Logger for Scanning and Storing Readings from 5TM and TEROS21 Sensors." Operator's User Manual, METER Group, United States of America (USA).

218. METER Group. (2016). "5TM for Measuring Volumetric Water Content and Temperature." Operator's User Manual, METER Group, United States of America (USA).

219. METER Group. (2017). "TEROS21 Sensor for Measuring Water Potential." Operator's User Manual, METER Group, Pullman, WA, United States of America (USA).

220. Mijares, R. G., Khire, M. V., and Johnson, T. (2012). "Field-scale evaluation of lysimeters versus actual earthen covers." Geotechnical Testing Journal, 35(1), 31–40.

221. Minet, J., Lambot, S., Delaide, G., Huisman, J. A., Vereecken, H., and Vanclooster, M. (2010). "A Generalized Frequency Domain Reflectometry Modeling Technique for Soil Electrical Properties Determination." Vadose Zone Journal, 9(4), 1063–1072.

222. Mitchell, J. K., and Jaber, M. (1990). Factors controlling the long-term properties of clay liners. Waste Containment Systems: Construction, Regulation, and Performance, ASCE, New York.

223. Monteith, J. L. (1981). "Evaporation and surface temperature." Quarterly Journal of the Royal Meteorological Society, 107(451), 1–27.

224. Montgomery, R., and Parsons, L. (1989). "The Omega Hills final cover test pilot study: Three-year data summary." Annual Meeting of the National Solid Waste Management Association, Washington, DC.

225. Montgomery, R., and Parsons, L. (1990). "The Omega Hills cover test pilot study: fourth year data summary." Proceedings of the 22nd Mid-Atlantic Industrial Waste Conference, Drexel University Philadelphia, USA, 24–27.

226. Morgan, K. T., Parsons, L. R., Wheaton, T. A., Pitts, D. J., and Obreza, T. A. (1999). "Field Calibration of a Capacitance Water Content Probe in Fine Sand Soils." Soil Science Society American Journal, 63(6), 987–989.

227. Morris, C. E., and Stormont, J. C. (1997). "Capillary barriers and subtitle D covers: Estimating equivalency." Journal of environmental engi, 123(1), 3–10.

228. Morris, C. E., and Stormont, J. C. (1998). "Evaluation of numerical simulations of capillary barrier field tests." Geotechnical and Geological Engineering, 16(3), 201–213.

229. Morris, D. V. (1990). "Settlement and Engineering Considerations in Landfill and Final Cover Design." Geotechnics of Waste Fills - Theory and Practice, ASTM STP 1070, 9.

230. Mualem, Y. (1976). "Hysteretical models for prediction of the hydraulic conductivity of unsaturated porous media." Water Resources Research, 12(6), 1248–1254.

231. Mwale, S. S., Azam-Ali, S. N., and Sparkes, D. L. (2005). "Can the PR1 capacitance probe replace the neutron probe for routine soil-water measurement?" Soil Use and Management, 21(3), 340–347.

232. Nemes, A., Rawls, W. J., and Pachepsky, Y. A. (2005). "Influence of Organic Matter on the Estimation of Saturated Hydraulic Conductivity." Soil Science Society of America Journal, 69(4), 1330–1337.

233. Ng, C. W. W., Coo, J. L., Chen, R., Guo, H. W., Ni, J., Chen, Y. M., Lu, B. W., Liu, J., and Zhan, T. L. T. (2019a). "A novel vegetated three-layer landfill cover system using recycled construction wastes without geomembrane." Canadian Geotechnical Journal, (in Press), 1–49.

234. Ng, C. W. W., Coo, J. L., Chen, Z. K., and Chen, R. (2016). "Water infiltration into a new three-layer landfill cover system." Journal of Environmental Engineering, 142(5), 04016007-1–12.

235. Ng, C. W. W., Liu, J., Chen, R., and Xu, J. (2015). "Physical and numerical modeling of an inclined three-layer (silt/gravelly sand/clay) capillary barrier cover system under extreme rainfall." Waste Management, 38(1), 210–221.

236. Ng, W. W., Charles, Ni, J., Chen, Y., Chen, R., and Gou, H. (2019b). "Effects of vegetation type on water infiltration in a three-layer cover system using recycled concrete." Journal of Zhejiang University Science A, 20(1), 1–9.

237. Noborio, K. (2001). "Measurement of soil water content and electrical conductivity by time domain reflectometry: A review." Computers and Electronics in Agriculture, 31(3), 213–237.

238. Noel, M., and Rykaart, E. M. (2003). "Comparative Study of Surface Flux Boundary Models to Design Soil Covers for Mine Waste Facilities." 6th International Conference on Acid Rock Drainage, Canada, 1–8.

239. Norris, A., Saafi, M., and Romine, P. (2008). "Temperature and moisture monitoring in concrete structures using embedded nanotechnology/microelectromechanical systems (MEMS) sensors." Construction and Building Materials, 22(2), 111–120.

240. Nyhan, J. W. (2005). "A Seven-Year Water Balance Study of an Evapotranspiration Landfill Cover Varying in Slope for Semiarid Regions." Vadose Zone Journal, 4(3), 466.

241. Nyhan, J. W., Shofield, T. G., and Starmer, R. H. (1997). "A water balance study of four landfill cover designs varying in slope for semiarid regions." Journal of Environmental Quality, 26, 1385–1392.

242. Ogorzalek, A. S., Bohnhoff, G. L., Shackelford, C. D., Benson, C. H., and Apiwantragoon, P. (2008). "Comparison of field data and water-balance predictions

for a capillary barrier cover." Journal of Geotechnical and Geoenvironmental Engineering, 134(4), 470–486.

243. Orense, R. P., Shimoma, S., Maeda, K., and Towhata, I. (2004). "Instrumented Model Slope Failure due to Water Seepage." Journal of Natural Disaster Science, 26(1), 15–26.

244. Othman, M. A., and Benson, C. H. (1993). "Effect of freeze–thaw on the hydraulic conductivity and morphology of compacted clay." Canadian Geotechnical Journal, 30(2), 236–246.

245. Othman, M. A., Benson, C. H., Chamberlain, E. J., and Zimmie, T. F. (1994). "Laboratory Testing to Evaluate Changes in Hydraulic Conductivity of Compacted Clays Caused by Freeze-Thaw." Hydraulic Conductivity and Waste Containment Transport in Soil, ASTM, D. E. and S. J. T. Daniel, ed., ASTM Publication, Philadelphia, 227–254.

246. Othman, M. A., Bonaparte, R., BV.A., G., and Warren, D. (2002). Evaluation of Liquids Management Data for Double-Lined Landfills. U.S. Environmental Protection Agency, National Risk Management Research Laboratory, Cincinnati, OH.

247. Øygarden, L., Kværner, J., and Jenssen, P. D. (1997). "Soil erosion via preferential flow to drainage systems in clay soils." Geoderma, 76(1–2), 65–86.

248. Paige, G. B., Stone, J. J., Lane, L. J., and Hakonson, T. E. (1996). "Calibration and Testing of Simulation Models for Evaluation of Trench Cap Designs." Journal of Environment Quality, 25(1), 136–136.

249. Palmeira, E. M., and Silva, A. R. L. (2007). "a Study on the Behaviour of Alternative Drainage Systems in Landfills." Proceedings Sardinia 2007, Eleventh International Waste Management and Landfill Symposium, Margherita di Pula, Italy.

250. Paltineanu, I. C., and Starr, J. L. (1997). "Real-time Soil Water Dynamics Using Multisensor Capacitance Probes: Laboratory Calibration." Soil Science Society of America Journal, 61(6), 1576–1585.

251. Parent, S. É., and Cabral, A. (2006). "Design of inclined covers with capillary barrier effect." Geotechnical and Geological Engineering, 24(3), 689–710.

252. Park, K. D., and Fleming, I. R. (2006). "Evaluation of a geosynthetic capillary barrier." Geotextiles and Geomembranes, 24(1), 64–71.

253. Parvin, N., and Degré, A. (2016). "Soil-specific calibration of capacitance sensors considering clay content and bulk density." Soil Research, 54(1), 111–119.

254. Penman, H. L. (1948). "Natural evaporation from open water, bare soil and grass." Nature, 158, 120–145.

255. Perkins, K. S., Nimmo, J. R., Medeiros, A. C., Szutu, D. J., and von Allmen, E. (2014). "Assessing effects of native forest restoration on soil moisture dynamics and potential aquifer recharge, Auwahi, Maui." Ecohydrology, 7(5), 1437–1451.

256. Polyakov, V., Fares, A., and Ryder, M. H. (2005). "Calibration of a Capacitance System for Measuring Water Content of Tropical Soil." Vadose Zone Journal, 4(4), 1004–1010.

257. Preston, G. M., and McBride, R. A. (2004). "Assessing the use of poplar tree systems as a landfill evapotranspiration barrier with the SHAW model." Waste Management and Research, 22(4), 291–305.

258. Priestley, C. H. B., and Taylor, R. J. (1972). "On the assessment of surface heat flux and evaporation using large scale parameters." Monthly Weather Review, 100, 81–92.

259. Qi, Z., and Helmers, M. J. (2008). "Field calibration of a multisensor capacitance probe for Des Moines Lobe Soils." Agricultural and Biosystems Engineering Conference Proceedings and Presentations, Rhode Island Convention Center Province, Rhode Island, 1–20.

260. Qian, T., Huo, L., and Zhao, D. (2010). "Laboratory Investigation into Factors Affecting Performance of Capillary Barrier System in Unsaturated Soil." Water Air and Soil Pollution, 206, 295–306.

261. Rahardjo, H., Santoso, V. A., Leong, E. C., Ng, Y. S., and Hua, C. J. (2012). "Performance of an instrumented slope covered by a capillary barrier system." Journal of Geotechnical and Geoenvironmental Engineering, 138(4), 481–490.

262. Rahardjo, H., Satyanaga, A., Harnas, F. R., and Leong, E. C. (2016). "Use of Dual Capillary Barrier as Cover System for a Sanitary Landfill in Singapore." Indian Geotechnical Journal, Springer India, 46(3), 228–238.

263. Rana, A., Foster, K., Bosshard, T., Olsson, J., and Bengtsson, L. (2014). "Impact of climate change on rainfall over Mumbai using Distribution-based Scaling of Global Climate Model projections." Journal of Hydrology: Regional Studies, Elsevier B.V., 1, 107–128.

264. Reddy, K. R., Stark, T. D., and Marella, A. (2010). "Beneficial Use of Shredded Tires as Drainage Material in Cover Systems for Abandoned Landfills." Practice

Periodical of Hazardous, Toxic, and Radioactive Waste Management, 14(1), 47–60.

265. Reddy, K., Stark, T., & Marella, A. (2008). "Clogging potential of tire-shred drainage layer in landfill cover systems." International Journal of Geotechnical Engineering, 2(4), 407-418.

266. Richards, L. A. (1931). "Capillary conduction of liquids thqough porous mediums." Physics, 1(1), 318–333.

267. Richardson, G. N., and Waugh, W. J. (1996). "The design of final cover systems for arid and semi-arid regions of the West." Mined and Reclamation, Carolina, 645–655.

268. Robinson, D. A., and Friedman, S. P. (2001). "Effect of particle size distribution on the effective dielectric permittivity of saturated granular media." Water Resources Research, 37(1), 33–40.

269. Robinson, D. A., Gardner, C. M. K., and Cooper, J. D. (1999). "Measurement of relative permittivity in sandy soils using TDR, capacitance and theta probes: Comparison, including the effects of bulk soil electrical conductivity." Journal of Hydrology, 223(3), 198–211.

270. Rock, S., Myers, B., and Fiedler, L. (2012). "Evapotranspiration (ET) covers." International Journal of Phytoremediation, 14(Sup 1), 1–25.

271. Roseen, R. M., Ballestero, T. P., Houle, J. J., Briggs, J. F., and Houle, K. M. (2012). "Water Quality and Hydrologic Performance of a Porous Asphalt Pavement as a Storm-Water Treatment Strategy in a Cold Climate." Journal of Environmental Engineering, 138(1), 81–89.

272. Roth, C. H., Malicki, M. A., and Plagge, R. (1992). "Empirical evaluation of the relationship between soil dielectric constant and volumetric water content as the basis for calibrating soil moisture measurements by TDR." Journal of Soil Science, 43(1), 1–13.

273. Rowe, R. K. (2005). "Long-term performance of contaminant barrier systems." Géotechnique, 55(9), 631–678.

274. Rowe, R. K. (2011). "Systems engineering: The design and operation of municipal solid waste landfills to minimize contamination of groundwater." Geosynthetics International, 18(6), 391–404.

275. Rowe, R. K. (2012). "Short- and long-term leakage through composite liners. The 7th Arthur Casagrande Lecture 1 1 This lecture was presented at the 14th Pan-American

Conference on Soil Mechanics and Geotechnical Engineering, Toronto, Ont., October 2011." Canadian Geotechnical Journal, 49(2), 141–169.

276. Rowe, R. K., and Yu, Y. (2012). Clogging of finger drain systems in MSW landfills. Waste management, 32(12), 2342-2352.

277. Yu, Y., & Rowe, R. K. (2012). Modelling leachate-induced clogging of porous media. Canadian Geotechnical Journal, 49(8), 877-890.

278. Rowe, R. K. (2014). "Performance of GCLS in liners for landfill and mining applications." Environmental Geotechnics, 1, 3–21.

279. Sadek, S., Ghanimeh, S., and El-Fadel, M. (2007). "Predicted performance of clay-barrier landfill covers in arid and semi-arid environments." Waste Management, 27(4), 572–583.

280. Saito, T., Fujimaki, H., Yasuda, H., and Inoue, M. (2009). "Empirical Temperature Calibration of Capacitance Probes to Measure Soil Water." Soil Science Society of America Journal, 73(6), 1931–1937.

281. Salt, M., Jaksa, M., Cox, J., and Lightbody, P. (2006). "Water balance modelling for phytocovers and cpnventional final covers at landfill closure." Common Ground Proceedings 10th Australia New Zealand Conference on Geomechanics, Brisbane, Australia, 392–397.

282. Sayer, M. A. S., Brissette, J. C., and Barnett, J. P. (2005). "Root growth and hydraulic conductivity of southern pine seedlings in response to soil temperature and water availability after planting." New Forests, 30(2–3), 253–272.

283. Scanlon, B. R., Christman, M., Reedy, R. C., Porro, I., Simunek, J., and Flerchinger, G. N. (2002). "Intercode comparisons for simulating water balance of surficial sediments in semiarid regions." Water Resources Research, 38(12), 59-1-59–16.

284. Scanlon, B. R., Levitt, D. G., Reedy, R. C., Keese, K. E., and Sully, M. J. (2005a). "Ecological controls on water-cycle response to climate variability in deserts." Proceedings of National Academy of Sciences of the USA, 102(17), 6033–6038.

285. Scanlon, B. R., Reedy, R. C., Keese, K. E., and Dwyer, S. F. (2005b). "Evaluation of evapotranspirative covers for waste containment in arid and semiarid regions in the Southwestern USA'." Vadose Zone Journal, 4, 55–71.

286. Schnabel, W. E., Munk, J., Lee, W. J., and Barnes, D. L. (2012). "Four-year performance evaluation of a pilot-scale evapotranspiration landfill cover in Southcentral Alaska." Cold Regions Science and Technology, 82, 1–7.

287. Schnabel, W., Lee, W., and Barnes, D. L. (2005). "A Numerical Simulation of Evapotranspiration Landfill Cover Performance at Three Cold-Region Locations." Impact of Global Climate Change, 1–8.

288. Schneider, A., Arnold, S., Doley, D., Mulligan, D. R., and Baumgartl, T. (2012). "The importance of plant water use on evapotranspiration covers in semi-arid Australia." Hydrology and Earth System Sciences Discussions, 9(10), 11911–11940.

289. Sharma, H. D., and Lewis, S. P. (1994). Waste containment systems, waste stabilization, and landfills: design and evaluation. Wiley and Sons, Wiley and Sons, New York.

290. Sherard, J. L., Dunnigan, L. P., and Decker, R. S. (1976). "Identification and Nature of Dispersive Soils." Journal of the Geotechnical Engineering Division, 102(GT4), 287–301.

291. Shivam, Goyal, M. K., and Sarma, A. K. (2017). "Analysis of the change in temperature trends in Subansiri River basin for RCP scenarios using CMIP5 datasets." Theoretical and Applied Climatology, 129(3–4), 1175–1187.

292. Schroeder, P. R., Aziz, N. M., Lloyd, C. M., and Zappi, P. A. (1994). The hydrologic evaluation of landfill performance (HELP) model: user's guide for version 3 (p. 233). Washington, DC: Risk Reduction Engineering Laboratory, Office of Research and Development, US Environmental Protection Agency.

293. Simon, F. G., and Müller, W. W. (2004). "Standard and alternative landfill capping design in Germany." Environmental Science and Policy, 7(4), 277–290.

294. Šimůnek, J., Šejna, M., and van Genuchten, M. T. (1999). "The Hydrus-2D software package for simulating water flow and solute transport in two-dimensional variably saturated media: Technical Manual." PC Progress, Prague, Czech Republic.

295. Sinnathamby, G., Pasky, A., Phillips, D. H. H., and Sivakumar, V. (2014). "Landfill cap models under simulated climate change precipitation: impacts of cracks and root growth." Géotechnique, 64(2), 95–107.

296. Sivaprakasam Subburayan, A. M. and S. M. (2011). "Modified Hargreaves Equation for Estimation of ETo in a Hot and Humid Location in Tamilnadu State, India." International Journal of Engineering Science and Technology (IJEST), 3(1), 592–600.

297. Skierucha, W., and Wilczek, A. (2010). "A FDR sensor for measuring complex soil dielectric permittivity in the 10-500 MHz frequency range." Sensors, 10(4), 3314–3329.

298. Smirnova, E., Bussière, B., Tremblay, F., and Bergeron, Y. (2011). "Vegetation Succession and Impacts of Biointrusion on Covers Used to Limit Acid Mine Drainage." Journal of Environment Quality, 40(1), 133.

299. Song, L., Li, J. H., Zhou, T., and Fredlund, D. G. (2017). "Experimental study on unsaturated hydraulic properties of vegetated soil." Ecological Engineering, 103, 207–216.

300. Steiniger, F. (1968). "The Effect of Burrower Attack on Dike Liners." Wasser and Boden, Berlin.

301. Sterpi, D. (2015). "Effect of freeze-thaw cycles on the hydraulic conductivity of a compacted clayey silt and influence of the compaction energy." Soils and Foundations, Elsevier, 55(5), 1326–1332.

302. Stormont, J. C. (1996). "The effectiveness of two capillary barriers on a 10% slope." Geotechnical and Geological Engineering, 14(4), 243–267.

303. Stormont, J. C., and Anderson, C. E. (1999). "Capillary barrier effect from underlying coarser soil layer." Journal of Geotechnical and geoenvironmental engineer, 125(8), 641–648.

304. Stormont, J. C., and Morris, C. E. (1999). "Method to Estimate Water Storage Capacity of Capillary Barriers." Journal of Geotechnical and Geoenvironmental Engineering, 124(4), 297–302.

305. Subedi, S., Hamamoto, S., Komatsu, T., Kawamoto, K., and Engineering, E. (2013). Development of Hydrophobic Capillary Barriers for Landfill Covers System: Assessment of Water Repellency and Hydraulic. Saitama University, Saitama.

306. Sui, R. (2018). "Irrigation Scheduling Using Soil Moisture Sensors." Journal of Agricultural Science, 10(1), 1–11.

307. Sun, J., Yuen, S. T. S., and Fourie, A. B. (2010). "The effect of using a geotextile in a monolithic (evapotranspiration) alternative landfill cover on the resulting water balance." Waste Management, 30(11), 2074–2083.

308. Suter, G. W., Luxmoore, R. J., and Smith, E. D. (1993). "Compacted Soil Barriers at Abandoned Landfill Sites are Likely to Fail in the Long Term." Journal of Environment Quality, 22(2), 217–226.

309. Swope, G. L. (1975). "Revegetation of Landfill Cover Sites." Pennsylvania State University, State Park, PA.

310. Tami, D., Rahardjo, H., Leong, E. C., and Fredlund, D. G. (2003). "A physical model for sloping capillary barriers." Geotechnical Testing Journal, 27(2), 173–183.

311. Tan, S. H., Wong, S. W., Chin, D. J., Lee, M. L., Ong, Y. H., Chong, S. Y., and Kassim, A. (2018). "Soil column infiltration tests on biomediated capillary barrier systems for mitigating rainfall-induced landslides." Environmental Earth Sciences, 77(589), 1–13.

312. Thompson, R. B., Gallardo, M., Valdez, L. C., and Fernández, M. D. (2007). "Determination of lower limits for irrigation management using in situ assessments of apparent crop water uptake made with volumetric soil water content sensors." Agricultural Water Management, 92(2), 13–28.

313. Topp, G. C., and Davis, J. L. (1985). "Measurement of soil water content using time-domain reflectometry (TDR): A Field Evaluation." Soil Science Society of America Journal, 49, 19–24.

314. Topp, G. C., Davis, J. L., and Annan, A. P. (1980). "Electromagnetic determination of soil water content: measruements in coaxial transmission lines." Water Resources Research, 16(3), 574–582.

315. Touma, J., Vachaud, G., and Parlange, J. Y. (1984). "Air and water flow in a sealed, ponded vertical soil column: Experiment and model." Soil Science, 137(3), 181–187.

316. USDOE. (2000). Innovative Technology Summary Report-Alternative Landfill Cover. U.S. Office of environmental management, New Mexico.

317. USEPA. (1989a). Final Cover on Hazardous Waste Landfills and Surface Impoundment. Washington DC.

318. USEPA. (1989b). "Requirements for hazardous waste landfill design, construction, and closure." Seminar publication, EPA (625/4–89/022), 1–127.

319. Vallejo, L. E. (2009). "Fractal analysis of temperature-induced cracking in clays and rocks." Géotechnique, 59(3), 283–286.

320. van Genuchten, M. T. (1980). "A Closed-form Equation for Predicting the Hydraulic Conductivity of Unsaturated Soils." Soil Science Society of America Journal, 44(5), 892–898.

321. Vangpaisal, T., Management, H. W., and Ratchathani, U. (2008). "Estimated Gas Migration through Landfill Cover Systems." (August).

322. Vaz, C. M. P., and Hopmans, J. W. (2001). "Simultaneous measurement of soil penetration resistance and water content with a combined penetrometer - TDR moisture probe." Soil Science Society of America Journal, 65(3), 4–12.

323. Vaz, C. M. P., Jones, S., Meding, M., and Tuller, M. (2013). "Evaluation of Standard Calibration Functions for Eight Electromagnetic Soil Moisture Sensors." Vadose Zone Journal, 12(2), 1–16.

324. Verburg, K., Ross, P. J., and Bristow, K. L. (1996). "SWIM v2.1 User Manual." Commonwealth Scientific and Industrial Research Organisation, Canberra, Australia.

325. Vereecken, H., Kollet, S., and Simmer, C. (2010). "Patterns in Soil–Vegetation–Atmosphere Systems: Monitoring, Modeling, and Data Assimilation." Vadose Zone Journal, 9(4), 821–827.

326. Vinnarasi, R., and Sarma, A. K. (2011). Impact of climate change on a Southern Tributary of Brahmaputra Basin.

327. Visconti, F., de Paz, J. M., Martínez, D., and Molina, M. J. (2014). "Laboratory and field assessment of the capacitance sensors Decagon 10HS and 5TE for estimating the water content of irrigated soils." Agricultural Water Management, 132, 111–119.

328. Wang, Z., Feyen, J., Nielsen, D. R., and Van Genuchten, M. T. (1997). "Two-phase flow infiltration equations accounting for air entrapment effects." Water Resources Research, 33(12), 2759–2767.

329. Wells, A. N., and Crooks, M. E. (1987). "Solid Waste Landfill Design Manual." Washington State Department of Ecology.

330. Whalley, W. R., Cope, R. E., Nicholl, C. J., and Whitmore, A. P. (2004). "In-field calibration of a dielectric soil moisture meter designed for use in an access tube." Soil Use and Management, 20(2), 203–206.

331. Whalley, W. R., Dean, T. J., and Izzard, P. (1992). "Evaluation of the capacitance technique as a method for dynamically measuring soil water content." Journal of Agricultural Engineering Research, 52, 147–155.

332. Widomski, M. K., Broichsitter, S. B., Zink, A., Fleige, H., Horn, R., and Ste, W. (2015). "Numerical modeling of water balance for temporary landfill cover in North Germany." Journal of Plant Nutrition and Soil Science, 178(3), 401–412.

333. Wilby, R. L., and Dawson, C. W. (2007). "SDSM 4.2— A decision support tool for th e assessment of regional climate change impacts, User Manual." Department of Geography, Lancaster University, UK, (August), 1–94.

334. Wilby, R. L., and Wigley, T. M. L. (1997). "Downscaling general circulation model output : a review of methods and limitations." Progress in Physical Geography, 21(4), 530–548.

335. Wilby, R. L., Dawson, C. W., and Barrow, E. M. (2002). "SDSM-a decision support tool for the assessment of regional climate change impacts." Environmental Modelling & Software, 17, 147–159.

336. Wong, L. C., and Haug, M. D. (1991). "Cyclical closed-system freeze–thaw permeability testing of soil liner and cover materials." Canadian Geotechnical Journal, 28(6), 784–793.

337. Wosten, J. H. M., Lilly, A., Nemes, A., and Bas, C. Le. (1999). "Development and use of a database of hydraulic properties of European soils." Geoderma, 90, 169–185.

338. Woyshner, M. R., and Yanful, E. K. (1995). "Modelling and field measurements of water percolation through an experimental soil cover on mine tailings." Canadian Geotechnical Journal, 32(4), 601–609.

339. Wraith, J. M., Robinson, D. A., Jones, S. B., and Long, D. S. (2005). "Spatially characterizing apparent electrical conductivity and water content of surface soils with time domain reflectometry." Computers and Electronics in Agriculture, 46, 239–261.

340. Xu, J., Ma, X., Logsdon, S. D., and Horton, R. (2012). "Short, Multineedle Frequency Domain Reflectometry Sensor Suitable for Measuring Soil Water Content." Soil Science Society of America Journal, 76(6), 1929–1937.

341. Xue, Q., Li, J. shan, and Liu, L. (2013). "Experimental study on anti-seepage grout made of leachate contaminated clay in landfill." Applied Clay Science, The Authors, 80–81, 438–442.

342. Yanful, E. K., Morteza Mousavi, S., and De Souza, L. P. (2006). "A numerical study of soil cover performance." Journal of Environmental Management, 81(1), 72–92.

343. Yanful, E. K., Mousavi, S. M., and Yang, M. (2003). "Modeling and measurement of evaporation in moisture-retaining soil covers." Advances in Environmental Research, 7(4), 783–801.

344. Yang, H., Rahardjo, H., and Leong, E.-C. (2006). "Behavior of Unsaturated Layered Soil Columns during Infiltration." Journal of Hydrologic Engineering, 11(4), 329–337.

345. Yang, H., Rahardjo, H., Leong, E. C., & Fredlund, D. G. (2004a). "Factors affecting drying and wetting soil-water characteristic curves of sandy soils." Canadian Geotechnical Journal, 41(5), 908-920.

346. Yang, H., Rahardjo, H., Leong, E. C., and Fredlund, D. G. (2004b). "A study of infiltration on three sand capillary barriers." Canadian Geotechnical Journal, 41(4), 629–643.

347. Yidong, G., Xin, C., Shuai, Z., and Ancheng, L. (2012). "Performance of multi-soil-layering system (MSL) treating leachate from rural unsanitary landfills." Science of the Total Environment, 420, 183–190.

348. Yoder, R. E., Johnson, D. L., Wilkerson, J. B., and Yoder, D. C. (1998). "Soil water sensor performance." Applied Engineering in Agriculture, 14(2), 121–133.

349. Yu, Y., and Rowe, R. K. (2012). "Effect of grain size on service life of MSW landfill drainage systems." Canadian Geotechnical Journal, 50(1), 1-14.

350. Yuen, S. T. S., Michael, R. N., Salt, M., Jaksa, M. B., and Sun, J. (2010). "Phytocapping as a Cost-Effective and Sustainable Cover Option for Waste Disposal Sites in Developing Countries." International Conference on Sustainable Built Environment (ICSBE-2010), (December 13-14), 13–14.

351. Zhan, T. L. T., Li, H., Jia, G. W., Chen, Y. M., and Fredlund, D. G. (2014). "Physical and numerical study of lateral diversion by three-layer inclined capillary barrier covers under humid climatic conditions." Canadian Geotechnical Journal, 51(12), 1438–1448.

352. Zhan, T. L., Ng, C. W., and Fredlund, D. G. (2007). "Field study of rainfall infiltration into a grassed unsaturated expansive soil slope." Canadian Geotechnical Journal, 44(4), 392–408.

353. Zhang, W., and Sun, C. (2014). "Parametric analyses of evapotranspiration landfill covers in humid regions." Journal of Rock Mechanics and Geotechnical Engineering, 6(4), 356–365.

354. Zhang, W., Sun, C., and Qiu, Q. (2016). "Characterizing of a capillary barrier evapotranspirative cover under high precipitation conditions." Environmental Earth Sciences, 75(6), 1–11.

355. Zhang, W., Zhang, Z., and Wang, K. (2009). "Experimental study and simulations of infiltration in evapotranspiration landfill covers." Water Science and Engineering, 2(3), 96–109.

356. Zhang, Z. F., Strickland, C. E., and Link, S. O. (2017). "Design and performance evaluation of a 1000-year evapotranspiration-capillary surface barrier." Journal of Environmental Management, 187, 31–42.

357. Žiliūte, L., Motiejūnas, A., Kleiziene, R., Gribulis, G., and Kravcovas, I. (2016). "Temperature and Moisture Variation in Pavement Structures of the Test Road." Transportation Research Procedia, 14(6), 778–786.

358. Zornberg, J. G., Bouazza, A., and McCartney, J. S. (2010). "Geosynthetic capillary barriers: current state of knowledge." Geosynthetics International, 17(5), 273–300.

359. Zornberg, J. G., LaFountain, L., and Caldwell, J. A. (2003). "Analysis and design of evapotranspirative cover for hazardous waste landfill." Journal of Geotechnical and Geoenvironmental Engineering, 129(6), 427–438.

List of Publications

Journal papers

1. **Shaikh, J.,** Yamsani, S.K., Sekharan, S., Rakesh, R.R., (2018). "Performance Evaluation of Profile Probe for Continuous Monitoring of Volumetric Water Content in Multilayered Cover System" 144(9): 040180781, *Journal of Environmental Engineering, ASCE*

2. **Shaikh, J.,** Yamsani, S.K., Sreedeep, S., and Rakesh, R.R. (2019). "Performance evaluation of 5TM sensor for real time monitoring of volumetric water content in multi-layered cover system" Vol. 8, No. 1, Pp. 322-335., *Advances in Civil Engineering Materials, ASTM*

3. **Shaikh, J.,** Bordoloi, S., Yamsani, S. K., Sekharan, S., Rakesh, R. R., & Sarmah, A. K. (2019). "Long-term hydraulic performance of landfill cover system in extreme humid region: Field monitoring and numerical approach." *Science of the total environment*, 688, 409-423.

4. **Shaikh, J.,** Yamsani, S. K., Bora, M. J., Sekharan, S., Rakesh, R. R., Mungale, A. and Bordoloi, S. (2019). "Impact Assessment of Vegetation Growth on Soil Erosion of a Landfill Cover Surface" *Acta Horticulturae et Regiotecturae 2 Nitra*, Slovaca Universitas Agriculturae Nitriae, pp. 76–80.

Manuscripts under review

1. **Shaikh, J.,** Bordoloi, S., Yamsani, S.K., Sekharan, S., and Rakesh, R.R., (2019). "Field hydraulic assessment of an instrumented three-layer landfill cover for a high humid region" Environmental Geotechnics, ICE.
2. **Shaikh, J.,** Bordoloi, S., Yamsani, S.K., Sekharan, S., and Rakesh, R.R., (2019). "Percolation characteristics assessment of different configuration of landfill cover system under constant flooding" Canadian Geotechnical Journal, NRC
3. **Shaikh, J.,** Yamsani, S.K., Sekharan, S., and Rakesh, R.R., (2019). "Hydraulic performance assessment of a multi-layered landfill cover system under constant water ponding" Environmental Earth Sciences, ELSEVIER.
4. **Shaikh, J.,** Bordoloi, S., Yamsani, S.K., Sekharan, S., and Rakesh, R.R., (2019). "A critical review on hydraulic performance assessment of landfill cover system considering climate change aspects" Critical Reviews in Environmental Science and Technology, Tailor & Francis.

Conference paper

1. Rout, A., **Shaikh, J.,** and Sreedeep, S. (2015). "Performance evaluation of three volumetric water content sensors" 50th Indian Geotechnical Conference,December, 2015, Pune, India. (Best paper award)